

MILD METHODS OF GLYCOSYL RADICAL GENERATION FOR C-GLYCOSIDE SYNTHESIS

Robert Stephen Andrews

A dissertation submitted to the faculty of the University of North Carolina at Chapel Hill in partial fulfillment of the requirements for the degree of Doctor of Philosophy in the Department of Chemistry.

Chapel Hill
2012

Approved by

Professor Michel R. Gagné

Professor Maurice Brookhart

Professor Michael Crimmins

Professor Jeffrey Johnson

Professor Joseph Templeton

Abstract

ROBERT STEPHEN ANDREWS: Mild Methods of Glycosyl Radical Generation for *C*-Glycoside Synthesis

(Under the direction of Prof. Michel R. Gagné)

Carbohydrates are a promising and expanding class of therapeutic drugs for a disparate group of diseases. As the anomeric linkages in these compounds are subject to enzymatic degradation, carbon-linked analogs of therapeutic glycosides have been developed and shown to increase the efficacy and bioavailability of the drug. Radical-mediated methods for the synthesis of anomeric carbon-carbon bonds feature excellent anomeric stereoselectivity and high functional group tolerance, making them ideal approaches to synthesis of *C*-glycosides. However, these methods often require the use of highly-toxic materials, elevated temperatures, or the use of a large excess radical acceptor to achieve high yields.

To improve upon these limitations, a nickel-catalyzed, room temperature approach to generate glycosyl radicals has been developed. Notably, this methodology requires only a slight excess of radical acceptor and does not use toxic tin reagents. Yields range from 20-98%, with highly electron-deficient alkenes providing the best results. Glycosyl radical addition into 1,1-disubstituted alkenes initially provided low diastereoselectivities, but by incorporating bulky alcoholic proton sources, the diastereoselectivity was improved up to 5:1.

A second-generation method of forming glycosyl radical was developed based on a single electron transfer from photo-generated $\text{Ru}(\text{bpy})_3^+$ to glycosyl bromides. Yields in these reactions were moderate to excellent, meeting or exceeding the previous best reported yields for each substrate class. Control experiments confirmed that the reaction is light-driven, and initial mechanistic

investigations led to a proposed mechanism. Further investigation into the rate of the photoredox process utilized trapping of the generated glycosyl radical with thiols. It was determined that catalyst hydrophobicity and solvent composition significantly affect the rate of the reaction, and these concepts were successfully applied to an improved synthesis of *C*-glycosides.

In an effort to apply these concepts to the synthesis of biologically relevant *C*-linked isosteres, a key aldehyde intermediate was synthesized using a photo-flow reactor. These reactors demonstrated improved formal turnover frequencies as compared to traditional “batch” reactions. Continuous-flow experiments were able to generate >5 g of the key intermediate in 24 hours, and this intermediate was successfully derivatized into the desired *C*-linked glycoconjugates.

To My Family and Elise.

Acknowledgements

Over the course of my graduate career, I have had the pleasure of interacting with so many people, many of whom I will never forget. Each person has changed me in some way, and I'd like to thank everyone for the experience. To anyone I do not specifically mention, please know that I am grateful.

I would like to thank Mike for the pleasure it has been to work in his lab for the past five years. He has given me the freedom to direct my own research and the support necessary to achieve my goals. His patience and guidance have been instrumental to my success, for which I am truly thankful. I am also very grateful for the trips to conferences in exotic lands he has funded, which were fantastic experiences. Thanks, Mike!

Thanks to my former teachers and professors who have helped me pursue a career in science. Special thanks to Mr. Jason Calhoun, (Gar-Field SHS), Mr. Jeff Malloy (JMU), Dr. Kevin Caran (JMU), Dr. Scott Lewis (JMU), Dr. Tom DeVore (JMU) and especially Dr. Kevin Minbiole (JMU) for his continued help long after I graduated and stopped working in his lab. Without your influence, I would not have even come to graduate school.

Thanks to my labmates at JMU for their help and companionship: Andrew (Super Duper) Blanchard, (the now) Dr. Erik Stang, Marita Lawler, Kevin Jellerson, Seth Kingree, and Kerry O'Neil. The long summers were far more pleasant around these guys, and I thank them for that.

A special thanks to former and current members of the Gagné lab, especially Dr. Hegui Gong for helping me get on my feet and set me in the right direction. (Dr. Michael) Tarselli for setting me straight, keeping me on my toes, and serving as an ongoing sounding board for chemistry, life-related

gripes, and everything in between. Dr. Colleen Munro-Leighton for the years of companionship while bringing the lab up to T. Brent Gunnoe standards. Dieter Weber for our long discussions about chemistry over the years that I have enjoyed, as well the numerous discussions of Deutschland. Joe Sokol and (Mike) Geier for the endless hours discussing the finer points of sports, as well as for forming a wonderfully successful trivia team. Ryan Felix for serving as the sole person in lab with whom I can discuss games, much to the chagrin of the rest of the lab. Laura Adduci for her endless patience and constant upbeat attitude, which is necessary to survive in a bay with me for as long as she has. Thanks everyone for the wonderful time, and I wish you all the best.

I would like to especially thank Elise. You have suffered along with me and been a source of constant support and optimism, regardless of my dour moods. I was only able to make it this far with your help. I cannot express how much this means to me, and I can only hope to return the favor.

Thanks to Holly, Vic, Mike, Christi, James, Cynthia, and Sergey for the invaluable friendship and helping me see the bright side of things. Thanks to the Poker Guys for the great times over the years I will not soon forget (looking at you, Stu).

Finally, I'd like to thank my family, who has supported me unconditionally throughout my life. Grandma and Grandpa A, Grandma and Grandpa B, Alan, Julie, Dave, Carolyn, Joyce, Wilbur, all my cousins, thank you for your love and guidance. Donnie, Mom and Dad, I can't thank you guys enough for everything you've done for me.

Table of Content

List of Tables	ix
List of Schemes	x
List of Figures	xiv
List of Abbreviations and Symbols	xvi
Chapter 1 - Introduction.	1
Carbohydrates and Glycosides.	1
Glycosides in Biology.	5
C-Glycosides.	8
Methods of C-Glycoside Synthesis.	12
Radical C-Glycoside Synthesis.	27
Research Objectives.	33
Chapter 2 : Radical Intermediates in Negishi Cross-Couplings.	34
Nickel-Catalyzed Radical Formation.	34
Application of Nickel Catalysts to Glycosyl Radical Generation (Dr. Hegui Gong).....	37
Substrate Scope: Alkenes and Carbohydrates.	40
Diastereoselectivity of 1,1-Disubstituted Alkenes.	43
Proposed Mechanism and Stereochemical Model.....	46
Diastereoselectivity: Chiral Auxiliaries.	50
Second Generation Catalysts: Atom-Transfer Radical Generation.	52
Conclusion.....	54
Experimental Section.	55

Chapter 3 – Light Mediated Radical <i>C</i> -Glycoside Synthesis.....	73
Photoredox Catalysis: Background.....	73
Initial Optimization.....	83
Substrate Scope: Carbohydrates and Alkenes.....	86
Control Experiments and Mechanistic Investigations.	88
Proposed Mechanism and Attempted Application to Propiolates.....	90
Conclusion.	95
Experimental Section.....	95
Chapter 4 - Rate of Glucosyl Radical Generation.....	107
Effect of Alkenes and Catalyst on Rate.	107
Rate of Photoredox Cycle.	110
Experimental Design.....	112
Rate Dependence on Reagent Concentration.....	114
Application to <i>C</i> -Glycoside Synthesis.	121
Conclusion.	122
Experimental Section.....	122
Chapter 5 - Large Scale Synthesis of <i>C</i> -Glycoconjugates	130
Synthesis of <i>C</i> -Glycoconjugates.....	130
Planned Synthesis of <i>C</i> -Glycoamino acids via Key Aldehyde Intermediate.....	136
Large Scale Synthesis of <i>C</i> -Glycosides.	140
Evaluation of Photo-Flow Reactor.....	144
Synthesis of <i>C</i> -Glycoconjugates.	147
Conclusion and Future Work.....	152
Experimental Section.....	153
Bibliography	171

List of Tables

Table 2.1: Optimization of Nickel-Catalyzed Radical Addition into Alkenes by Dr. Hegui Gong.	38
Table 2.2: Substrate Scope of Acrylate-Based Alkenes.	40
Table 2.3: Radical Addition into Substituted Styrenes.	41
Table 2.4: Sugar Substrates in Ni-Catalyzed Addition into Alkenes.	43
Table 2.5: Optimization of Diastereoselectivity of Addition into Disubstituted Alkenes.	44
Table 2.6: Diastereoselective Addition into Alkenes Scope.	46
Table 2.7: Influence of Oxazolidinone-based Chiral Auxiliaries on Diastereoselectivity.	50
Table 2.8: Investigation of Copper Catalysts for <i>C</i> -Glycoside Synthesis.	53
Table 3.1: Initial Optimization of Ru(bpy) ₃ ²⁺ -Mediated <i>C</i> -Glycoside Synthesis.	83
Table 3.2: Optimization of Additives for the Synthesis of <i>C</i> -Glycosides.	84
Table 3.3: Final Optimization of Radical-Mediated <i>C</i> -Glycoside Synthesis.	85
Table 3.4: Substrate Scope of Radical-Mediated <i>C</i> -Glycoside Synthesis.	86
Table 3.5: Control Experiments in the Light-Mediated Synthesis of <i>C</i> -Glycosides.	88
Table 4.1: Yield and Conversion of <i>C</i> -Glycoside Synthesis with Optimized Conditions.	121
Table 4.2: % Conversion of 4 for various cosolvent concentrations	125
Table 5.1: 24-hour Continuous Flow Reaction for Ac- and Piv-Protected Sugars.	145
Table 5.2: Calculation of % Transmittance Based on Path Length and [Ru(dmb) ₃ ²⁺]	155
Table 5.3: Conversion, Yield, and TOF of Flow Reactor Based on Design.	158

List of Schemes

Scheme 1.1: Equilibrium between Aldohexose and Pyranose Form of Glucose.....	2
Scheme 1.2: Electrophilic Activation of Saccharides for C-Glycoside Synthesis.....	13
Scheme 1.3: Stereoselectivity of Cyanide Addition to Glucosyl Fluorides Based on Conditions.....	13
Scheme 1.4: Alkylation of Glycosyl Halides with Various Nucleophiles.	14
Scheme 1.5: Synthesis of C-Allyl Glycosides.	14
Scheme 1.6: Examples of Electrophilic Substrates for C-Glycoside Synthesis.....	15
Scheme 1.7: Synthesis of C-linked Glycerolipid via Ramberg-Bäcklund Rearrangement.....	16
Scheme 1.8: Nucleophilic Addition of Glycals into Aldehydes.	17
Scheme 1.9: Synthesis of Iodo-Glycals for Cross-Coupling Reactions.....	17
Scheme 1.10: Stereospecific Addition of Lithium-Saccharides via Direct Metal-Metal Exchange. ...	18
Scheme 1.11: Stereoselective Addition of Lithium-Glycosides into Aldehydes via Reduction.....	18
Scheme 1.12: Deprotonation of Sulfonyl Glycosides and Stereoselective Protonation.	19
Scheme 1.13: Addition of 1,3-Diketones into Ally-Palladium Complex.	19
Scheme 1.14: Palladium-Catalyzed Heck-type Coupling for Aryl-C-Glycoside Synthesis.	20
Scheme 1.15: Palladium-Catalyzed Stille Reaction of Stannyl Glycals.	21
Scheme 1.16: Negishi Cross-Coupling of Iodo-Glycals.	21
Scheme 1.17: Stereoselective Rhodium-Catalyzed α -Arylation of Glycosyl Enones.	22
Scheme 1.18: Divergent Synthesis of Aryl-C-Glycosides Based on Oxidant.	22
Scheme 1.19: Saturated, Unsaturated, and Fully Oxygenated Glycosyl Electrophiles.....	23
Scheme 1.20: Nickel-Catalyzed Negishi Cross-Coupling of sp^3 -Hybridized Electrophiles.....	24
Scheme 1.21: Negishi Cross-Coupling of Glucosyl Bromides and Alkylzinc Reagents.....	25
Scheme 1.22: Negishi Cross-Coupling of Mannosyl Bromides and Alkylzinc Reagents.	25
Scheme 1.23: Selectivity of Negishi Cross-Coupling with Glucosyl Bromides and Arylzinc.	26
Scheme 1.24: Selectivity of Negishi Cross-Coupling with Mannosyl Bromides and Arylzincs.	26

Scheme 1.25: Orientation of Glucosyl Radicals.....	28
Scheme 1.26: Tin-Mediated of Glycosyl Halides into Alkenes.	28
Scheme 1.27: Rate of Glycosyl Radical Generation Based on Orientation of C2 Substituent.....	29
Scheme 1.28: Mechanism of Tin-Catalyzed Radical Addition into Alkenes.	30
Scheme 1.29: Examples of Tin-Catalyzed Radical Generation for the Synthesis of C-Disaccharides.	31
Scheme 1.30: Generation of Glycosyl Radicals by Titanocene(III) Chloride.	32
Scheme 1.31: Nickel-Catalyzed Radical Generation and Addition into Acrylates.	33
Scheme 2.1: Reaction of Ni(I) and Ni(II) Complexes with Alkyl Coupling Partners.	34
Scheme 2.2: Proposed Catalytic Cycle of Ni-Catalyzed Negishi Reactions.	35
Scheme 2.3: Observed Radical Cyclization by Cárdenas in Negishi Cross-Coupling.	37
Scheme 2.4: Radical Clock Reaction in Negishi Cross-Coupling.....	37
Scheme 2.5: Ring-Opening of Vinyl Cyclopropane 58	47
Scheme 2.6: Proposed Mechanism of Ni-Catalyzed Synthesis of C-Glycosides.	47
Scheme 2.7: Proposed Stereochemistry Model.	49
Scheme 2.8: General Mechanism for ATRP.	52
Scheme 3.1: Reduction of Glycosyl Bromides by Nickel(I) Complex	73
Scheme 3.2: Metal to Ligand Charge Transfer to Form Ligand-Centered Radical.....	74
Scheme 3.3: Redox Behavior of Excited State Ru(bpy) ₃ ²⁺	75
Scheme 3.4: Reduction of Phenacylsulfonium Salt by 1,4-Dihydropyridine with Ru(bpy) ₃ Cl ₂	76
Scheme 3.5: Reduction of Phenacyl Bromide 12 Catalyzed by Ru(bpy) ₃ Cl ₂	77
Scheme 3.6: Ru(bpy) ₃ Cl ₂ -Catalyzed Enantioselective α -Functionalization of Aldehydes.	78
Scheme 3.7: Proposed Organocatalytic and Photoredox Mechanism by MacMillan and Nicewicz....	79
Scheme 3.8: Formal [2+2] Intramolecular Cyclization of Enones.	80
Scheme 3.9: Ru(bpy) ₃ ²⁺ -Catalyzed [2+2] Cycloaddition of Crossed Enones.	81
Scheme 3.10: Radical-Mediated Reduction Debromination with Ru(bpy) ₃ ²⁺	81
Scheme 3.11: Radical-Cascade Synthesis of Polycycles Initiated by Ru(bpy) ₃ Cl ₂	82

Scheme 3.12: Planned Reactivity of $\text{Ru}(\text{bpy})_3^+$ and Glycosyl Bromides.....	82
Scheme 3.13: Thiol-Trapping Control Experiment.	89
Scheme 3.14: Radical-Mediated Conjugate Additions into Vinyl Cyclopropane 51	90
Scheme 3.15: Proposed Mechanism of $\text{Ru}(\text{bpy})_3^{2+}$ -Catalyzed C-Glycoside Synthesis.	91
Scheme 3.16: Attempted Conjugate Addition into Propiolates.	92
Scheme 3.17: Potential Mechanism for Synthesis of 61	93
Scheme 3.18: Reaction of 23 with Propiolate 59	93
Scheme 4.1: Proposed Mechanism of Reductive Quenching of $\text{Ru}(\text{bpy})_3^{2+}$ with Amines.	110
Scheme 4.2: Proposed Trapping of Glycosyl Radicals with Thiols.....	112
Scheme 4.3: Varying Concentration of Thiol on Consumption of 4	114
Scheme 5.1: Synthesis of C-Alanine via Radical Addition into a Chiral Alkene.....	131
Scheme 5.2: Wittig-Approach to β -C-Alanine Glycoamino Acid.....	131
Scheme 5.3: Wittig-Approach to Glycosyl C-Serines.	132
Scheme 5.4: Synthesis of β -C-Serine via Ramberg-Bäcklund Rearrangement.	132
Scheme 5.5: Synthesis of C-Serines via Nucleophilic Addition of Chiral Zinc Reagent to Glycal. .	133
Scheme 5.6: Synthesis of α -C-Serine via Olefination and Asymmetric Hydrogenation.	134
Scheme 5.7: Organocatalytic α -Amination of Aldehydes for C-Alanine Synthesis.....	135
Scheme 5.8: Organocatalytic α -Amination of Aldehydes for C-Serine Synthesis.	136
Scheme 5.9: Planned Synthesis of C-Glycoconjugates from Common Aldehyde Intermediate.	137
Scheme 5.10: One-Pot Organocatalytic Asymmetric Strecker Cyanation of Aldehydes.	138
Scheme 5.11: L-Prolinamide Catalyzed α -Chlorination of Aldehydes for Amino Acid Synthesis...	139
Scheme 5.12: α -Substitution of Aldehydes with Iminoglyoxalate 56 for Amino Acid Synthesis.....	139
Scheme 5.13: Conversion and TOF Based on Vessel Size.....	140
Scheme 5.14: One-Pot Organocatalytic Synthesis of Glycosyl Amino Nitriles.....	147
Scheme 5.15: Platinum-Catalyzed Hydration of Nitrile to Amide.	148
Scheme 5.16: Alcoholysis of Primary Amide to Methyl Ester.....	148

Scheme 5.17: α -Chlorination of Aldehydes and Subsequent Derivatization to Azido Ester.	149
Scheme 5.18: α -Addition of Aldehyde into Iminoglyoxalate, Reduction, and Lactonization.....	150
Scheme 5.19: α -Addition of Aldehyde into Iminoglyoxalate and Protection.	151
Scheme 5.20: Synthesis of Model C-glycolipid.	151

List of Figures

Figure 1.1: Structure of Aldose and Ketose Carbohydrates.....	1
Figure 1.2: General Structure for X-Glycosides.....	2
Figure 1.3: α - and β -Anomeric Forms of Common Pyranose Monosaccharides.....	3
Figure 1.4: Anomeric Effect in Pyranose Monosaccharides.....	4
Figure 1.5: Energy Diagram for the Anomerization of Glucosyl Bromides.....	5
Figure 1.6: Absence of Anomeric Effect in C-Glycosides.	8
Figure 1.7: Nojirimycin-Glucose Dimer as Glucosidase Enzyme Inhibitor.	9
Figure 1.8: O- and C-Glycoside Analogs of KRN7000.....	10
Figure 1.9: Presence of Sporozites based on Dosage of O- and C-linked KRN7000.	11
Figure 1.10: Polymer-based Sialic Acid C-Glycosides for Inhibition of Influenza Binding.	12
Figure 1.11: Catalyst- and Substrate-Control in Negishi Cross-Couplings of Glycosyl Halides.	27
Figure 2.1: Common Byproducts in the Nickel-Catalyzed Radical Addition into Alkenes.	39
Figure 2.2: Structure of Pincer Ligands Used in Optimization.....	39
Figure 2.3: Plot of % Yield vs σ -value of Substituent for a Series of Substituted-Styrenes.....	42
Figure 2.4: Reduction Potentials of Terpy-Nickel Complexes.	48
Figure 2.5: Chiral Auxiliaries Investigated and Resulting Diastereoselectivity.	51
Figure 3.1: Structure of Trisbipyridine Ruthenium(II).	74
Figure 3.2: Time-Based EPR of Carbon-Based Radicals in Light-Mediated Reactions.....	90
Figure 3.3: Attempted Amine Quenchers for Addition of Radicals into Propiolates.	94
Figure 4.1: Reaction of Glucosyl Bromide 4 with Methyl Acrylate.....	108
Figure 4.2: Reaction of Glucosyl Bromide 4 with Methyl Vinyl Ketone.....	109
Figure 4.3: Experimental Setup for CFL Irradiation of NMR Tubes.	113
Figure 4.4: Amount of 1 consumed after 3 h of irradiation with a 14 W CFL light source versus initial concentration of 1.....	114

Figure 4.5: Conversion after 3 h of irradiation with increasing [Ru(bpy) ₃ ²⁺] for CFL and blue LED light sources.	115
Figure 4.6: Experimental Setup for the Irradiation of NMR Tubes with Blue LEDs.....	116
Figure 4.7: % Conversions after 3 h of irradiation as a function of initial EtNiPr ₂ concentration....	117
Figure 4.8: % conversion of 1 (20 min) after photolysis with blue LEDs versus cosolvent additive..	118
Figure 4.9: Conversion after 20 min of irradiation with blue LEDs with increasing [Ru(bpy) ₃ ²⁺].	119
Figure 4.10: Conversion after 20 min of irradiation with blue LEDs for Ru(L) ₃ ²⁺	120
Figure 5.1: % Transmittance vs distance (d) from the Wall from the Beer-Lambert law.	141
Figure 5.2: Diagram of the Designed Photo-flow Reactor.	143
Figure 5.3: TOF vs [Ru(dmb) ₃ ²⁺] at Two Tubing Diameters.	144
Figure 5.4: Experimental Setup for the Synthesis of Acetate-Protected C-Glycosides.....	146
Figure 5.5: Experimental Setup for the Synthesis of Pivaloate-Protected C-Glycosides.....	146
Figure 5.6: Flow Reactor Design A.....	156

List of Abbreviations and Symbols

°C	degrees Celcius
%T	% transmittance (light)
Å	angstrom
Abs	absorbance (light)
Ac	acetyl
α	alpha – opposite sides of pyranose ring (stereochemistry)
AIBN	2,2'-azobis(2-methylpropionitrile)
aq	aqueous
β	beta – same side of the pyranose ring (stereochemistry)
BINOL	1,1'-bi-2-naphthol
Boc	<i>tert</i> -butoxycarbonyl
bpy	2,2'-bipyridine
Bn	benzyl
brms	based on remaining starting material (yield)
<i>n</i> BuLi	<i>n</i> -butyllithium
<i>t</i> Bu	<i>tert</i> -butyl
<i>t</i> BuLi	<i>tert</i> -butyllithium
<i>t</i> BuOH	<i>tert</i> -butyl alcohol
Bz	benzoate
C-	carbon (linkage in saccharides)
Cbz	carboxylbenzyl
CFL	compact fluorescent light
COD	1,5-cyclooctadiene
δ	delta – change from standard value (NMR)

d	doublet (NMR)
<i>d</i>	distance
D	dextrorotary (stereochemistry, relative to glyceraldehyde)
de	diastereomeric excess
DFT	density functional theory (calculations)
DMA	<i>N,N</i> -dimethylacetamide
DMAP	4-(dimethylamino)pyridine
dmb	4,4'-dimethyl-2,2'-bipyridine
DMF	<i>N,N</i> -dimethylformamide
DMI	1,3-dimethyl-2-imidazolidinone
DMSO	dimethylsulfoxide
dr	diastereomeric ratio
dtb-bpy	4,4'-di- <i>tert</i> -butyl-2,2'-bipyridine
<i>E</i>	entgegen – opposite (German)
E _a	activation energy
ee	enantiomeric excess
epi.	epimer (stereochemistry)
EPR	Electroparamagnetic resonance (spectroscopy)
eq.	equivalent
ESI	electrospray ionization
Et	ethyl
EtOH	ethanol
φ	quantum yield
FEP	fluorinated ethylene propylene
g	gram
mg	milligram

μg	microgram
GCMS	gas chromatography – mass spectroscopy
h	hour
hν	energy (from light)
HEH	Diethyl 1,4-dihydro-2,6-dimethyl-3,5-pyridine dicarboxylate
HMETA	1,1,4,7,10,10-hexamethyltriethylenetetramine
HPLC	high performance liquid chromatography
HRMS	high resolution mass spectrum
Hz	hertz (NMR coupling constants)
I.D.	inner diameter (tubing)
L	liter
L	any unspecified ligand
L	levorotary (stereochemistry, relative to glyceraldehyde)
mL	milliliter (10^{-3} liter)
μL	microliter (10^{-6} liter)
λ	lambda - wavelength
LC-TOF	liquid chromatography time of flight mass spectrometry
LDA	lithium diisopropylamide
LED	light emitting diode
m	multiplet (NMR)
<i>m</i> -	meta – 1,3 relationship on aromatic
M	molar – 1 mol / liter (concentration)
Me	methyl
MeOH	methanol
mg	milligram
MHz	megahertz

min	minutes
MLCT	metal to ligand charge transfer
mM	millimolar – 10^{-3} mol / liter (concentration)
mmol	millimole
mol %	mole percent (catalyst loading)
mp	melting point
MS	molecular sieves
m/z	mass-to-charge ratio (mass spectrometry)
ν	nu – frequency (cm^{-1})
n	non-bonding (orbital)
NCS	<i>N</i> -chlorosuccinimide
ND	not determined
NMR	nuclear magnetic resonance
Nuc	any unspecified nucleophile
<i>o</i> -	ortho, 1,2-relationship on aromatic
<i>p</i> -	para, 1,4-relationship on aromatic
P	any unspecified protecting group
Ph	phenyl
π	pi – electrons involved in C-C multiple bonds
1,10-phen	1,10-phenanthroline
Piv	pivaloate
PMETA	Tris[2-(dimethylamino)ethyl]amine
ppm	parts per million (NMR relative difference)
ppy	2-phenylpyridine
<i>i</i> Pr	<i>iso</i> -propyl
<i>i</i> PrOH	isopropyl alcohol

pyr	pyridine
q	quartet (NMR)
R-	any unspecified carbon-containing group
rt	room temperature
σ	sigma – electrons involved in C-C single bonds
σ^*	antibonding orbital in C-C single bonds
s	seconds
s	singlet (NMR)
SCE	saturated calomel electrode
SFC	supercritical fluid chromatography
STP	standard temperature and pressure (296 Kelvin and 1 atmosphere)
t	triplet (NMR)
TBDMS	<i>tert</i> -butyldimethylsilyl
THF	tetrahydrofuran
TIPS	triisopropylsilyl
TMEDA	<i>N,N,N',N''</i> -tetramethylethylenediamine
TMS	trimethylsilyl
TOF	turnover frequency
Ts	<i>p</i> -toluenesulfonate
PhMe	toluene
W	watt (energy)
X-	any unspecified heteroatom (saccharides)
Xc	any unspecified chiral auxiliary
Z	zusammen – together (German)

Chapter 1 - Introduction.

Carbohydrates and Glycosides.

Carbohydrates, or saccharides, are biological macromolecules primarily comprised of carbon, oxygen, and hydrogen atoms. These molecules are responsible for essential biological processes in living organisms, such as energy storage and intercellular recognition events.¹ Carbohydrates have an empirical formula of $(\text{CH}_2\text{O})_n$, or “hydrated carbon”, from which the term “carbohydrate” is derived. While formaldehyde ($n = 1$) can be considered the simplest carbohydrate, it has little biological relevance due to its toxicity, so instead trioses ($n = 3$, e.g. glyceraldehyde **1**) are generally regarded as the smallest carbohydrate.^{1c} Monosaccharides typically range in size from trioses through heptoses and can exist as two distinct structural isomers based on the location of the carbonyl. Aldoses terminate in an aldehyde, whereas ketoses contain an internal carbonyl (Figure 1.1).

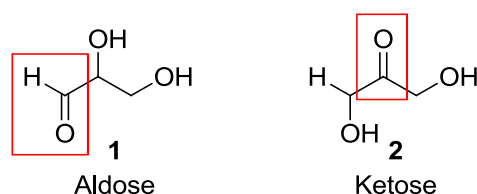


Figure 1.1: Structure of Aldose and Ketose Carbohydrates.

¹ a) Collins, P.; Ferrier, R., *Monosaccharides. Their Chemistry and Their Roles in Natural Products*. West Sussex, England, 1995. b) Varki, A., *Essentials of glycobiology*. Cold Spring Harbor Laboratory Press: Cold Spring Harbor, N.Y., 2009. c) Mathews, C. K.; van Holde, K. E.; Ahern, K. G., *Biochemisry*. 3rd Ed.; Addison Wesley Longman, Publishers, San Francisco, 2000; pp. 278-312.

Monosaccharides are the basic building blocks of more complex biological structures. By connecting multiple monosaccharides, oligo- and polysaccharides are formed, such as the disaccharide sucrose and the polysaccharide α -amylose.¹ Carbohydrates can exist as pure saccharides, containing only carbohydrate monomers, or as glycosides in which the carbohydrate is covalently linked to a non-saccharide group called the aglycone (Figure 1.2). Glycosylation of other biological macromolecules creates glycoconjugates such as glycopeptides and glycolipids, which separates carbohydrates from other classes of biological macromolecules.

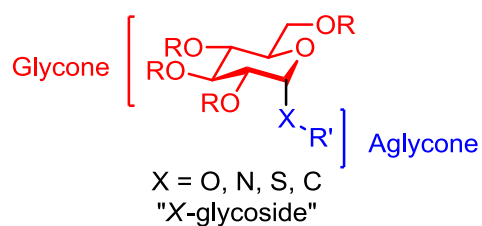
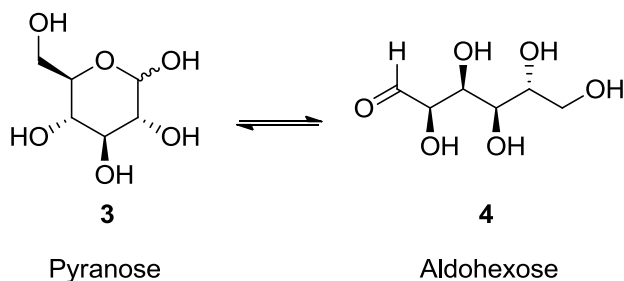


Figure 1.2: General Structure for X-Glycosides.

Carbohydrates adopt multiple conformations based on substitution, stereochemistry, and the molecule's environment.^{1a,c} For example, aldohexoses are of particular interest because of their ability to form stable 6-member cyclic hemiacetals called pyranoses. The carbonyl moiety allows the saccharide to undergo an internal cyclization in order to form the hemiacetal. Glucose is the most prevalent member of the pyranose class of saccharides, and its pyranose (**3**) and ring-opened (**4**) forms are shown in Scheme 1.1.



Scheme 1.1: Equilibrium between Aldohexose and Pyranose Form of Glucose.

These ring-forms are in a thermodynamic equilibrium dependent on the environment and structure of the monosaccharide. Generally the cyclic hemiacetal is strongly favored under physiological conditions. Glucose exists solely as the pyranose form in water at 40 °C.¹ In the case of pyranose monosaccharides, the hemiacetal can adopt two distinct anomers defined by the orientation of the alcohol at C1 relative to the C-5 substituent (compounds **5-7**, Figure 1.3). When the substituents are on the same face of the ring, the hemiacetal is the α -anomer, and when the substituents are on opposite of the ring, the hemiacetal is the β -anomer (compounds **8-10**, Figure 1.3). In the case of glucose, mannose and galactose, this coincides with the axial and equatorial position of the alcohol, respectively.

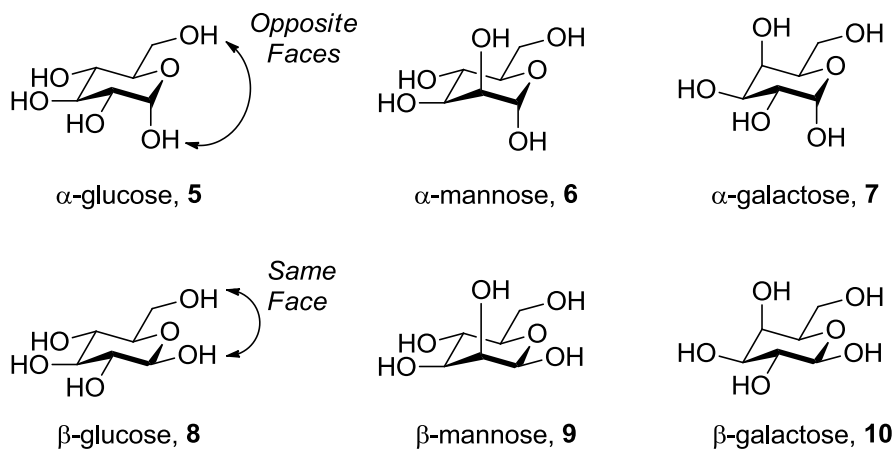


Figure 1.3: α - and β -Anomeric Forms of Common Pyranose Monosaccharides.

These cyclic hemiacetals benefit from anomeric stabilization. This is a non-bonding secondary orbital overlap between the lone-pair on the ethereal oxygen and the σ^* antibonding orbital of the C-X bond, where X is an electron-deficient atom such as oxygen, nitrogen, or sulfur (Figure 1.4).² Although populating antibonding orbitals weakens the C-X bond, the molecule is stabilized as a whole. The equatorial anomer has poor orbital overlap due to the equatorial orientation

² Carey, F. A.; Sundberg, R. J. In *Advanced Organic Chemistry, Part A*, 4th ed.; Kluwer Academic / Plenum Publishers: New York, 2000; pp 151-156.

and does not exhibit any anomeric stabilization, thus the anomeric effect favors the axial conformation in pyranose monosaccharides.³

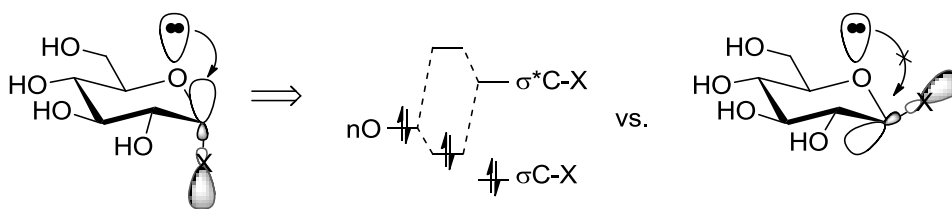


Figure 1.4: Anomeric Effect in Pyranose Monosaccharides.

The anomeric effect directly controls the reactivity of saccharides and can be used to control stereochemistry of substitution at the anomeric position. An example of this was reported by Lemieux and co-workers in 1975.⁴ The authors developed a halide ion-catalyzed glycosylation reaction for the selective synthesis of α -O-glycosides based on the thermodynamic stability of anomers. Adding bromide salts to a solution of glycosyl bromide **11** allows for the interconversion of the anomers to create an equilibrium between the α - and β -anomers (**11** and **12**, Figure 1.5).

³ a) Juaristi, E.; Cuevas, G., *Tetrahedron* **1992**, 48 (24), 5019-5087. b) Takahashi, O.; Yamasaki, K.; Kohno, Y.; Ohtaki, R.; Ueda, K.; Suezawa, H.; Umezawa, Y.; Nishio, M., *Carbohydr. Res.* **2007**, 342, 1202-1209.

⁴ Lemieux, R. U.; Hendricks, K. B.; Stick, R. V.; James, K., *J. Am. Chem. Soc.* **1975**, 97, 4056-4062.

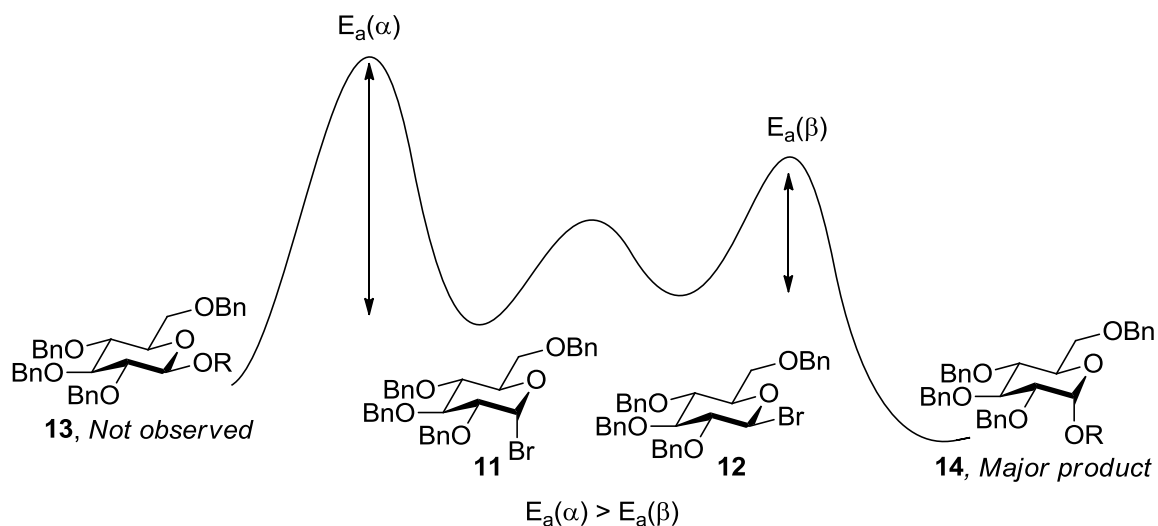


Figure 1.5: Energy Diagram for the Anomerization of Glucosyl Bromides.

Because the absence of the anomeric effect destabilizes the β -anomer, the activation energy for substitution is lower, making the β -anomer more reactive towards substitution. The reaction proceeds under Curtin-Hammett control, and a second S_N2 displacement of bromide by the nucleophile gives the net-retentive product (**14**) as the major isomer.⁵

Glycosides in Biology.

Biological macromolecules can be divided into four major classes: DNA, proteins, carbohydrates and lipids.^{1b} Carbohydrates are unique among these for two reasons: they often exhibit a high degree of branching, and carbohydrate monomers may be connected to each other through linkages. These attributes allow for highly complex carbohydrate structures, which control how carbohydrates and glycoconjugates to participate in a plethora of biological processes.⁶ Perhaps the

⁵ Carey, F. A.; Sundberg, R. J. In *Advanced Organic Chemistry, Part A*, 4th ed.; Kluwer Academic / Plenum Publishers: New York, 2000; pp 220-222.

⁶ a) Varki, A., *Glycobiology* **1993**, 3, 97-130. b) Struwe, W. B.; Cosgrave, E. F. J.; Byrne, J. C.; Saldova, R.; Rudd, P. M.; Owens, R.; Nettleship, J., Glycoproteomics in Health and Disease. In *Functional and Structural Proteomics of Glycoproteins*, Springer Netherlands: 2011; pp 1-38. c) Dwek, R. A., *Chem. Rev.* **1996**, 96, 683-720.

most important carbohydrate functions is as a source of energy for organisms, as monosaccharides are converted into energy in the form of adenosine triphosphate (ATP) through metabolism.⁷ Plants convert solar energy and CO₂ into carbohydrates through photosynthesis, and polysaccharides serve as a method to store these monosaccharides for later conversion to energy (i.e. ATP). It is through this conversion of monosaccharides into ATP that carbohydrates provide the necessary energy for the majority of complex living organisms, but the importance of carbohydrates extends far beyond this function.

Aside from their role in energy conversion and storage, the biological roles of carbohydrates can be classified into two broad categories.^{1^b} The first is to provide structure and modulate biological components. For example, all cells in nature are covered by a complex array of glycans, or complex polysaccharides, that serve as a physical protective barrier and define the shape of the cell. In the same fashion, the glycans on glycoproteins provide a physical shield to protect the underlying polypeptide from enzymatic degradation. These same glycans also ensure proper folding of the protein after synthesis in the endoplasmic reticulum (ER). Failure to fold properly due to incorrect glycosylation will prevent the protein from exiting the ER, which serves to regulate the formation of these glycoproteins.

The other major biological role of carbohydrates is to act as targets in specific recognition events.^{1^b} These recognition events can either be within the same organism (intrinsic) or between organisms (extrinsic). Receptors can recognize specific glycans in a variety of different types of interactions within an organism, which allows these receptors to control critical functions, ranging from the clearance of soluble blood-plasma glycoproteins to cell-cell interactions in the compaction of mouse embryos. Glycans also serve as ligands for the specific binding of pathogens, such as

⁷ Mathews, C. K.; van Holde, K. E.; Ahern, K. G., *Biochemisry*. 3rd Ed.; Addison Wesley Longman, Publishers, San Francisco, 2000; pp. 594-624.

bacteria, viruses and parasites, to host sites. These interactions can be highly selective, specific to the structure and modification of the host site.

The role of glycans in these recognition events suggests the potential of glycosides and glycoconjugates as therapeutics. For example, it is known that carbohydrates attached to a protein carrier can trigger an antibody response to protect an organism from infection.⁸ Furthermore, if a carbohydrate is able to mimic the antigens of a malignant tumor, it has the potential to act as a vaccine to prevent reoccurrence or metastasis of the cancer. Danishefsky has detailed progress toward a carbohydrate-based cancer vaccine, and other examples of carbohydrate-based cancer vaccines are in various stages of clinical trials.⁹ Additionally, several carbohydrate-based therapeutics are currently on the market for conditions such as epilepsy, gastric ulceration, and sepsis, and a carbohydrate-based vaccine against childhood meningitis is also approved for use.^{9,10} It is clear that carbohydrates are an emerging class of pharmaceuticals with the capability of treating a disparate group of conditions.

In general, glycosides, and thus glycoside-based therapeutics, suffer from significant problems under physiological conditions that can limit bioavailability. Glycosidase enzymes can cause glycan degradation through ionic cleavage of anomeric linkages, in particular *O*-linkages.¹¹ This serves to decrease the lifetime of the glycoside and consequently its efficacy. Significant effort has been devoted to the development of carbohydrate mimetics that have more desirable

⁸ a) Osborn, H. M. I.; Evans, P. G.; Gemmell, N.; Osborne, S. D., *J. Pharm. Pharmacol.* **2004**, *56*, 691-702. b) Kuberan, B.; Lindhardt, R. J., *Curr. Org. Chem.* **2000**, *4*, 653-677.

⁹ Danishefsky, S.; Allen, J. R., *Angew. Chem., Int. Ed.* **2000**, *39*, 836-863.

¹⁰ Doores, K. J.; Gambelin, D. P.; Davis, B. G., *Chem. Eur. J.* **2006**, *12*, 656-665.

¹¹ a) Sears, P.; Wong, C.-H., *Angew. Chem., Int. Ed.* **1999**, *38*, 2300-2324. b) Marcaurelle, L. A.; Bertozzi, C. R., *Chem. Eur. J.* **1999**, *5*, 1384-1390.

pharmacokinetic properties. Modifications of naturally occurring glycosides can alter the lifetime, bioavailability, binding affinity, and selectivity of the therapeutic.

C-Glycosides.

One approach to prevent the enzymatic or hydrolytic cleavage of *O*-glycosides is to synthesize the corresponding *C*-glycoside as a more stable isostere.¹¹ By replacing the anomeric carbon-oxygen bond with a carbon-carbon bond, the nature of the anomeric center has been changed in several significant ways. The carbon-carbon bond is no longer polarized, and the oxidation state of the anomeric center is reduced. These combine to prevent the formation of an oxonium intermediate at the anomeric position through acid-catalyzed or enzymatic activation. Furthermore, the σ^*_{C-C} orbital is a poor acceptor and does not allow for the anomeric non-bonding interaction (Figure 1.6). This significantly stabilizes the anomeric bond in *C*-glycosides, because these molecules do not exhibit the anomeric effect.

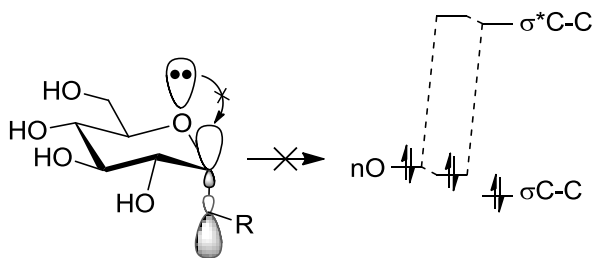


Figure 1.6: Absence of Anomeric Effect in *C*-Glycosides.

C-linked glycosides have been shown to resist enzymatic cleavage by glycosidase enzymes, which cleave anomeric C-O bonds in *O*-glycosides and carbohydrate dimers such as sucrose. The utility of these stabilized isosteres in pharmaceutical and biological research has been recognized for years.¹² Liu demonstrated this ability to inhibit α -glucosidase through the development of an enzyme

¹² a) Zou, W., *Curr. Top. Med. Chem.* **2005**, 5, 1363-1391. b) Lin, C. H.; Lin, H. C.; Yang, W. B., *Curr. Top. Med. Chem.* **2005**, 5, 1431-1457. c) Hultin, P. G., *Curr. Top. Med. Chem.* **2005**, 5, 1299-1331. d) Compain, P.;

transition-state inhibitor.¹³ Based on the key binding interactions in the α -glucosidase binding pocket, a nojirimycin-glucose dimer (**15**, Figure 1.7) was chosen as the inhibitor to both bind tightly to the enzyme and to resist hydrolysis once in the binding pocket. The molecule demonstrated an *in vitro* inhibition constant (K_i) of 2×10^{-6} M for the α -glucosidase enzyme, as compared to a K_m of 2×10^{-2} M for sucrose. When administered to mice in a dosage of 2.5 mg/kg along with sucrose or starch, postprandial hyperglycemia was significantly suppressed, indicating the sucrose or starch was not being hydrolyzed to glucose monomers. The authors attribute this to the ability of the developed C-glycoside to bind to the enzyme and resist degradation.

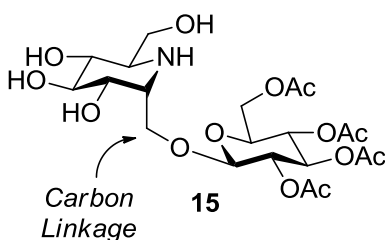


Figure 1.7: Nojirimycin-Glucose Dimer as Glucosidase Enzyme Inhibitor.

C-glycosides also demonstrate improved therapeutic properties due to the increased bioavailability of the drug. The α -galactosyl ceramide immunostimulant KRN7000 (**16**, Figure 1.8), has been extensively studied for its activity as a treatment for several types of cancers,¹⁴ malaria,¹⁵

Martin, O. R., *Bioorg. Med. Chem.* **2001**, 9, 3077-3092. e) Nicotra, F.; Driguez, H.; Thiem, J., Synthesis of C-glycosides of biological interest

In *Glycoscience Synthesis of Substrate Analogs and Mimetics*, Springer Berlin / Heidelberg: 1997; Vol. 187, pp 55-83.

¹³ Liu, P. S., *J. Org. Chem.* **1987**, 52, 4717-4721.

¹⁴ a) Kikuchi, A.; Nieda, M.; Schmidt, C.; Koezuka, Y.; Ishihara, S.; Ishikawa, Y.; Tadokoro, K.; Durrant, S.; Boyd, A.; Juji, T.; Nicol, A., *Br. J. Cancer* **2001**, 85, 741-746. b) Nakagawa, R.; Motoki, K.; Ueno, H.; Iijima, R.; Nakamura, H.; Kobayashi, E.; Shimosaka, A.; Koezuka, Y., *Cancer Res.* **1998**, 58, 1202-1207. c) Hayakawa, Y.; Rovero, S.; Forni, G.; Smyth, M. J., *Proc. Natl. Acad. Sci. U.S.A.* **2003**, 100, 9464-9469.

diabetes,¹⁶ and hepatitis B.¹⁷ Franck and co-workers were the first to synthesize the nearest C-analog of KRN7000 (**17**) and test its activity in a variety of assays.¹⁸

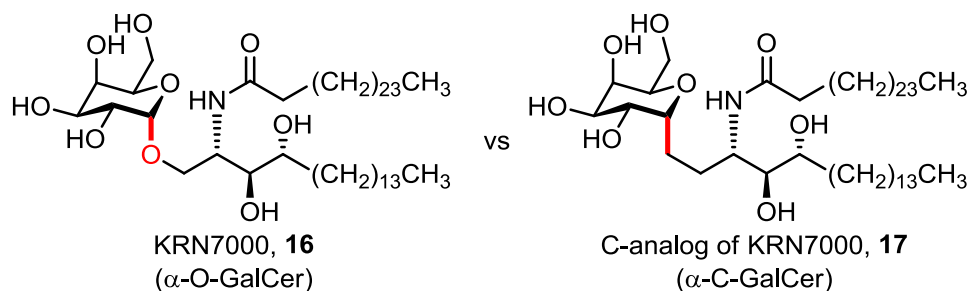


Figure 1.8: O- and C-Glycoside Analogs of KRN7000.

Mice were treated with KRN7000 and its C-analog and exposed to malaria. After an incubation interval, the mice livers were assayed for the sporozoite stage of the disease. While both KRN7000 and C-KRN7000 were effective at reducing sporozoite levels, the C-analog showed excellent suppression of the disease at 1-ng dosage, whereas KRN7000 required 1 μ g to achieve similar activity, a 1000-fold increase in protection for **17** over **16** (Figure 1.9).

The authors then carried out experiments to determine the length of activity of galactosyl ceramides **16** and **17**. The initial interval between dosing and malaria exposure was varied. The O-glycoside showed activity for only one day, whereas the C-glycoside continued to be effective for up to four days. The authors postulate this could be due to either the increased stability of the C-glycoside, which increases the bioavailability of the therapeutic, or different binding of the C-

¹⁵ Gonzalez-Aseguinolaza, G.; de Oliveira, C.; Tomaska, M.; Hong, S.; Bruna-Romero, O.; Nakayama, T.; Taniguchi, M.; Bendelac, A.; Van Kaer, L.; Koezuka, Y.; Tsuji, M., *Proc. Natl. Acad. Sci. U.S.A.* **2000**, 97, 8461-8466.

¹⁶ Hong, S.; Wilson, M. T.; Serizawa, I.; Wu, L.; Singh, N.; Naidenko, O. V.; Miura, T.; Haba, T.; Scherer, D. C.; Wei, J.; Kronenberg, M.; Koezuka, Y.; Van Kaer, L., *Nat. Med.* **2001**, 7, 1052-1056.

¹⁷ Kakimi, K.; Guidotti, L. G.; Koezuka, Y.; Chisari, F. V., *J. Exp. Med.* **2000**, 192, 921-930.

¹⁸ Yang, G.; Schmieg, J.; Tsuji, M.; Franck, R. W., *Angew. Chem., Int. Ed.* **2004**, 43, 3818-3822.

glycoside to the receptor to favor more effective signaling cascades. While the authors favor the latter proposal, it nevertheless clearly demonstrates the potential of *C*-glycoside analogs.

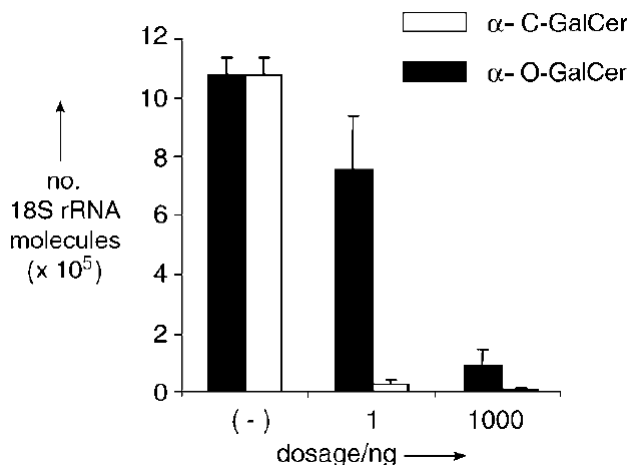


Figure 1.9: Presence of Sporozites based on Dosage of *O*- and *C*-linked KRN7000.

In another example, Nagy and co-workers attempt to prevent the attachment of the influenza virus to the surface of erythrocytes using sialic acids.¹⁹ It has been shown that polyvalent sialic acids can bind to the surface of these cells to prevent the binding of virus lectins, which in turn inhibits viral binding and plaque formation. However, neuraminidases present on the surface of the virus specifically target and hydrolyze *O*-glycosidic linkages, limiting the efficacy of *O*-sialic acid therapeutics. The authors synthesized a polymer containing *C*-sialic acid-bound monomers and were able to achieve 50% binding inhibition of the virus with only 0.2 μ M of 30 wt% sialic acid polymer and 50% reduction in plaque formation at 100 μ M (**18**, Figure 1.10). Most importantly, the authors were able to demonstrate that the polymers were resistant to hydrolysis by the neuraminidases on the surface of the virus.

¹⁹ Nagy, J. O.; Wang, P.; Gilbert, J. H.; Schaefer, M. E.; Hill, T. G.; Callstrom, M. R.; Bednarski, M. D., *J. Med. Chem.* **1992**, 35, 4501-4502.

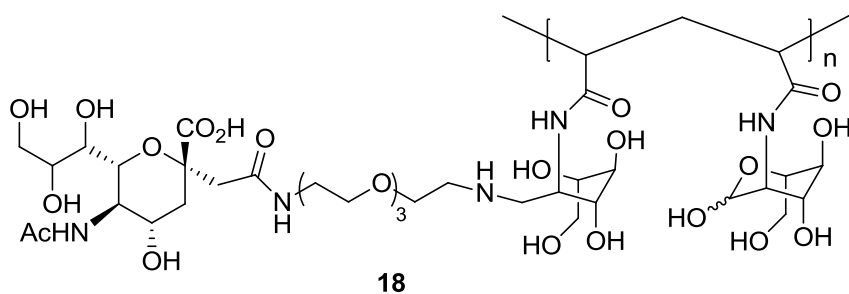


Figure 1.10: Polymer-based Sialic Acid C-Glycosides for Inhibition of Influenza Binding.

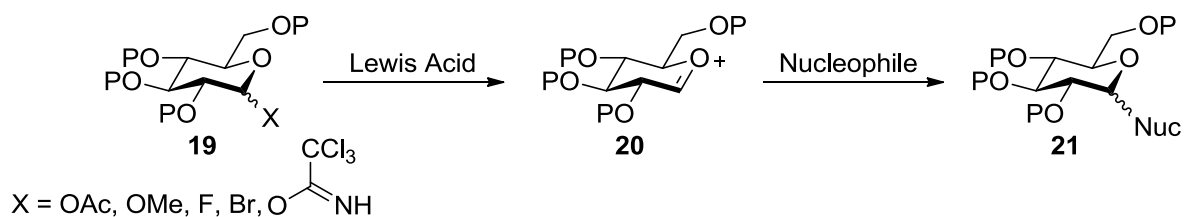
Methods of C-Glycoside Synthesis.

As these examples clearly show the potential of C-glycosides as stable isosteres of glycoconjugates, significant research has been devoted to the synthesis of these analogs.²⁰ Methods that create a new C-C anomeric bond in pyranose monosaccharides are the most direct method of synthesizing C-glycosyl analogs. These methods can generally be divided into four major classes of reactions determined by the reactivity of the anomeric carbon: electrophilic, nucleophilic, transition metal complexes, and radical.

Electrophilic reactions are a widely used glycosylation method for the synthesis of both C-glycosides and O-glycosides.^{20,21} In this approach, the saccharide serves as an electrophile which reacts with a carbon-based nucleophile to create a new carbon-carbon linkage. The substrate can be rendered electrophilic in several ways, the most common of which is activation of the anomeric substituent under Lewis acidic conditions to generate an oxocarbenium ion (**20**, Scheme 1.2). The nucleophile then attacks the C1 position to form the C-glycoside, and the resulting stereochemistry is primarily substrate controlled.

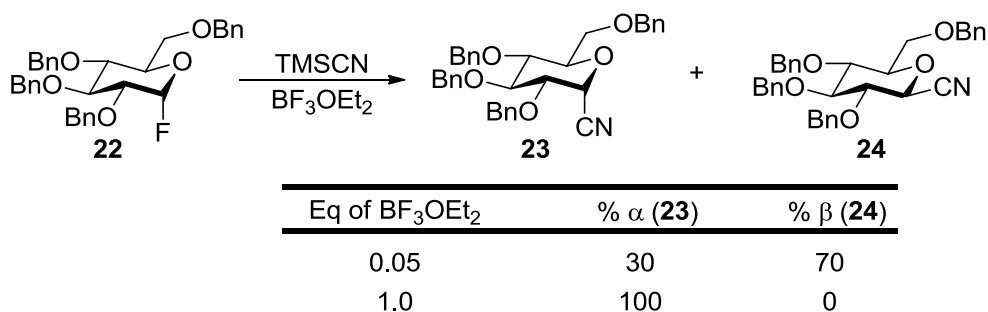
²⁰ a) Postema, M. H. D., *C-Glycoside Synthesis*. CRC Press, Inc.: Boca Raton, 1995. b) Levy, D. E.; Tang, C., *The Chemistry of C-Glycosides*. Pergamon: Tarrytown, 1995.

²¹ Toshima, K.; Tatsuta, K., *Chem. Rev.* **1993**, 93, 1503-1531.



Scheme 1.2: Electrophilic Activation of Saccharides for C-Glycoside Synthesis.

In these reactions, each component must be carefully selected in order to obtain high yields and selectivities. Acetates, ethers, halides, and trichloroacetimidates are examples of viable leaving groups, and typical Lewis acids include BF_3OEt_2 , TiCl_4 , TMSOTf , and SnCl_4 . This methodology has been successfully demonstrated with a range of nucleophiles, the simplest of which is cyanide. For example, reacting tetrabenzyl glucosyl fluoride (**22**, Scheme 1.3) in the presence of BF_3OEt_2 results in a mixture of anomers that is dependent on the Lewis acid concentration.²² While the substrate has a strong influence on the stereochemistry of the product, the reaction conditions can be tailored to override this natural selectivity, which is a common feature of electrophilic activation for C-glycoside synthesis.



Scheme 1.3: Stereoselectivity of Cyanide Addition to Glucosyl Fluorides Based on Conditions.

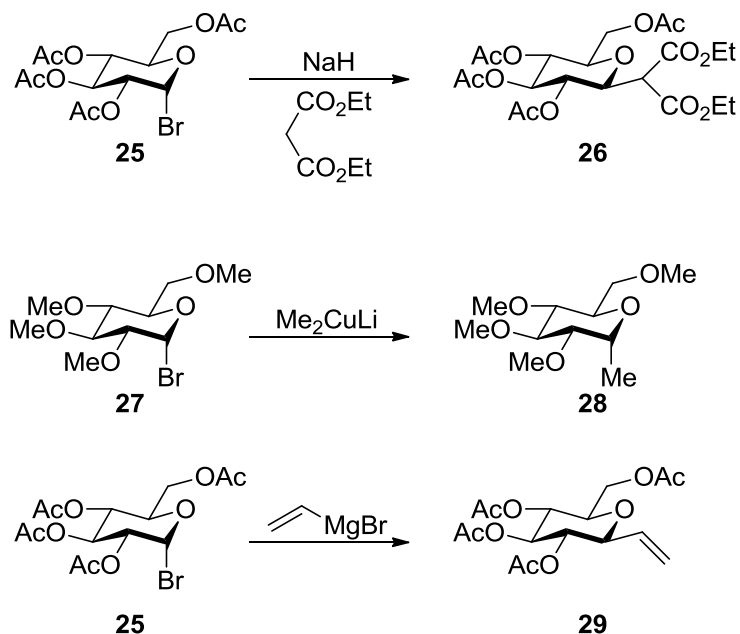
Alkylations with anionic carbon nucleophiles other than cyanide have been demonstrated with malonates,²³ organocuprates,²⁴ and Grignard reagents (Scheme 1.4).²⁵ In these reactions, the superior

²² Araki, Y.; Kobayashi, N.; Watanabe, K.; Ishido, Y., *J. Carbohydr. Chem.* **1985**, 4, 565-585.

²³ Hanessian, S.; Pernet, A. G., *Can. J. Chem.* **1974**, 52, 1266-1279.

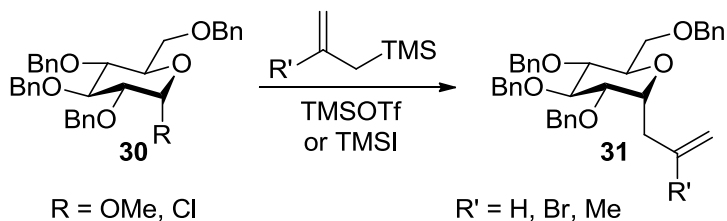
²⁴ Bihovsky, R.; Selick, C.; Giusti, I., *J. Org. Chem.* **1988**, 53, 4026-4031.

nucleophilicity of the carbanions allows these reactions to proceed in the absence of a Lewis acid promoter.



Scheme 1.4: Alkylation of Glycosyl Halides with Various Nucleophiles.

Allylations are possible with allyltrimethyl silanes but require a Lewis acid due to the poor nucleophilicity of allylsilanes (Scheme 1.5).²⁶ This method has been used to synthesize substituted allyl-C-glycosides, which are useful for further derivatization.

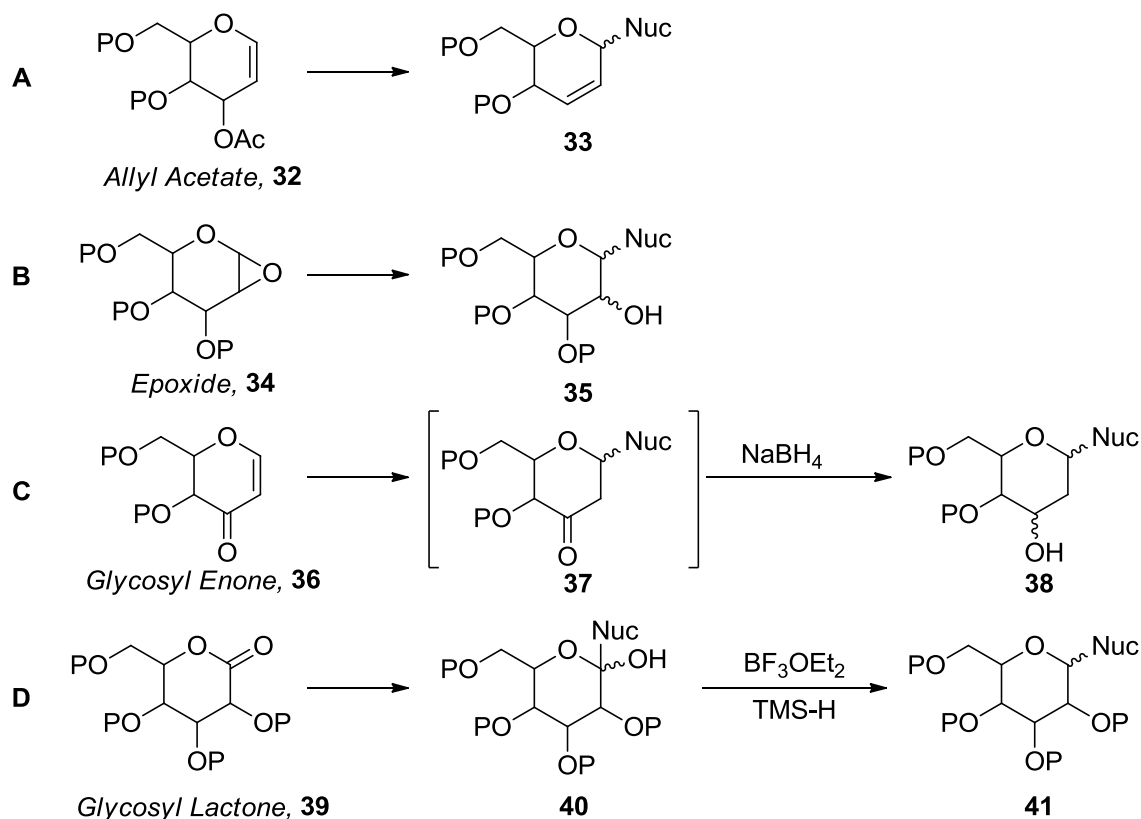


Scheme 1.5: Synthesis of C-Allyl Glycosides.

²⁵ Shulman, M. L.; Shiyan, S. D.; Khorlin, A. Y., *Carbohydr. Res.* **1974**, 33, 229-235.

²⁶ Hosomi, A.; Sakata, Y.; Sakurai, H., *Carbohydr. Res.* **1987**, 171, 223-232.

While less prevalent, other electron deficient saccharides serve as electrophilic substrates for substitution (Scheme 1.6).



Scheme 1.6: Examples of Electrophilic Substrates for C-Glycoside Synthesis.

Examples of these include sugar allyl acetates,²⁷ epoxides,²⁸ enones,²⁹ and lactones,³⁰ which utilize electron-withdrawing oxygen substituents to activate the substrate for nucleophilic attack. However, these substrates require further modification to arrive at a fully-substituted saccharide. For example,

²⁷ Herscovici, J.; Delatre, S.; Antonakis, K., *Tetrahedron Lett.* **1991**, 32, 1183-1186

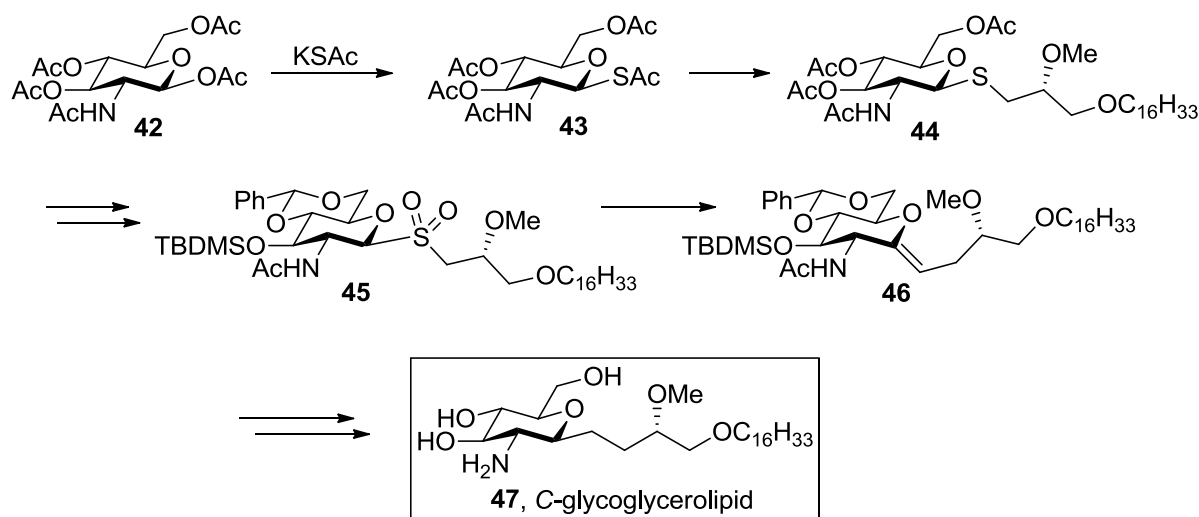
²⁸ Bellosta, V.; Czernecki, S., *J. Chem. Soc., Chem. Commun.* **1989**, 199-200.

²⁹ Goodwin, T. E.; Crowder, C. M.; White, R. B.; Swanson, J. S.; Evans, F. E.; Meyer, W. L., *J. Org. Chem.* **1983**, 48, 376-380.

³⁰ a) Kraus, G. A.; Molina, M. T., *J. Org. Chem.* **1988**, 53, 752-753. b) Czernecki, S.; Ville, G., *J. Org. Chem.* **1989**, 54, 610-612.

glycosyl lactones must be reduced in order to generate a *C*-glycoside without a hemiacetal (**41**), and glycosyl enones must be reduced to form 2-deoxy-*C*-glycosides (**38**).

Frank and co-workers have applied the basic concept of electrophilic activation for a different approach to *C*-glycoside synthesis.³¹ In this approach, potassium thioacetate was reacted with *N*-acetyl-D-acetylglucosamine to form the *S*-acetyl glycoside (**43**, Scheme 1.7). This intermediate was selectively cleaved and substituted with a glycerolipid backbone, which was then oxidized to the sulfone. Ramberg-Bäcklund rearrangement afforded the *Z*-isomer of the glycosyl alkene (**46**), which after hydrogenation and deprotection afforded the desired glycoglycerolipid (**47**).



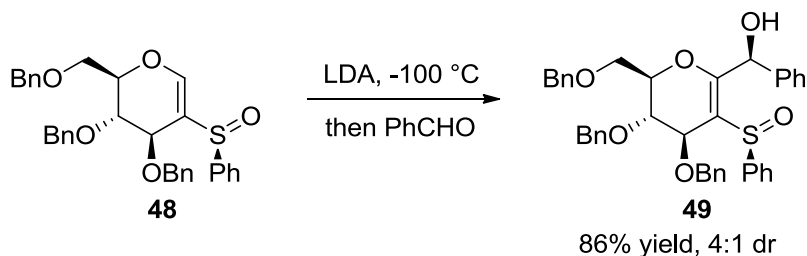
Scheme 1.7: Synthesis of *C*-linked Glycerolipid via Ramberg-Bäcklund Rearrangement.

Complimentary to electrophilic activations of saccharides are nucleophilic sugar substitutions, which are unavailable to other glycoside isosteres (e.g. *O*-, *N*-, *S*-glycosides).^{20,32} In this class of reactions, the sugar serves as the nucleophile, typically in the form of lithiated sugar

³¹Yang, G.; Franck, R. W.; Bittman, R.; Samadder, P.; Arthur, G., *Org. Lett.* **2001**, 3, 197-200.

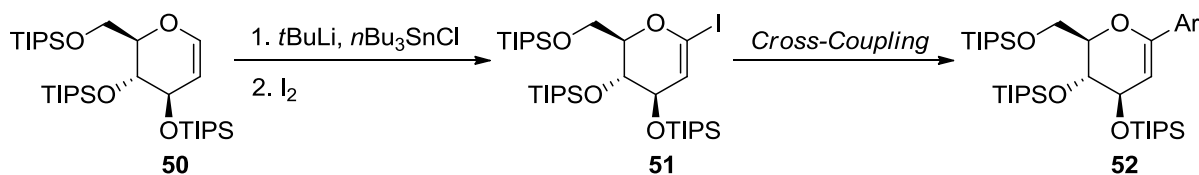
³² Beau, J.-M.; Gallagher, T.; Driguez, H.; Thiem, J., Nucleophilic *C*-glycosyl donors for *C*-glycoside synthesis. In *Glycoscience Synthesis of Substrate Analogs and Mimetics*, Springer Berlin / Heidelberg: 1997; Vol. 187, pp 1-54.

derivatives, to react with a carbon electrophile. These nucleophiles are synthesized through direct hydrogen- or metal-metal exchange, substituent reduction, or deprotonation. Hydrogen-metal exchange can be used for the lithiation of glycols with common lithiating reagents such as *t*BuLi or LDA. Aldehydes can serve as competent electrophiles (Scheme 1.8),³³ and Schmidt and Dietrich have reported the stereoselective synthesis of *C*-substituted glycosides in this manner.



Scheme 1.8: Nucleophilic Addition of Glycols into Aldehydes.

In a multistep approach to *C*-glycosides, lithium-glycols have also been utilized for the synthesis of *C*₁ iodoglycols (Scheme 1.9).³⁴ These electrophiles can be used as substrates for transition-metal catalyzed cross-coupling reactions, which will be discussed later.



Scheme 1.9: Synthesis of Iodo-Glycols for Cross-Coupling Reactions.

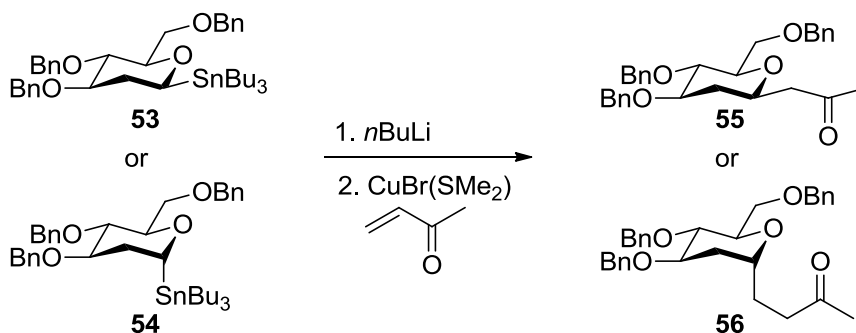
Direct metal-metal exchange has been used on fully-saturated carbohydrates in nucleophilic glycosidations.³⁵ In these reactions, trialkylstannyl glycosides are again reacted with common lithiating reagents to generate the alkyl-lithium glycoside nucleophile. Competent electrophiles for

³³ Schmidt, R. R.; Dietrich, H., *Angew. Chem., Int. Ed. Engl.* **1991**, 30, 1328-1329.

³⁴ Friesen, R. W.; Loo, R. W., *J. Org. Chem.* **1991**, 56, 4821-4823.

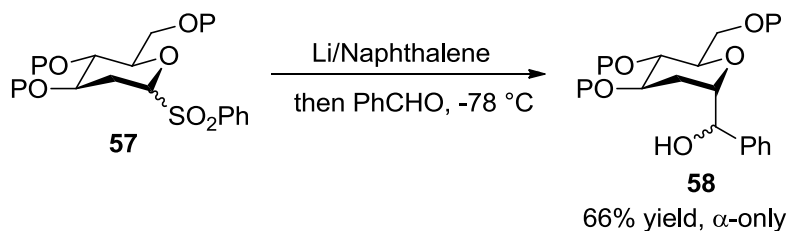
³⁵ Hutchinson, D. K.; Fuchs, P. L., *J. Am. Chem. Soc.* **1987**, 109, 4930-4939.

these reactions include enones, epoxides, and allyl halides (Scheme 1.10). Importantly, the stereochemistry of the starting material is retained in the product through a stereospecific lithium-metal exchange; thus, β -stannyl glycosides (**53**) provide the β -C-glycosides (**55**).



Scheme 1.10: Stereospecific Addition of Lithium-Saccharides via Direct Metal-Metal Exchange.

Reduction of glycosyl halides with lithium-naphthalide provides a complimentary mechanism for preparation of alkyl lithium glycosides.³⁶ However, these reactions are stereoselective for α -C-glycosides via the interconversion of the lithium-glycoside anomers, which favors the more stable axial carbanion. For example, exposure of a mixture of α - and β -pyranosyl phenylsulfones to lithium-naphthalide and subsequent reaction with aldehydes yields only α -products (Scheme 1.11).

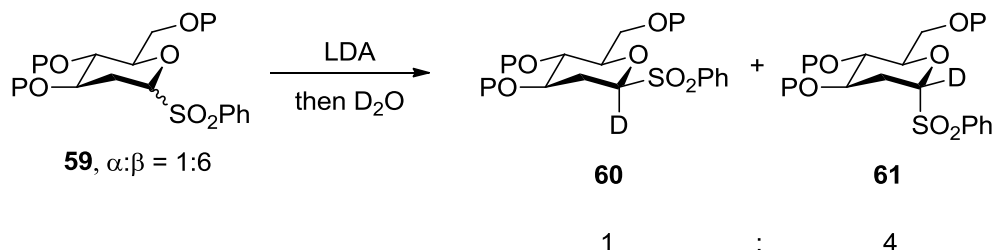


Scheme 1.11: Stereoselective Addition of Lithium-Glycosides into Aldehydes via Reduction.

Glycosyl carbanions stabilized through the use of electron-withdrawing groups provide another alternative to lithium-naphthalide reductions.³⁶ In this case, the presence of a sulfone or ester in the anomeric position allows for deprotonation and subsequent reactivity to form β -C-glycosides.

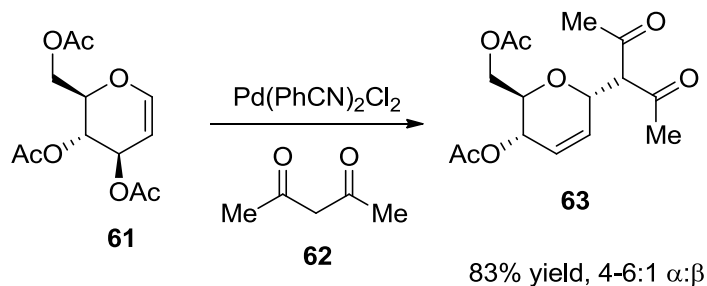
³⁶ Beau, J.-M.; Sinaÿ, P., *Tetrahedron Lett.* **1985**, 26, 6185-6188.

Exposure of a mixture of phenylsulfone glycoside anomers (**59**) to LDA or *n*BuLi followed by D₂O quenching results in a 4:1 β:α mixture anomers (**60** and **61**, Scheme 1.12). This concept has been applied to the stereoselective synthesis of *C*-disaccharides.³⁷



Scheme 1.12: Deprotonation of Sulfonfyl Glycosides and Stereoselective Protonation.

In general, electrophilic and nucleophilic activation of saccharides provides *C*-glycosides with reasonable stereocontrol but often require strong acidic or basic conditions. This limits the functionality on both the carbohydrate backbone as well as the aglycone, especially when attempting asymmetric syntheses on epimerizable substrates. Transition-metal catalysis has been applied to *C*-glycoside synthesis in an attempt to overcome the inherent limitations of these acid or base sensitive substrates.²⁰ The simplest metal-catalyzed examples utilize acetate-protected glycals (**61**) in the presence of a palladium catalyst in order to generate a palladium-allyl species, which then reacts with a nucleophile (e.g. malonates, 1,3-diketones, Scheme 1.13).³⁸

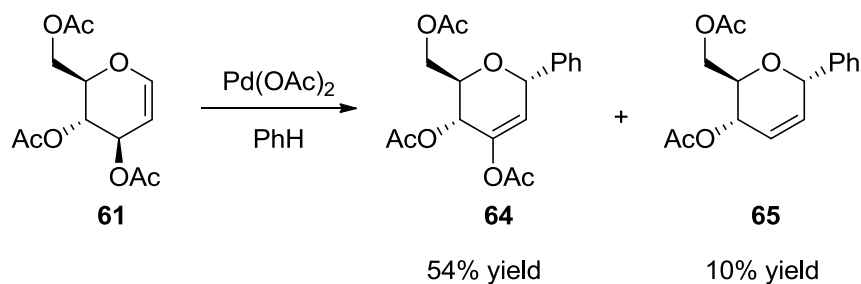


Scheme 1.13: Addition of 1,3-Diketones into Ally-Palladium Complex.

³⁷ Beau, J.-M.; Sinaÿ, P., *Tetrahedron Lett.* **1985**, 26, 6189-6192.

³⁸ Yougai, S.; Miwa, T., *J. Chem. Soc., Chem. Commun.* **1983**, 68-69.

While this approach is considered transition-metal catalyzed, it is limited in scope by the nucleophile and loses stereochemical information at C3. Transition-metal catalyzed cross-coupling reactions are an effective method for forming new carbon-carbon bonds.³⁹ Through prefunctionalized positions, a new anomeric bond can be formed with a wide variety of substrates. For example, acetate-protected glycals can undergo Heck-type coupling with various electrophiles to generate C-glycosides (Scheme 1.14).⁴⁰



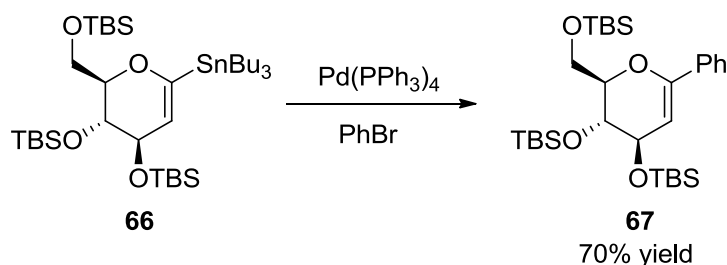
Scheme 1.14: Palladium-Catalyzed Heck-type Coupling for Aryl-C-Glycoside Synthesis.

Loss of stereochemistry on the saccharide occurs due to β -hydride elimination during the catalytic cycle, and while stereoselective hydrogenation can restore the stereocenter, this situation is not ideal. To circumvent this problem, Stille couplings with anomeric stannanes have been developed (Scheme 1.15).⁴¹ In these examples, the saccharide serves as the transmetallating reagent in a polarity-reversed cross-coupling.

³⁹ Hartwig, J. F., *Organotransition Metal Chemistry: From Bonding to Catalysis*. University Science Books: Sausalito. 2010; pp. 877-965.

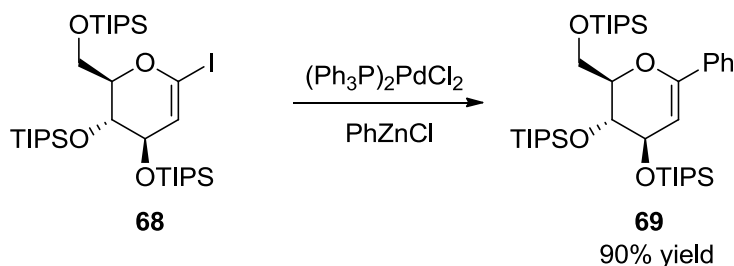
⁴⁰ Czernecki, S.; Dechavanne, V., *Can. J. Chem.* **1983**, 61, 533-540.

⁴¹ Friesen, R. W.; Sturino, C. F., *J. Org. Chem.* **1990**, 55, 2572-2574.



Scheme 1.15: Palladium-Catalyzed Stille Reaction of Stannyl Glycals.

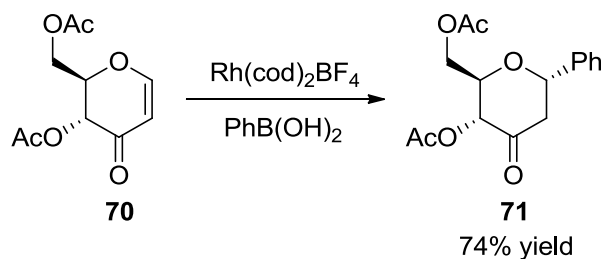
Vinyl halides can also serve as electrophiles in the presence of transmetallating reagents. This gives greater flexibility, as these substrates are generally easier to synthesize and a wider range of transmetallating reagents can be employed. For example, Friesen and co-workers have demonstrated a high-yielding palladium-catalyzed Negishi cross-coupling with glycosyl vinyl iodides and arylzinc halides (Scheme 1.16).³⁴



Scheme 1.16: Negishi Cross-Coupling of Iodo-Glycals.

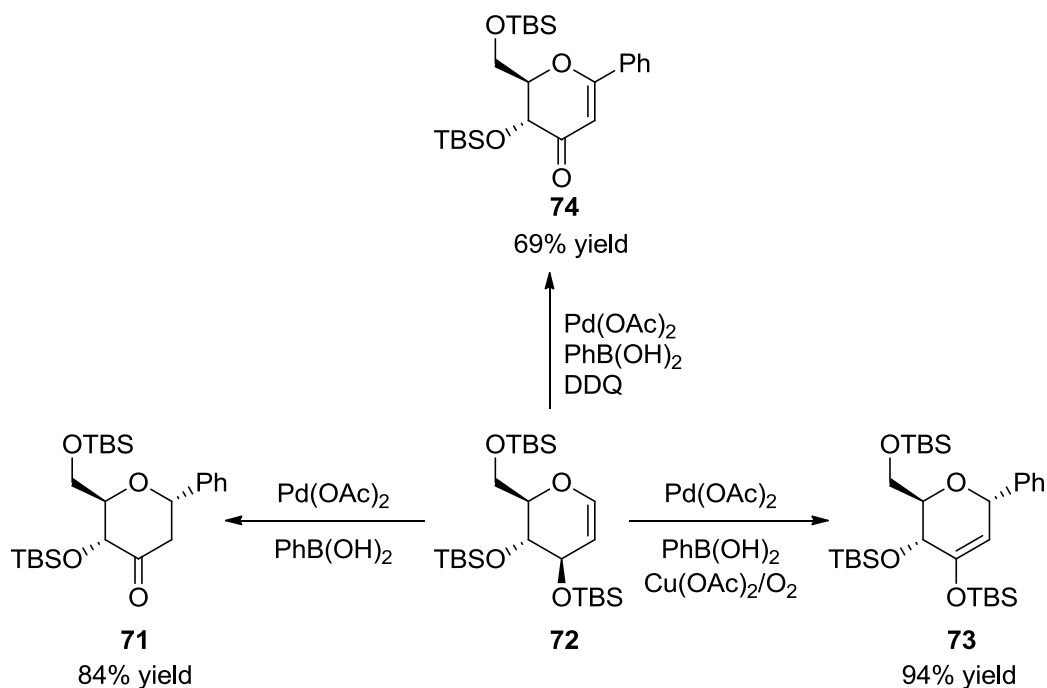
While high-yielding, these reactions with vinyl halides do not directly create a new anomeric stereocenter. In this regard, several stereoselective cross-coupling reactions of glycols have been reported. Maddaford and co-workers have described a rhodium-catalyzed arylation of 3-oxo-glycals that gives exclusive α -selectivity (Scheme 1.17).⁴²

⁴² Ramnauth, J.; Poulin, O.; Bratovanov, S. S.; Rakhit, S.; Maddaford, S. P., *Org. Lett.* **2001**, 3, 2571-2573.



Scheme 1.17: Stereoselective Rhodium-Catalyzed α -Arylation of Glycosyl Enones.

Ye and co-workers have shown the palladium-catalyzed arylation of trisilyl-glycals produces different products based on the oxidant in the reaction (Scheme 1.18).⁴³ In this manner, the authors are able to synthesize highly functionalized aryl-*C*-glycosides both with and without anomeric stereocenters.

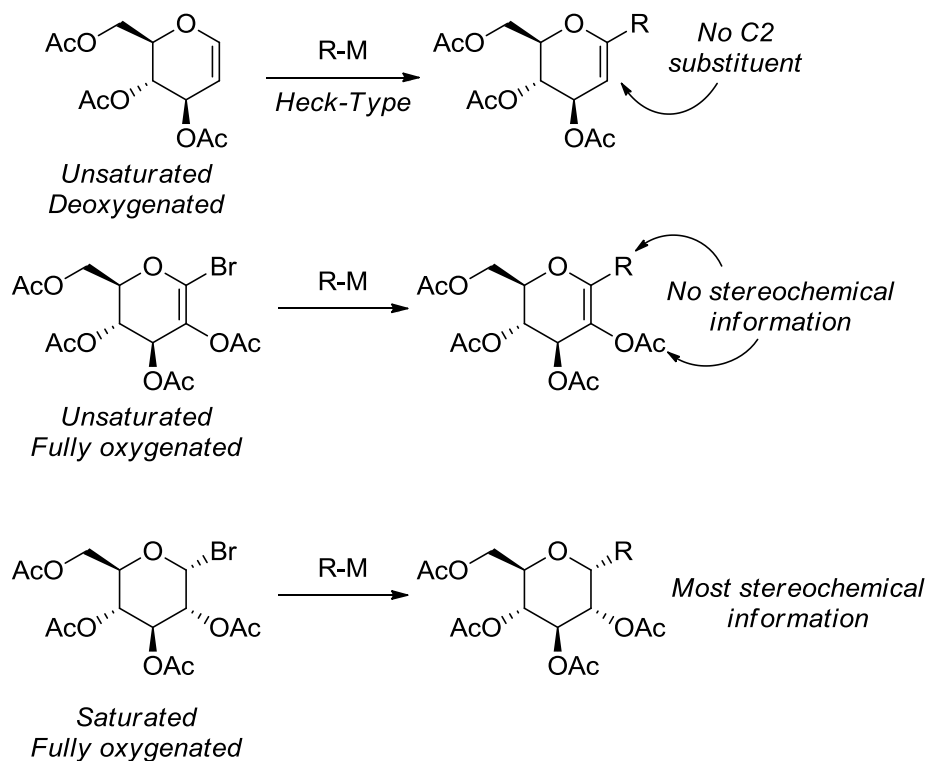


Scheme 1.18: Divergent Synthesis of Aryl-*C*-Glycosides Based on Oxidant.

As the stereochemistry of the carbohydrate backbone is a key to the behavior of glycosides in recognition events, it is imperative for future applications that methodologies for *C*-glycoside synthesis are tolerant of fully-oxygenated, saturated saccharide substrates. Many of the previously

⁴³ Xiong, D.-C.; Zhang, L.-H.; Ye, X.-S., *Org. Lett.* **2009**, *11*, 1709-1712.

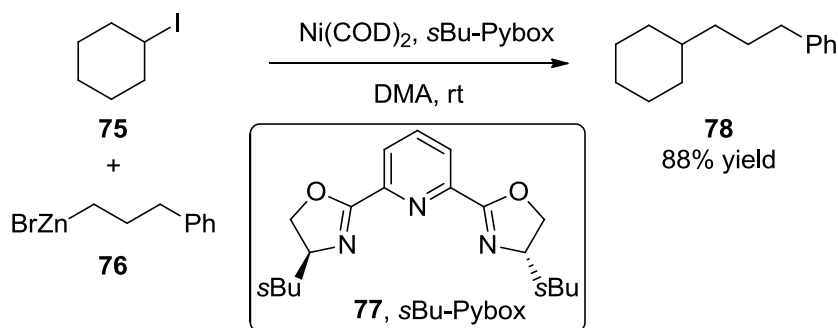
discussed methods require glycals or other unsaturated bonds on the saccharide to achieve reactivity, which then require further derivatization to achieve a fully-oxygenated glycoside. However, analogous cross-couplings with fully-saturated substrates would require an sp^3 -hybridized electrophile (Scheme 1.19), which can lose stereochemistry via β -hydride or β -acetoxy elimination after forming a metal-glycosyl intermediate.³⁹



Scheme 1.19: Saturated, Unsaturated, and Fully Oxygenated Glycosyl Electrophiles.

Fu and co-workers have reported their efforts to mitigate β -hydride elimination in sp^3 alkyl halides (Scheme 1.20).⁴⁴ They have found the use of Pybox pincer ligands sufficiently suppress β -hydride elimination. This knowledge was then applied to the Negishi cross-coupling of alkyl halides with aryl- and alkylzinc reagents.

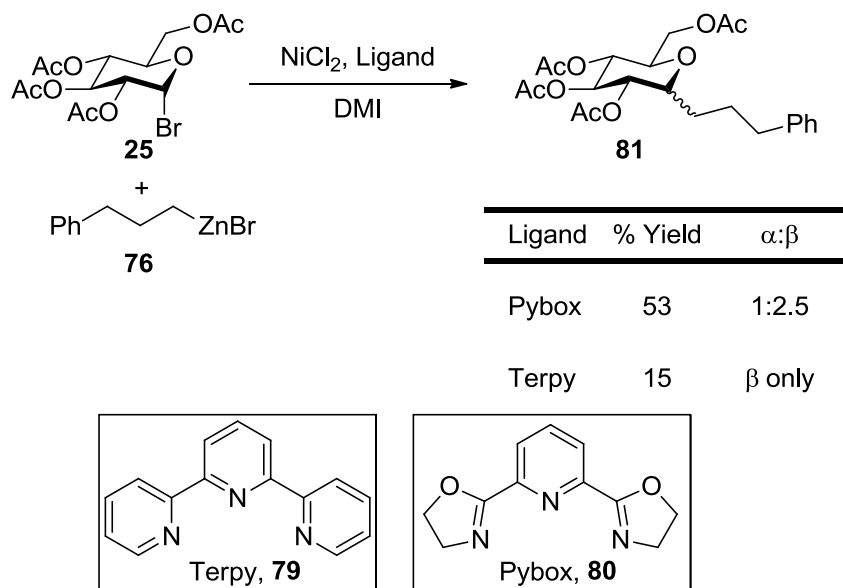
⁴⁴ For selected examples, see: a) Zhou, J.; Fu, G. C., *J. Am. Chem. Soc.* **2003**, *125*, 12527-12530. b) Zhou, J.; Fu, G. C., *J. Am. Chem. Soc.* **2003**, *125*, 14726-14727. c) Zhou, J. S.; Fu, G. C., *J. Am. Chem. Soc.* **2004**, *126*, 1340. d) Fischer, C.; Fu, G. C., *J. Am. Chem. Soc.* **2005**, *127*, 4594-4595.



Scheme 1.20: Nickel-Catalyzed Negishi Cross-Coupling of sp^3 -Hybridized Electrophiles.

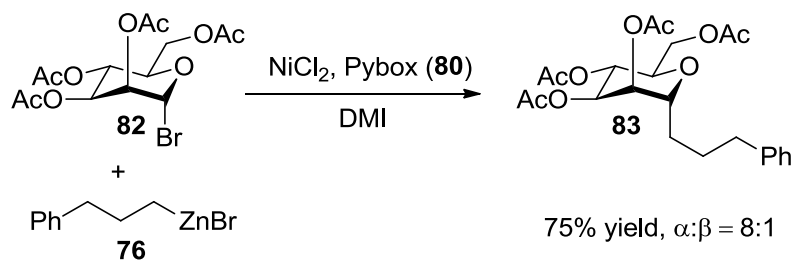
The concept developed by Fu and co-workers served as an inspiration for the seminal work of Gagné and Gong, who have reported a nickel-catalyzed Negishi cross-coupling of alkyl- and arylzinc halides with fully-oxygenated glycosyl halides for the synthesis of *C*-glycosides.⁴⁵ In these reactions, a protected glycosyl bromide is reacted in the presence of a nickel catalyst, a Pybox or Terpy ligand, and excess transmetallating zinc reagent to afford the corresponding *C*-glycoside. These studies focused on the anomeric stereoselectivity of the product based on both catalyst complex and substrate. Glucose-based substrates have exhibited an inherent preference for β -selectivity with alkylzinc reagents. This preference was further reinforced by utilizing Terpy as the pincer ligand although in diminished yields (Scheme 1.21).

⁴⁵ a) Gong, H.; Sinisi, R.; Gagné, M. R., *J. Am. Chem. Soc.* **2007**, *129*, 1908-1909. b) Gong, H.; Gagné, M. R., *J. Am. Chem. Soc.* **2008**, *130*, 12177-12183.



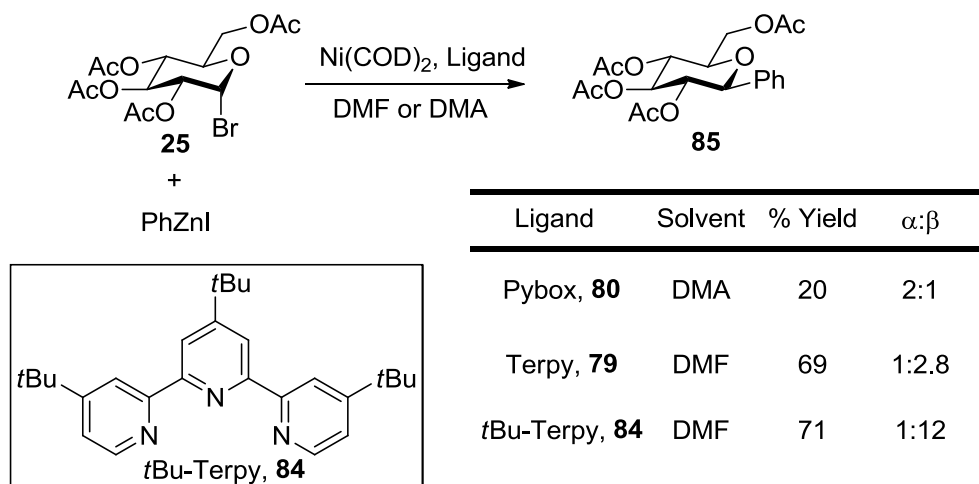
Scheme 1.21: Negishi Cross-Coupling of Glucosyl Bromides and Alkylzinc Reagents.

Conversely, mannosyl bromides exhibited exclusive α -selectivity, yielding alkyl-*C*-mannosides in high yields and selectivities (Scheme 1.22).



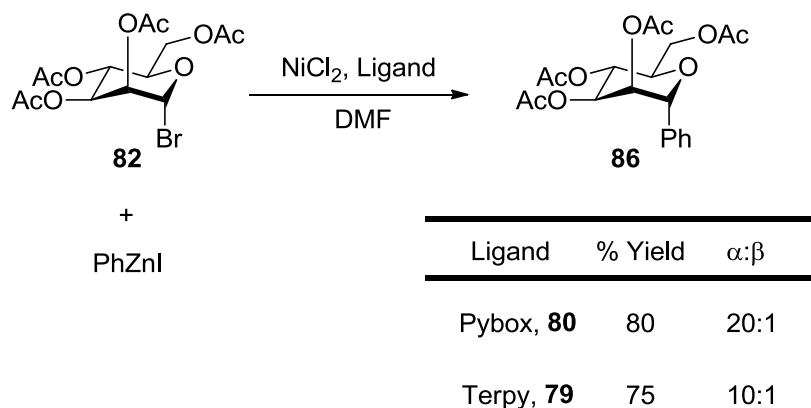
Scheme 1.22: Negishi Cross-Coupling of Mannosyl Bromides and Alkylzinc Reagents.

Arylzinc reagents provided similar results but required a separate optimization. Glucosyl bromides exhibited a slight preference for α -*C*-glucosides with Pybox, whereas Terpy reversed the selectivity. Increasing the steric bulk of the Terpy ligands served to further favor the β -products (Scheme 1.23).



Scheme 1.23: Selectivity of Negishi Cross-Coupling with Glucosyl Bromides and Arylzinc.

As seen with alkylations, mannose substrates favored the α -products with both classes of ligands, with Pybox resulting in higher α -selectivities (Scheme 1.23).



Scheme 1.24: Selectivity of Negishi Cross-Coupling with Mannosyl Bromides and Arylzincs.

From these results, it was concluded that the nickel-catalyzed Negishi cross-coupling reactions were both catalyst- and substrate-controlled. Glucose arylations and alkylations were inherently β -selective, and mannose substrates were α -selective. Pybox ligands favored the formation of α -products, whereas Terpy ligands favored β -products. However, both classes of ligands were insufficient to overcome the influence of the substrate and generally served to reinforce inherent selectivities. These observations are summarized in Figure 1.11.^{45b}

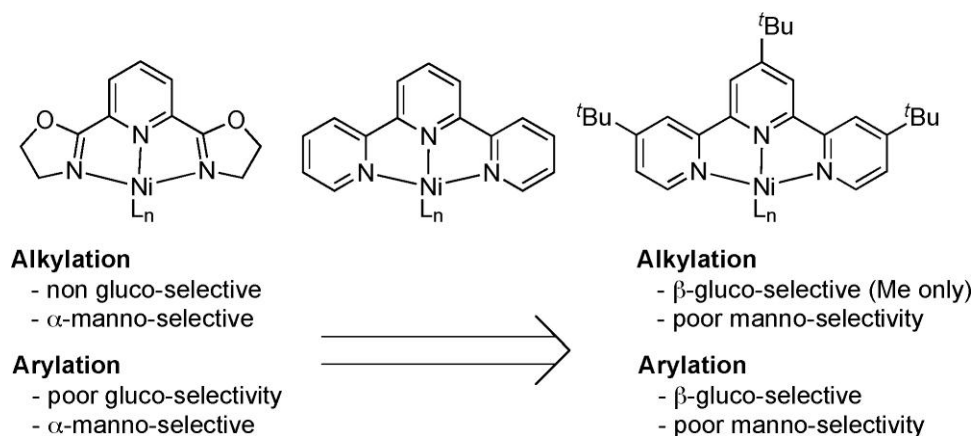


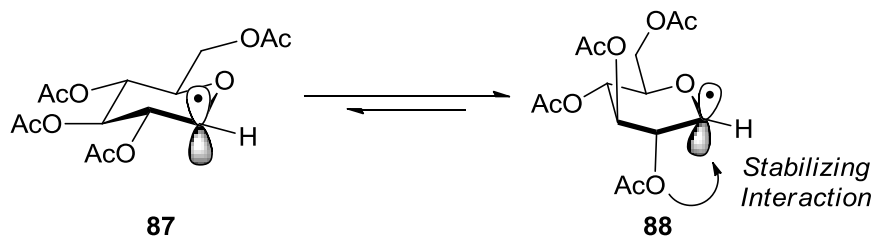
Figure 1.11: Catalyst- and Substrate-Control in Negishi Cross-Couplings of Glycosyl Halides.

Radical C-Glycoside Synthesis.

Each of the previously discussed methods of C-glycosidation has involved ionic mechanisms. Non-ionic, or radical, pathways represent another approach to the formation of C-glycosides.²⁰ As opposed to ionic pathways, radical mechanisms have a high functional group tolerance and are highly diastereoselective. Anomeric radicals tend to favor α -substitution, providing exclusive substrate control in C-glycosidations, differing from previously discussed protocols. Giese and co-workers have reported that a tetraacetyl glucosyl radical adopts a boat conformation that orients the C2 and C3 substituents axially (Scheme 1.25).⁴⁶ This then provides additional stabilization of the anomeric radical through a non-bonding interaction of the singly-occupied orbital of the radical and the σ^* of the C-OAc bond at C2.

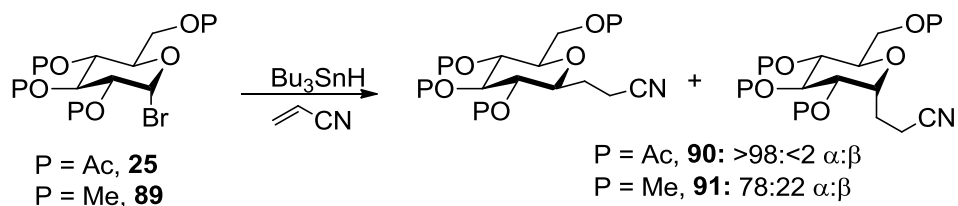
⁴⁶ a) Dupuis, J.; Giese, B.; Rüegge, D.; Fishcer, H.; Korth, H. G.; Sustmann, R., *Angew. Chem., Int. Ed. Engl.*

1984, 23, 896-898. b) Korth, H. G.; Sustmann, R.; Gröninger, K. S.; Witzel, T.; Giese, B., *J. Chem. Soc., Perkin Trans. 2* **1986**, 1461-1464.



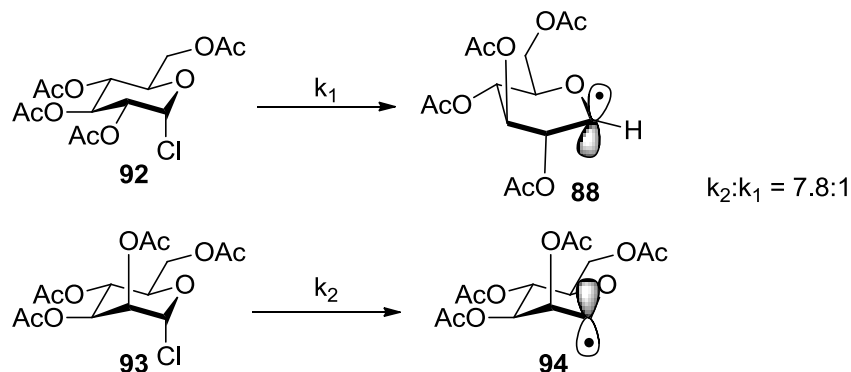
Scheme 1.25: Orientation of Glucosyl Radicals.

The SOMO/LUMO interaction is further enhanced by the increased electron density at the radical center as a result of anomeric donation from the lone-pair on the ethereal oxygen. The boat conformation then favors axial substitution to provide the α -products (Scheme 1.26). By contrast, methyl-protected glucosyl bromides give lower α -selectivities. The authors suggest this is due to the poorer electron-withdrawing ability of the methyl ethers as compared to the acetates, which disfavors the boat conformation.



Scheme 1.26: Tin-Mediated of Glycosyl Halides into Alkenes.

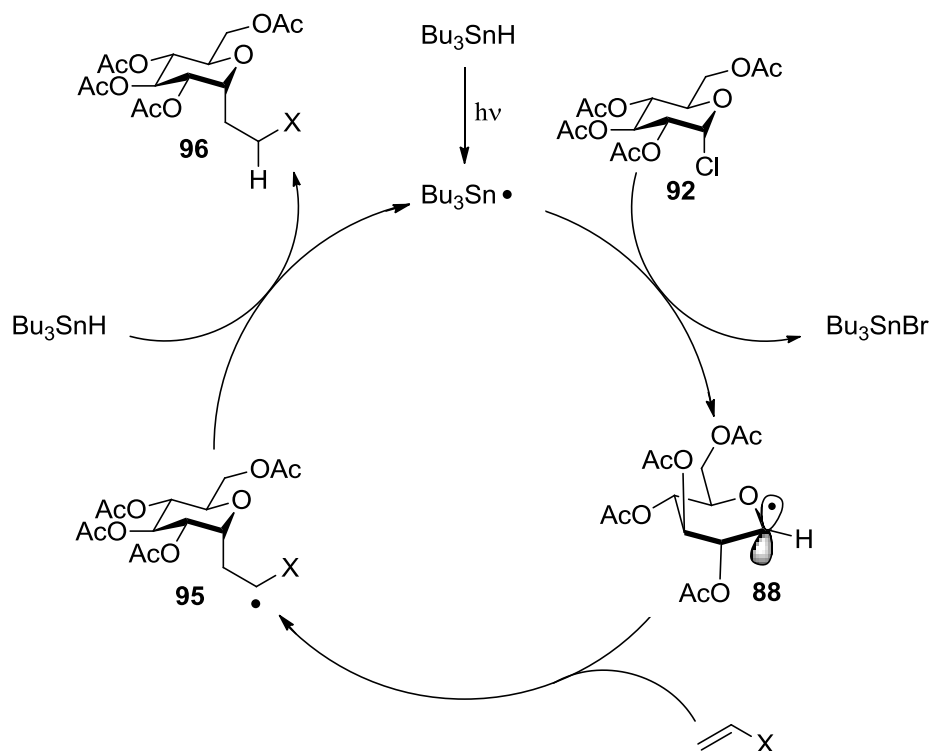
Further evidence for the role of axially-oriented acetates is provided by tetraacetate mannosyl chloride (**93**, Scheme 1.27), which adopts a chair conformation and reacts 7.8 times more rapidly toward chloride abstraction than the corresponding glucosyl chloride (**92**).^{46a}



Scheme 1.27: Rate of Glycosyl Radical Generation Based on Orientation of C2 Substituent.

Giese and co-workers have used this knowledge to develop a general method for C-glycoside synthesis from glycosyl halides and electron-deficient alkenes.⁴⁷ In these reactions, tributyltin hydride is photolyzed by UV light to generate a tin-radical, which abstracts bromine from the glycoside (Scheme 1.28). The resulting glycosyl radical then adds into the alkene, generating a new alkyl radical. Hydrogen abstraction from an additional equivalent of tin hydride affords the product and another tin radical, which propagates the radical chain.

⁴⁷ a) Giese, B.; Dupuis, J., *Angew. Chem., Int. Ed. Engl.* **1983**, 22, 622-623. b) Giese, B.; González-Gómez, J. A.; Witzel, T., *Angew. Chem., Int. Ed.* **1984**, 23, 69-70. c) Giese, B.; Witzel, T., *Angew. Chem., Int. Ed.* **1986**, 25, 450-451. d) Giese, B., *Angew. Chem., Int. Ed.* **1989**, 28, 969-980.

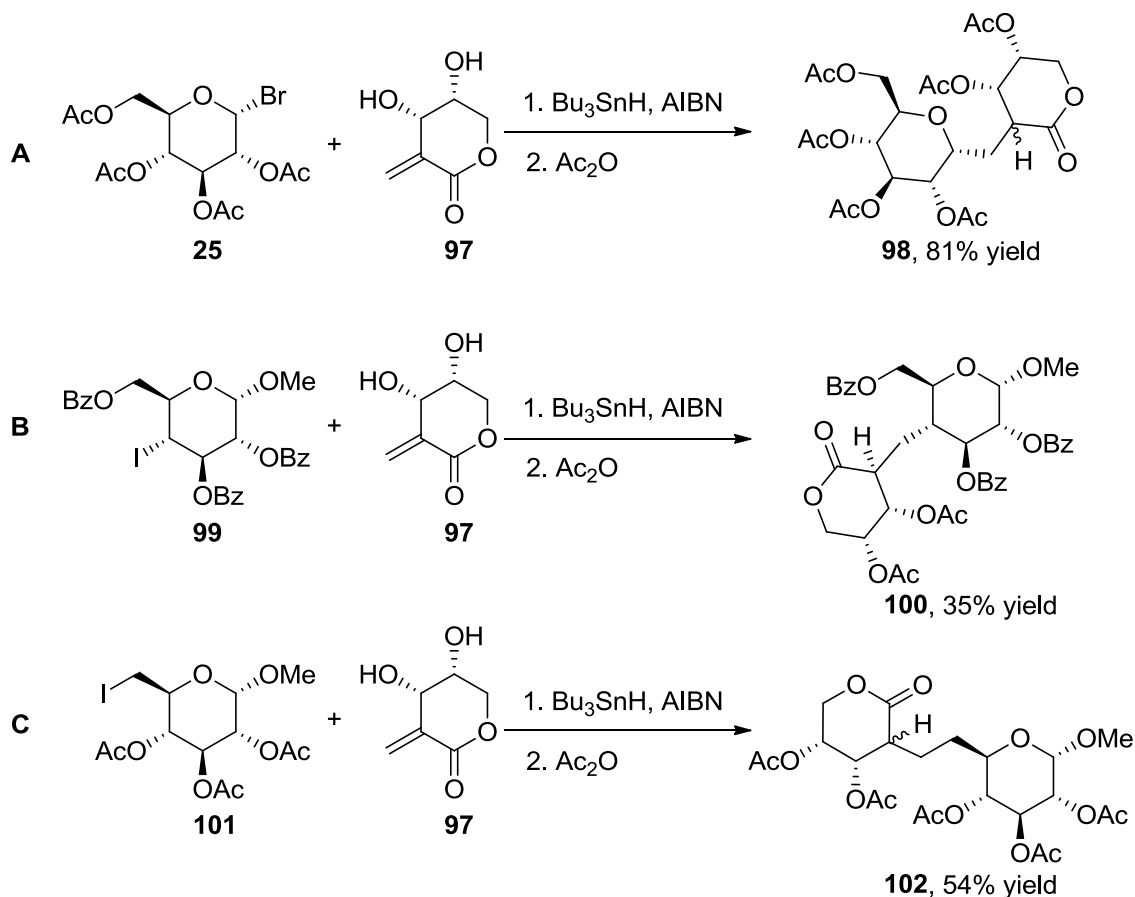


Scheme 1.28: Mechanism of Tin-Catalyzed Radical Addition into Alkenes.

This radical method is general for non-saccharide alkyl substrates; cyclohexyl bromide and non-anomeric sugar radicals both react well under these conditions.^{47b} Giese and co-workers have applied this methodology to the synthesis of C_{1-4} -disaccharides, a common linkage in naturally occurring glycosides (Scheme 1.29).^{47c} By varying the location of the halogen, the authors were able to affect the regio- and stereoselectivity of the addition into a carbohydrate-derived alkene.

In general, a radical approach offers several advantages over other methods of C -glycosidation. Since the reactions proceed through a non-ionic pathway, radical reactions offer increased functional group tolerance. This tolerance allows for the inclusion of epimerizable stereocenters and other reactive moieties into the aglycones to provide further flexibility in the synthesis of C -glycosides. Anomeric radicals also provide high α -selectivity regardless of the reaction conditions, which is not the case for other methods of glycoside activation. While addition of electron-rich anomeric radicals into electron-rich alkenes is kinetically disfavored, this provides a

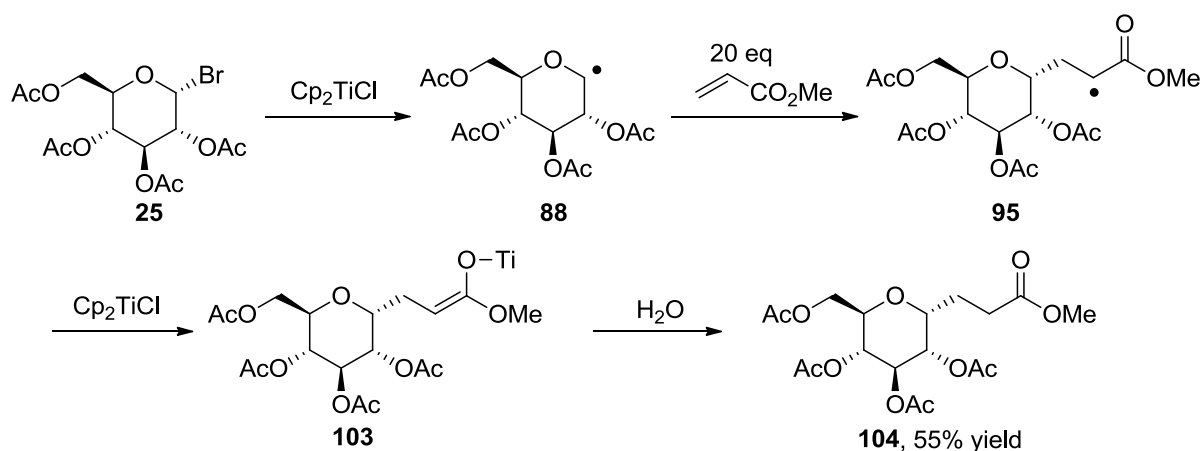
certain degree of chemoselectivity to the radical reactions. Since only electron-deficient alkenes can be expected to react, electron-rich alkenes can be incorporated into the aglycone for later derivatization.



Scheme 1.29: Examples of Tin-Catalyzed Radical Generation for the Synthesis of C-Disaccharides.

These advantages help explain the popularity of radical-mediated methods of C-glycosidation. However, tin-mediated radical methods exhibit several disadvantages. In general, a large excess (6-20 eq) of alkene is necessary for an effective reaction, which is wasteful and unsuitable for more precious alkenes. The use of toxic tin reagents presents a significant health hazard and technical challenge, as tin byproducts are often difficult to remove from crude reaction mixtures. Additionally, these reactions require the use of harsh photolysis conditions or high temperatures to initiate the reactions.

Alternative, tin-free radical C-glycosidations have been developed to avoid some of the disadvantages associated with the Giese protocol. Spencer and Schwartz report the use of titanium(III) reagents for the reaction of glycosyl bromides with electron-deficient alkenes (Scheme 1.30).⁴⁸ In this case, titanocene(III) chloride generates the glycosyl halide, which undergoes radical conjugate addition to form α -radical **95**. A second equivalent of titanocene(III) chloride reduces **95** to a titanium-enolate (**103**), which is then protonated upon workup to afford the desired product (**104**).

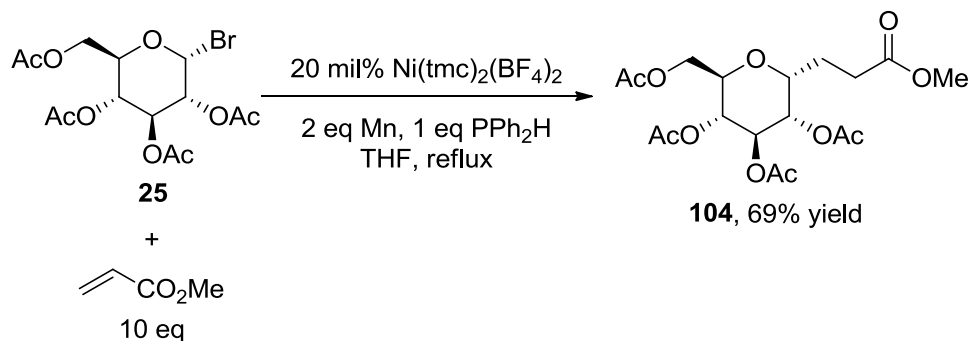


Scheme 1.30: Generation of Glycosyl Radicals by Titanocene(III) Chloride.

A similar methodology was reported by Marsden and co-workers, whereby glycosyl radicals were generated by $\text{Ni}(\text{tmc})_2(\text{BF}_4)_2$ in the presence of a Mn^0 reductant (Scheme 1.31).⁴⁹ The methodology provides the C-glycosides in modest yields as a single anomer without the use of toxic tin reagents. A phosphine reductant is required in this reaction in order to terminate the α -radical.

⁴⁸ a) Spencer, R. P.; Schwartz, J., *J. Org. Chem.* **1997**, 62, 4204-4205. b) Spencer, R. P.; Schwartz, J., *Tetrahedron* **2000**, 54, 2103-2112.

⁴⁹ Readman, S. K.; Marsden, S. P.; Hodgson, A., *Synlett* **2000**, 1628-1630.



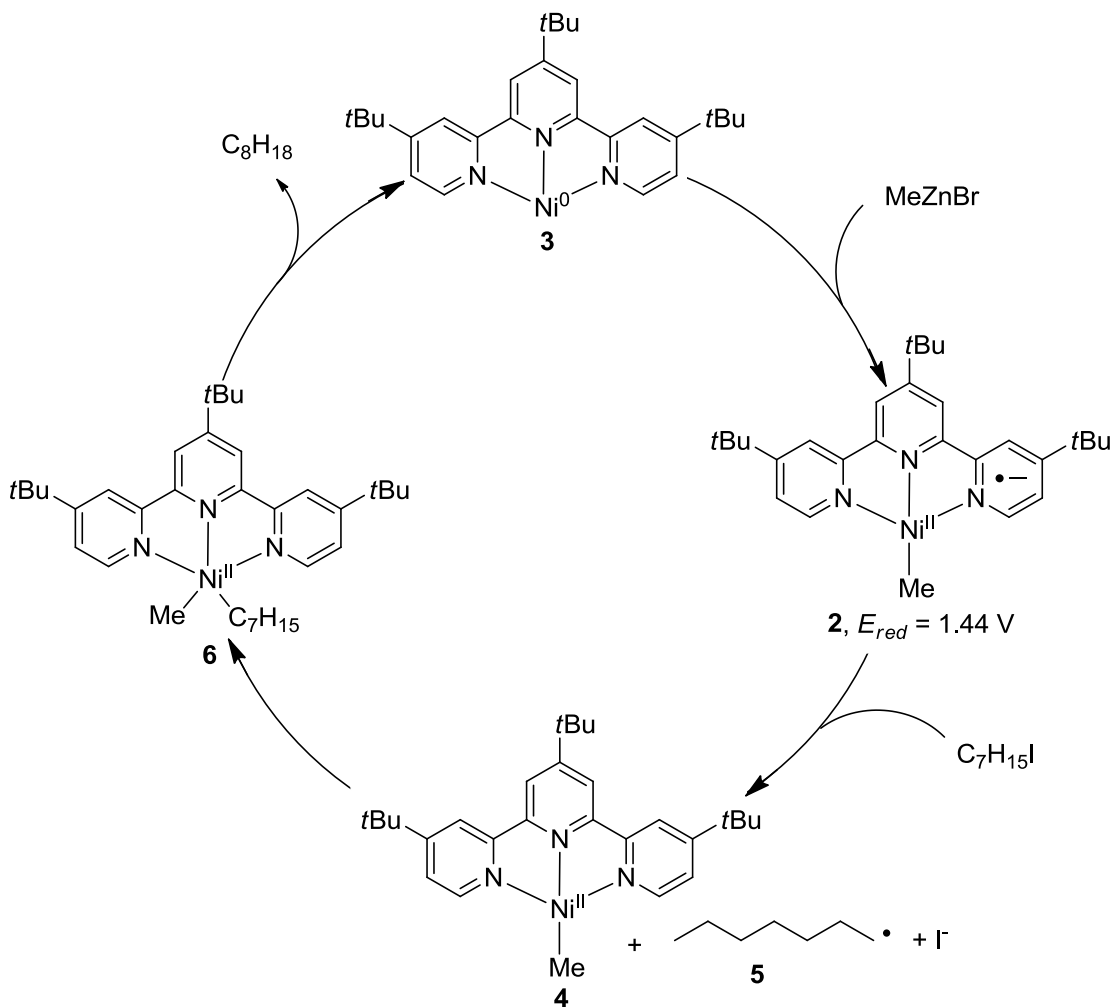
Scheme 1.31: Nickel-Catalyzed Radical Generation and Addition into Acrylates.

Research Objectives.

While alternative, tin-free radical glycosylation reactions exist, they still suffer from modest yields and require a large excess of alkene. There is still significant room for improvement in tin-free radical C-glycosidations. The purpose of the research reported herein was to develop *new methods to generate glycosyl radicals under mild conditions* and to apply these methods towards the synthesis of *biologically-relevant C-glycosides*. This work was initiated as an extension of the previously developed Negishi cross-coupling reaction in an attempt to solve the problems inherent to radical-mediated C-glycosidations. Initial work focused on the development of a room-temperature nickel-catalyzed radical conjugate addition into alkenes and applications toward diastereoselective C-glycoside synthesis (**Chapter 2**). Investigations into the mechanism led to the discovery of a light-mediated photoredox process which affords the same reactivity but with higher yields and broader substrate scope (**Chapter 3**). As this technology is relatively new in the realm of organic synthesis, the factors that control the rate of the photoredox cycle were studied (**Chapter 4**), and the concept was applied to a large-scale synthesis of C-glycoconjugates using a photo-flow process (**Chapter 5**).

⁵⁰ a) González-Bobes, F.; Fu, G. C., *J. Am. Chem. Soc.* **2006**, *128*, 5360-5361. b) Powell, D. A.; Maki, T.; Fu, G. C., *J. Am. Chem. Soc.* **2005**, *127*, 510-511. c) Vaupel, A.; Knochel, P., *J. Org. Chem.* **1996**, *61*, 5743-5753.

reactions.⁵¹ To differentiate between a M^0/M^{II} couple, common in palladium-catalyzed cross-coupling reactions, and a mechanism involving M^{I} species, the researchers synthesized and isolated $\text{Ni}^{\text{II}}(\text{Me})\text{I}$ (**1**) and $\text{Ni}^{\text{I}}\text{-Me}$ (**2**) complexes (Scheme 2.1).



Scheme 2.2: Proposed Catalytic Cycle of Ni-Catalyzed Negishi Reactions.

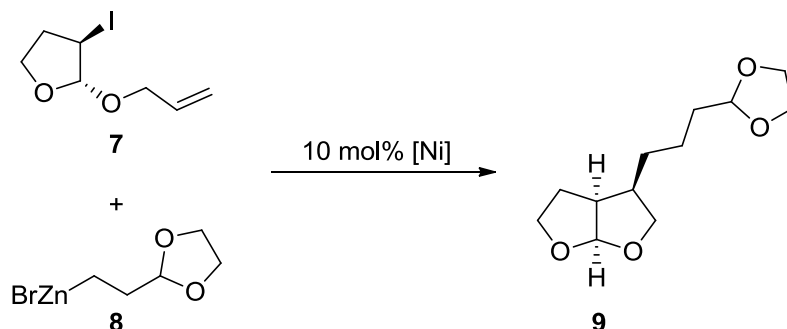
⁵¹ a) Anderson, T. J.; Jones, G. D.; Vicic, D. A., *J. Am. Chem. Soc.* **2004**, *126*, 8100-8101. b) Jones, G. D.; McFarland, C.; Anderson, T. J.; Vicic, D. A., *Chem. Commun.* **2005**, 4211-4213. c) Jones, G. D.; Martin, J. L.; McFarland, C.; Allen, O. R.; Hall, R. E.; Haley, A. D.; Brandon, R. J.; Konovalova, T.; Desrochers, P. J.; Pulay, P.; Vicic, D. A., *J. Am. Chem. Soc.* **2006**, *128*, 13175-13183.

Upon exposure to stoichiometric quantities of heptylZnBr, complex **1** provided only an 8% yield of octane, which suggests oxidative addition of alkyl halide followed by transmetallation and reductive elimination is not the mechanism of nickel-catalyzed Negishi cross-couplings (Scheme 2.1, reaction **A**). However, complex **2** was found to react with iodoheptane to generate octane in a 90% yield, indicating **2** is the catalytically active species in these reactions (Scheme 2.1, reaction **B**). The authors propose the Ni^I species (**2**) reacts with the alkyl halide to generate an alkyl radical. Upon further investigation, **2** was found to behave as a Ni^{II} complex with a ligand-centered radical anion that can serve as a strong reductant ($E_{red} = 1.44$ V vs Ag/Ag⁺ in THF).^{51b,c} The authors proposed that single electron transfer from **2** to the substrate reduces the alkyl halide to generate an alkyl radical (**5**). Radical recombination with the nickel catalyst (**6**) and reductive elimination produces the product and turns over the catalytic cycle (Scheme 2.2). This mechanism was later supported by DFT calculations by Lin and Phillips.⁵²

Similarly, Cárdenas and co-workers have demonstrated the intermediacy of alkyl radicals in nickel-catalyzed Negishi cross-coupling reactions through the use of internal radical traps (Scheme 2.3).⁵³ By incorporating an alkene into the substrate, the authors were able to induce radical-mediated cyclization prior to radical recombination with the catalyst and subsequent reductive elimination from the resulting complex.

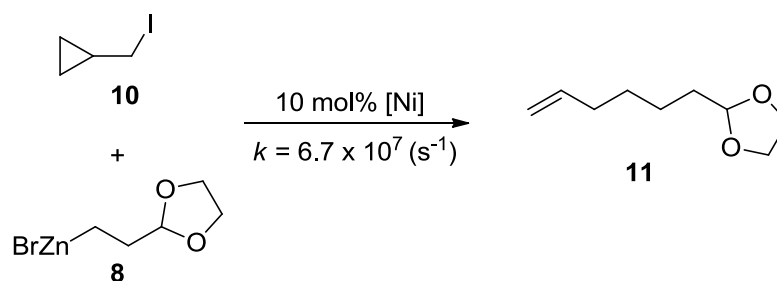
⁵² Lin, X.; Phillips, D. L., *J. Org. Chem.* **2008**, *73*, 3680-3688.

⁵³ Phapale, V. B.; Buñuel, E.; García-Iglesias, M.; Cárdenas, D. J., *Angew. Chem., Int. Ed.* **2007**, *46*, 8790-8795.



Scheme 2.3: Observed Radical Cyclization by Cárdenas in Negishi Cross-Coupling.

The authors attempted to determine the approximate lifetime of the radical through the use of radical clocks. While other internal alkenes failed to provide any rearrangements, it was found that cyclopropyl iodomethane (**10**) rearranged prior to radical recombination and transmetalation to provide alkene **11**. This suggests the key C-C coupling reaction has a rate comparable to a unimolecular process, in the range of 0.9×10^7 – 6.7×10^7 s⁻¹.



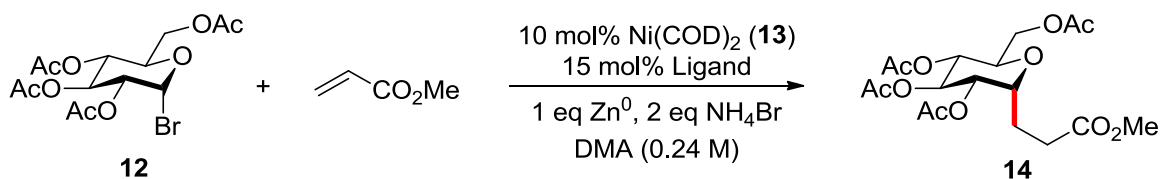
Scheme 2.4: Radical Clock Reaction in Negishi Cross-Coupling.

Application of Nickel Catalysts to Glycosyl Radical Generation (Dr. Hegui Gong).

These investigations suggest nickel catalysts generate free alkyl radicals with a finite lifetime under mild, room-temperature conditions. At this time, the Gagné group sought to utilize these conditions to generate glycosyl radicals as an alternative to previously reported methods. Our goal was to achieve a room-temperature, tin-free process that does not require a large excess of alkene. Initial investigations into this area and final optimization were conducted by Dr. Hegui Gong and are

summarized in Table 2.1.⁵⁴ Glucosyl bromide **12** was allowed to react with a mixture of 10 mol% Ni(COD)₂ (**13**), 15 mol% of a pincer-ligand, 2 eq. of methyl acrylate, 1 eq. of Zn⁰ as a stoichiometric reductant, and 2 eq. of a NH₄Br as a proton source to protonate the putative enolate formed after conjugate addition and reduction. It was found that C-glycoside **14** could be formed in a 37% yield along with glucal (**15**, 24% yield, Figure 2.1) from β-acetoxy elimination (Table 2.1, entry 11).

Table 2.1: Optimization of Nickel-Catalyzed Radical Addition into Alkenes by Dr. Hegui Gong.



Entry	Ligand/Solvent	% Product 14	% Glucal 15
1	Pybox/DMA	35	12
2	<i>R</i> -Ph-Pybox/DMA	70	<i>Trace</i>
3	R-iPr-Pybox/DMA	69	5
4	S-Ph-Pybox/DMA	52	Trace
5	Terpy/DMA	46	5
6	tBu-Terpy/DMA	54	8
7	R-Ph-Pybox/DMF	35	Trace
8	R-Ph-Pybox/DMI	30	Trace
9	R-Ph-Pybox/THF	Trace	Trace
10	R-Ph-Pybox/MeCN	40	12
11	None/DMA	37	24
12	None/DMA	5	Major

Additional byproducts, including hydrolysis from adventitious water (**16**) and over-conjugate addition (**17**, Figure 2.1), comprise the bulk of the mass balance.

⁵⁴ Gong, H.; Andrews, R. S.; Zuccarello, J. L.; Lee, S. J.; Gagné, M. R., *Org. Lett.* **2009**, *11*, 879-882.

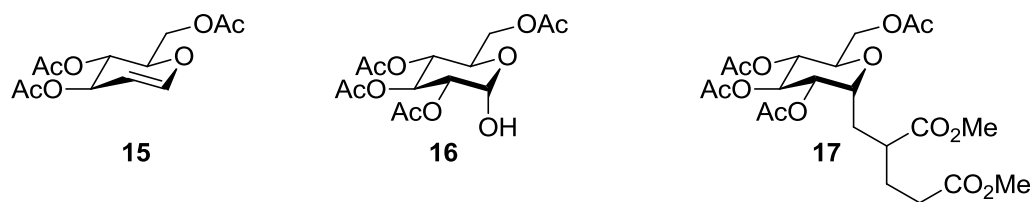


Figure 2.1: Common Byproducts in the Nickel-Catalyzed Radical Addition into Alkenes.

As has been seen in other activations of sp^3 -hybridized electrophiles, pincer ligands such as Pybox (**18**) and Terpy (**19**) suppress β -elimination and the formation of glucal **15** (Table 2.1, entries 1 and 5). While further substitution on Terpy ligands provided only a modest improvement in yield (Table 2.1, entries 5 and 6), substituted Pybox ligands significantly increased the yield of **14**. *R*-Ph-Pybox (**20**, Figure 2.2) afforded the highest yield (70%), although *S*-Ph-Pybox (**22**) was less effective, suggesting the existence of matched and mismatched combinations of catalyst-ligand complex and the chiral substrate.

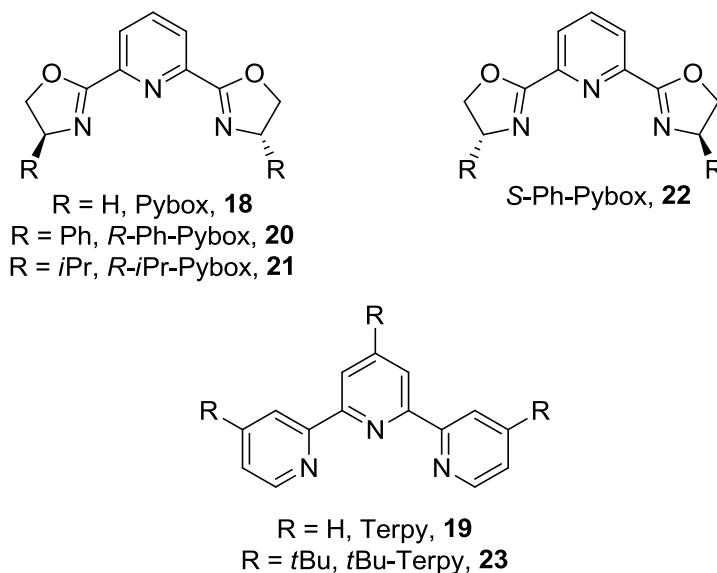


Figure 2.2: Structure of Pincer Ligands Used in Optimization.

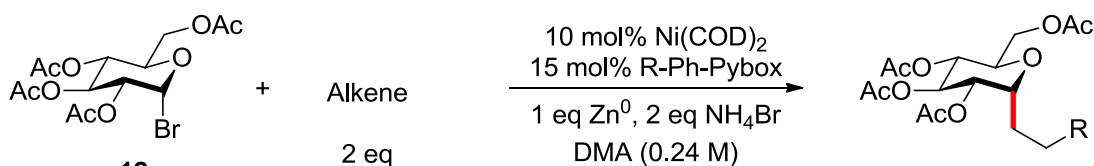

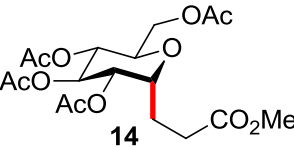

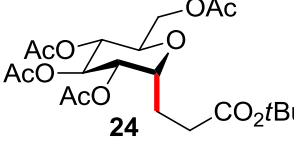
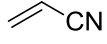
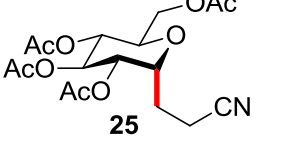
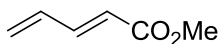
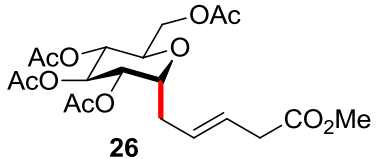
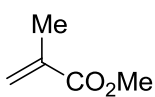
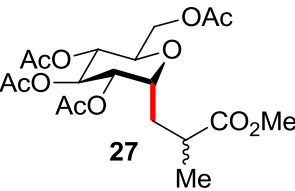
A brief solvent scan indicated DMA was the optimal solvent for this reaction. Similar solvents to DMA such as DMF or DMI significantly reduced the yield. Importantly, in the absence of a nickel catalyst, only 5% of product is formed, highlighting the importance of the catalyst. Exposing **15** to

the reaction conditions resulted in no detectable formation of product **14**, which indicates a Heck-type mechanism is unlikely.

Substrate Scope: Alkenes and Carbohydrates.

With the optimized conditions in hand, the substrate scope of the methodology was investigated (Table 2.2).

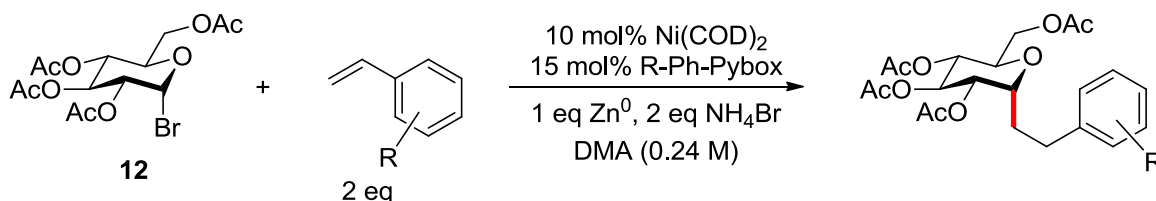
Table 2.2: Substrate Scope of Acrylate-Based Alkenes.

			
Entry	Alkene	Product	% Yield
1			70
2			75
3			75
4			65
5			88 1.4:1 dr

As expected, electron-deficient alkenes were well-tolerated in this reaction, providing modest to good yields. Acrylates and acrylonitrile were among the best substrates, providing the C-

glycosides in 65-88% yields; however, electron-rich alkenes (e.g. ethyl vinyl ether) were not successful in these reactions, and 1,1-disubstituted alkenes resulted in low diastereoselectivity on the aglycone.

Table 2.3: Radical Addition into Substituted Styrenes.



Entry	R	σ -value	Product	% Yield
1	H	-	28	trace
2	4-OMe	-0.27	29	trace
3	4-OAc	0.31	30	10
4	4-Cl	0.23	31	30
5	4-CF ₃	0.54	32	45
6	4-CO ₂ Me	0.45	33	62
7	4-CN	0.66	34	75
8	4-F	0.06	35	trace
9	3-F	0.34	36	35
10	2-F	-	37	20

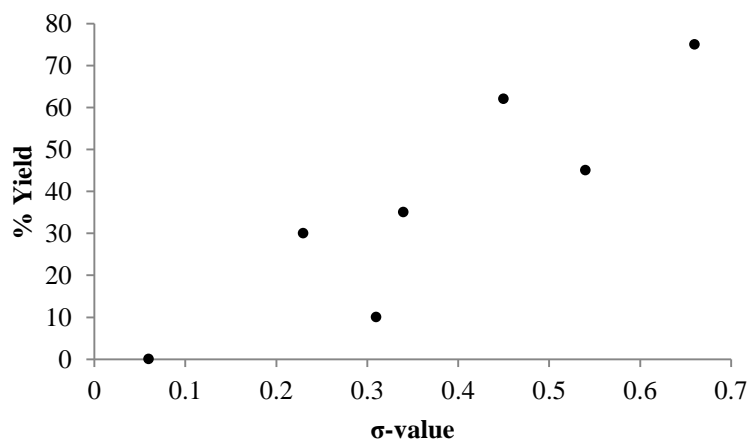
In an attempt to elucidate the electronic requirements of the alkenes, a series of substituted styrenes were subjected to the reaction conditions (Table 2.3). As expected, strong electron-withdrawing groups resulted in higher yields, whereas electron-donating substituents resulted in no reaction.⁵⁵ While there was significant variation among the alkenes tested, more positive Hammett σ -values of the substituent roughly correlated to higher yields,⁵⁶ which is consistent with the nucleophilic character of the glycosyl radical (Figure 2.3).⁵⁷

⁵⁵ Giese, B., *Angew. Chem., Int. Ed.* **1983**, 22, 753-764.

⁵⁶ For Hammett substitution constants, see: Hansch, C.; Leo, A.; Taft, R. W., *Chem. Rev.* **1991**, 91, 165-195.

Giese and co-workers have reported that the rate of nucleophilic radical addition into alkenes increases as the alkene substituent becomes more electron-deficient.⁵⁵ It is possible the higher yields in these reactions are a result of high rates of glucosyl radical addition into the alkene. This hypothesis also explains the prevalence of the β -hydride elimination product in reactions with less electron-deficient alkenes.

Figure 2.3: Plot of % Yield vs σ -value of Substituent for a Series of Substituted-Styrenes.



The nickel-catalyzed reductive coupling was successfully extended to other acetate-protected glycosyl bromides (glycosyl bromides (

Table 2.4). Both the mannosyl bromide **38** and galactosyl bromide **39** proceeded smoothly to the corresponding α -C-glycosides in 76% and 60% yield respectively. Benzoate-protected glucosyl bromide **41** was similarly well-tolerated and resulted in a 62% yield, whereas 5-dealkylated-C-arabinoside **40** was produced in 61% yield with diminished stereoselectivity. Benzyl-protected glucosyl bromide **42**, a common glycosidation reagent in *O*- and *C*-glycoside synthesis, was too susceptible to hydrolysis for this methodology, resulting in only 20% yield of **47**.

⁵⁷ For examples, see: a) SanMartin, R.; Tavassoli, B.; Walsh, K. E.; Walter, D. S.; Gallagher, T., *Org. Lett.*

2000, 2, 4051-4054. b) Liu, Y.; Gallagher, T., *Org. Lett.* **2004**, 6, 2445-2448.

Table 2.4: Sugar Substrates in Ni-Catalyzed Addition into Alkenes.

Entry	Starting Material	Product	% Yield (α : β)
1			76 (α)
2			60 (α)
3			61
4			62 (α)
5			20

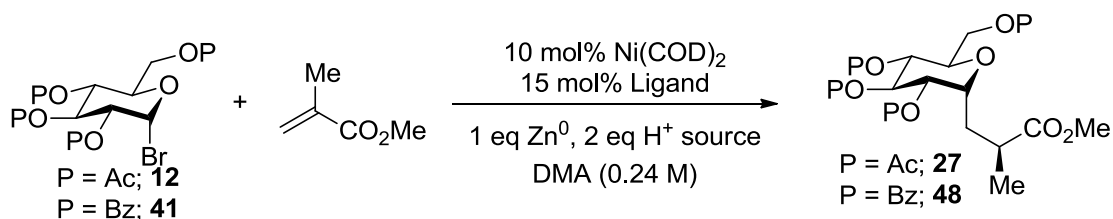
Diastereoselectivity of 1,1-Disubstituted Alkenes.

Glycosyl radical addition into 1,1-disubstituted alkenes resulted in high selectivity for the α -anomer but proved non-selective on the aglycone (Table 2.2, entry 5). In order to further improve the applicability of this methodology, we sought to re-optimize our initial reaction conditions to achieve

higher side-chain diastereoselectivity (Table 2.5). The bulkier benzoate-protected glycosyl bromide **41** did not significantly improve stereoselectivity, nor did varying the chiral ligand or increasing the steric bulk on the acrylate. Enantiopure methacryloyl esters and imides similarly failed to provide improved diastereoselectivities.

As protonation of the proposed enolate was presumed to be the stereodetermining step, we then investigated the proton source. Chiral ammonium salts resulted in a modest improvement in diastereoselectivity (2.3:1 vs 1.4:1) but were found to be inferior to alcohol proton sources (Table 2.5, entries 1 and 6).

Table 2.5: Optimization of Diastereoselectivity of Addition into Disubstituted Alkenes.

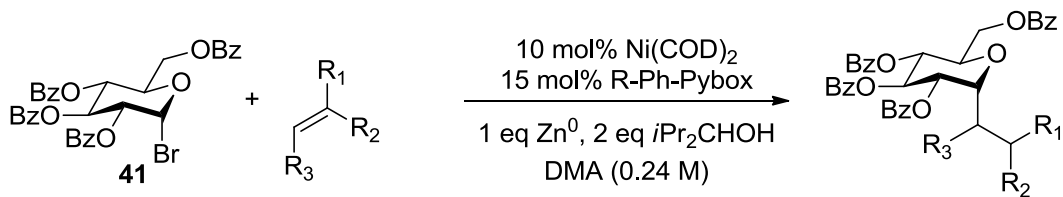


Entry	P =	Ligand	Proton Source	% Yield	dr
1	Ac	R-Ph-Pybox	NH ₄ Br	88	1.4:1
2	Bz	R-Ph-Pybox	NH ₄ Br	75	1.6:1
3	Ac	S-Ph-Pybox	NH ₄ Br	72	1:1
4	Ac	S- <i>i</i> Pr-Pybox	NH ₄ Br	87	1.4:1
5	Ac	Indeny-Pybox	NH ₄ Br	63	2:1
6	Ac	R-Ph-Pybox	(-) sparteine·H ₂ SO ₄	63	2.3:1
7	Bz	R-Ph-Pybox	H ₂ O	55	4:1
8	Bz	R-Ph-Pybox	EtOH	76	3.2:1
9	Bz	R-Ph-Pybox	<i>i</i> PrOH	81	4.2:1
10	Bz	R-Ph-Pybox	<i>i</i>Pr₂CHOH	80	5:1
11	Bz	R-Ph-Pybox	<i>t</i> BuOH	60	3.5:1
12	Bz	R-Ph-Pybox	(S)-Binol	ND	1:1
13	Bz	R-Ph-Pybox	(<i>R</i>)-2-butanol	ND	3.4:1
14	Bz	R-Ph-Pybox	(<i>S</i>)-2-butanol	ND	3.7:1
15	Ac	R-Ph-Pybox	<i>i</i> Pr ₂ CHOH	90	2:1

Simply allowing water to quench the enolate through the addition of wet silica resulted in a 4:1 ratio of diastereomers (Table 2.5, entry 7). Increasing the steric bulk and branching on the alcohol improved the diastereoselectivity up to a point, with *i*Pr₂CHOH providing a 5:1 dr (Table 2.5, entry 10), and the absolute stereochemistry was determined to be the *S*-isomer via single-crystal x-ray diffraction. Surprisingly, different enantiomers of chiral alcohols did not significantly affect the diastereoselectivity, with both enantiomers of 1-phenylethanol resulting in approximately the same ratio of diastereomers. Finally, it was determined that the benzoate protecting groups were essential to obtaining high diastereoselectivity, as acetate-protected glucosyl bromide **12** resulted in lower diastereoselectivity than observed for **41** (Table 2.5, entry 15).

To determine if the optimized conditions for diastereoselectivity were general for di- and trisubstituted alkenes, a series of geminally disubstituted alkenes were tested in the reaction (Table 2.6). Exposure of α -methylene- γ -butyrolactone (**49**) and 3-methacryloyloxazolidin-2-one (**50**) to **41** gave the desired C-glycosides with good diastereoselectivity. More sterically hindered alkenes such as methyl 2-phenyl acrylate (**51**) and (1*S*,4*R*)-3-methylenebicyclo[2.2.1]heptan-2-one (**52**) coupled successfully but with diminished diastereoselectivities. Trisubstituted alkene **53** provided C-glycoside **58** in 56% yield despite the fact that trisubstituted alkenes generally demonstrate poor reactivity. This reactivity is potentially due to the increased electron-withdrawing capability of the alkene as compared to methyl crotonate, which fails to react under nickel-catalyzed conditions.

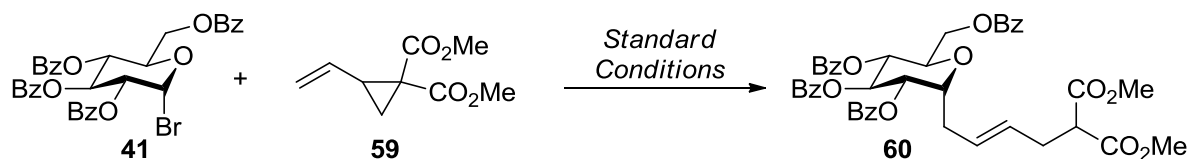
Table 2.6: Diastereoselective Addition into Alkenes Scope.



Entry	Alkene	Product	% Yield (dr)
1	 49	 54	50 (7:1)
2	 50	 55	74 (5:1)
3	 51	 56	46 (2.5:1)
4	 52	 57	76 (1.8:1)
5	 53	 58	56 (1.2:1)

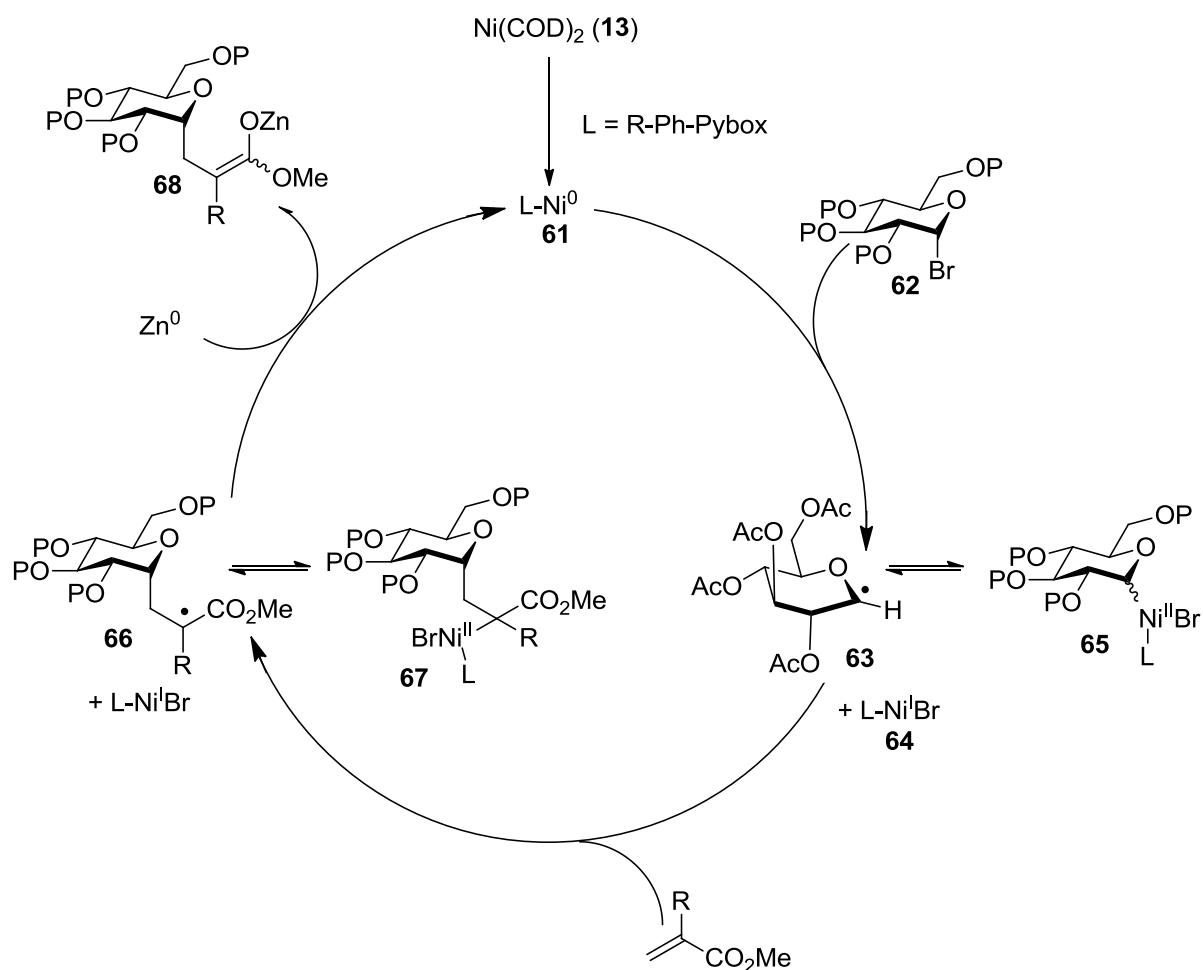
Proposed Mechanism and Stereochemical Model.

It was determined that vinyl cyclopropane **59** also reacted under these conditions but provided the ring-opened product **60**.



Scheme 2.5: Ring-Opening of Vinyl Cyclopropane 58.

Most importantly, this observation along with the faster rates of addition into electron-deficient alkenes and the exquisite α -selectivity can be explained by the intermediacy of radicals in this methodology. A proposed mechanism for the nickel-catalyzed glycosyl radical addition into alkenes is shown in Scheme 2.6.



Scheme 2.6: Proposed Mechanism of Ni-Catalyzed Synthesis of C-Glycosides.

Initial complexation of the pincer ligand to Ni^0 occurs rapidly (<10 min at room temperature) and can be observed *in situ* through a color change from colorless to purple. At this point, addition of the glucosyl bromide (**62**) to the reaction vessel results in another color change from purple to red, presumably due to the activation of the substrate to form nickel complex **64**. The precise nature of this complex is the subject of current investigations. In 2011, Vicic reported the synthesis and properties of Terpy-Ni(I)Br (**69**) as compared to Terpy-Ni(II)Br₂ (**70**) and Terpy-Ni(I)-Me (**71**) shown in Figure 2.4.⁵⁸ Interestingly, **70** and **71** exhibit similar potentials for ligand-centered reductions of the complex, suggesting this process is independent of the oxidation state of the metal center.

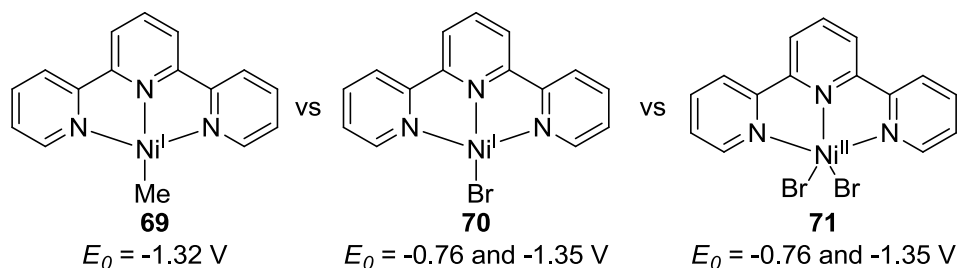
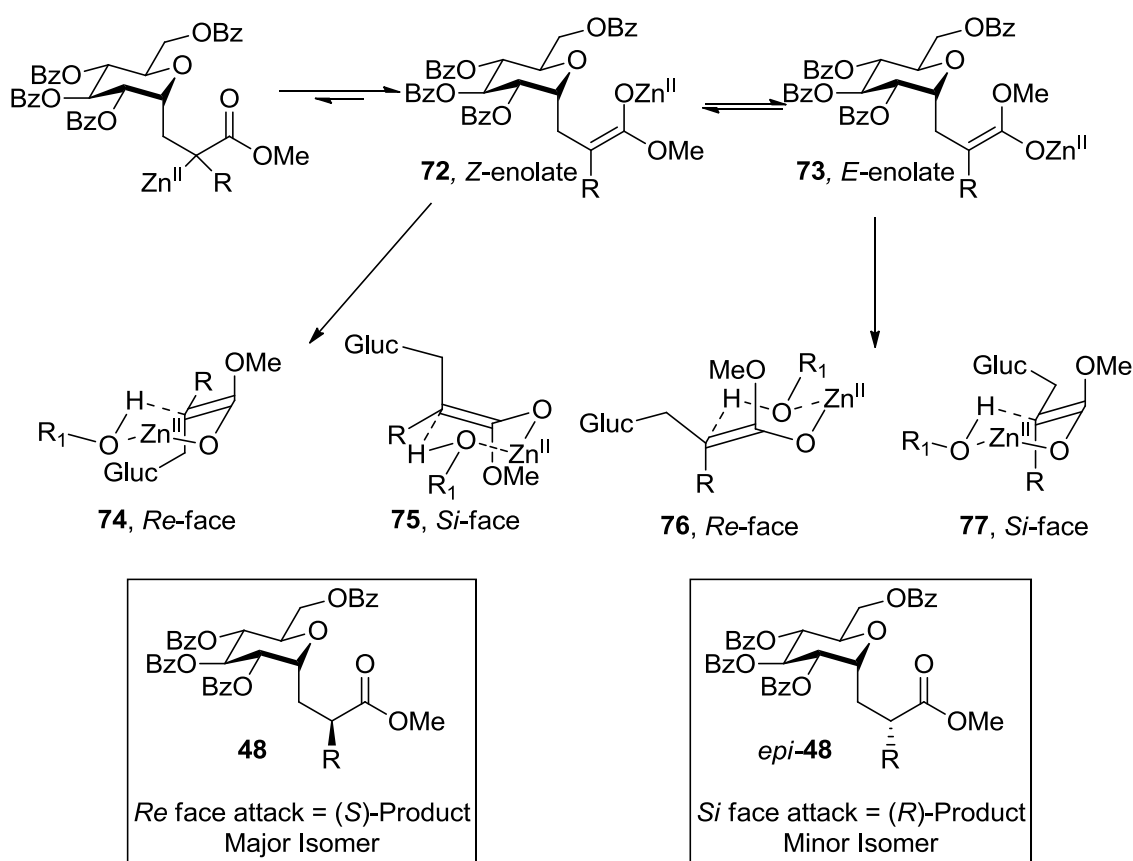


Figure 2.4: Reduction Potentials of Terpy-Nickel Complexes.

EPR analysis of **69** and **70** identified a ligand-centered radical on **69** and a metal-centered radical on **70**, which was further corroborated by DFT calculations. From these experiments, it is clear the active catalyst species in our nickel-catalyzed glucosyl radical generation for conjugate addition is different than the active species in a Negishi cross-coupling system. However, at this point the specific behavior of the catalyst is unknown. We speculate the nickel species **64** can exist alone in solution, as a $\text{Ni}^{\text{II}}(\text{Br})$ -alkyl species after radical recombination (**65**) or as an equilibrium between the two species (**64** and **65**). It is also possible species **64** is reduced directly by Zn^0 in order to regenerate **61**, which turns over the catalyst cycle (not shown). Regardless of the nature of this

⁵⁸ Ciszewski, J. T.; Mikhaylov, D. Y.; Holin, K. V.; Kadirov, M. K.; Budnikova, Y. H.; Sinyashin, O.; Vicic, D. A., *Inorg. Chem.* 50, 8630-8635.

species, it is clear that a glycosyl radical is formed, which reacts with alkene present to yield α -radical species **65**. Reduction of this intermediate with Zn^0 forms zinc enolate **67**, which is then protonated under the reaction conditions to form the product. Any high-valent nickel species present at this point will again be reduced by Zn^0 to turn over the catalytic cycle (Scheme 2.6).



Scheme 2.7: Proposed Stereochemistry Model.

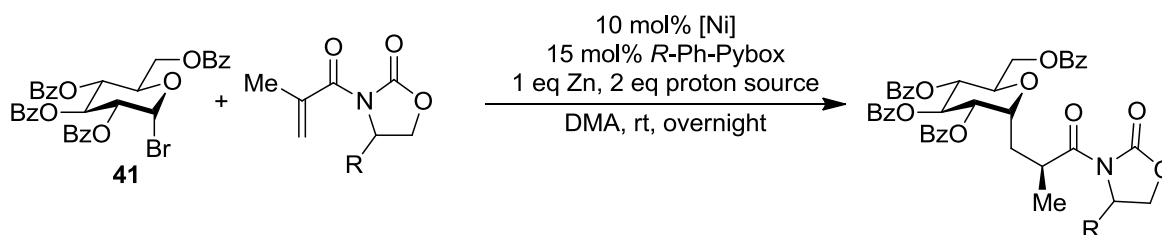
The stereochemistry on the aglycone is proposed to arise from stereoselective protonation of the zinc enolate (Scheme 2.7). The alcohol coordinates to the zinc enolate to form a Zimmerman-Traxler transition state, which then directs proton attack to the *re*-face of the enolate to form the *S*-isomer. Non-coordinating proton sources (i.e. ammonium salts) fail to produce this coordinated transition state and results in low diastereoselectivity. The precise stereochemistry of the enolate (*E* vs *Z*) is unknown, thus the precise origin of the stereoselectivity is unknown. However, it is clear the

steric bulk of the protecting groups is important, so it is possible the sugar substrate provides the differentiation between the faces.

Diastereoselectivity: Chiral Auxiliaries.

In an attempt to further improve the diastereoselectivity, several oxazolidinone-based chiral auxiliaries were investigated. As has been seen in a variety of enol reactions (e.g. aldol reactions, enol-substitution reactions),⁵⁹ these chiral auxiliaries are able to rigidly structure the Zimmerman-Traxler transition state, imparting high levels of diastereoselectivity.⁶⁰

Table 2.7: Influence of Oxazolidinone-based Chiral Auxiliaries on Diastereoselectivity.



Entry	R	[Ni]	Proton source	% Yield	dr ^a
1	<i>R</i> -Ph, 78	Ni(COD) ₂	NH ₄ Br	45, 84	3:1
2	<i>R</i> -Ph, 78	Ni(COD) ₂	<i>i</i> Pr ₂ CHOH	75, 84	3:1
3	<i>S</i> -Ph, 79	Ni(COD) ₂	NH ₄ Br	35, 85	1.4:1
4	<i>S</i> -Ph, 79	Ni(COD) ₂	<i>i</i> Pr ₂ CHOH	49, 85	1.5:1
5	<i>R</i> - <i>i</i> Pr, 80	NiBr ₂ (diglyme)	<i>i</i> Pr ₂ CHOH	ND ^b , 86	3.3:1
6	<i>S</i> - <i>i</i> Pr, 81	Ni(COD) ₂	<i>i</i> Pr ₂ CHOH	ND ^b , 87	1.5:1
7	<i>R</i> -Bn, 82	Ni(COD) ₂	<i>i</i> Pr ₂ CHOH	ND ^b , 88	3.3:1
8	<i>S</i> -Bn, 83	Ni(COD) ₂	<i>i</i> Pr ₂ CHOH	ND ^b , 89	~1:1

^a Determined by ¹H NMR ^b Not determined

As DMA is a highly polar solvent, it is possible the modest diastereoselectivities are a result of a loosely-coordinated transition state. We proposed the diastereoselectivity of enolate protonation

⁵⁹ For a review on oxazolidinone-based chiral auxiliaries, see Evans D. A. *Aldrichim. Acta* **1982**, 15, 23-32.

⁶⁰ For a recent review on chiral auxiliaries, see Gnass, Y.; Glorius, F., *Synthesis* **2006**, 2006, 1899-1930.

in these reactions could be increased even further by using methacryloyl-derived chiral auxiliaries. More importantly, we hoped to use this concept for the diastereoselective synthesis of C-glycoamino acids, which would ideally exist as a single isomer.

Initial work towards increasing the diastereoselectivity focused on the use of oxazolidinone-based chiral auxiliaries under the previously optimized reaction conditions. Comparison of the proton source with both enantiomers of phenyl-substituted oxazolidinones demonstrated no significant effect on diastereoselectivity, although the yields were notably higher with *i*Pr₂CHOH. The *R*-isomers of the auxiliaries consistently gave a 3:1 ratio of diastereomers, regardless of the substituent on the auxiliary, while the *S*-isomers were found to give lower selectivities. However, none of the auxiliaries tested were able to supersede the diastereoselectivity as compared to achiral methyl methacrylate. Adding coordinating Lewis acids into the reaction mixture (Sm(OTf)₃ or MgBr₂(OEt₂)), which have been shown to improve the diastereoselectivity of other reactions involving oxazolidinone-based chiral enolates,⁶⁰ suppressed formation of the product. Other chiral auxiliaries were tested and the results of each are shown in Figure 2.5. “SuperQuat” oxazolidinone **90** failed to improve the diastereoselectivity, and camphorsultam-based alkene **91** resulted in almost no selectivity. Epinephrine-derived acrylamide **92** failed to react, which is consistent with the previous observation that acrylamides are unreactive under the reaction conditions.

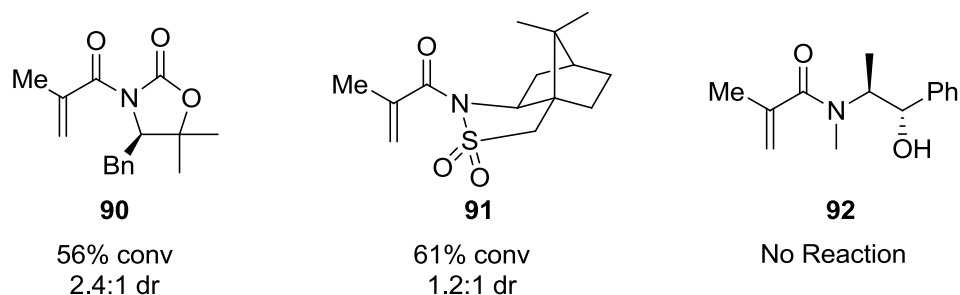
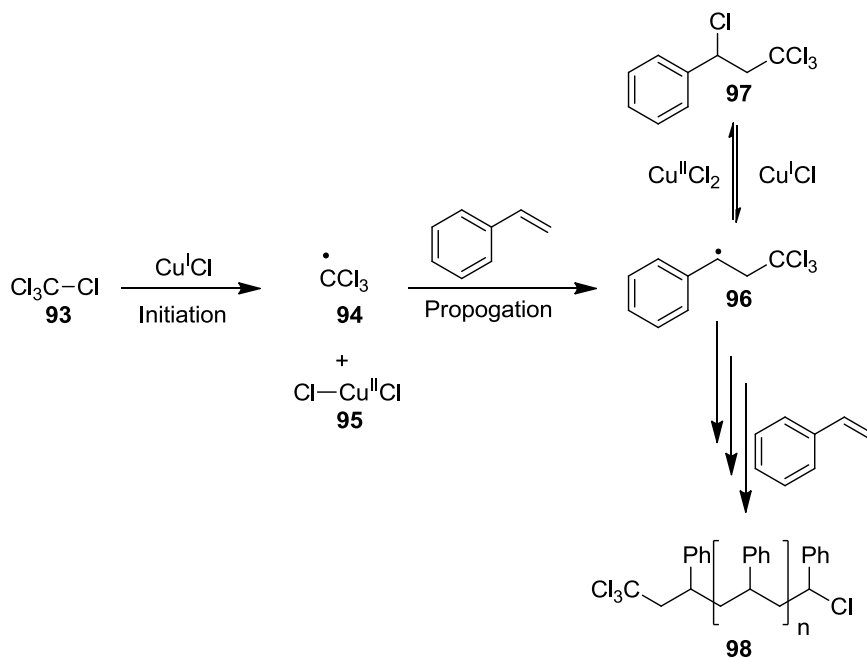


Figure 2.5: Chiral Auxiliaries Investigated and Resulting Diastereoselectivity.

Second Generation Catalysts: Atom-Transfer Radical Generation.

Chiral auxiliaries failed to improve the diastereoselectivity of conjugate addition into 1,1-disubstituted alkenes, and observation we initially attributed to the high polarity of DMA. A less-polar solvent would not be able to solvate developing charges in the transition state as well as DMA, resulting in a tightly-coordinated transition state. However, any attempts to change the solvent in this methodology resulted in significantly lower yields; therefore, a second-generation methodology was needed to conduct the reaction in non-polar solvents. For this we considered two possible mechanisms of glycosyl bromide activation: atom abstraction and outer-sphere electron transfer.



Scheme 2.8: General Mechanism for ATRP.

We envisioned an atom abstraction mechanism similar to an atom transfer radical addition (ATRA) or polymerization (ATRP) mechanism (Scheme 2.8).⁶¹ In these reactions, a transition-metal catalyst initially abstracts a halide from the substrate (**93**) to form an alkyl radical (**94**). This radical

⁶¹ a) Matyjaszewski, K.; Xia, J., *Chem. Rev.* **2001**, *101*, 2921-2990. b) Patten, T. E.; Matyjaszewski, K., *Acc. Chem. Res.* **1999**, *32*, 895-903.

then undergoes conjugate addition into an appropriate alkene, and the resulting radical (**96**) then abstracts the halide from the catalyst (**97**).

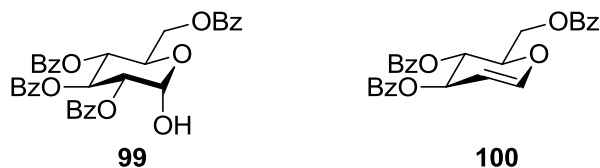
Table 2.8: Investigation of Copper Catalysts for C-Glycoside Synthesis.

Br[C@@H]1O[C@H](OC(=O)c2ccccc2)[C@@H](OC(=O)c3ccccc3)[C@H](OC(=O)c4ccccc4)[C@@H](OC(=O)c5ccccc5)[C@H]1O + C=CC(=O)OC
 $\xrightarrow[\text{NH}_4\text{Br, Solvent}]{[\text{Cu}], \text{Ligand, Zn}}$
COC(=O)CC[C@@H]1O[C@H](OC(=O)c2ccccc2)[C@@H](OC(=O)c3ccccc3)[C@H](OC(=O)c4ccccc4)[C@@H](OC(=O)c5ccccc5)[C@H]1O

41 **46**

Entry	[Cu]	Ligand	Solvent	% Conv ^a	46 ^a	99 ^{a,b}	100 ^{a,b}
1	CuI	R-Ph-Pybox	DMA	>98%	1	1	0.17
2	CuBr ₂	R-Ph-Pybox	DMA	>98%	1	1	0.17
3	CuBr ₂	Bpy	DMA	>98%	1	2.5	trace
4	CuBr ₂	1,10-Phen	DMA	>98%	1	6.7	trace
5	CuBr ₂	TMEDA	DMA	>98%	1	0.67	0.15
6	CuBr ₂	PMETA	DMA	>98%	1	0.67	0.15
7	CuBr₂	HMETA	DMA	>98%	1	0.2	0.2
8	CuBr ₂	HMETA	CH ₂ Cl ₂	42%	1	4.4	trace
9	CuBr₂	HMETA	THF	~5%	1	trace	trace
10	CuBr ₂	HMETA	Et ₂ O	~4%	1	trace	trace

^a Determined by ¹H NMR, ^b Equivalents relative to **46**



In the case of ATRP, the catalyst can re-abstract the halide from the organic substrate to allow for conjugate additions to occur, creating a “living” polymerization (**98**).⁶² As we do not see any bromine incorporation into the product, we postulated if halide abstraction was the mechanism of activation in our system, the organic α -radical was simply being reduced to the enolate prior to halide abstraction. Thus, we decided to probe the competency of ATRA/ATRP catalysts in this methodology.

To test this hypothesis, glucosyl bromide **41** and methyl acrylate were subjected to different catalyst and ligand combinations known for their activity in ATRP reactions (Table 2.1). Using CuI or CuBr₂ as catalysts instead of Ni(COD)₂ resulted in full conversion of starting material (**41**) but produced equimolar amounts of the C-glycoside product and hydrolysis (**99**) along with glucal (**100**) (β -elimination product). Bidentate aromatic ligands resulted in significantly more hydrolysis, whereas TMEDA suppressed hydrolysis. While the tridentate ligand PMETA did not improve the ratio of desired product to byproducts, the tetradentate ligand HMETA produced the desired product as the major product with only 0.2 eq of hydrolysis and glucal relative to product. Less polar solvents effectively suppressed formation of glucal, and non-polar ethereal solvents successfully prevented hydrolysis. However, these non-polar solvents suffered from poor conversions, and ultimately ATRP-based catalysts were deemed unsuitable for this reaction.

Conclusion.

We have demonstrated a mild, tin-free nickel-catalyzed method of glycosyl radical generation for conjugate addition into electron-deficient alkenes for the synthesis of C-glycosides. This methodology features low alkene stoichiometry and temperature requirements. The diastereoselectivity of reactions with 1,1-disubstituted alkenes was significantly improved through the use of *i*Pr₂CHOH as a bulky proton source. Attempts to further improve the diastereoselectivity with

⁶² a) Bisht, H. S.; Chatterjee, A. K., *J. Macromol. Sci. Pol. R.* **2001**, *41*, 139-173. b) Kamigaito, M.; Ando, T.; Sawamoto, M., *Chem. Rev.* **2001**, *101*, 3689-3746. c) Uegaki, H.; Kotani, Y.; Kamigaito, M.; Sawamoto, M., *Macromolecules* **1997**, *30*, 2249-2253.

chiral auxiliaries were unsuccessful, potentially due to the highly polar solvents required for successful reactivity. A second generation copper catalyst system was proposed based on the concepts of ATRA/ATPR reactions in order to provide a more robust reaction, but these reactions generally suffered from poor reactivity or selectivity.

Experimental Section.

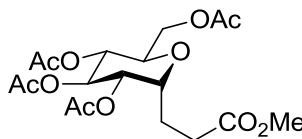
All reagents were reagent grade quality and used as received from Aldrich unless otherwise indicated. All reactions were carried out under an atmosphere of argon or nitrogen unless otherwise indicated. Anhydrous THF was distilled from sodium/ benzophenone ketyl prior to use. All other solvents were technical grade unless noted. Anhydrous N,N-dimethylacetamide (DMA), anhydrous N,N-dimethylimidazolidinone (DMI; Fluka), anhydrous DMF (Acros), NiCl₂ • glyme, Ni(COD)₂ (Strem), terpyridine (**20**), and 4, 4', 4''-tri-tert-butyl-2,2',6,2''-terpyridine (*t*Bu-terpy, **23**), methyl benzoylformate, methyl triphenylphosphonium bromide, diisopropylamine, and n-butyllithium (1.6 M in hexanes) were used as received. The unsubstituted Pybox was prepared according to a literature procedure.⁶³ Acetobromo- α -D-glucose (**12**, 1% CaCO₃) and acetobromo- α -D-galactose (**39**, 1% CaCO₃) were purified by passing through a silica column prior to use. Acetobromo- α -D-mannose (**38**),⁶⁴ and benzylbromo- α -D-glucose (**42**) were prepared according to reported procedures.⁶⁵ Tri-O-acetyl- β -D-arabinosyl bromide (**40**) and α -D-glucopyranosyl bromide tetrabenzoate (**41**) were used as received. Alkenes were used as received unless otherwise mentioned. Chiral methacryloyl imides

⁶³ a) Nishiyama, H.; Kondo, M.; Nakamura, T.; Itoh, K. *Organometallics* **1991**, *10*, 500-508. b) Motoyama, Y.; Kurihara, O.; Murata, K.; Aoki, K.; Nishiyama, H. *Organometallics* **2000**, *19*, 1025-1034.

⁶⁴ Ravindranathan Karcha, K. P.; Jennings, H. J. *J. Carbohydr. Chem.* **1990**, *9*, 777-781.

⁶⁵ a) Blom, P.; Ruttens, B.; Van Hoof, S.; Hubrecht, I.; Van der Eycken, J.; Sas, B.; Van hemel, J.; Vandenkerckhove, J. *J. Org. Chem.* **2005**, *70*, 10109-10112. b) Takeo, K.; Nakagen, M.; Teramoto, Y.; Nitta, Y. *Carbohydr. Res.* **1990**, *201*, 261-275.

78-83 were synthesized according to reported procedures.⁶⁶ Column chromatography was performed using Merck silica gel 60 as the solid support. All NMR spectra were recorded on Bruker Avance 500 MHz, 400 MHz, or 300 MHz spectrometer at STP and with CDCl₃ as the NMR solvent unless otherwise indicated. All deuterated solvents were used as received from Cambridge Isotope Laboratories, Inc. ¹H NMR and ¹³C NMR chemical shifts are reported in δ units, parts per million (ppm) relative to the chemical shift of residual solvent. Reference peaks for chloroform in ¹H NMR and ¹³C NMR spectra were set at 7.26 ppm and 77.0 ppm, respectively; for methanol the reference peaks in ¹H NMR and ¹³C NMR spectra were set at 3.30 ppm and 49.0 ppm, respectively. High-resolution mass spectra (HRMS) were obtained using a Micromass Q-ToF Ultima or Brucker Biotof-II instrument. Melting point was recorded on Uni-melt (Thoms Hoover) capillary melting point apparatus. Infrared (IR) spectra were obtained using a Jasco 460 Plus Fourier transform infrared spectrometer. Specific rotations were obtained using a Jasco DIP-1000 polarimeter with CH₂Cl₂ as the solvent.

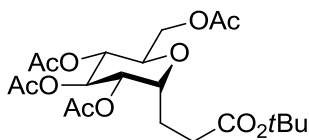


Methyl 3-(2,3,4,6,-tetra-*O*-acetyl- α -D-glucopyranosyl)propanoate (14).

This compound was prepared according to the General Procedure A using aceto-1-bromo- α -D-glucose **12** (100 mg, 0.243 mmol, 100 mol%) and methyl acrylate (42 mg, 0.486 mmol, 200 mol%).

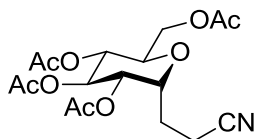
⁶⁶ Evans, D. A.; Chapman, K. T.; Bisaha, J., *J. Am. Chem. Soc.* **1988**, *110*, 1238-1256.

Flash column chromatography (SiO₂: 20% ethyl acetate in hexanes) gave the desired product⁶⁷ as a colorless oil (71 mg, 0.17 mmol, 70% yield).



***t*-Butyl 3-(2,3,4,6,-tetra-*O*-acetyl- α -D-glucopyranosyl)propanoate (24).**

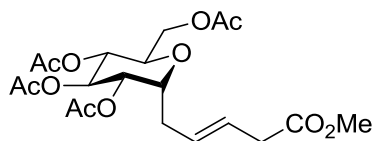
This compound was prepared according to the General Procedure A using aceto-1-bromo- α -D-glucose **12** (100 mg, 0.243 mmol, 100 mol%) and *tert*-butyl acrylate (71 μ L, 0.488 mmol, 200 mol%). Flash column chromatography (SiO₂: 20% ethyl acetate in hexanes) gave the desired product as a colorless oil (80 mg, 0.174 mmol, 72% yield). $[\alpha]_D^{25} = +27$ ($c = 29.4$). ¹H NMR (400 MHz, CDCl₃): δ 5.30(t, $J = 9.3$ Hz, 1H, *H*3), 5.06(dd, $J = 9.6$ and 5.7 Hz, 1H, *H*2), 4.98 (t, $J = 9.0$ Hz, 1H, *H*4), 4.23 (dd, $J = 12.3$ and 4.8 Hz, 1H, *H*6), 4.15 (ddd, $J = 11.6$, 5.6, and 3.2, 1H, *H*1), 4.04 (dd, $J = 12$ and 2 Hz, 1H, *H*7), 3.83 (ddd, $J = 9.2$, 4.8, and 2.4 Hz, 1H, *H*5), 2.22-2.33 (m, 2H), 2.08 (s, 3H), 2.04 (s, 3H), 2.02 (s, 6H), 1.87-1.65 (m, 2H), 1.42 (s, 9H). ¹³C NMR (100 MHz, CDCl₃): δ 172.0, 170.6, 170.0, 169.6, 169.5, 80.7, 72.1, 70.4, 70.2, 68.79, 68.75, 62.2, 30.8, 28.0, 20.7, 20.66, 20.59. IR (film) 3472, 2977, 2939, 1751, 1644, 1455, 1368, 1227, 1153, 1096, 1034, 977, 912, 848, 731, 602, 537, 505 cm⁻¹. HRMS (ESI): m/z [M+H]⁺ found 461.2022, calcd 461.2023 for C₂₁H₃₃O₁₁.



3-(2,3,4,6,-tetra-*O*-acetyl- α -D-glucopyranosyl)propionitrile (25).

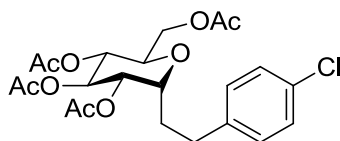
⁶⁷ a) Adlington, R. M.; Baldwin, J. E.; Basak, A.; Kozyrod, R. P. *J. Chem. Soc., Chem. Comm.* **1983**, 17, 944-945. (b) For full characterization of ester **14**, see: Gotanda, K.; Matsugi, M.; Suemura, M.; Ohira, C.; Sano, A.; Oka, M.; Kita, Y. *Tetrahedron* **1999**, 55, 10315-1324.

This compound was prepared according to the General Procedure A using aceto-1-bromo- α -D-glucose **12** (100 mg, 0.243 mmol, 100 mol%) and acrylonitrile (32 μ L, 0.486 mmol, 200 mol%). Flash column chromatography (SiO₂: 25% EtOAc in hexanes) gave the desired product⁶⁸ as a colorless oil (70 mg, 0.18 mmol, 75% yield).



Methyl 5-(2,3,4,6-tetra-O-acetyl- α -D-glucopyranosyl)prop-3-enoate (26).

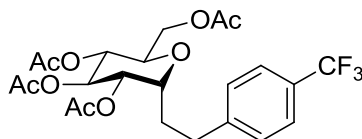
This compound was prepared according to the General Procedure A using aceto-1-bromo- α -D-glucose **12** (100 mg, 0.243 mmol, 100 mol%) and (*E*)-methyl penta-2,4-dienoate (55 mg, 0.486 mmol, 200 mol%). Flash column chromatography (SiO₂: 20% ethyl acetate in hexanes) gave the desired product as a colorless oil (70 mg, 0.158 mmol, 65% yield). $[\alpha]_D^{25} = +53$ ($c = 46.4$). ¹H NMR (400 MHz, CDCl₃): δ 5.66 (dt, $J = 21.6$ and 6.4 Hz, 1H), 5.46 (dt, $J = 21.6$ and 6.8 Hz, 1H), 5.28 (t, $J = 9.2$ Hz, 1H; *H*3), 5.04 (dd, $J = 9.2$ and 5.6 Hz, 1H; *H*2), 4.95 (t, $J = 9.2$ Hz, 1H; *H*4), 4.20 (dd, $J = 12.0$ and 4.4 Hz, 1H; *H*6), 4.15-4.25 (m, 1H; *H*1), 4.01 (dd, $J = 12.0$ and 2.8 Hz, 1H, *H*7), 3.81 (ddd, $J = 9.2, 5.6, 2.8$ Hz, 1H, *H*5), 3.64 (s, 3H), 3.03 (d, $J = 6.8$ Hz, 2H), 2.46-2.57 (m, 1H), 2.24-2.33 (m, 1H), 2.04 (s, 3H), 2.01 (s, 3H), 1.99 (s, 6H). ¹³C NMR (100 MHz, CDCl₃): δ 171.9, 170.6, 170.0, 169.6, 169.4, 128.4, 125.1, 71.9, 70.2, 70.0, 68.7, 68.5, 61.9, 51.8, 37.7, 29.1, 20.61, 20.56. IR (film) 3011, 2955, 2852, 1746, 1436, 1390, 1226, 1165, 1034, 976, 911.2, 603 cm⁻¹. HRMS (ESI): m/z $[M+H]^+$ found 445.1694, calcd 445.1710 for C₂₀H₂₉O₁₁.



⁶⁸ Giese, B.; Dupuis, J.; Nix, M. *Org. Synth.* **1987**, 65, 236-239.

1-(2,3,4,6,-tetra-*O*-acetyl- α -D-glucopyranosyl)-2-(4-chlorophenyl)ethane (31).

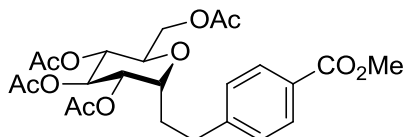
This compound was prepared according to the General Procedure A using aceto-1-bromo- α -D-glucose **12** (100 mg, 0.243 mmol, 100 mol%) and 4-chlorostyrene (0.058 mL, 0.488 mmol, 200 mol %). Flash column chromatography (SiO₂: 20% ethyl acetate in hexanes) gave the desired product as a colorless oil (35 mg, 0.074 mmol, 30% yield). $[\alpha]_{\text{D}}^{25} = +28$ ($c = 2.2$). ¹H NMR (400 MHz, CDCl₃): δ 7.27 (d, $J = 7.2$ Hz, 2H, Ar), 7.12 (d, $J = 8.4$ Hz, 2H, Ar), 5.30 (t, $J = 9.2$ Hz, 1H, *H*3), 5.08 (dd, $J = 9.4$ and 5.8 Hz, 1H, *H*2), 4.99 (t, $J = 9.2$ Hz, 1H, *H*4), 4.25 (dd, $J = 12.2$ and 5.4 Hz, 1H, *H*6), 4.16 (m, 1H, *H*1), 4.09 (dd, $J = 12.2$ and 2.2 Hz, 1H, *H*7), 3.86 (m, 1H, *H*5), 2.74 (ddd, $J = 14, 10.4$, and 4.8 Hz, 1H, -CH₂Ar), 2.57 (m, 1H, -CH₂Ar), 2.02-2.10 (m, 13H, OAc (x4), CH₂CH₂Ar), 1.75 (m, 1H, CH₂CH₂Ar). ¹³C NMR (100 MHz, CDCl₃): δ 170.6, 170.1, 169.5, 139.3, 132.0, 129.7, 138.7, 71.8, 70.5, 70.3, 69.0, 62.5, 30.4, 29.7, 20.7, 20.65, 20.60. IR (film) 3346, 2094, 1644, 1226, 543 cm⁻¹. HRMS (ESI): m/z [M+H]⁺ found 471.1419, calcd 471.1422 for C₂₂H₂₈O₉Cl.



1-(2,3,4,6,-tetra-*O*-acetyl- α -D-glucopyranosyl)-2-(4-trifluorophenyl)ethane (32).

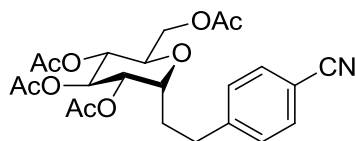
This compound was prepared according to the General Procedure A using aceto-1-bromo- α -D-glucose **12** (100 mg, 0.243 mmol, 100 mol%) and 4-trifluorostyrene (84 mg, 0.486 mmol, 200 mol%). Flash column chromatography (SiO₂: 20% ethyl acetate in hexanes) gave the desired product as a colorless oil (55 mg, 0.109 mmol, 45% yield). $[\alpha]_{\text{D}}^{25} = +23$ ($c = 28.2$). ¹H NMR (400 MHz, CDCl₃): δ 7.94 (d, $J = 7.2$ Hz, 2H), 7.24 (d, $J = 8.0$ Hz, 2H), 5.28 (t, $J = 9.2$ Hz, 1H; *H*3), 5.06 (dd, $J = 9.2$ and 5.6 Hz, 1H; *H*2), 4.96 (t, $J = 9.2$ Hz, 1H; *H*4), 4.22 (dd, $J = 12.0$ and 5.6 Hz, 1H; *H*6), 4.12-4.27 (m, 1H; *H*1), 4.05 (dd, $J = 12.0$ and 2.8 Hz, 1H, *H*7), 3.88 (s, 3H), 3.85 (ddd, $J = 9.6, 5.6, 2.8$ Hz, 1H, *H*5), 2.78 (td, $J = 9.6$ and 4.8 Hz, 1H), 2.60-2.70 (m, 1H), 2.05-2.15 (m, 1H), 2.08 (s, 3H), 2.01 (s,

3H), 2.00 (s, 3H), 1.99 (s, 3H), 1.70-1.90 (m, 1H). ^{13}C NMR (100 MHz, CDCl_3): δ 170.5, 170.0, 169.5, 169.45, 166.8, 146.2, 129.8, 128.4, 128.1, 71.7, 70.2, 70.1, 68.7, 62.2, 52.0, 31.0, 26.8, 20.7, 20.6, 20.59, 20.56. IR (film) 3459, 2959, 2924, 2848, 2109, 1747, 1645, 1419, 1369, 1327, 1226, 1162, 1119, 1067, 1034, 977, 600 cm^{-1} . HRMS (ESI): m/z $[\text{M}+\text{H}]^+$ found 505.1669, calcd 505.1685 for $\text{C}_{23}\text{H}_{28}\text{F}_3\text{O}_9$. MP = 103-105 $^\circ\text{C}$.



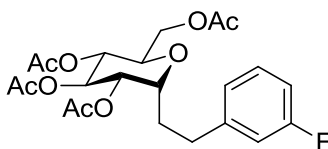
Methyl 4-(2-[2,3,4,6-tetra-O-acetyl- α -D-glucopyranosyl]ethyl)benzoate (33).

This compound was prepared according to the General Procedure A using aceto-1-bromo- α -D-glucose **12** (100 mg, 0.243 mmol, 100 mol%) and 4-methoxycarbonylstyrene (79 mg, 0.486 mmol, 200 mol%). Flash column chromatography (SiO_2 : 20% ethyl acetate in hexanes) gave a mixture of diastereomers (5:1 dr based on NMR) as a colorless oil (75 mg, 0.151 mmol, 62% yield). $[\alpha]_{\text{D}}^{25} = +41$ ($c = 44.8$). ^1H NMR (400 MHz, CDCl_3): δ 7.56 (d, $J = 8.0$ Hz, 2H), 7.31 (d, $J = 8.0$ Hz, 2H), 5.31 (t, $J = 9.2$ Hz, 1H; $H3$), 5.10 (dd, $J = 9.6$ and 5.6 Hz, 1H; $H2$), 4.99 (t, $J = 9.2$ Hz, 1H; $H4$), 4.26 (dd, $J = 12.0$ and 5.6 Hz, 1H; $H6$), 4.15-4.20 (m, 1H; $H1$), 4.10 (dd, $J = 12.0$ and 2.8 Hz, 1H, $H7$), 3.88 (ddd, $J = 9.6, 5.6, 2.8$ Hz, 1H, $H5$), 2.80-2.87 (m, 1H), 2.60-2.70 (m, 1H), 2.10-2.20 (m, 1H), 2.11 (s, 3H), 2.05 (s, 3H), 2.04 (s, 3H), 2.03 (s, 3H), 1.76-1.85 (m, 1H). ^{13}C NMR (100 MHz, CDCl_3): δ 170.6, 170.1, 169.6, 169.5, 128.7, 125.5, 125.4, 71.6, 70.3, 70.1, 68.8, 62.3, 30.9, 27.0, 20.7, 20.65, 20.6. IR (film) 3446, 2954, 2013, 1748, 1718, 1645, 1436, 1368, 1281, 1226, 1108, 1035 cm^{-1} . HRMS (ESI): m/z $[\text{M}+\text{H}]^+$ found 495.1849, calcd 495.1866 for $\text{C}_{24}\text{H}_{31}\text{O}_{11}$.



1-(2,3,4,6,-tetra-*O*-acetyl- α -D-glucopyranosyl)-2-(4-cyanophenyl)ethane (34).

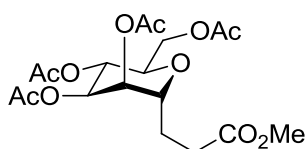
This compound was prepared according to the General Procedure A using aceto-1-bromo- α -D-glucose **12** (100 mg, 0.243 mmol, 100 mol%) and 4-cyanostyrene (63 mg, 0.488 mmol 200 mol%). Flash column chromatography (SiO₂: 25% ethyl acetate in hexanes) gave the product as a colorless oil (82 mg, 0.178 mmol, 73% yield). $[\alpha]_D^{25} = +57 (c = 20.6)$. ¹H NMR (400 MHz, CDCl₃): δ 7.60 (d, $J = 8.4$ Hz, 2H), 7.31 (d, $J = 8$ Hz, 2H), 5.30 (t, $J = 9.2$ Hz, 1H, *H*2), 5.08 (dd, $J = 9.2$ and 5.6 Hz, 1H, *H*4), 4.99 (t, $J = 9.2$ Hz, 1H, *H*3), 4.26 (dd, $J = 12.0$ and 5.6 Hz, 1H, *H*6), 4.16 (ddd, $J = 12$, 5.6, and 3.6 Hz, 1H, *H*1), 4.09 (dd, $J = 12$ and 2.8 Hz, 1H, *H*7), 3.86 (ddd, $J = 9.2$, 5.6, 2.8, 1H, *H*5), 2.83 (ddd, $J = 14.4$, 10, and 4.8 Hz, 1H, CH₂Ar), 2.68 (m, 1H, CH₂Ar), 2.207-2.17 (m, 13H, OAc (x4), CH₂CH₂Ar), 1.79 (ddd, $J = 10.8$, 7.6, and 3.6 Hz, 1H, CH₂CH₂Ar). ¹³C NMR (100 MHz, CDCl₃) δ 170.6, 170.1, 169.56, 169.52, 146.5, 132.4, 129.3, 118.9, 110.2, 71.6, 70.2, 70.1, 68.9, 68.8, 62.3, 31.2, 26.8, 20.77, 20.70, 20.65. IR (film) 3432, 2962, 2227, 2107, 1747, 1644, 1506, 1434, 1368, 1226, 1093, 1035, 977, 909, 732, 641, 602, 562 cm⁻¹. HRMS (ESI): m/z [M+H]⁺ found 462.1768, calcd 462.1764 for C₂₃H₂₈NO₉.



1-(2,3,4,6,-tetra-*O*-acetyl- α -D-glucopyranosyl)-2-(3-fluorophenyl)ethane (36).

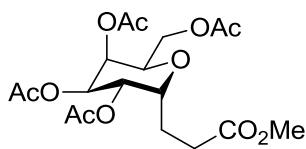
This compound was prepared according to the General Procedure A using aceto-1-bromo- α -D-glucose **12** (100 mg, 0.243 mmol, 100 mol%) and 3-fluorostyrene (58 μ L, 0.448 mmol, 200 mol%). Flash column chromatography (SiO₂: 20% ethyl acetate in hexanes) gave the product as a colorless oil (39 mg, 0.086 mmol, 35% yield). $[\alpha]_D^{25} = +49 (c = 8.8)$. ¹H NMR (400 MHz, CDCl₃): δ 7.25 (m, 1H), 6.96 (d, $J = 7.6$ Hz, 1H), 6.90 (d, $J = 9.2$ Hz, 2H), 5.30 (t, $J = 9.2$ Hz, 1H *3H*), 5.09 (dd, $J = 9.2$ and 5.6 Hz, 1H, *H*2), 4.99 (t, $J = 9.2$ Hz, 1H *H*4), 4.25 (dd, $J = 12.0$ and 5.6 Hz, 1H, *H*6), 4.17 (ddd, J

= 9.2, 5.6, and 3.6 Hz, 1H, *H1*) 4.08 (dd, *J* = 12.0 and 2.4 Hz, 1H, *H7*), 3.86 (ddd, *J* = 8.8, 5.6, and 2.4 Hz, 1H, *H5*), 2.77 (ddd, *J* = 14, 9.6, and 4.8 Hz, 1H, -CH₂Ar), 2.60 (m, 1H, -CH₂Ar), 2.02-2.14 (m, 13H, 4 - OAc + -CH₂-), 1.80 (m, 1H, -CH₂-). ¹³C NMR (100MHz, CDCl₃): δ 170.9, 170.1, 169.63, 169.57, 164.2, 161.7, 143.44, 143.38, 130.1, 130.0, 124.1, 124.0, 115.4, 115.2, 113.27, 113.07, 71.8, 70.4, 70.2, 68.85, 68.79, 30.86, 27.0, 20.8, 20.73, 20.71, 20.67. IR (film) 3430, 2096, 1745, 1645, 1368, 1226, 1034 cm⁻¹. HRMS (ESI): *m/z* [M+H]⁺ found 455.1702, calcd 455.1717 for C₂₂H₂₈O₉F.



Methyl 3-(2,3,4,6-tetra-*O*-acetyl- α -D-mannopyranosyl)propanoate (43).

This compound was prepared according to the General Procedure A using 2,3,4,6-tetra-*O*-acetyl- α -mannosyl bromide (100 mg, 0.243 mmol, 100 mol%) and methyl acrylate (42 mg, 0.486 mmol, 200 mol%). Flash column chromatography (SiO₂: 20% ethyl acetate in hexanes) gave the desired product⁶⁹ as a colorless oil (77 mg, 0.18 mmol, 76% yield).



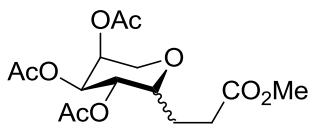
Methyl 3-(2,3,4,6-tetra-*O*-acetyl- α -D-galactopyranosyl)propanoate (44).

This compound was prepared according to the General Procedure A using 2,3,4,6-tetra-*O*-acetyl- α -D-galactosyl bromide (100 mg, 0.243 mmol, 100 mol%) and methyl acrylate (42 mg, 0.486 mmol, 200

⁶⁹ a) Maity, S. K.; Dutta, S. K.; Banerjee, A. K.; Achari, B.; Singh, M. *Tetrahedron* **1994**, 50, 6965-6974. b)

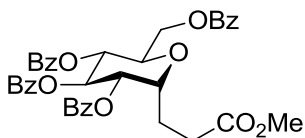
Ghosez, A.; Göbel, T.; Giese, B. *Chem. Ber.* **1988**, 121, 1807-1811.

mol%). Flash column chromatography (SiO₂: 20% ethyl acetate in hexanes) gave the desired product^{67b} as a colorless oil (61 mg, 0.15 mmol, 60% yield).



Methyl 3-(2,3,4-tri-*O*-acetyl-β-D-arabinopyranosyl)propanoate (45).

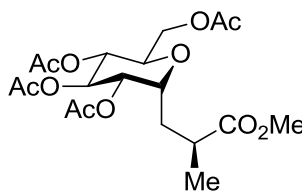
This compound was prepared according to the General Procedure A using tri-*O*-acetyl- β -D-arabinosyl bromide (83 mg, 0.243 mmol, 100 mol%) and methyl acrylate (42 mg, 0.486 mmol, 200 mol%). Flash column chromatography (SiO₂: 20% ethyl acetate in hexanes) gave an inseparable mixture of diastereomers (2.5:1 dr based on NMR) as a colorless oil (51 mg, 0.148 mmol, 61% yield). ¹H NMR (400 MHz, CDCl₃) for the major isomer: [α]_D²⁵ = -12 (*c* = 24.6). δ 5.28 (t, *J* = 3.2 Hz, 1H), 5.14 (ddd, *J* = 10.4, 5.2 and 1.6 Hz, 1H), 4.92 (d, *J* = 2.8 Hz, 1H), 3.81 (dd, *J* = 11.2 and 5.2 Hz, 1H), 3.77 (dd, *J* = 10.0 and 2.4 Hz, 1H), 3.66 (s, 3H), 3.60 (t, *J* = 10.8 Hz, 1H), 2.42 (ddd, *J* = 16.0, 7.6, 2.4 Hz, 2H), 2.14 (s, 3H), 2.12 (s, 3H), 1.98 (s, 3H), 1.64-1.85 (m, 2H). ¹³C NMR (100 MHz, CDCl₃): δ 173.5, 169.7, 169.2, 72.9, 69.8, 66.6, 65.5, 63.5, 51.6, 29.9, 25.2, 21.0, 20.8, 20.7. IR (film) 3434, 2090, 1741, 1645, 1437, 1372, 1224, 1056, 604 cm⁻¹. HRMS (ESI): *m/z* [M+H]⁺ found 347.1329, calcd 347.1342 for C₁₅H₂₃O₉.



Methyl 3-(2,3,4,6-tetra-*O*-benzoyl-α-D-glucopyranosyl)propanoate (46).

This compound was prepared according to the General Procedure A using benzoyl-1-bromo- α -D-glucose **41** (160 mg, 0.243 mmol, 100 mol%) and methyl acrylate (42 mg, 0.486 mmol, 200 mol%). Flash column chromatography (SiO₂: 15% ethyl acetate in hexanes) gave the desired product as a

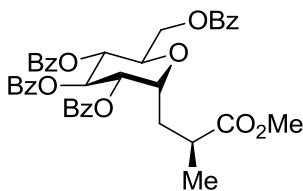
white solid (100 mg, 0.151 mmol, 62% yield). $[\alpha]_D^{25} = +33$ ($c = 32.5$). ^1H NMR (400 MHz, CDCl_3): δ 8.06 (dd, $J = 6.8$ and 1.6 Hz, 2H), 7.99 (dd, $J = 7.2$ and 1.2 Hz, 2H), 7.90-7.94 (m, 4H), 7.31-7.56 (m, 12H), 6.00 (t, $J = 8.8$ Hz, 1H; $H3$), 5.60 (t, $J = 8.8$ Hz, 1H; $H4$), 5.54 (dd, $J = 8.8$ and 5.6 Hz, 1H; $H2$), 4.56 (dd, $J = 12.0$ and 5.6 Hz, 1H; $H6$), 4.53 (dd, $J = 12.0$ and 3.2 Hz, 1H; $H7$), 4.50-4.54 (m, 1H; $H1$) 4.34 (ddd, $J = 8.8$, 5.6 Hz, 3.2 Hz, 1H; $H5$), 3.65 (s, 3H), 2.36-2.61 (m, 3H), 1.99-2.08 (m, 1H). ^{13}C NMR (100 MHz, CDCl_3): δ 173.3, 166.1, 165.6, 165.3, 165.2, 133.5, 133.4, 133.3, 133.1, 129.84, 129.81, 129.7, 129.5, 129.0, 128.8, 128.7, 128.5, 128.3, 71.9, 70.9, 70.2, 69.7, 69.3, 62.9, 51.7, 29.6, 21.2. IR (film) 3459, 2359, 2341, 2096, 1725, 1645, 1451, 1315, 1269, 1177, 1093, 1069, 1026, 709 cm^{-1} . HRMS (ESI): m/z $[\text{M}+\text{H}]^+$ found 667.2204, calcd 667.2179 for $\text{C}_{38}\text{H}_{35}\text{O}_{11}$. MP = 123-124 $^{\circ}\text{C}$.



(2S)-methyl 2-methyl-3-(2,3,4,6-tetra-O-acetyl- α -D-glucopyranosyl)propanoate (27).

To a flame-dried Schlenk tube equipped with a stir bar was loaded (*S*)-Ph-PyBox, (**22**) (0.014 g, 0.037 mmol, 15 mol%) and NH_4Br (48 mg, 0.49 mmol). The tube was moved to a dry glove box, at which point $\text{Ni}(\text{COD})_2$ (0.007 g, 0.024 mmol, 10 mol%) and Zn powder (0.016 g, 0.243 mmol, 100 mol%) were added. After the tube was moved out of the glove box, DMA (1.0 mL) was added. The mixture was allowed to stir for 5 min, and a typical dark blue solution formed. Under N_2 atmosphere, aceto-1-bromo- α -D-glucose **12** (100 mg, 0.243 mmol, 100 mol%) was added in one portion followed by the addition of methyl methacrylate (52 μL , 0.488 mmol, 200 mol%). After the resulting mixture was stirred for 12 h at 25 $^{\circ}\text{C}$, it was directly loaded onto a silica column without work-up (the residue was rinsed with small amount of CH_2Cl_2). Flash column chromatography (SiO_2 : 20% ethyl acetate in hexanes) gave an inseparable mixture of diastereomers (1:1 dr based on ^1H NMR) as a

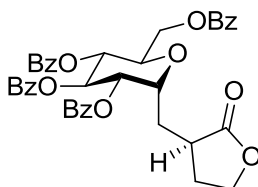
colorless oil (75 mg, 0.174 mmol, 72% yield). $[\alpha]_D^{25} = +48$ ($c = 14.2$). ^1H NMR (500 MHz, C_6D_6): δ 5.57 (t, $J = 9.0$ Hz, 1H, $H3$ 1st diast.), 5.56 (t, $J = 9.5$ Hz, 1H, $H3$ 2nd diast.), 5.29 (t, $J = 9.25$ Hz, 1H, $H4$ 2nd diast.), 5.25-5.27 (2 dd, $J = 6$ and 2 Hz, $H2$ 1st and 2nd diast.), 5.18 (t, $J = 9.25$ Hz, 1H, $H4$ 1st diast.), 4.37 (ddd, $J = 11.5$, 5.5, and 3 Hz, 1H, $H1$ 2nd diast.), 4.05-4.29 (m, 5H, $H1$ 1st diast. + $H6$ 1st and 2nd diast. + $H7$ 1st and 2nd diast.), 3.88 (ddd, $J = 10$, 4.5, and 3 Hz, 1H, $H5$ 2nd diast.), 3.71 (ddd, $J = 9$, 5.5, and 2.5 Hz, 1H, $H5$ 1st diast.), 3.37 (s, 3H, -OMe 2nd diast.), 3.28 (s, 3H, -OMe 1st diast.), 2.58 (ddd, $J = 7$, 7, and 4 Hz, 1H, 2nd diast.), 2.38 (sextet, $J = 7$ Hz, 1H, 1st diast.), 2.18 (ddd, $J = 15$, 12, and 7.5 Hz, 1H, 1st diast.) 1.94 (ddd, $J = 17.5$, 14.5, 8, 1H, 2nd diast.) 1.55-1.73 (m, 24H 1st and 2nd diast + 1H 2nd diast.), 1.42 (ddd, $J = 15$, 7, and 3 Hz, 1H, 1st diast.), 1.02 (d, $J = 7$ Hz, 3H, 1st diast.), 0.97 (d, $J = 7$ Hz, 3H, 2nd diast.). ^{13}C NMR (125 MHz, C_6D_6): δ 175.4, 174.8, 169.3, 169.2, 169.0, 168.9, 168.42, 168.36, 168.31, 168.2, 71.0, 70.3, 70.2, 69.9, 69.83, 69.76, 68.4, 68.6, 68.5, 68.3, 61.5, 61.2, 61.5, 61.2, 50.6, 50.5, 35.9, 34.8, 19.49, 19.46, 19.43, 19.4, 19.38, 19.30, 19.28, 17.38, 16.33. IR (film) 3448, 2956, 2110, 1748, 1646, 1436, 1369, 1226, 1142, 1097, 1035, 982, 909, 603 cm^{-1} . HRMS (ESI): m/z $[\text{M}+\text{H}]^+$ found 433.1701, calcd 433.1710 for $\text{C}_{19}\text{H}_{29}\text{O}_{11}$.



(2S)-methyl 2-methyl-3-(2,3,4,6-tetra-O-benzoyl- α -D-glucopyranosyl)propanoate (48).

This compound was prepared according to the General Procedure B using benzoyl-1-bromo- α -D-glucose **41** (160 mg, 0.243 mmol, 100 mol%) and methyl methacrylate (49 mg, 0.486 mmol, 200 mol%). Flash column chromatography (SiO_2 : 15% ethyl acetate in hexanes) gave a mixture of diastereomers (5:1 dr based on NMR) as a white solid (133 mg, 0.194 mmol, 80% yield). The major isomer was isolated by recrystallization from diethyl ether. $[\alpha]_D^{25} = +47$ ($c = 22.4$). ^1H NMR (400

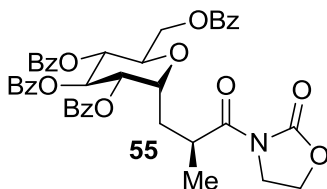
MHz, CDCl₃): δ 8.07 (dd, J = 7.6 and 0.8 Hz, 2H), 8.01 (dd, J = 7.6 and 1.2 Hz, 2H), 7.91-7.94 (m, 4H), 7.31-7.57 (m, 12H), 5.95 (t, J = 8.4 Hz, 1H; H_3), 5.56 (t, J = 8.4 Hz, 1H; H_4), 5.52 (dd, J = 8.8 and 3.6 Hz, 1H; H_2), 4.50-4.60 (m, 3H; H_6 , H_7 and H_1), 4.31-4.35 (m, 1H; H_5), 2.70-2.85 (m, 2H), 2.05-2.13 (m, 2H), 1.26 (d, J = 7.2 Hz, 3H). ¹³C NMR (100 MHz, CDCl₃): δ 176.0, 166.2, 165.6, 165.3, 133.4, 133.3, 133.1, 129.84, 129.8, 129.7, 129.5, 129.0, 128.8, 128.4, 128.37, 128.3, 70.7, 70.6, 70.1, 69.3, 63.0, 51.7, 35.3, 29.9, 18.1. IR (film) 3435, 2092, 1721, 1645, 1451, 1315, 1268, 1177, 1093, 1069, 1026, 709 cm⁻¹. HRMS (ESI): m/z [M+H]⁺ found 681.2351, calcd 681.2336 for C₃₉H₃₇O₁₁. MP = 169-170 °C.



α -[2,3,4,6-tetra-*O*-benzoyl- α -D-glucopyranosyl-1-methyl]- γ -butyrolactone (54).

This compound was prepared according to the General Procedure B using benzoyl-1-bromo- α -D-glucose **41** (79 mg, 0.12 mmol), Ni(COD)₂ (3.3 mg, 0.012 mmol), (*R*)-PhPyBox **20** (6.6 mg, 0.018 mmol), α -methylene- γ -butyrolactone (**49**) (20 μ L, 0.24 mmol), 2,4-dimethyl-3-pentanol (34 μ L, 0.24 mmol), Zn (7.8 mg, 0.12 mmol), and DMA (0.8 mL). Flash column chromatography (SiO₂: 60-70% Et₂O in hexanes) provided the pure major isomer as a white solid (40 mg, 0.060 mmol, 50%). $[\alpha]_D^{25}$ = +29 (c = 2.5). ¹H NMR (400 MHz): δ = 8.06-7.89 (m, 8H), 7.59-7.25 (m, 12H), 5.90 (t, J = 7.8 Hz, 1H), 5.51 (t, J = 7.4 Hz, 1H), 5.48 (dd, J = 8.1, 4.9 Hz, 1H), 4.78-4.72 (m, 2H), 4.52 (dd, J = 12.1, 3.4 Hz, 1H), 4.42 (ddd, J = 3.4, 7.0, 14.1 Hz, 1H), 4.18 (td, J = 8.7, 1.9 Hz, 1H), 3.90 (ddd, J = 10.4, 9.2, 6.3 Hz, 1H), 2.67 (m, 1H), 2.37 (dddd, J = 14.7, 10.6, 6.3, 1.9 Hz, 1H), 2.20 (t, J = 6.7 Hz, 2H), 2.03 (m, 1H). ¹³C NMR (100 MHz): δ = 178.7, 166.1, 165.384, 165.375, 165.3, 133.6, 133.49, 133.48, 133.3, 130.0, 129.9, 129.8, 129.7, 129.6, 128.9, 128.1, 128.6, 128.51, 128.48, 128.4, 70.9, 70.7, 70.3, 69.5, 68.8, 66.5, 62.5, 37.0, 29.2, 27.2. IR (film) 3067, 2948, 2359, 1769, 1724, 1646,

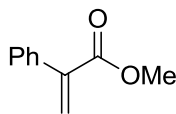
1601, 1451, 1375, 1315, 1269, 1176, 1093, 1069, 1026, 710 cm⁻¹. HRMS (ESI): m/z [M+H]⁺ found 679.2200, calcd 679.2179 for C₃₉H₃₅O₁₁. MP = 195-197 °C



(2S)-3-(2-methyl-3-[2,3,4,6-tetra-O-benzoyl- α -D-glucopyranosyl]propanoyl)oxazolidin-2-one (55).

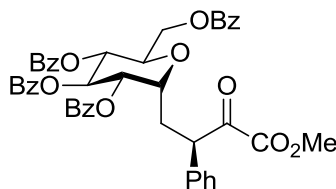
This compound was prepared according to the General Procedure B using benzoyl-1-bromo- α -D-glucose **41** (0.160 mg, 0.243 mmol, 100 mol%) and 3-methacryloyloxazolidin-2-one⁷⁰ (0.074 g, 0.486 mmol, 200 mol%). Flash column chromatography (SiO₂: 30% ethyl acetate in hexanes) gave a mixture of diastereomers (5:1 dr based on NMR) as a white solid (0.132 g, 0.180 mmol, 74% yield). The major isomer was isolated by recrystallization from diethyl ether. $[\alpha]_D^{25} = +60$ ($c = 16.1$). ¹H NMR (400 MHz, CDCl₃): δ 8.07 (d, $J = 7.2$ Hz, 2H), 8.02 (d, $J = 7.2$ Hz, 2H), 7.91-7.93 (m, 4H), 7.31-7.56 (m, 12H), 5.97 (t, $J = 8.8$ Hz, 1H; H_3), 5.63 (t, $J = 8.8$ Hz, 1H; H_4), 5.51 (dd, $J = 8.8$ and 5.6 Hz, 1H; H_2), 4.62 (dd, $J = 12.4$ and 3.2 Hz, 1H; H_6), 4.52 (dd, $J = 12.0$ and 4.8 Hz, 1H; H_7), 4.50-4.56 (m, 1H; H_1), 4.36 (t, $J = 8.4$ Hz, 2H; O=C(N)O-CH₂), 4.31 (ddd, $J = 8.8$, 4.4 and 3.2 Hz, 1H; H_5), 3.92-4.06 (m, 3H; (O=C)N(C=O)-CH₂ and Me-CH(CH₂)CON-), 2.20 (m, 2H), 1.32 (d, $J = 6.8$ Hz, 3H). ¹³C NMR (100 MHz, CDCl₃): δ 175.8, 166.1, 165.6, 165.3, 165.1, 152.9, 133.3, 133.26, 133.1, 129.8, 129.77, 129.7, 129.67, 129.50, 129.0, 128.9, 128.8, 128.4, 128.37, 128.3, 70.7, 70.6, 70.2, 70.1, 69.1, 62.5, 61.8, 42.6, 33.8, 29.4, 18.5. IR (film) 3434, 2091, 1777, 1723, 1646, 1451, 1386, 1269, 1093, 1069, 1026, 710 cm⁻¹. HRMS (ESI): m/z [M+H]⁺ found 736.2380, calcd 736.2394 for C₄₁H₃₇NO₁₂. MP = 157-160 °C.

⁷⁰ Sibi, M. P.; Sausker, J. B. *J. Am. Chem. Soc.* **2002**, *124*, 984-991.



Methyl 2-phenylacrylate (51).

A 50 mL flame dry round bottom flask under nitrogen was charged with 18 mL THF, and the flask was cooled to -78 °C. Methyl triphenylphosphonium bromide (2.3 g, 6.4 mmol, 105 mol%) and diisopropylamine (85 μ L, 0.61 mmol, 10 mol%) were added, followed by a dropwise addition of *n*butyllithium (2.44 mL of 2.5M in hexanes, 6.1 mmol, 100 mol%). The solution was allowed to warm to room temperature. After 1 hour, the solution was then cooled to -78 °C, and methyl benzoyl formate (1 g, 6.1 mmol, 100 mol%) was added dropwise. This created a yellow suspension, which was warmed to room temperature and allowed to stir for 18 h. The reaction was quenched with 1 M HCl (1 mL) and diluted with brine (10 mL). The layers were separated, and the aqueous layer was extracted twice with diethyl ether. The combined organic layers were washed twice with brine, dried with MgSO₄, filtered, and concentrated in vacuo. Flash column chromatography (SiO₂: 5% ethyl acetate in hexanes) gave the desired product⁷¹ as a clear oil (550 mg, 3.4 mmol, 56% yield)

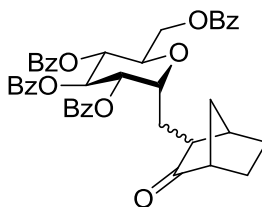


(2R)-methyl 2-phenyl-3-(2,3,4,6-tetra-*O*-benzoyl- α -D-glucopyranosyl)propanoate (56).

This compound was prepared according to the General Procedure B using benzoyl-1-bromo- α -D-glucose **41** (0.160 mg, 0.243 mmol, 100 mol%) and methyl 2-phenylacrylate (80 mg, 0.488 mmol, 200 mol%). Flash column chromatography (SiO₂: 5%-20% ethyl acetate in hexanes) gave an

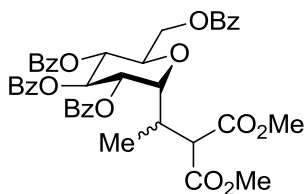
⁷¹ Peng, C., Wang, Y., Wang, J.; *J. Am. Chem. Soc.* **2008**, *130*, 1566-1567.

inseparable mixture of diastereomers (dr = 1.6:1) as a white amorphous solid (84 mg, 0.113 mmol, 46% yield). $[\alpha]_D^{25} = +32$ ($c = 15.0$). ^1H NMR (500 MHz, C_6D_6): δ 7.95–8.34 (m, Ar), 6.79–7.27 (m, Ar), 6.41 (t, $J = 9.1$ Hz, 1H, $H3$ minor diast.) 6.32 (t, $J = 8.9$ Hz, 1H, $H3$ major diast.), 5.92 (t, $J = 9.0$ Hz, 1H, $H4$ minor diast.), 5.79 (dd, $J = 9.2$ and 5.7 Hz, 1H, $H2$ major diast.), 5.75 (t, $J = 8.6$ Hz, 1H, $H4$ major diast.), 5.69 (dd, $J = 9.4$ and 5.8 Hz, 1H, $H2$ minor diast.), 4.91 (ddd, $J = 11.6$, 5.6, and 3 Hz, 1H, $H1$ major diast.), 4.70 (dd, $J = 12.1$ and 3 Hz, 1H, $H6/7$ minor diast.), 4.43–4.58 (m, 1H CH major diast., 1H $H6/7$ major diast., 1H $H6/7$ minor diast., 1H $H5$ minor diast., 1H $H1$ minor diast.), 4.22 (ddd, $J = 15$, 6.3, and 3.2 Hz, 1H, $H5$ major diast.), 4.06 (dd, $J = 11.1$ and 3.8 Hz, 1H, $H6/7$ major diast.), 3.89 (dd, $J = 8.2$ and 6.7 Hz, 1H, CH minor diast.), 3.29 (s, 3H, -OMe minor diast.), 3.10 (s, 3H, -OMe major diast.), 3.05 (m, 1H, CH_2 minor diast.), 2.84 (ddd, $J = 14.4$, 11.2, and 3 Hz, 1H, CH_2 major diast.), 2.40 (ddd, $J = 14.8$, 11.6, and 3.8 Hz, 1H, CH_2 major diast.), 2.35 (ddd, $J = 14.6$, 8.2, and 2.5 Hz, 1H, CH_2 minor diast.). ^{13}C NMR (125 MHz, C_6D_6): δ 173.2, 172.4, 165.4, 165.32, 165.29, 164.88, 164.83, 164.77, 164.5, 138.9, 137.6, 132.54, 132.51, 132.47, 132.34, 132.30, 132.9, 129.8, 129.49, 129.45, 129.44, 129.41, 129.38, 129.31, 128.26, 129.24, 128.94, 128.90, 128.86, 128.81, 128.76, 128.68, 128.45, 128.40, 128.34, 127.94, 127.90, 127.85, 127.83, 127.82, 127.78, 127.63, 128.11, 126.9, 71.1, 70.86, 70.80, 70.76, 70.5, 70.2, 69.8, 69.7, 69.6, 69.4, 62.8, 62.5, 47.7, 46.8, 29.6, 29.1. IR (film) 3438, 3063, 2952, 2279, 1729, 1601, 1493, 1452, 1315, 1268, 1177, 1093, 1069, 1027, 710 cm^{-1} . HRMS (ESI): m/z $[\text{M}+\text{H}]^+$ found 743.2461, calcd 743.2492 for $\text{C}_{44}\text{H}_{39}\text{O}_{11}$.



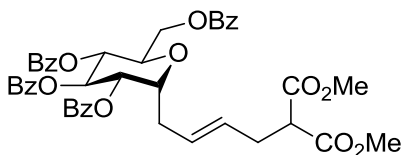
3-[2,3,4,6-tetra-*O*-benzoyl- α -D-glucopyranosyl-1-methyl]-bicyclo[2.2.1]heptan-2-one (57).

This compound was prepared according to the General Procedure B using benzoyl-1-bromo- α -D-glucose **41** (79 mg, 0.12 mmol), Ni(COD)₂ (3.3 mg, 0.012 mmol), (*R*)-PhPyBox **20** (6.6 mg, 0.018 mmol), 3-methylene-2-norbornanone **52** (30 μ L, 0.24 mmol), 2,4-dimethyl-3-pentanol (34 μ L, 0.24 mmol), Zn (7.8 mg, 0.12 mmol), and DMA (0.8 mL). Flash column chromatography (SiO₂: 30-40% EtOAc in hexanes) provided the product as a white solid (68 mg, 0.097 mmol, 79%, 1.7:1 mixture of diastereomers). $[\alpha]_D^{25} = +29$ ($c = 2.5$). A small sample was purified via SFC (CO₂/THF) to obtain ¹H NMR (400 MHz) for the major and minor diastereomers. Major isomer: δ 8.05-7.86 (m, 8H), 7.59-7.25 (m, 2H), 5.89 (t, $J = 6.2$ Hz, 1H), 5.48 (dd, $J = 8.1, 4.7$ Hz, 1H), 5.47 (t, $J = 7.4$ Hz), 4.71-4.64 (m, 2H), 4.54 (dd, $J = 12.1, 3.5$ Hz, 1H), 4.33 (td, $J = 7.3, 3.5$ Hz, 1H), 2.62 (br m, 1H), 2.52 (d, $J = 4.5$ Hz, 1H), 2.17 (m, 1H), 1.98 (ddd, $J = 14.8, 5.9, 3.7$ Hz, 1H), 1.87 (ddd, $J = 14.9, 10.7, 7.3$ Hz, 1H), 1.75 (m, 1H), 1.57 (m, 2H), 1.45-1.33 (m, 3H). Minor Diastereomer: $\delta = 8.03$ -7.84 (m, 8H), 7.58-7.26 (m, 12H), 6.02 (t, $J = 7.2$ Hz, 1H), 5.56 (t, $J = 9.2$ Hz, 1H), 5.48 (dd, $J = 9.5, 5.8$ Hz, 1H), 4.57 (dd, $J = 12.1, 6.5$ Hz, 1H), 4.49-4.42 (m, 2H), 4.34 (ddd, $J = 12.0, 6.6, 2.8$ Hz, 1H), 2.63 (br m, 1H), 2.58 (d, $J = 4.9$ Hz, 1H), 2.50 (ddd, $J = 15.6, 13.6, 3.7$ Hz, 1H), 2.24 (dt, $J = 11.4, 3.6$ Hz, 1H), 1.98 (m, 1H), 1.78 (m, 1H), 1.45 (m, 2H), 1.42 (m, 1H), 1.31 (m, 2H). For the mixture: ¹³C NMR (100 MHz): $\delta = 219.6$ (minor), 218.8 (major), 166.1 (major), 166.0 (minor), 165.6 (minor), 165.43 (minor), 165.41 (major), 165.34 (major), 165.32 (major), 165.3 (minor), 133.6 (minor), 133.5 (minor), 133.43 (minor), 133.40 (major), 133.22 (minor), 133.19 (major), 133.16 (minor), 129.88, 129.85, 129.83, 129.73, 129.67, 129.65, 129.60, 129.57, 129.0, 128.9, 128.82, 128.81, 128.68, 128.67, 128.53, 128.47, 128.44, 128.41, 128.38, 128.33, 128.32, 77.2, 71.7, 71.4, 70.7, 70.5, 70.4, 70.3, 69.6, 69.5, 69.4, 69.0, 63.1 (minor), 62.7 (major), 50.8 (major), 50.2 (minor), 50.1 (major), 49.0 (minor), 39.8 (major), 37.4 (minor), 37.0 (major), 36.9 (minor), 25.5, 25.4, 24.0, 21.9, 21.7, 21.0. IR (film) 3064, 2958, 2878, 2340, 2254, 1968, 1914, 1729, 1601, 1584, 1451, 1315, 1269, 1177, 1093, 1027, 911, 710 cm⁻¹. HRMS (ESI): m/z [M+H]⁺ found 703.2552, calcd 703.2543 for C₄₂H₃₉O₁₀. MP = 177-180 °C.



Dimethyl 2-(1-[2,3,4,6-tetra-*O*-benzoyl- α -D-glucopyranosyl]ethyl)malonate (58**).**

This compound was prepared according to the General Procedure B using benzoyl-1-bromo- α -D-glucose **41** (0.160 g, 0.243 mmol, 100 mol%) and dimethyl 2-ethylidenemalonate **53** (0.077 g, 0.486 mmol, 200 mol%). Flash column chromatography (SiO₂: 15% ethyl acetate in hexanes) gave an inseparable mixture of diastereomers (1.2:1 dr based on NMR) as an amorphous solid (0.100 g, 0.136 mmol, 56% yield). $[\alpha]_D^{25} = +50$ ($c = 26.8$). ¹H NMR (400 MHz, CDCl₃) for the major isomer: δ 7.13-8.21 (m, 20H), 5.81 (t, $J = 4.4$ Hz, 1H; *H3*), 5.53 (dd, $J = 4.4$ and 2.4 Hz, 1H; *H2*), 5.37 (t, $J = 4.0$ Hz, 1H; *H4*), 5.02 (dd, $J = 12.0$ and 8.8 Hz, 1H; *H6*), 4.57-4.65 (m, 1H, *H7*), 4.44-4.51 (m, 2H, *H1* and *H5*), 4.04 (d, $J = 4.4$ Hz, 1H), 3.64 (s, 3H), 3.57 (s, 3H), 2.75-2.90 (m, 1H), 1.20 (d, $J = 6.8$ Hz, 1H). ¹H NMR (400 MHz, CDCl₃) for the minor isomer: δ 7.13-8.21 (m, 20H), 5.76 (t, $J = 3.2$ Hz, 1H; *H3*), 5.44 (dd, $J = 3.2$ and 2.4 Hz, 1H; *H2*), 5.39 (t, $J = 3.2$ Hz, 1H; *H4*), 4.90 (dd, $J = 11.2$ and 8.0 Hz, 1H; *H6*), 4.57-4.65 (m, 2H, *H5* and *H1*), 4.49 (dd, $J = 12.0$ and 4.4 Hz, 1H, *H7*), 3.69 (d, $J = 5.6$ Hz, 1H), 3.68 (s, 3H), 3.63 (s, 3H), 2.75-2.90 (m, 1H), 1.06 (d, $J = 6.8$ Hz, 1H). For the mixture: ¹³C NMR (100 MHz, CDCl₃): δ 169.6, 168.8, 168.3, 166.2, 165.4, 165.3, 164.6, 164.4, 133.8, 133.7, 133.6, 133.5, 133.3, 133.2, 130.2, 130.0, 129.8, 129.7, 129.6, 129.5, 129.1, 128.9, 128.7, 128.65, 128.6, 128.5, 128.4, 128.35, 128.2, 128.15, 73.4, 73.2, 70.1, 68.2, 67.8, 67.3, 67.0, 66.8, 61.2, 52.5, 52.3, 52.2, 52.1, 51.5, 33.9, 33.5, 13.0, 12.1. IR (film) 3434, 2092, 1778, 1724, 1644, 1451, 1386, 1315, 1269, 1177, 1094, 1069, 1026, 710 cm⁻¹. MS (ESI): m/z [M+H]⁺ found 739.2, calcd 739.2 for C₄₁H₃₉O₁₃.



(E)-Dimethyl 2-(4-[2,3,4,6-tetra-O-benzoyl- α -D-glucopyranosyl]but-2-enyl)malonate (60).

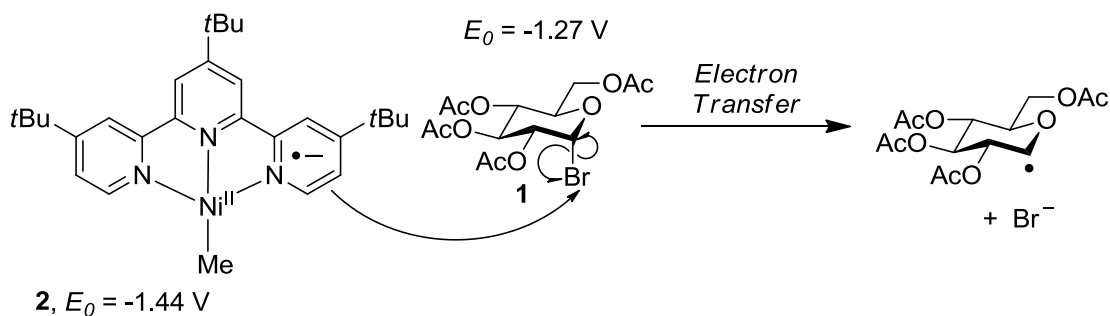
This compound was prepared according to the General Procedure A using benzoyl-1-bromo- α -D-glucose **41** (0.320 g, 0.488 mmol, 100 mol%) and cyclopropyl malonate⁷² **59** (180 mg, 0.976 mmol). Flash column chromatography (SiO₂: 20% ethyl acetate in hexanes) followed by purification on preparative SFC in MeCN gave the desired ring-opened product as a clear oil. $[\alpha]_D^{25} = +34$ ($c = 1.1$). ¹H NMR (500 MHz, C₆D₆): δ 6.82-8.25 (m, 20H, -OBz), 6.31 (t, $J = 9$ Hz, 1H, H_3), 5.79 (t, $J = 8.5$ Hz, 1H, H_4), 5.70 (dd, $J = 9$ and 5.5 Hz, 1H, H_2), 5.32-5.42 (m, 2H, -HC=CH-), 4.59-4.66 (m, 2H, $H_6 + H_7$), 4.47 (ddd, $J = 10.5, 4.5$, and 4.5 Hz, 1H, H_1), 3.29-3.33 (m, 4H, -OMe + CH), 2.52 (t, $J = 7$ Hz, 2H, -CH₂CH(CO₂Me)₂), 2.49 (ddd, $J = 17, 11.5$, and 6.5 Hz, 1H, -CH₁CH₂CH=C), 2.18-2.24 (m, 1H, -CH₁CH₂CH=C). ¹³C NMR (125 MHz, C₆D₆): δ 169.08, 169.07, 166.1, 166.0, 165.5, 165.3, 133.3, 133.2, 133.0, 130.5, 130.1, 130.0, 129.9, 129.7, 129.6, 129.5, 129.1, 128.62, 128.6, 128.5, 128.1, 127.9, 72.4, 71.6, 71.0, 70.2, 70.0, 63.2, 53.2, 51.9, 32.1, 31.9, 29.8, 23.0, 14.3. IR (film) 3066, 3030, 2953, 2922, 2849, 1754, 1729, 1452, 1268, 1094, 1069, 1027, 711 cm⁻¹. HRMS (ESI): m/z [M+H]⁺ found 765.2538, calcd 765.2547 for C₄₃H₄₁O₁₃.

⁷² Perreault, C.; Goudreau, S. R.; Zimmer, L. E.; Charette, A. B. *Org. Lett.* **2008**, *10*, 689-692, and references therein.

Chapter 3 – Light Mediated Radical C-Glycoside Synthesis.

Photoredox Catalysis: Background.

Since ATRP-based catalysts were ineffective for C-glycosylations with glycosyl bromides, we considered the possibility of glycosyl radical generation via outer-sphere electron transfer. Vicic and Phillips both proposed electron transfer as the key step in the activation of alkyl halides in nickel-catalyzed Negishi cross-couplings.^{51,52} While our nickel-catalyzed conjugate addition likely proceeds through a different mechanism, it is possible that activation of the glycosyl halide to form the radical is a redox process rather than a halide abstraction. The E_0 of α -acetobromo-D-glucose (**1**) was reported as -1.27V (vs SCE),⁷³ whereas a (*t*Bu-Terpy)Ni^IMe (**2**) has a $E_0 = -1.44$ V (vs SCE).⁵¹ These reduction potentials suggest these nickel catalysts can serve as a reductant in order to generate glycosyl radicals via electron transfer (Scheme 3.1).



Scheme 3.1: Reduction of Glycosyl Bromides by Nickel(I) Complex

To test this hypothesis, we envisioned the use of polypyridine ruthenium complexes as outer-sphere reductants, namely tris(bipyridine)ruthenium(II), or Ru(bpy)₃²⁺ (**3**, Figure 3.1).

⁷³ Rondinini, S. B.; Mussini, P. R.; Crippa, F.; Sello, G., *Electrochem. Commun.* **2000**, 2, 491-496.

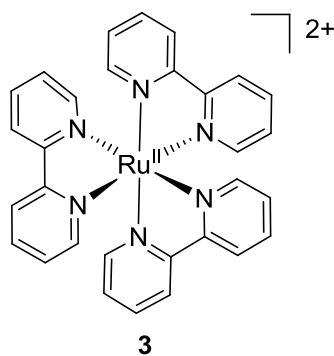
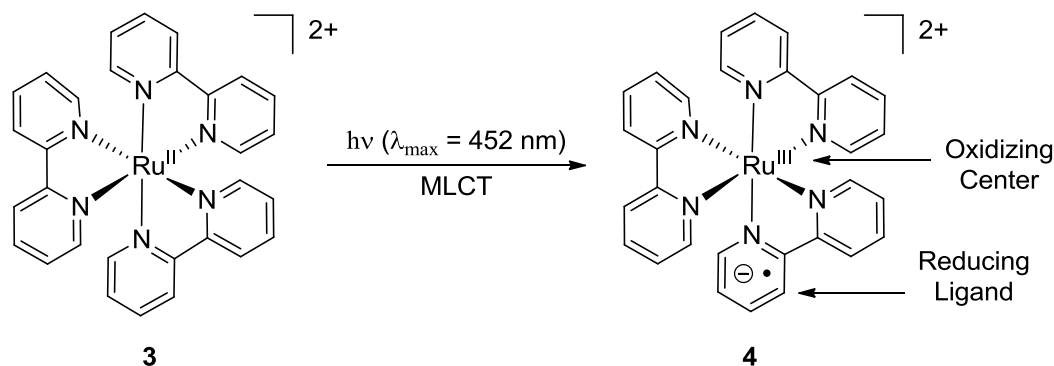


Figure 3.1: Structure of Trisbipyridine Ruthenium(II).

First reported in 1936 by Burstall,⁷⁴ $\text{Ru}(\text{bpy})_3^{2+}$ has been used to study a plethora of processes, from the photophysical properties of polypyridine ruthenium complexes to the redox transformations including reduction and oxidation of water.⁷⁵ This chemically robust complex serves as a photosensitizer, absorbing visible light ($\lambda_{\text{max}} = 452 \text{ nm}$ in MeCN), which triggers a metal-ligand charge transfer (MLCT) to either a singlet or triplet excited state.



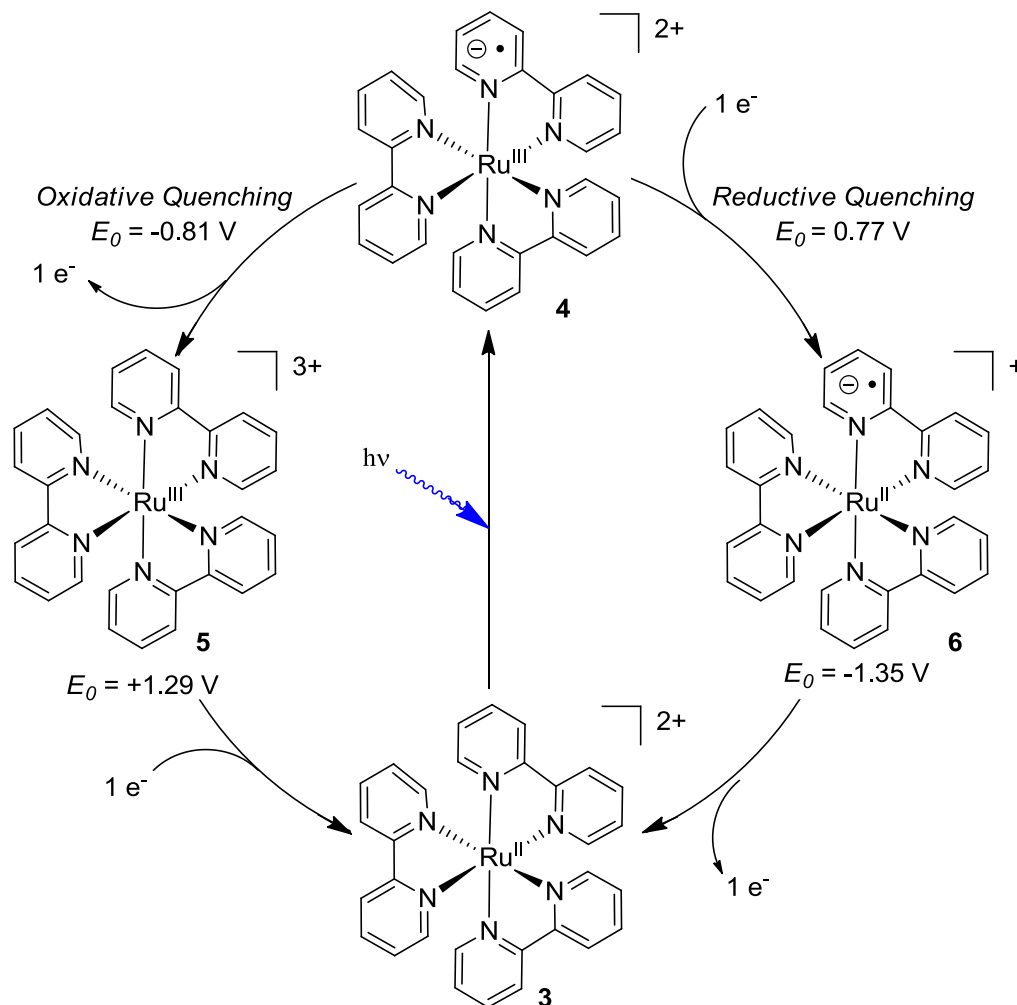
Scheme 3.2: Metal to Ligand Charge Transfer to Form Ligand-Centered Radical.

The singlet state undergoes a highly efficient intersystem crossing ($\phi = 1$) to the triplet state ($^3\text{Ru}(\text{bpy})_3^{2+}$, **4**, Scheme 3.2), which has an emission lifetime of approximately 1.1 μs in MeCN.

⁷⁴ Burstall, F. H., *J. Chem. Soc.* **1936**, 173-175.

⁷⁵ For a comprehensive review on polypyridine ruthenium complexes, see Juris, A.; Balzani, V.; Barigelletti, F.; Campagna, S.; Belser, P.; von Zelewsky, A., *Coord. Chem. Rev.* **1988**, 84, 85-277.

$^3\text{Ru}(\text{L})_3^{2+}$ has a +3 oxidation state at the metal center with a ligand centered radical anion, similar to the nickel complexes reported by Vicic.

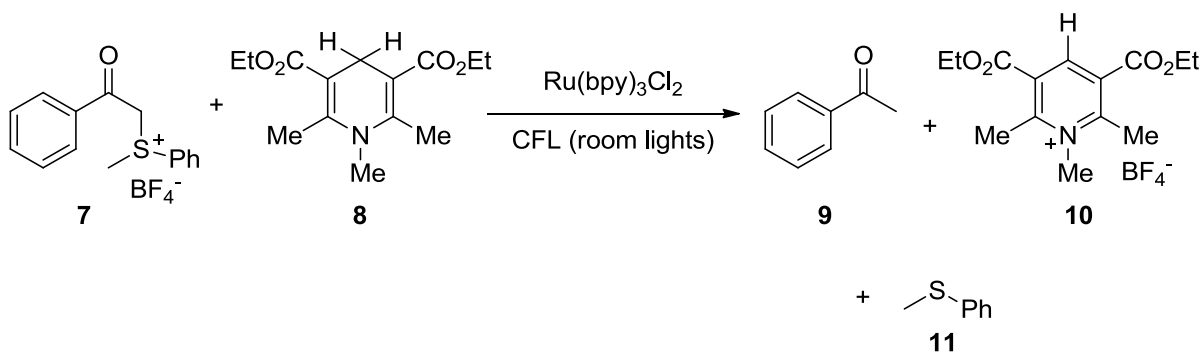


Scheme 3.3: Redox Behavior of Excited State $\text{Ru}(\text{bpy})_3^{2+}$.

The relatively long excited state lifetime enables the triplet state to react in intermolecular processes.⁷⁵ The triplet state exhibits both oxidizing and reducing properties due in part to the energy gained by absorbing a photon (2.1 eV). This energy alters the redox potentials of the triplet state. Oxidative quenching ($E_0 = -0.81 \text{ V}$ vs SCE) of the excited state species removes the ligand-centered electron to generate $\text{Ru}(\text{bpy})_3^{3+}$ (5, Scheme 3.3), which in turn serves as a strong oxidant ($E_0 = 1.29 \text{ V}$

vs SCE). Reductive quenching ($E_0 = 0.77$ V vs SCE) of the excited state reduces the metal center to generate $\text{Ru}(\text{bpy})_3^+$ (**6**, Scheme 3.3), which is a strong reductant ($E_0 = -1.33$ V vs SCE).

While many investigations involving $\text{Ru}(\text{bpy})_3^{2+}$ have focused on the photophysical properties and applications to energy-related problems, little effort was initially devoted to developing photosensitized synthetic methodologies.⁷⁶ Early examples included the reduction of redox-labile functional groups. In 1978, Kellogg and co-workers reported the light-induced reduction of phenacylsulfonium salts by 1,4-dihydropyridine **8** (Scheme 3.4).⁷⁷



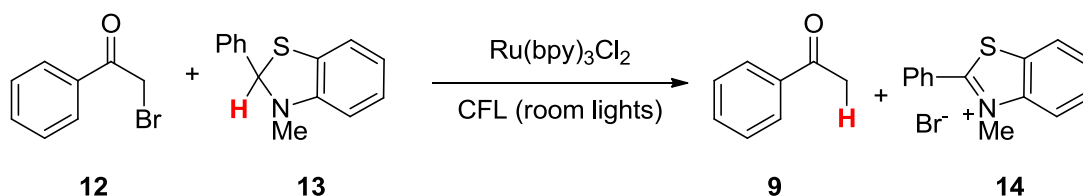
Scheme 3.4: Reduction of Phenacylsulfonium Salt by 1,4-Dihydropyridine with $\text{Ru}(\text{bpy})_3\text{Cl}_2$.

Control experiments indicated the reaction proceeds slowly under ambient light in the absence of sensitizer (48 h) but could be greatly accelerated by adding $\text{Ru}(\text{bpy})_3^{2+}$, TPP, or eosin disodium salt. Although mechanistic investigations failed to produce any conclusive evidence for the specific role of $\text{Ru}(\text{bpy})_3^{2+}$ in these reactions, the authors suggest that the photosensitizer affects the single electron transfer steps of the reaction. In a similar reaction, Kellogg and co-workers reported the reduction of

⁷⁶ For recent reviews on synthetic applications of $\text{Ru}(\text{bpy})_3^{2+}$, see: a) Tucker, J. W.; Stephenson, C. R. J. *J. Org. Chem.* **2012**, 77, ASAP. DOI: 10.1021/jo202538x. b) Teplý, F., *Collect. Czech. Chem. Commun.* **2011**, 76, 859-917. c) Narayanam, J. M. R.; Stephenson, C. R. J., *Chem. Soc. Rev.* **2011**, 40, 102-113. d) Yoon, T. P.; Ischay, M. A.; Du, J., *Nat Chem* **2010**, 2, 527-532.

⁷⁷ Hedstrand, D. M.; Kruizinga, W. H.; Kellogg, R. M., *Tetrahedron Lett.* **1978**, 19, 1255-1258.

phenacylbromide (**12**) under $\text{Ru}(\text{bpy})_3^{2+}$ catalysis with benzothiazole **13** as the terminal reductant (Scheme 3.5).⁷⁸



Scheme 3.5: Reduction of Phenacyl Bromide 12 Catalyzed by $\text{Ru}(\text{bpy})_3\text{Cl}_2$.

Over the next two decades, more examples of organic transformations catalyzed by $\text{Ru}(\text{bpy})_3^{2+}$ were reported, including reduction of dimethyl maleate to methyl succinate,⁷⁹ reduction of ketones to alcohols,⁸⁰ elimination of vicinal dibromides to give alkenes,⁸¹ conjugate addition into alkenes,⁸² sulfide oxidation,⁸³ and nitroarene reduction.⁸⁴ However, it wasn't until 2008 that the field began to attract significant interest. In this year, Nicewicz and MacMillan reported the merging of $\text{Ru}(\text{bpy})_3^{2+}$ photoredox chemistry with asymmetric organocatalysis for the intermolecular α -alkylation of aldehydes (Scheme 3.6).⁸⁵

⁷⁸ Mashraqui, S. H.; Kellogg, R. M., *Tetrahedron Lett.* **1985**, 26, 1453-1456.

⁷⁹ Pac, C.; Ihama, M.; Yasuda, M.; Miyauchi, Y.; Sakurai, H., *J. Am. Chem. Soc.* **1981**, 103, 6495-6497.

⁸⁰ Ishitani, O.; Yanagida, S.; Takamuku, S.; Pac, C., *J. Org. Chem.* **1987**, 52, 2790-2796.

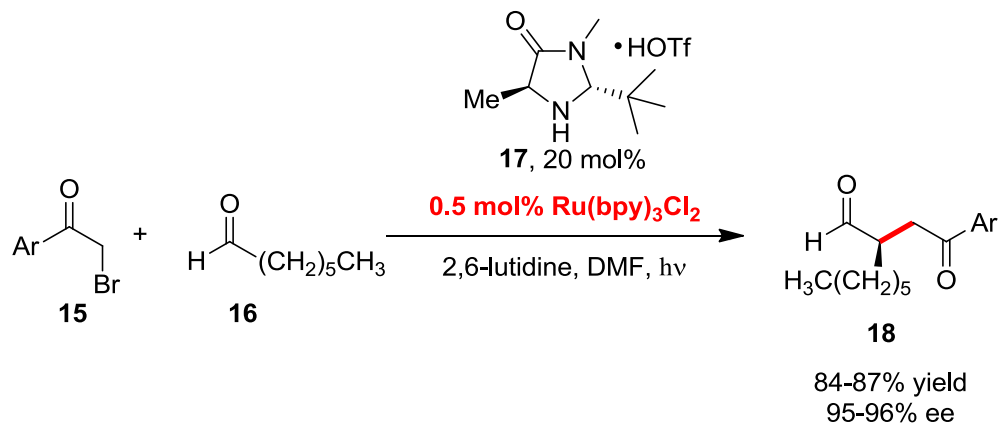
⁸¹ Maidan, R.; Goren, Z.; Becker, J. Y.; Willner, I., *J. Am. Chem. Soc.* **1984**, 106, 6217-6222.

⁸² Okada, K.; Okamoto, K.; Morita, N.; Okubo, K.; Oda, M., *J. Am. Chem. Soc.* **1991**, 113, 9401-9402.

⁸³ Zen, J.-M.; Liou, S.-L.; Kumar, A. S.; Hsia, M.-S., *Angew. Chem., Int. Ed.* **2003**, 42, 577-579.

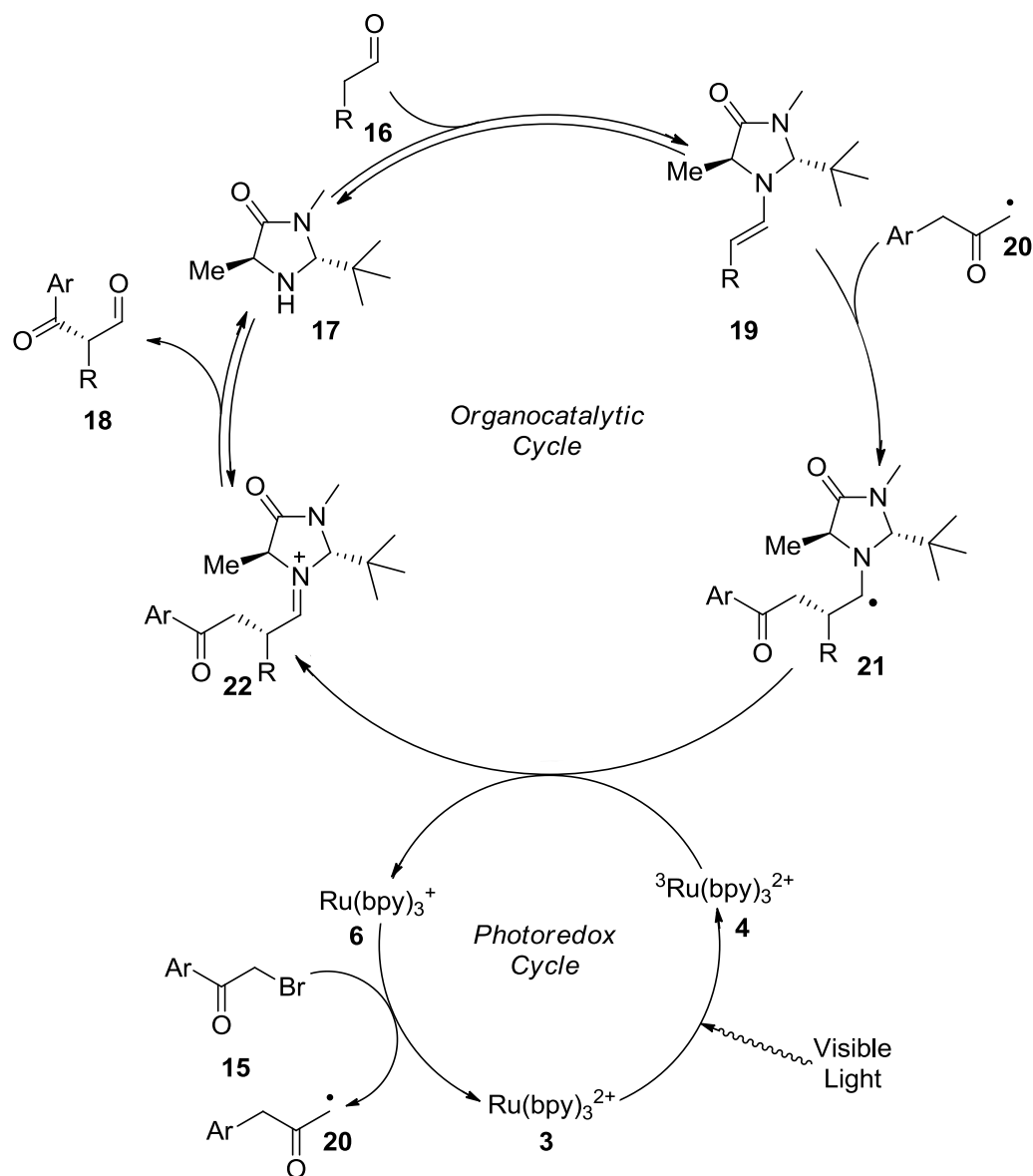
⁸⁴ Hirao, T.; Shiori, J.; Okahata, N., *Bull. Chem. Soc. Jpn.* **2004**, 77, 1763-1764.

⁸⁵ Nicewicz, D. A.; MacMillan, D. W. C., *Science* **2008**, 322, 77-80.



Scheme 3.6: Ru(bpy)₃Cl₂-Catalyzed Enantioselective α -Functionalization of Aldehydes.

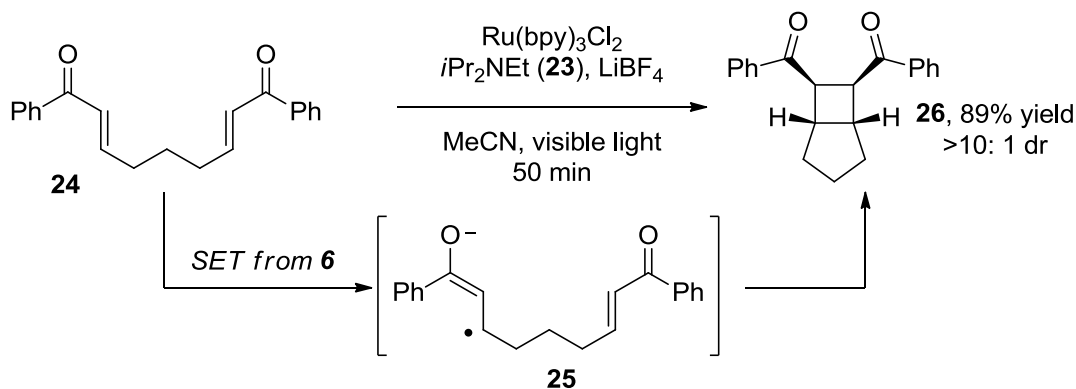
In the proposed mechanism for this reaction, enamine **19** (Scheme 3.7), formed upon condensation of imidazolidinone **17** with aldehyde **16**, serves as a sacrificial reductant to generate Ru(bpy)₃⁺ (**6**). This ruthenium species in turn reduces the alkyl halide (e.g. phenacylbromide, **20**) to generate an alkyl radical, which then attacks the SOMOphilic enamine **19** to generate radical intermediate **21**. Oxidation of this intermediate to iminium **22** by photoexcited ³Ru(bpy)₃²⁺ (**4**) generates additional Ru(bpy)₃⁺ (**6**) and the product (**18**) after hydrolysis of the organocatalyst (**17**).



Scheme 3.7: Proposed Organocatalytic and Photoredox Mechanism by MacMillan and Nicewicz.

This example establishes an important and exciting precedent in the development of enantioselective radical reactions, and this approach has been applied to other α -functionalizations of aldehydes. Moreover, it clearly demonstrates the potential of $\text{Ru}(\text{bpy})_3^{2+}$ as a catalyst for complex synthetic transformations.

In the same year, Yoon and co-workers applied photoredox catalysis to intramolecular formal [2+2] cyclizations of enones (Scheme 3.9).⁸⁶ $\text{Ru}(\text{bpy})_3^{2+}$ reacts with Hünig's base (*i*Pr₂NEt, **23**) to generate $\text{Ru}(\text{bpy})_3^+$ (**6**), which reduces an aryl enone to form enolate radical anion **25** and triggers cyclization. Control experiments in the absence of *i*Pr₂NEt failed to react, indicating that excited state $\text{Ru}(\text{bpy})_3^{2+}$ does not directly interact with the substrate.



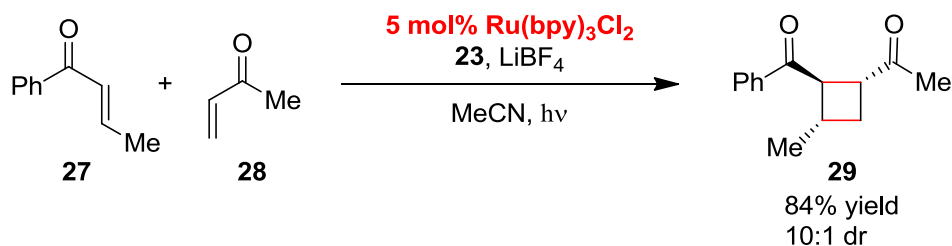
Scheme 3.8: Formal [2+2] Intramolecular Cyclization of Enones.

The authors were also able to induce large-scale (1 g) cyclizations using only sunlight to promote the reaction, highlighting the long-term potential of $\text{Ru}(\text{bpy})_3^{2+}$ as an energy-efficient catalyst. This concept later applied to intermolecular cyclization of crossed-enones (Scheme 3.9)⁸⁷ and the intramolecular cyclization of electron-rich styrenes via an oxidative pathway.⁸⁸

⁸⁶ Ischay, M. A.; Anzovino, M. E.; Du, J.; Yoon, T. P., *J. Am. Chem. Soc.* **2008**, *130*, 12886-12887.

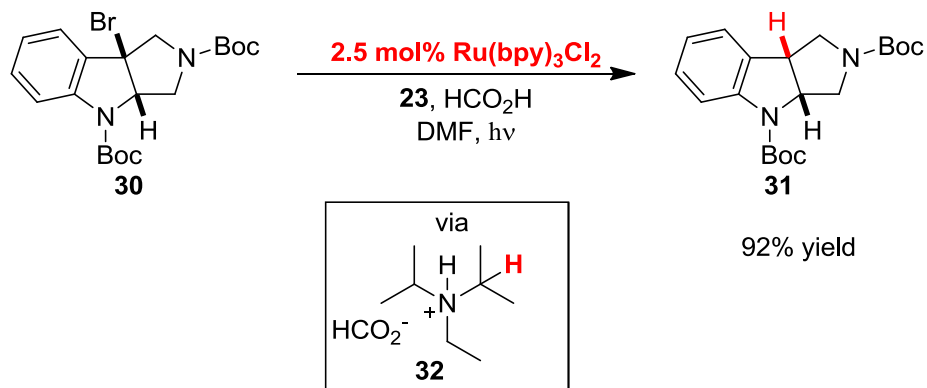
⁸⁷ Du, J.; Yoon, T. P., *J. Am. Chem. Soc.* **2009**, *131*, 14604-14605.

⁸⁸ Ischay, M. A.; Lu, Z.; Yoon, T. P., *J. Am. Chem. Soc.* **2010**, *132*, 8572-8574.



Scheme 3.9: Ru(bpy)₃²⁺-Catalyzed [2+2] Cycloaddition of Crossed Enones.

Stephenson and co-workers reported chemoselective reductive dehalogenation with Ru^{II}(bpy)₃²⁺ and trialkylammonium formate as terminal reductant (Scheme 3.10).⁸⁹ Acyl and benzyl halides were selectively reduced in the presence of aryl and vinyl halides due to their lower and more accessible reduction potential. Deuterium labeling studies on the *i*Pr₂NHEtO₂CH (32) salt indicate reduction of the alkyl radical occurs primarily via hydrogen abstraction from the methine on the amine rather than from the formate hydrogen.



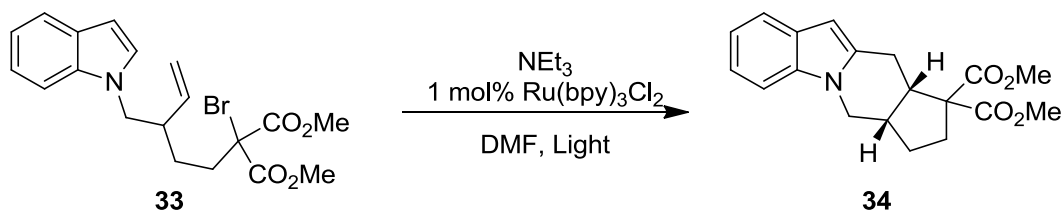
Scheme 3.10: Radical-Mediated Reduction Debromination with Ru(bpy)₃²⁺.

Shortly thereafter, Stephenson and co-workers applied a Ru^{II}(bpy)₃²⁺/amine system to a radical cyclization for the synthesis of complex indoles and pyrroles.⁹⁰ In this example, a pendant alkyl radical is generated via halogen reduction, which subsequently attacks the indole to form a new

⁸⁹ Narayanam, J. M. R.; Tucker, J. W.; Stephenson, C. R. J., *J. Am. Chem. Soc.* **2009**, *131*, 8756-8757.

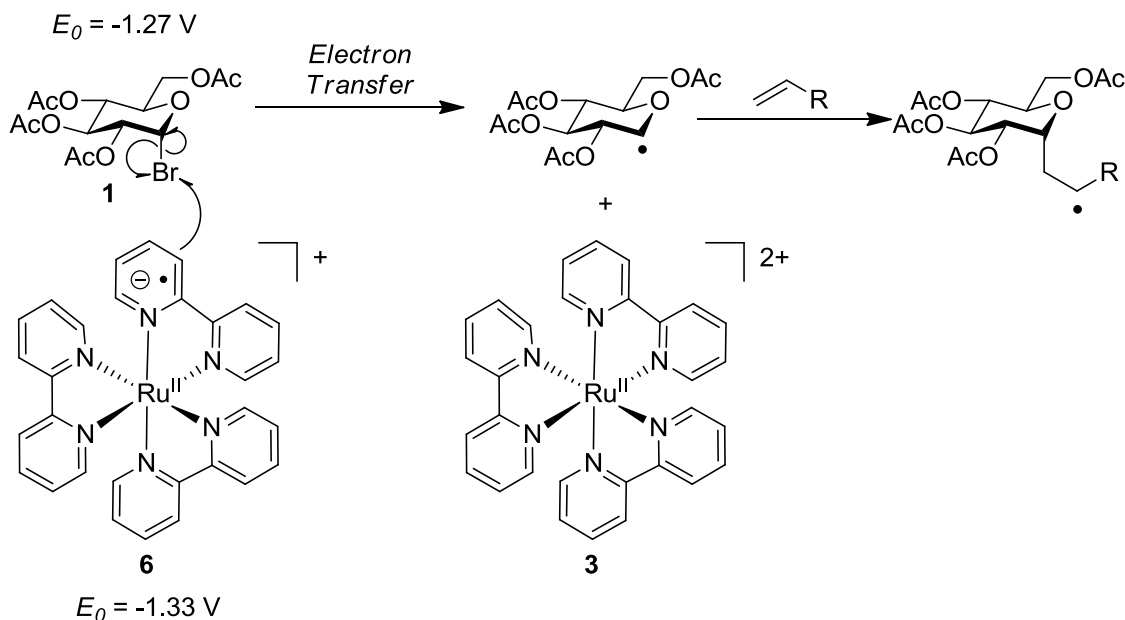
⁹⁰ Tucker, J. W.; Narayanam, J. M. R.; Krabbe, S. W.; Stephenson, C. R. J., *Org. Lett.* **2009**, *12*, 368-371.

C-C bond. The authors then detail a radical-mediated cascade polycyclization through the incorporation of an alkene for the synthesis of tetracycles (Scheme 3.11).



Scheme 3.11: Radical-Cascade Synthesis of Polycycles Initiated by Ru(bpy)₃Cl₂.

This work, along with research presented by Okada and Oka,⁸² represent the first examples of intramolecular and intermolecular addition of radicals generated via reduction by Ru(bpy)₃²⁺ into alkenes. Based on this precedence, we concluded it was possible to initiate similar reactivity in glycosyl halides through single electron transfer from Ru(bpy)₃²⁺ (Scheme 3.12). We also hoped this would allow us to access products or diastereoselectivities unobtainable with our nickel methodology.

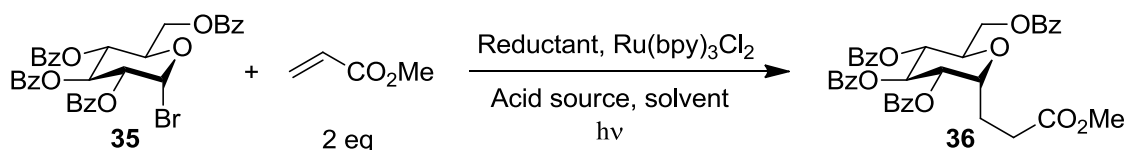


Scheme 3.12: Planned Reactivity of Ru(bpy)₃⁺ and Glycosyl Bromides.

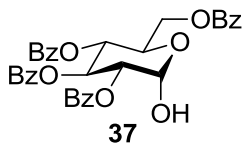
Initial Optimization.

Initial investigations focused on reaction conditions similar to our nickel-catalyzed glycosyl radical generation. In the first attempt to use photoredox catalysts, glucosyl bromide **35**, Mn^0 , NH_4Br , and $\text{Ru}^{\text{II}}(\text{bpy})_3^{2+}$ in DMA were irradiated by a compact fluorescent light bulb (CFL, 14 W) for 2 hours to afford a 47% isolated yield of **36** along with hydrolysis **37**.

Table 3.1: Initial Optimization of $\text{Ru}(\text{bpy})_3^{2+}$ -Mediated C-Glycoside Synthesis.



Entry	Reductant	Acid source	Solvent (0.12 M)	Result
1	Mn	NH_4Br	MeCN	37
2	Mn	MeOH	DMA	trace 36 + 37
3	NEt_3	NH_4Br	DMA	37
4	23	NH_4Br	DMA	No reaction
5	23	23 ·HBr	DMA	37
6	23	23 ·HBr	CH_2Cl_2	trace 36
7	23	23 ·HBr	MeCN	26% 36

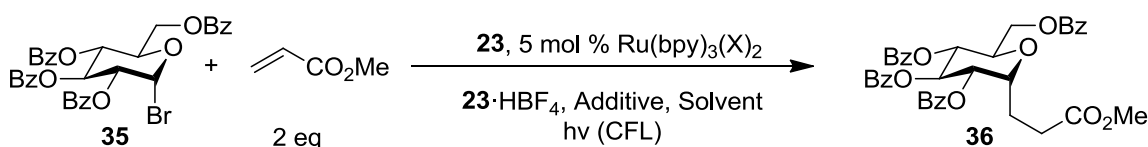


By halving the concentration of the photosensitizer, a 30% yield was obtained, and initial optimization of this reaction began with this catalyst loading.⁹¹ Changing the solvent from DMA to the less-polar MeCN to suppress hydrolysis of the starting material failed to produce any product (Table 3.1, entry 1). Unlike in the nickel-catalyzed method, alcohol proton sources were found to be

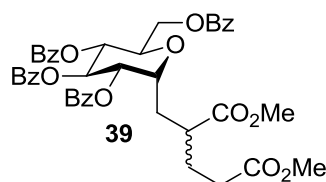
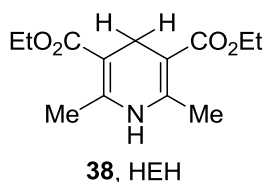
⁹¹ Andrews, R. S.; Becker, J. J.; Gagné, M. R., *Angew. Chem., Int. Ed.* **2010**, 49, 7274-7276.

unsuitable. As described in previous reports, amines can reductively quench $^3\text{Ru}(\text{bpy})_3^{2+}$ in order to generate $\text{Ru}(\text{bpy})_3^+$ and an amine radical cation.⁹² In our hands, triethylamine was ineffective for this reaction (Table 3.1, entry 3), but *i*Pr₂NEt (**23**) did produce detectable amounts of product (Table 3.1, entry 6). However, using *i*Pr₂NEt to quench $^3\text{Ru}(\text{bpy})_3^{2+}$ required the use of **23**·HBF₄ in order to create a buffer of appropriate pH along with a less-polar solvents to obtain a 26% yield of **36** (Table 3.1, entry 7).

Table 3.2: Optimization of Additives for the Synthesis of C-Glycosides.



Entry	Solvent	X	Additive	Result
1	MeCN (0.12 M)	Cl	Bu ₄ NPF ₆	44%
2	MeCN (0.06 M)	Cl	Bu ₄ NPF ₆	50%
3	MeCN (0.06 M)	BF ₄	Bu ₄ NPF ₆	61%
4	MeCN (0.06 M)	BF ₄	Bu ₄ NPF ₆ HEH (38)	72%
5	CH₂Cl₂ (0.06 M)	BF ₄	Bu ₄ NPF ₆ HEH (38)	80%



Yields were further improved by adding 10 equivalents of an ammonium salt with a non-coordinating counter anion (Table 3.2, entry 1). Similar improvements in yield were obtained by decreasing the overall concentration of the reaction and by using a catalyst with a non-coordinating counter anion in order to suppress hydrolysis (Table 3.2, entries 2 and 3). Avoiding the use of

⁹² DeLaive, P. J.; Sullivan, B. P.; Meyer, T. J.; Whitten, D. G., *J. Am. Chem. Soc.* **1979**, *101*, 4007-4008.

nucleophilic counterions presumably reduces the overall concentration of nucleophilic anions in solution, which can induce a Lemieux anomerization to make the substrate more susceptible to hydrolysis. Other manipulations of concentrations and additives did not lead to any improvements. The mass balance of these reactions was dominated by over-conjugate addition (**39**), as determined by mass spectrometry. We supposed this product arose from poor termination of the radical after conjugate-addition, which would allow the radical to react with an additional equivalent of alkene. Inspired by Stephenson's successful reductive debromination with Hantzsch ester **38** or formic acid, we found that including 1.1 equivalents of Hantzsch ester **38** resulted in less oligomerization and higher yields (Table 3.2, entry 4).⁸⁹ Non-polar CH₂Cl₂ further improved the yields through suppression of hydrolysis (Table 3.2, entry 5). Final optimization determined that the tetraalkylammonium salt and acid additives were unnecessary in the reaction. These results are summarized in Table 3.3.

Table 3.3: Final Optimization of Radical-Mediated C-Glycoside Synthesis.

Entry	Acid (Eq)	Salt (Eq)	Conc (M)	% Yield
1	-	-	0.06	63
2	-	1	0.06	68
3	2	2	0.06	83
4	-	5	0.06	73
5	-	10	0.06	77
6	10	-	0.06	88
7	10	-	0.12	90
8	2.5	-	0.12	91
9	-	-	0.12	92

Substrate Scope: Carbohydrates and Alkenes.

With the optimized conditions in hand, the substrate scope of the methodology was investigated (Table 3.4). Acetate-protected glucosyl bromide **1** resulted in equally high yields as compared to benzoate-protected sugar **35**, indicating protecting group had no effect on the reaction (Table 3.4, entry 1).

Table 3.4: Substrate Scope of Radical-Mediated C-Glycoside Synthesis.

<div><div><div><div><div><div>R'O</div><div>R'O</div><div>R'O</div><div>R'O</div><div>OR'</div></div></div><div><div><div><div><div>R'O</div><div>R'O</div><div>R'O</div><div>R'O</div><div>Br</div></div></div><div><div><div><div><div>R_2</div><div>CH_2</div><div>R_1</div></div></div><div><div><div><div><div>Ru(bpy)_3(BF_4)_2</div><div>23, 38</div></div></div><div><div><div>CH_2Cl_2, h\nu</div></div></div></div></div></div><div><div><div><div><div>R'O</div><div>R'O</div><div>R'O</div><div>R'O</div><div>OR'</div></div></div><div><div><div><div><div>R'O</div><div>R'O</div><div>R'O</div><div>R'O</div><div>OR'</div></div></div><div><div><div><div><div>R</div></div></div></div></div></div></div></div></div></div></div></div></div></div></div> </		
------------------------------------------------------------------------------------------------------------------------------------------------------------------------------------------------------------------------------------------------------------------------------------------------------------------------------------------------------------------------------------------------------------------------------------------------------------------------------------------------------------------------------------------------------------------------------------------------------------------------------------------------------------------------------------------------------------------------------------------------------------------------------	--	--

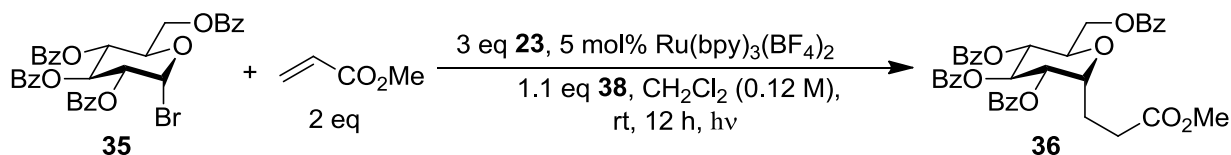
[a] R'=Ac or Bz. [b] Yield of isolated product; conditions: glycosyl bromide (0.12 mmol, 0.12 mm in CH₂Cl₂), alkene (0.24 mmol), **3** (0.36 mmol), [Ru(bpy)₃](BF₄)₂ (0.06 mmol), **5** (0.24 mmol), irradiation overnight at room temperature with a 14W fluorescent bulb. [c] 0.134 mmol **5**. [d] 1.2 mmol glycosyl bromide. [e] 1.2 mmol alkene.

However, initial application of this methodology to more electron-deficient alkenes (e.g. acrolein) resulted in significantly lower yields (46%). It was determined that over-conjugate addition accounted for the bulk of the mass balance despite the incorporation of Hantzsch ester **38**. However, increasing the concentration of **38** sufficiently suppressed oligomerization and afforded the products in excellent yields.

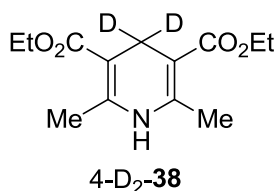
As seen in our nickel-catalyzed reaction, only electron deficient alkenes were successful in this reaction, and the products showed exclusive α -selectivity. However, this methodology demonstrated a broader functional group tolerance, as methyl vinyl ketone and acrolein resulted in excellent yields (Table 3.4, entries 2 and 3). More importantly, the yields for several of the substrates meet or exceed the highest previously reported yield by any method, demonstrating the value of this approach as a method of *C*-glycoside synthesis (Table 3.4, entries 1-4). Higher alkene concentrations improved yields when over-conjugate addition was non-problematic (Table 3.4, entry 6). In these instances, the major byproduct observed was reductive debromination of the starting material, which suggests radical addition into the alkene is slow. Increasing the concentration of alkene serves to increase the rate of conjugate addition and thus the yield of the desired *C*-glycoside. Mannosyl and galactosyl bromides were also well tolerated (Table 3.4, entries 9 and 10), and these reactions could be scaled to 1.2 mmol of substrate without complication (Table 3.4, entries 1 and 8). Although 1,1-disubstituted alkenes were tolerated in the reactions, β -substituted enoates were not (e.g. methyl crotonate, methyl maleate). In an attempt to increase diastereoselectivity of conjugate addition by using chiral auxiliaries in non-polar solvents, chiral-auxiliary derived 1,1-disubstituted alkenes were tested but failed to produce diastereoselectivities comparable to the nickel methodology.

Control Experiments and Mechanistic Investigations.

Table 3.5: Control Experiments in the Light-Mediated Synthesis of C-Glycosides.

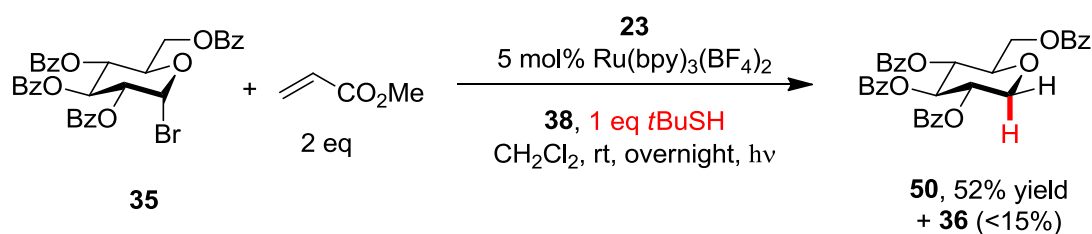


Entry	Deviation from Std Conditions	Result
1	None	92% yield
2	No cat/light	<5%
3	No 23	<20% (all 23 consumed)
4	No 38	<25%
5	No 38 , 10 eq 23 ·HBF ₄	60%
6	4-D ₂ - 38	<25% D incorporation
7	23 ·DBF ₄	No D incorporation



A series of control experiments were conducted in order to elucidate a possible mechanism for this reaction (Table 3.5). Omission of either the photosensitizer or light resulted in no detectable product formation. In the absence of Hantzsch ester **38** and acid additive, <20% yield of **36** is obtained, although **35** is fully consumed. Adding 10 eq of acid improved the yields to 60%. Based on the proposed mechanism for reductive debromination according to Stephenson and co-workers,⁸⁹ it is plausible that the protonated acid serves as a hydrogen atom source in a similar fashion. As our initial hypothesis that Hantzsch ester serves as a hydrogen atom source, deuterium-labeled Hantzsch

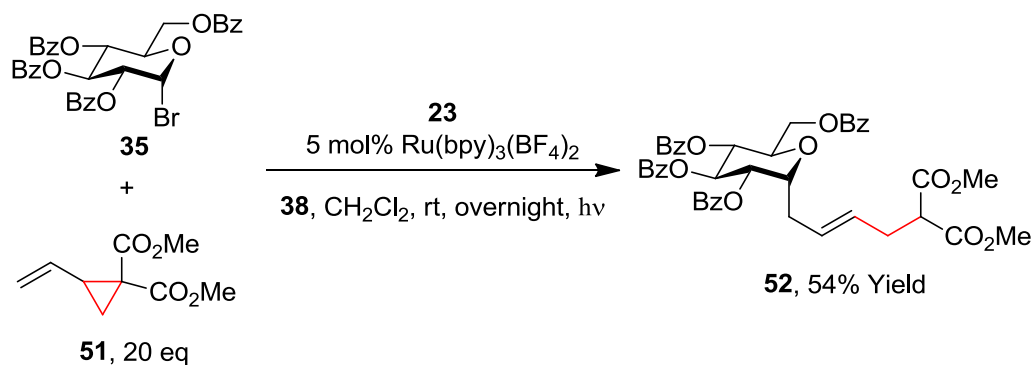
ester (4-D₂-**38**) was used in an attempt to demonstrate this through deuterium-incorporation in the product. However, little deuterium incorporation was detected (<25% of the product), and no deuterium incorporation is observed in CD₂Cl₂ or CD₃CN. **23**•DBF₄ was used as the acid additive in D₂O-washed glassware but similarly failed to show any deuterium incorporation. These simple labeling experiments suggest the termination of the reaction is not simple hydrogen abstraction or a protonation of an enolate. However, the high yields obtained with Hantzsch ester **38** clear indicate its importance in the reaction.



Scheme 3.13: Thiol-Trapping Control Experiment.

To provide further evidence for a radical mechanism, additional control experiments were conducted. A competition experiment in which *t*BuSH was added to the reaction under standard conditions resulted in reductive debromination (**50**) as the primary product in 52% yield along with <15% of the C-glycoside (Scheme 3.13). This result is consistent with previously reported radical conditions in which the addition of thiols gives exclusive C1-reduction.⁹³ As with our nickel-catalyzed conditions, vinyl cyclopropane **51** resulted in formation of the ring-opened product (Scheme 3.14).⁵⁴ These observations along with the exclusive formation of α -C-glycosides suggest the intermediacy of a glycosyl radical which undergoes conjugate addition into the alkene.

⁹³ Praly, J.-P.; Ardakani, A. S.; Bruyère, I.; Marie-Luce, C.; Bing Qin, B., *Carbohydr. Res.* **2002**, 337, 1623-1632.



Scheme 3.14: Radical-Mediated Conjugate Additions into Vinyl Cyclopropane 51.

The presence of a radical was tentatively confirmed through the use of time-resolved EPR studies.⁹⁴ In these experiments, a laser is used to trigger the reaction, and the EPR signal is monitored at different time intervals. Through this method, different radicals are identified by their different lifetimes and G values. In these experiments, 2-3 different carbon-centered radicals were identified, supporting a radical-based mechanism for this reaction (Figure 3.2).

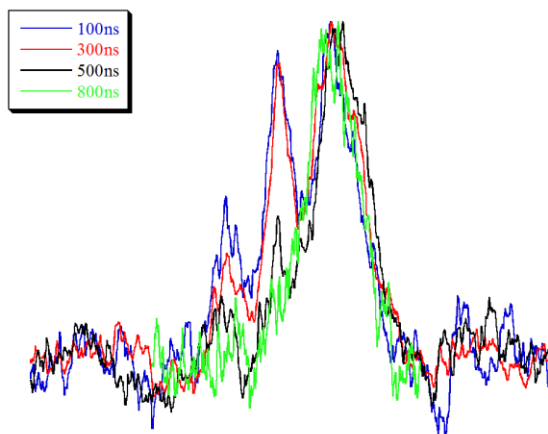


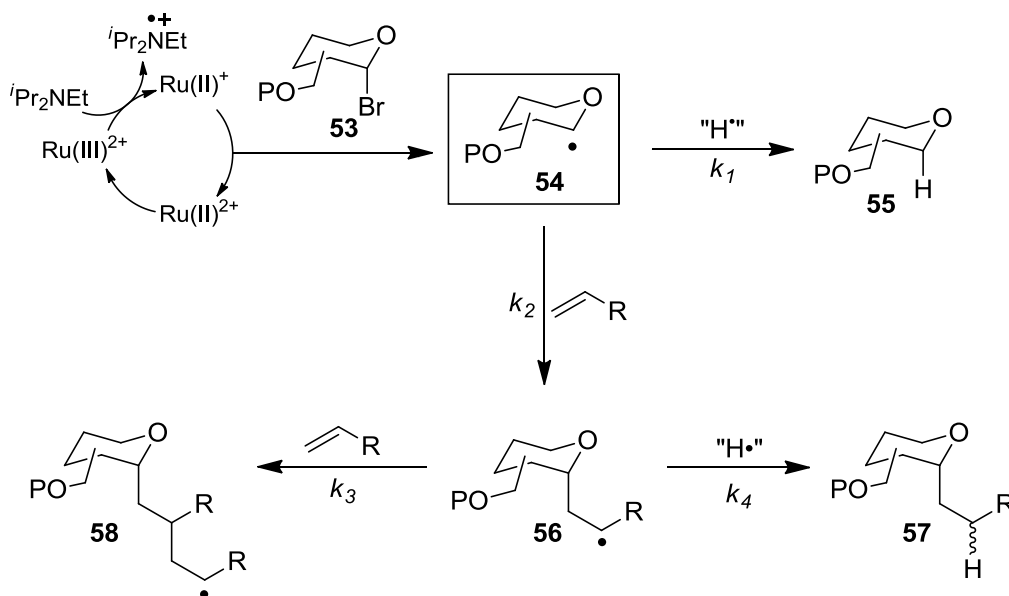
Figure 3.2: Time-Based EPR of Carbon-Based Radicals in Light-Mediated Reactions.

Proposed Mechanism and Attempted Application to Propiolates.

Based on these experiments, we propose the reaction proceeds via photoreduction of the glycosyl bromide (53) to generate a glycosyl radical (54, Scheme 3.15). The radical can then undergo

⁹⁴ In collaboration with Prof. Malcolm Forbes at UNC-CH.

one of two possible reactions. In the presence of an electron-deficient alkene, conjugate addition occurs to generate α -radical **56** (k_2). As the electron-withdrawing ability of the alkene substituent decreases, the rate of conjugate addition decreases and becomes competitive with reductive debromination of the substrate (**55**, Scheme 3.15, k_1 vs k_2). After conjugate addition, two more possible pathways exist. In the case of strong electron-withdrawing substituents, over-conjugate addition is possible in order to provide oligomerized products (**58**, Scheme 3.15, via k_3). Competitive with this is reduction by Hantzsch ester **38** to provide the desired C-glycoside (**57**, k_4), and increasing the concentration of **38** can serve to favor reduction over conjugate addition (i.e. $k_4 > k_3$).



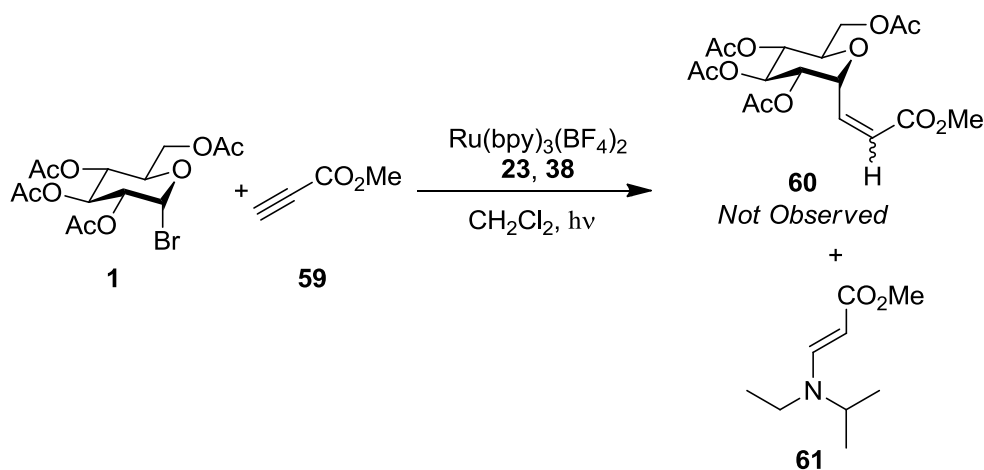
Scheme 3.15: Proposed Mechanism of $\text{Ru}(\text{bpy})_3^{2+}$ -Catalyzed C-Glycoside Synthesis.

The specific nature of the reduction of α -radical **56** is unclear, as evidenced by the deuterium-labeling experiments. Hantzsch ester **38** is known to serve as a reductant in a variety of different mechanisms, including both direct hydrogen abstraction and single electron transfer followed by proton transfer.⁹⁵ It is possible **38** serves in this latter capacity, serving to reduce the radical to an enolate, which then rapidly protonates under the reaction conditions. Since the oxidation of aliphatic

⁹⁵ Cheng, J.-P.; Lu, Y.; Zhu, X.-Q.; Sun, Y.; Bi, F.; He, J., *J. Org. Chem.* **2000**, 65, 3853-3857.

amines by $^3\text{Ru}(\text{bpy})_3^{2+}$ is known to generate acid, this could explain why deuterium incorporation was low with deuterium-labeled **38**. However, at this point we cannot exclude any possible mechanism.

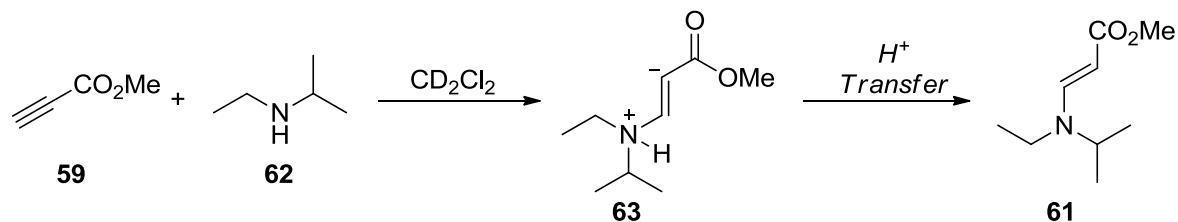
We sought to apply this chemistry to the radical conjugate addition into propiolates in an attempt to expand this methodology to alternative coupling partners. Initial work in this area was investigated by Aaron Francis, who exposed glycosyl bromide **1** and methyl propiolate (**59**) to the optimized reaction conditions (Scheme 3.16). It was found that the glycosyl bromide was not consumed in the reaction, and instead **61** was formed as the major product as determined by ^1H NMR.



Scheme 3.16: Attempted Conjugate Addition into Propiolates.

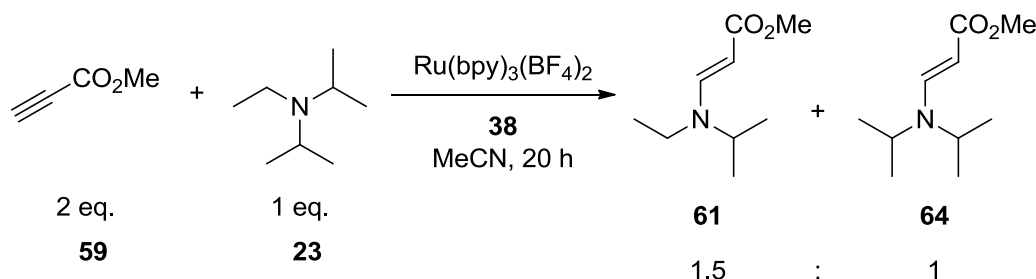
We presumed **61** was the product of a Baylis-Hillman-type reaction, wherein *N*-isopropylethylamine undergoes conjugative addition into propiolate **59** to form enolate **63**. Either intra- or intermolecular protonation of this intermediate would result in product **61**, as depicted in Scheme 3.17. This was later confirmed independently by reacting **59** with **62** in CD_2Cl_2 , which cleanly provided **51**⁹⁶ in 30 minutes.

⁹⁶ ^1H NMR matches reported spectrum: Lee, K. Y.; Lee, C. G.; Na, J. E.; Kim, J. N., *Tetrahedron Lett.* **2005**, 46, 69-74.



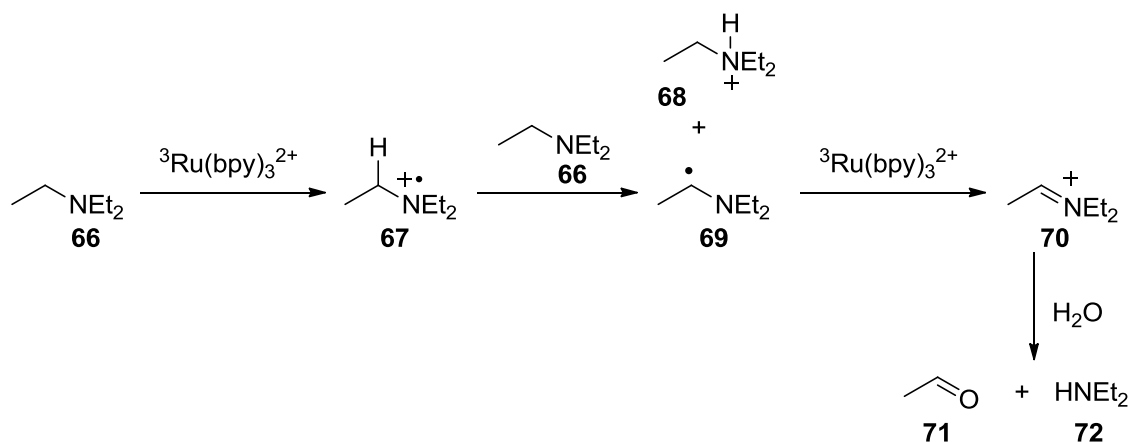
Scheme 3.17: Potential Mechanism for Synthesis of 61.

To confirm the glycosyl bromide was unnecessary for the formation of **62**, *i*Pr₂NEt (**23**) and methyl propiolate were irradiated with light and photocatalyst in the absence of glycosyl bromide. This reaction resulted in a 1.5:1 formation of **61** to **64**, as determined by ¹H NMR and GCMS.



Scheme 3.18: Reaction of 23 with Propiolate 59.

From these experiments, it is clear **23** forms a mixture of **62** and diisopropylamine (**65**) in the presence of $\text{Ru}(\text{bpy})_3^{2+}$ and Hantzsch ester **38**. It has been reported by Meyer and co-workers that triethylamine (**66**) reacts with excited state $^3\text{Ru}(\text{bpy})_3^{2+}$ to generate the amine radical cation (**67**). They propose this intermediate is deprotonated by an additional equivalent of amine to form triethylammonium cation (**68**) and the neutral alkyl radical **69**, which is then be oxidized by $^3\text{Ru}(\text{bpy})_3^{2+}$ in generate an iminium ion (**70**). We propose this intermediate is hydrolyzed under the reaction conditions by adventitious water in order to form the 2° amine necessary for conjugate addition into the propiolate (e.g. **72**).



To circumvent this reactivity, stable amine reductants were investigated in this reactivity (Figure 3.3). Arylamine reductants **72** and **73** have been shown by Stephenson and co-workers to affect the addition of malonate radicals into indoles where trialkylamines were found to be problematic.⁹⁷

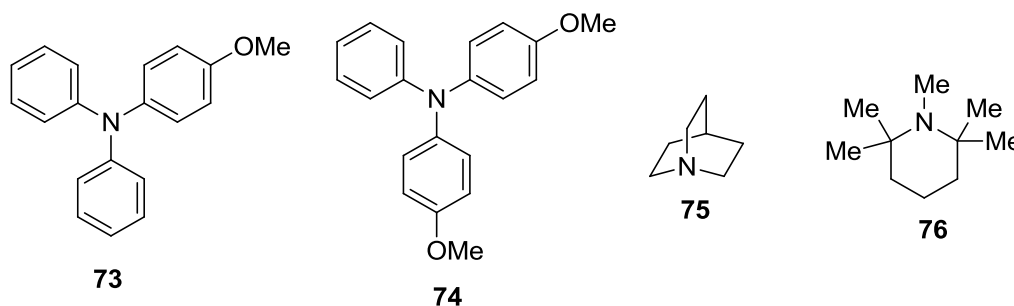


Figure 3.3: Attempted Amine Quenchers for Addition of Radicals into Propiolates.

However, each failed to produce the desired reactivity and often resulted in a complex mixture of products. Moreover, thiol trapping experiments with reductants **72** and **73** suggest the glycosyl radical is not being formed under the reaction conditions. This highlights one of the key challenges in utilizing RuL_3^{2+} catalysts for organic synthesis; modification of one reaction partner has a profound effect on the reaction. In this case, changing the amine from an irreversible trialkylamine reductant to a reversible triarylamine reductant likely changes the nature of reductive quenching of the photo-

⁹⁷ Furst, L.; Matsuura, B. S.; Narayanam, J. M. R.; Tucker, J. W.; Stephenson, C. R. J., *Org. Lett.* **2010**, *12*, 3104-3107.

excited catalyst ($^3\text{Ru}(\text{bpy})_3^{2+}$). This subtle change shuts down productive reactivity, and the glycosyl radical is not formed. Further investigations into the reductive quenching of the catalyst and the subtle changes that affect the rate could allow this methodology to be applied to new and exciting systems

Conclusion.

A mild, room-temperature, visible-light mediated method of glycosyl radical generation has been developed and applied to the radical conjugate addition into alkenes for C-glycoside synthesis. The procedure serves an attractive and effective alternative to Giese's tin mediated methodologies and provides near best results for each substrate class. The intermediacy of radicals in the reaction was confirmed through the nature of the C-glycosides formed and the use of *in situ* EPR monitoring. Attempts to expand the scope of suitable radical acceptors to propiolates instead provided insight into the subtleties of the reductive quenching of the photo-excited catalyst. Current efforts focus on the nature of this reductive quenching step and the role amine reductants serve in this process.

Experimental Section.

General. All reagents were reagent grade quality and used as received from Aldrich or Acros unless otherwise indicated. All reactions were conducted under inert conditions (Ar or N₂) unless otherwise indicated. Anhydrous THF was distilled from sodium/benzophenone prior to use. Anhydrous CH₂Cl₂ was passed through a column of alumina, sparged with N₂ for 20 minutes, and stored in a sealed Schlenk flask. Anhydrous acetonitrile (MeCN), N,N-diisopropylethylamine (*i*Pr₂NEt), and diisopropylamine (*i*Pr₂NH) were distilled from CaH₂ prior to use. Acetobromo- α -D-glucose (1% CaCO₃) and acetobromo- α -D-galactose (1% CaCO₃) were purified by passing through a silica column prior to use. α -D-glucopyranosyl bromide tetrabenzoate, α -D-mannopyranosyl bromide tetrabenzoate were synthesized according to literature procedure.⁶⁴ Ru(bpy)₃Cl₂ was synthesized by reported

procedure,⁹⁸ and $\text{Ru}(\text{bpy})_3(\text{BF}_4)_2$ was synthesized in an analogous manner to reported anion metathesis.⁹⁹ Dimethyl 3-vinylcyclopropane-1,1-dicarboxylate was synthesized according to literature procedure.¹⁰⁰ Acrylonitrile, acrolein, methyl vinyl ketone, were distilled prior to use. Supercritical fluid chromatography (SFC) was conducted on a Berger Minigram SFC. Column chromatography was performed using Silicycle silica gel 60 as the solid support. All NMR spectra were recorded on Bruker Avance 500 MHz or 400 MHz spectrometer at STP and with CDCl_3 as the NMR solvent unless otherwise indicated. All deuterated solvents were used as received from Cambridge Isotope Laboratories, Inc. ^1H NMR, ^{13}C NMR, and ^{31}P NMR chemical shifts are reported in δ units, parts per million (ppm) relative to the chemical shift of residual solvent or an external standard. Reference peaks for chloroform in ^1H NMR and ^{13}C NMR spectra were set at 7.26 ppm and 77.0 ppm, respectively. ^{31}P reference peak was set at -18.0 ppm for triphenylphosphite in CDCl_3 as an external standard. High-resolution mass spectra (HRMS) were obtained using a Micromass Q-ToF Ultima or Agilent Accurate LC-TOF Mass Spectrometer (ESI+, 175 eV). Melting point was recorded on Uni-melt (Thomas Hoover) capillary melting point apparatus. Infrared (IR) spectra were obtained using a ASI ReactIR 1000 infrared spectrometer. Specific rotations were obtained using a Jasco DIP-1000 polarimeter with CH_2Cl_2 as the solvent.

General Procedures.

General Procedure A (liquid alkene): A flame-dried Schlenk tube equipped with a stir bar under Ar was charged with $\text{Ru}(\text{bpy})_3(\text{BF}_4)_2$ (5 mol%), Hantzsch ester **38** (2.2 mol eq) and glycosyl bromide (1 mol eq.). The flask was evacuated and then backfilled with Ar. Solvent (to a sugar concentration of 0.12 mM) was added, forming a bright orange heterogeneous solution, followed by $^i\text{Pr}_2\text{NEt}$ (23, 3 mol

⁹⁸ Broomhead, J. A.; Young, C. G. *Inorg. Synth.* 1990, 28, 338.

⁹⁹ Masui, H.; Murray, R. W. *Inorg. Chem.* **1997**, 36, 5118.

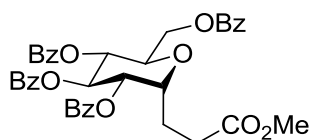
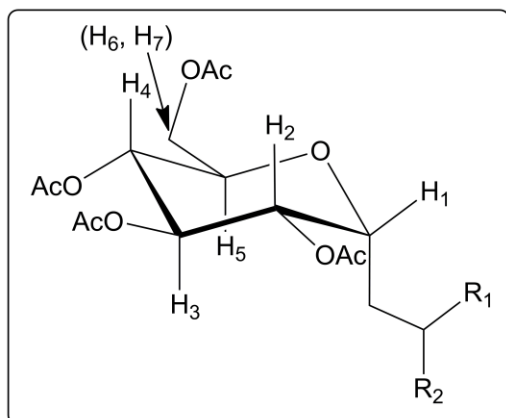
¹⁰⁰ Parsons, A. T.; Campbell, M. J.; Johnson, J. S. *Org. Lett.* **2008**, 10, 2541.

eq.) and alkene (2 mol eq.). The reaction tube was placed 6-10 cm from a 14W fluorescent light bulb and stirred at room temperature until TLC showed consumption of starting material. The reaction was quenched by passing through a plug of silica in Et₂O. Flash column chromatography provided the product as a white solid or a colorless oil after removal of solvents.

General Procedure B (solid alkene): A flame-dried Schlenk tube equipped with a stir bar under Ar was charged with Ru(bpy)₃(BF₄)₂ (5 mol%), alkene (2 mol eq.), Hantzsch ester **38** (2.2 mol eq) and glycosyl bromide (1 mol eq). The flask was evacuated and then backfilled with Ar. Solvent (to a sugar concentration of 0.12 mM) was added, forming a bright orange heterogeneous solution, followed by ⁱPr₂NEt (**23**, 3 mol eq.). The reaction tube was placed 6-10 cm from a 14W fluorescent light bulb and stirred at room temperature until TLC showed consumption of starting material. The reaction was quenched by passing through a plug of silica in Et₂O unless otherwise indicated. Flash column chromatography provided the product as a white solid or a colorless oil after removal of solvents.

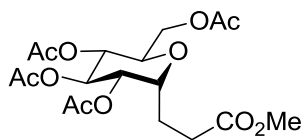
General Procedure for determination of yield by SFC: The sample for analysis was prepared by adding 100 µL of 6-*t*-butyl-2-methyl-phenol (0.588 mmol) to a solution of crude material in 10 mL THF. The sample was injected (5 µL) onto a silica column (4.6 mm x 250 mm) in 30% THF in CO₂ at 100 bar with a 4 mL/min flow rate. Standard retention time = 1.10 min; sample retention time = 2.38 min. The ratio of areas was then compared to a calibration curve to determine yield.

Proton labeling: For the purpose of spectral assignment, the proton labeling outlined in the following box was used throughout the text (including mannosides and galactosides).



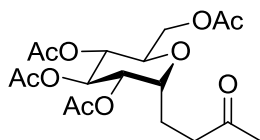
Methyl 3-(2,3,4,6-tetra-*O*-benzoyl- α -D-glucopyranosyl)propanoate (36).

This compound was prepared according to the General Procedure A using α -D-glucopyranosyl bromide tetrabenzoate **35** (80 mg, 0.12 mmol, 2 mol eq.) and methyl acrylate (22 μ L, 0.244 mmol, 2 mol eq.). The yield was determined by SFC for reaction optimization. Alternatively, purification of the crude material by flash column chromatography (SiO₂: 20/80 to 30/70 ethyl acetate in hexanes) gave the desired product⁵⁴ as a white solid.



Methyl 3-(2,3,4,6-tetra-*O*-acetyl- α -D-glucopyranosyl)propanoate (40).

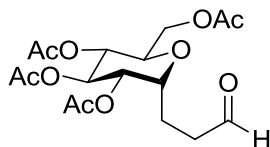
This compound was prepared according to the General Procedure A using aceto-1-bromo- α -D-glucose **1** (50 mg, 0.12 mmol, 1 mol eq.) and methyl acrylate (22 μ L, 0.244 mmol, 2 mol eq.). Flash column chromatography (SiO₂: 40/60 to 50/50 ethyl acetate in hexanes gradient) gave the desired product⁶⁷ as a white solid (48 mg, 0.115 mmol, 94% yield).



Methyl 3-(2,3,4,6,-tetra-*O*-acetyl- α -D-glucopyranosyl)propyl ketone (41).

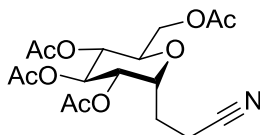
This compound was prepared according to the General Procedure A using aceto-1-bromo- α -D-glucose **1** (50 mg, 0.12 mmol, 1 mol eq.) and methyl vinyl ketone (20 μ L, 0.244 mmol, 2 mol eq.). Flash column chromatography (SiO₂: 50/50 ethyl acetate in hexanes) gave the desired product¹⁰¹ as a

white solid (42 mg, 0.104 mmol, 86% yield).



3-(2,3,4,6,-tetra-*O*-acetyl- α -D-glucopyranosyl)propionaldehyde (42).

This compound was prepared according to the General Procedure A using aceto-1-bromo- α -D-glucose **1** (50 mg, 0.12 mmol, 1 mol eq.) and acrolein (16 μ L, 0.244 mmol, 2 mol eq.). Flash column chromatography (SiO₂: 50/50 ethyl acetate in hexanes) gave the desired product^{67b} as a white solid (40 mg, 0.103 mmol, 85% yield).

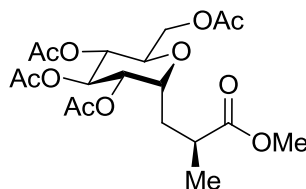


3-(2,3,4,6,-tetra-*O*-acetyl- α -D-glucopyranosyl)propionitrile (43).

This compound was prepared according to the General Procedure A using aceto-1-bromo- α -D-glucose **1** (50 mg, 0.122 mmol, 1 mol eq.) and acrylonitrile (16 μ L, 0.244 mmol, 2 mol eq.). Flash

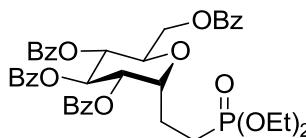
¹⁰¹ Abrecht, S.; Scheffold, R. *Chimia* **1985**, 39, 211.

column chromatography (SiO₂ in 50/50 to 60/40 ethyl acetate in hexanes) gave the desired product⁶⁸ as a white solid (40 mg, 0.104 mmol, 85% yield).



(2S)-methyl 2-methyl-3-(2,3,4,6-tetra-O-acetyl-α-D-glucopyranosyl)propanoate (44).

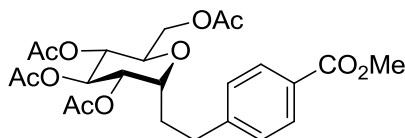
This compound was prepared according to the General Procedure A using aceto-1-bromo-α-D-glucose **1** (50 mg, 0.12 mmol, 1 mol eq.) and methyl methacrylate (28 μL, 0.244 mmol, 2 mol eq.). Flash column chromatography (SiO₂: 30:70 to 40:60 ethyl acetate in hexanes) gave the desired product⁵⁴ as a white solid (52 mg, 0.120 mmol, 98% yield, 1.5:1 dr of isomers).



Diethyl-2-(2,3,4,6-tetra-O-benzoyl-α-D-glucopyranosyl)ethylphosphonate (45).

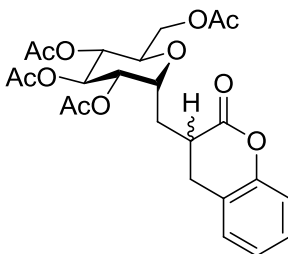
This compound was prepared according to the General Procedure A using aceto-1-bromo-α-D-glucose **35** (50 mg, 0.12 mmol, 2 mol eq.) and diethyl vinylphosphonate (188 μL, 1.22 mmol, 10 mol eq.). The reaction was placed directly on column for purification. Flash column chromatography (SiO₂: 80/20 ethyl acetate in hexanes) gave the desired product as a white solid (57 mg, 0.077 mmol, 63% yield). $[\alpha]_D^{25} = 33.9$ ($c = 2.45$). ¹H NMR (500 MHz, CDCl₃): δ 7.90-8.04 (m, 8H), 7.29-7.53 (m, 12H), 5.96 (t, ³J(H,H) = 9 Hz, 1H, *H*3), 5.53 (t, ³J(H,H) = 8.5 Hz, 1H, *H*4), 5.50 (dd, ³J(H,H) = 5.5 and 9 Hz, 1H, *H*2), 4.60 (dd, ³J(H,H) = 6.5 and 12 Hz, 1H, *H*6/7), 4.51 (dd, ³J(H,H) = 3 and 12 Hz, 1H, *H*6/7), 4.44 (m, 1H, *H*1), 4.28 (ddd, ³J(H,H) = 3, 6.5 and 8.5 Hz, 1H, *H*5) 4.02 (m, 4H, -OCH₂CH₃), 2.32 (m, 1H), 1.97 (m, 2H), 1.73 (m, 1H), 1.24 (t, ³J(H,H) = 7.5 Hz, 3H), 1.21 (t, ³J(H,H)

= 7 Hz, 3H). ^{13}C NMR (125 MHz, CDCl_3): δ 166.1, 165.6, 165.4, 165.3, 133.6, 133.5, 133.4, 133.2, 129.91, 129.89, 129.7, 129.6, 128.9, 128.84, 128.78, 128.5, 128.45, 128.43, 72.4, 72.2, 70.9, 70.1, 69.8, 69.3, 63.0, 61.72, 61.66, 21.8, 20.6, 19.67, 19.64, 16.46, 16.43, 16.42, 16.38. ^{31}P = δ 30.9. IR (film) $\tilde{\nu}$ = 3057, 2988, 2308, 1733, 1652, 1602, 1552, 1420, 1177, 1096, 1069, 1207 cm^{-1} . HRMS (ESI): m/z $[\text{M}+\text{H}]^+$ found 745.2400, calcd 745.2414 for $\text{C}_{40}\text{H}_{41}\text{O}_{12}\text{P}$. m.p. = 123-124°C.



Methyl 4-(2-[2,3,4,6,-tetra-*O*-acetyl- α -D-glucopyranosyl]ethyl)benzoate (46).

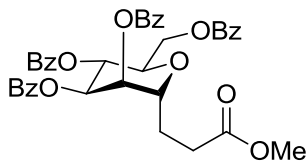
This compound was prepared according to the General Procedure B using aceto-1-bromo- α -D-glucose **1** (50 mg, 0.122 mmol, 1 mol eq.) and 4-methoxycarbonylstyrene (40 mg, 0.244 mmol, 2 mol eq.). Flash column chromatography (SiO_2 : 30/70 to 40/60 ethyl acetate in hexanes) gave the product as a colorless oil⁵ (31 mg, 0.063 mmol, 51% yield).



2-([2,3,4,6,-tetra-*O*-acetyl- α -D-glucopyranosyl]methylene)dihydrocoumarin (47).

This compound was prepared according to the General Procedure B using aceto-1-bromo- α -D-glucose **1** (492 mg, 1.2 mmol, 1 mol eq.) and 2-methylene-3-hydrocoumarin (**77**) (384 mg, 2.4 mmol, 2 mol eq.). Flash column chromatography (SiO_2 : 30/70 ethyl acetate in hexanes) gave the product as a 1.8:1 mixture of diastereomers as a white solid (525 mg, 1.07 mmol, 89% yield). The material was

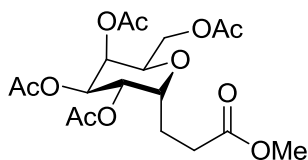
then recrystallized from benzene/hexanes to give analytically pure product as a 1:1 mixture of diastereomers. $[\alpha]_D^{25} = +107.2$ ($c = 0.60$). ^1H NMR (500 MHz, CDCl_3): δ 7.26 (t, $^3J(\text{H,H}) = 7.7$ Hz, 1H + 1H, major + minor) 7.18 (d, $^3J(\text{H,H}) = 7.1$ Hz, 1H + 1H, major + minor), 7.10 (t, $^3J(\text{H,H}) = 7.5$ Hz, 1H + 1H, major + minor), 7.04 (dd, $^3J(\text{H,H}) = 3.2$ and 8 Hz, 1H + 1H, major + minor) 5.36 (t, $^3J(\text{H,H}) = 9.2$ Hz, 1H, *H3*, minor), 5.27 (t, $^3J(\text{H,H}) = 8.5$ Hz, 1H, *H3*, major), 5.13 (dd, $^3J(\text{H,H}) = 1.6$ and 5.25 Hz, 1H, *H2*, major), 5.11 (dd, $^3J(\text{H,H}) = 3.2$ and 5.9 Hz, 1H, *H2*, minor), 4.98 (t, $^3J(\text{H,H}) = 9.1$ Hz, 1H, *H4*, minor), 4.95 (t, $^3J(\text{H,H}) = 8.3$ Hz, 1H, *H4*, major), 4.52 (ddd, $^3J(\text{H,H}) = 2.8$, 5.3 and 11.6 Hz, 1H, *H1*, major), 4.39 (ddd, $^3J(\text{H,H}) = 3.0$, 5.8 and 12.5 Hz, 1H, *H1*, minor), 4.25-4.17 (m, 1H + 1H, *H6/7*, major + minor), 4.10 (dd, $^3J(\text{H,H}) = 2.9$ and 12.2 Hz, 1H, *H6/7*, major), 3.99 (dd, $^3J(\text{H,H}) = 2.3$ and 12.2 Hz, 1H, *H6/7*, minor), 3.92-3.83 (m, 1H + 1H, *H5*, major + minor), 3.10-2.92 (m, 2H + 1H, major + minor), 2.88-2.79 (m, 1H + 2H, major + minor), 2.66 (dt, $^3J(\text{H,H}) = 2.8$ and 13.5 Hz, 1H, minor), 2.20 (ddd, $^3J(\text{H,H}) = 2.7$, 8.3 and 14.8 Hz, 1H, major), 2.09 (s, 3H, OAc), 2.05-1.95 (m, 17H, major + minor), 1.92 (s, 3H, OAc), 1.86 (s, 3H, OAc), 1.71-1.64 (m, 1H, minor). ^{13}C NMR (125 MHz, CDCl_3): δ 170.7, 170.6, 170.5, 170.3, 170.0, 169.9, 169.8, 169.6, 169.5, 151.5, 151.4, 128.5, 128.5, 128.1, 127.8, 124.6, 124.4, 122.8, 122.3, 116.7, 116.7, 70.7, 70.1, 70.1, 69.8, 69.7, 69.6, 69.2, 69.1, 68.5, 60.4, 62.2, 62.1, 35.6, 35.1, 31.6, 30.3, 28.2, 26.7, 25.1, 22.7, 20.8, 20.7, 20.7, 20.6, 20.5, 20.4. IR (film) $\tilde{\nu} = 3057, 2988, 1750, 1617, 1590, 1490, 1459, 1424, 1370, 1227, 1146, 1096, 1038\text{ cm}^{-1}$. HRMS (ESI): m/z $[\text{M}+\text{H}]^+$ found 493.1698, calcd 493.1710 for $\text{C}_{24}\text{H}_{28}\text{O}_{11}$.



Methyl 3-(2,3,4,6-tetra-*O*-benzoyl- α -D-mannopyranosyl)propanoate (48).

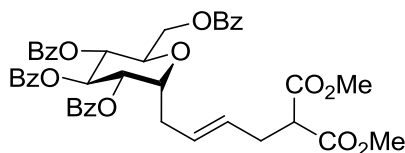
This compound was prepared according to a modified General Procedure A using α -D-mannopyranosyl bromide tetrabenzoate **35** (80 mg, 0.12 mmol, 1 mol eq.) and methyl acrylate (22 μL , 0.244 mmol, 2 mol eq.) and Hantzsch ester **4** (34 mg, 0.134 mmol, 1.1 eq). Flash column chromatography (SiO_2 : 40/60 to 50/50 ethyl acetate in hexanes gradient) gave the desired product as a

white solid (66 mg, 0.099 mmol, 81% yield). $[\alpha]_D^{25} = -16.68$ ($c = 1.68$) ^1H NMR (400 MHz, CDCl_3): δ 8.09 (dd, $^3J(\text{H,H}) = 1.6$ and 6.8 Hz, 2H), 8.03 (dd, $^3J(\text{H,H}) = 1$ and 8 Hz, 2H), 7.98 (dd, $^3J(\text{H,H}) = 1.2$ and 6 Hz, 2H), 7.3-7.6 (m, 12 H), 6.02 (t, $^3J(\text{H,H}) = 9.2$ Hz, 1 H, H_4), 5.81 (dd, $^3J(\text{H,H}) = 3.2$ and 9.2 Hz, 1H, H_3), 5.65 (t, $^3J(\text{H,H}) = 3.2$ Hz, 1H, H_2), 4.60 (m, 2H, H_6 and H_7), 4.29-4.35 (m, 2H H_1 and H_5), 3.69 (s, 3H, -OMe), 2.55 (m, 2H), 2.41 (m, 1H), 2.10 (m, 1H). ^{13}C NMR (125 MHz, CDCl_3): δ 173.2, 166.2, 165.6, 165.5, 165.4, 133.5, 133.4, 133.3, 129.81, 129.78, 129.73, 129.4, 128.9, 128.5, 128.47, 128.41, 128.40, 74.7, 71.6, 70.6, 69.9, 62.8, 51.8, 30.1, 23.8. IR (film) 3067, 2960, 2929, 2856, 1729, 1605, 1455, 1285, 1250, 1181, 1111, 1073, 1026 cm^{-1} . HRMS (ESI): m/z $[\text{M}+\text{H}]^+$ found 667.2163, calcd 667.2174 for $\text{C}_{38}\text{H}_{34}\text{O}_{11}$. m.p. = 54-57°C.



Methyl 3-(2,3,4,6-tetra-*O*-acetyl- α -D-galactopyranosyl)propanoate (49).

This compound was prepared according to the General Procedure A using aceto-1-bromo- α -D-galactose (50 mg, 0.12 mmol, 1 mol eq.) and methyl acrylate (22 μL , 0.244 mmol, 2 mol eq.). Flash column chromatography (SiO_2 : 30/70 to 50/50 ethyl acetate in hexanes gradient) gave the desired product^{67b} as a white solid (41 mg, 0.098 mmol, 80% yield).

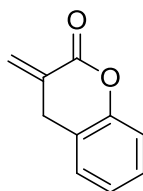


(*E*)-Dimethyl 2-(4-[2,3,4,6-tetra-*O*-benzoyl- α -D-glucopyranosyl]but-2-enyl)malonate (50).

This compound was prepared according to the General Procedure A using α -D-mannopyranosyl bromide tetrabenzoate **35** (80 mg, 0.122 mmol, 1 mol eq.) and dimethyl 3-vinylcyclopropane-1,1-dicarboxylate (450 mg, 2.44 mmol, 20 mol eq.). Flash column chromatography (SiO_2 : 25/75 ethyl acetate in hexanes) gave the product as a white powder⁵ (51 mg, 0.065 mmol, 54% yield).

***N,N*-diisopropylammonium tetrafluoroborate (23·HBF₄).**

To a round bottom flask fitted with a stir bar was added acetone (20 mL) and *i*Pr₂NEt **23** (10 mL, 57 mmol). The solution was cooled to 0° C, and HBF₄·Et₂O (7.7 mL, 57 mmol) was added dropwise. The solution was allowed to stir for 10 minutes, and a white precipitate formed. Additional acetone was added to dissolve precipitate. The solution was dried with MgSO₄, filtered, and concentrated in vacuo. The resulting solid was redissolved in a minimal amount of acetone, and 200 mL Et₂O was added. A white solid formed which was collected via suction filtration and rinsed with Et₂O to give the product as a white powder (10.0 g, 81% yield). ¹H NMR (500 MHz, CDCl₃): δ 6.75 (br, 1H, N-H), 3.69 (m, 2H), 3.15 (m, 2H), 1.40 (m, 15H). ¹³C NMR (125 MHz, CDCl₃): δ 55.3, 43.4, 18.5, 17.1. IR (film) $\tilde{\nu}$ = 3134, 3057, 2991, 2953, 1482, 1424, 1405, 1181, 1131, 1073, 996, 926, 895 cm⁻¹.



2-methylene-3-hydrocoumarin (77).

To a flame dry round bottom flask under Ar with a stir bar was added THF (100 mL) and *i*Pr₂NH (6.6 mL, 47 mmol, 3 mol eq.). The flask was cooled to -78° C, and *n*BuLi (29.3 mL, 1.6 M in hexanes, 47 mmol, 3 mol eq.) was added. The reaction was allowed to stir 10 minutes. Dihydrocoumarin (2 mL, 15.8 mmol, 1 mol eq.) was added as a solution in dry THF (12 mL with an 8 mL rinse). The reaction was allowed to stir 30 minutes at -78° C, and Eschenmoser's salt (10.2 g, 55.2 mmol, 3.5 mol eq.) was added all at once. A yellow suspension resulted, which was allowed to warm to room temperature and stir for 75 minutes. The reaction was quenched with NH₄Cl_(aq). The layers were separated, and the aqueous layer was extracted 2 x Et₂O. The combined organic layers were rinsed with brine, dried with MgSO₄, and filtered. The solvent was evaporated in vacuo to afford the crude product as a yellow oil. The crude mixture was then dissolved in THF (not anhydrous), which

resulted in a yellow solution. To this solution was added a stir bar and MeI (5 mL, 80 mmol, 5 mol eq.). The reaction was allowed to stir open to air at room temperature for 18 hours. The resulting suspension was quenched by filtering through a plug of silica and rinsing with Et₂O. The solvent was removed in vacuo in order to afford the crude product as a yellow oil. Flash column chromatography (SiO₂: 10/90 ethyl acetate in hexanes) afforded the product as a white solid (1.2 g, 7.5 mmol, 47% yield over 2 steps). ¹H NMR (500 MHz, CDCl₃): δ 7.25 (t, ³J(H,H) = 8 Hz, 1H), 7.19 (d, ³J(H,H) = 7.4 Hz, 1H), 7.12 (t, ³J(H,H) = 7.4 Hz, 1H), 7.08 (d, ³J(H,H) = 8 Hz, 1H), 6.44 (s, 1H), 5.80 (s, 1H), 3.83 (s, 2H). ¹³C NMR (125 MHz, CDCl₃): δ 163.3, 150.8, 131.7, 128.6, 128.2, 127.7, 124.5, 121.1, 117.0, 32.0. IR (film) $\tilde{\nu}$ = 3057, 2988, 1749, 1637, 1617, 1557, 1490, 1459, 1424, 1227, 1193, 1170, 1139, 1110. HRMS (ESI): *m/z* [M+H]⁺ found 161.0603, calcd 161.0603 for C₁₀H₈O₂. m.p. = 65-67°C.

Time-Resolved EPR Measurements.

Our TREPR apparatus has been described previously in several recent publications.¹⁰² Briefly, a YAG pumped OPO laser system with output at 460 nm (5 mJ) is fired at a repetition rate of 10 Hz, while sampling the direct detection EPR signal from the microwave bridge (CW mode) using a gated boxcar signal averager. The external magnetic field is swept over 2 or 4 minutes with 100 or 300 ns wide gates sampling the EPR signal 5-10 times at each magnetic field point. The flow system was flushed and a solvent blank was run before all experiments. All spectra have center field of 3270 G, sweep width of 200 G, microwave frequency 9.47 GHz, microwave power 10 mW. Samples were

¹⁰² (a) Lebedeva, N. V.; Forbes, M. D. E. Acrylic Polymer Radicals: Structural Characterization and Dynamics in Carbon-Centered Radicals and Radical Cations. In *Wiley Series on Reactive Intermediates in Chemistry and Biology*; Forbes, M.D.E., Ed; Wiley: New York, 2010, Vol. 3; p 323-355. (b) Forbes, M. D. E. *Photochem. Photobiol.* **1997**, 65, 73.

flowed through the microwave resonator using a micropump from a reservoir that was constantly purged with nitrogen gas bubbles (for 10 minutes prior to and during TREPR).

Chapter 4 - Rate of Glucosyl Radical Generation.

Effect of Alkenes and Catalyst on Rate.

During the investigations detailed in Chapter 3, the required reaction times for the visible-light mediated radical conjugate addition into alkenes were observed to be dependent on the nature of the alkene. For example, addition into methyl acrylate required only 12 hours to achieve full-conversion, whereas addition into methyl vinyl ketone required 48 hours. In an effort to further probe these observations, reactions with methyl acrylate and methyl vinyl ketone were monitored *in situ* by ^1H NMR. In addition to $\text{Ru}(\text{bpy})_3^{2+}$, two additional photocatalysts were investigated in order to investigate the effect these catalysts might have on the rate of the reaction. $\text{Ru}(\text{dmb})_3^+$ is a stronger reductant than $\text{Ru}(\text{bpy})_3^+$ (-1.47 V vs -1.35 V), so it is possible the rate could be accelerated due to a more thermodynamically favorable electron transfer from catalyst to substrate. We envisioned $\text{Ru}(\text{dtb-bpy})_3^{2+}$ could exacerbate these differences, as it is an even stronger reductant (-1.68 V vs SCE). $\text{Ir}(\text{ppy})(\text{dtb-bpy})^+$ has been shown by the MacMillan group to afford higher yields than $\text{Ru}(\text{bpy})_3^{2+}$ in certain reactions,¹⁰³ and we hoped to apply this to our system in an attempt to further improve the reaction. Initial investigations into this area were conducted with the help of Stephanie Kramer and are reported in Figure 4.1 and Figure 4.2.

¹⁰³ Nagib, D. A.; Scott, M. E.; MacMillan, D. W. C., *J. Am. Chem. Soc.* **2009**, *131*, 10875-10877.

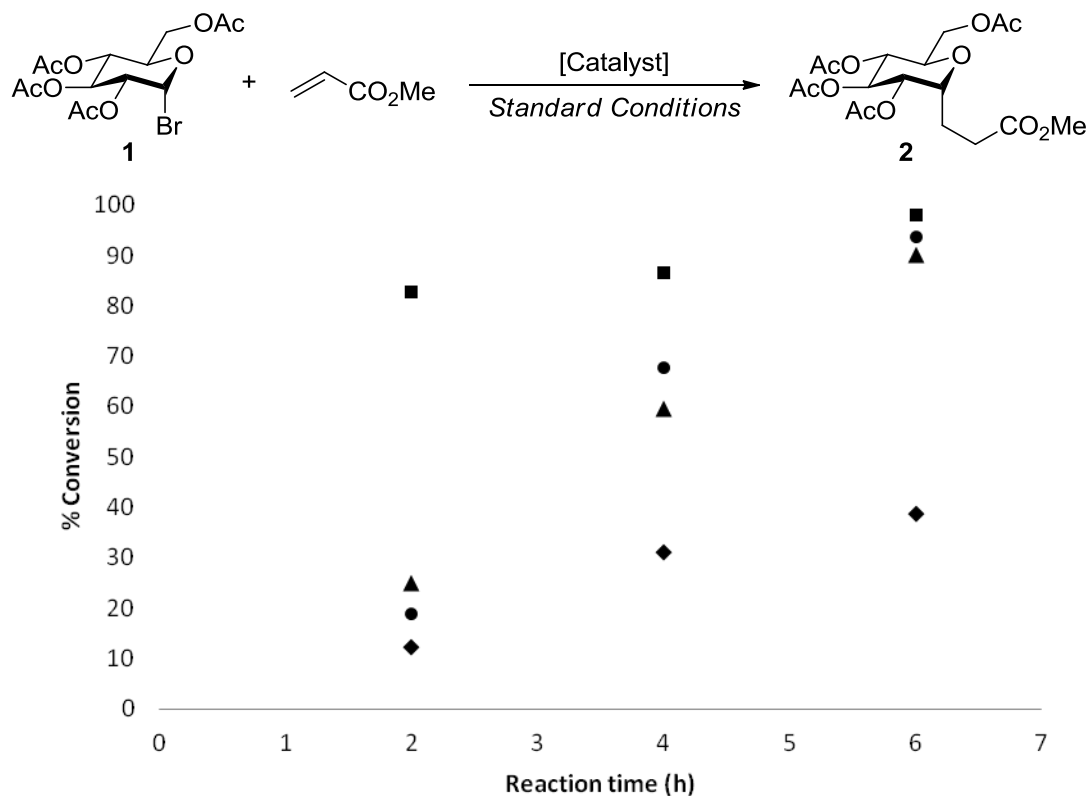


Figure 4.1: Reaction of Glucosyl Bromide 4 with Methyl Acrylate. Diamond = $\text{Ru}(\text{bpy})_3^{2+}$; circle = $\text{Ru}(\text{dmb})_3^{2+}$; triangle = $\text{Ru}(\text{dtb-bpy})_3^{2+}$; square = $\text{Ir}(\text{ppy})_2(\text{dtb-bpy})^+$.

For the reaction with methyl acrylate, it was found $\text{Ir}(\text{ppy})_2(\text{dtb-bpy})^+$ provided the fastest reaction, achieving full conversion in approximately 4 hours of reaction time (Figure 4.1). $\text{Ru}(\text{bpy})_3^{2+}$ was the slowest catalyst, providing only 40% conversion after 6 hours of irradiation. Interestingly, while $\text{Ru}(\text{dmb})_3^{2+}$ did provide the expected acceleration in rate to give 90% conversion in 6 hours, $\text{Ru}(\text{dtb-bpy})_3^{2+}$ did not further enhance the rate of the reaction.

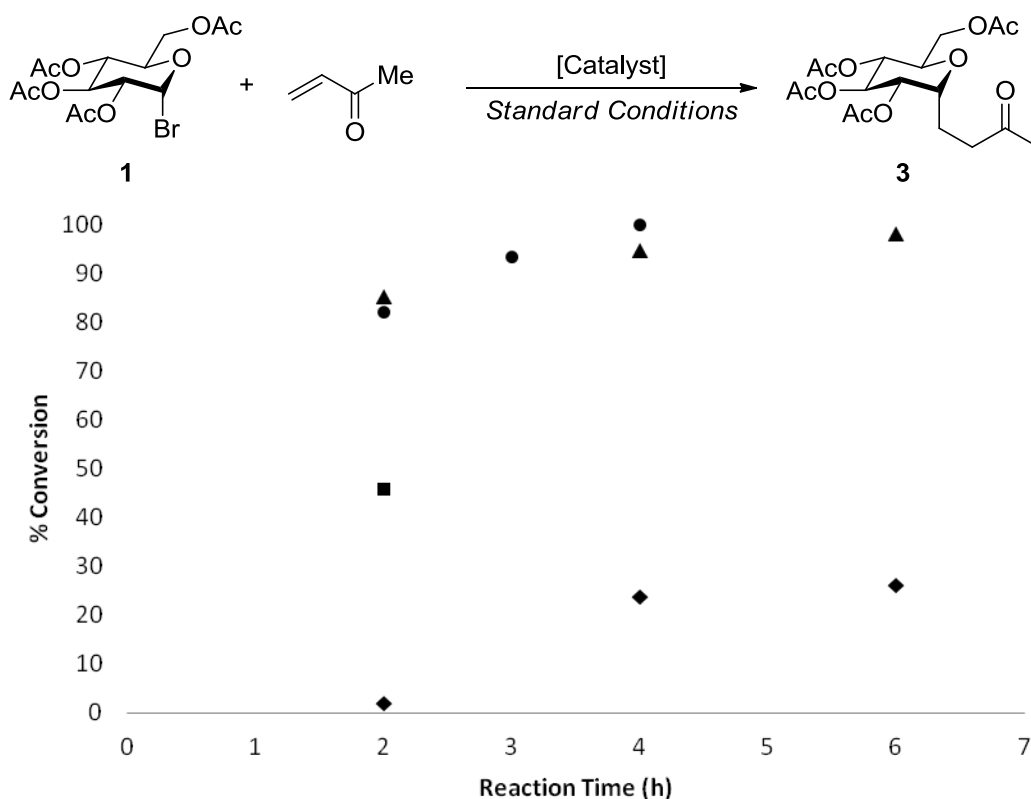
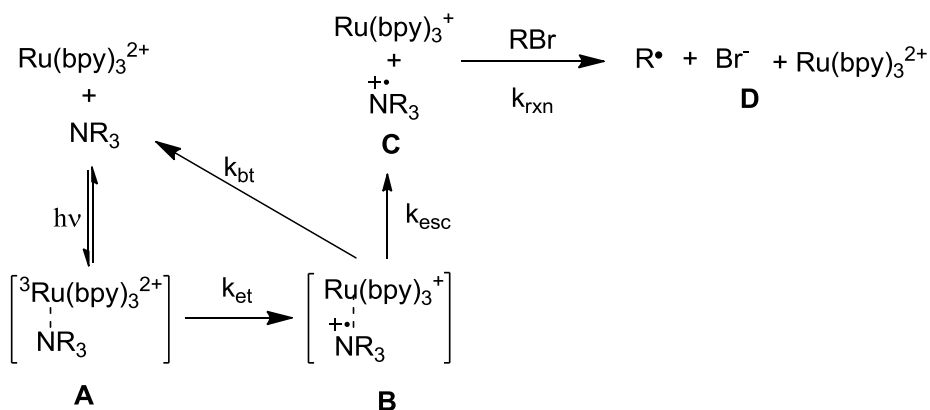


Figure 4.2: Reaction of Glucosyl Bromide **4** with Methyl Vinyl Ketone. Diamond = Ru(bpy)₃²⁺; circle = Ru(dmb)₃²⁺; triangle = Ru(dtb-bpy)₃²⁺; square = Ir(ppy)₂(dtb-bpy)⁺.

Surprisingly, reactions with methyl vinyl ketone provided drastically different results. It was found that Ru(bpy)₃²⁺ again provided the slowest rate of reaction but resulted in only 30% conversion after 6 hours (Figure 4.2). Both Ru(dmb)₃²⁺ and Ru(dtb-bpy)₃²⁺ dramatically increased the rate of reaction, requiring only 2 hours of irradiation to provide approximately 85% conversion. Ir(ppy)₂(dtb-bpy)⁺ also resulted in a significant increase in reaction rate but simultaneously consumed methyl vinyl ketone, presumably through radical-mediated oligomerization after reduction from the catalyst. From these results, it is clear that both catalyst and alkene influence the rate of the reaction. To further understand these effects and how to take advantage of them, we sought to investigate the nature of the photoredox cycle and its effect on the rate and efficiency of the reaction.

Rate of Photoredox Cycle.

The proposed mechanism in Chapter 3 details the fate of the glycosyl radical in terms of product and byproduct formation. The nature of the photoredox cycle is still a mystery. While much is known about the behavior of RuL_3^{2+} complexes and the mechanism of reductive quenching,¹⁰⁴ little work has been devoted to investigating the mechanism of the photoredox cycle as applied to generation of alkyl radicals. Moreover, little is known about the rate and efficiency of this process. Based on previous reports, a generalized mechanism for reductive quenching of $^3\text{RuL}_3^{2+}$ is depicted in Scheme 4.1.¹⁰⁴



Scheme 4.1: Proposed Mechanism of Reductive Quenching of $\text{Ru}(\text{bpy})_3^{2+}$ with Amines.

In this mechanism, $\text{Ru}(\text{bpy})_3^{2+}$ is excited by visible light to its triplet-excited state, $^3\text{Ru}(\text{bpy})_3^{2+}$. In the presence of an amine quencher, the photoexcited catalyst and the quencher exist as a solvent-separated pair in equilibrium with an associated precursor complex **A**. Outer-sphere electron transfer (k_{et}) from the amine to the metal complex in precursor complex **A** generates an ion-pair, called a successor complex (Scheme 4.1, **B**). Solvent-cage escape (k_{esc}) leads to an amine radical-cation and activated photocatalyst (Scheme 4.1, **C**), the latter of which can then react with

¹⁰⁴ a) Kavarnos, G. J.; Turro, N. J., *Chem. Rev.* **1986**, 86, 401-449. b) Julliard, M.; Chanon, M., *Chem. Rev.*

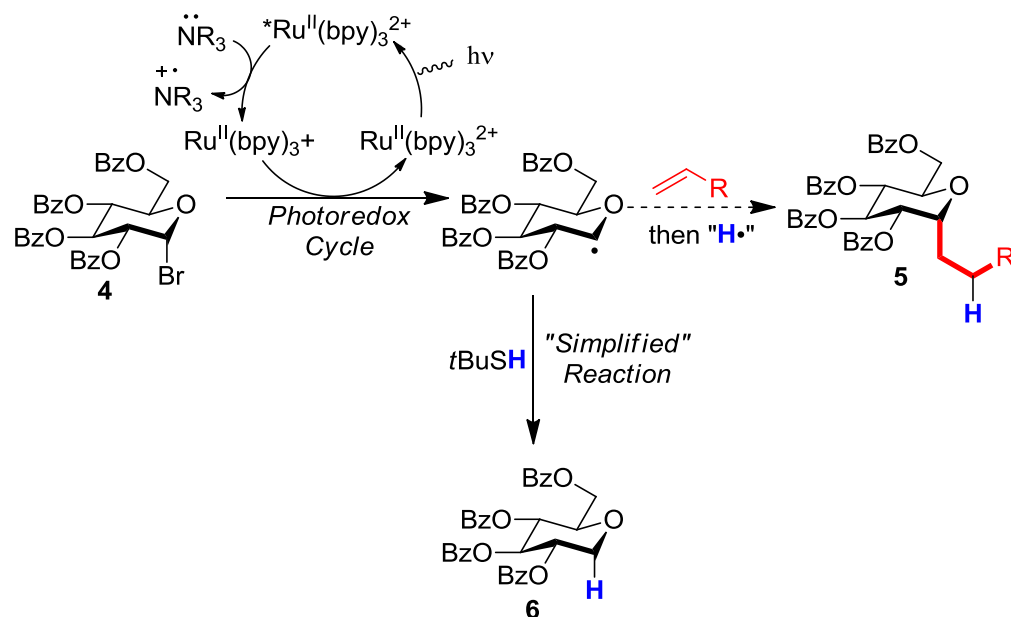
1983, 83, 425-506. c) Kitamura, N.; Kim, H. B.; Okano, S.; Tazuke, S., *J. Phys. Chem.* **1989**, 93, 5750-5756. d)

Ballardini, R.; Varani, G.; Indelli, M. T.; Scandola, F.; Balzani, V., *J. Am. Chem. Soc.* **1978**, 100, 7219-7223.

substrate to generate the desired organic radical. In a competitive pathway, back electron transfer (k_{bt}) returns the photocatalyst and quencher to the ground state after dissociation (not shown). Back-electron transfer is an energy-wasting process, as it converts light energy into thermal energy without generating the organic radical. This serves to slow the observed rate of the forward reaction (k_{rxn}).

The reaction times in our reported light-mediated *C*-glycoside synthesis were typically long (12-48 h),⁹¹ and we considered the possibility that nonproductive heat generation was the source of these long reaction times. Simply put, a significant proportion of the incoming energy from the light source was not driving the reaction forward and was therefore wasted. Based on the simplified reaction mechanism depicted in Scheme 4.1, we presumed the inefficiencies were localized in the photogeneration of the glycosyl radical, as trapping of a glycosyl radical with methyl acrylate is expected to be fast and efficient. Thus our initial goal was to probe the photoredox cycle to determine factors that affect the rate of radical generation.

In order to simplify the reaction, we planned to trap the C1 radical with *t*BuSH in lieu of an alkene, since the rate of the reaction has been shown to depend on the alkene.⁹¹ Thiols have been shown to effectively trap C1 radicals by preventing acetoxy migration to form a C2 radical (Scheme 4.2).⁹³ By avoiding trapping with alkenes, the formation of byproducts after radical generation is eliminated, and several possible variables in the mechanism are removed, such as the role of Hantzsch ester in the terminating step(s).



Scheme 4.2: Proposed Trapping of Glycosyl Radicals with Thiols.

Experimental Design.

In order to conduct the experiment without resorting to traditional kinetics, which require photon counting, we planned to irradiate parallel reactions for a specified length of time and compare the conversions between the reactions. Assuming the photon flux is consistent for each sample, this allows for direct comparison of the reactions. As glucosyl bromide **4** and its reductive bromination product **6** were amenable to identification and quantification by ^1H NMR, the reactions could be readily irradiated in NMR tubes to determine the conversion *in situ*. To ensure the rate of reaction was consistent, the NMR tubes were placed at an equal distance from the CFL source, as depicted in Figure 4.3.

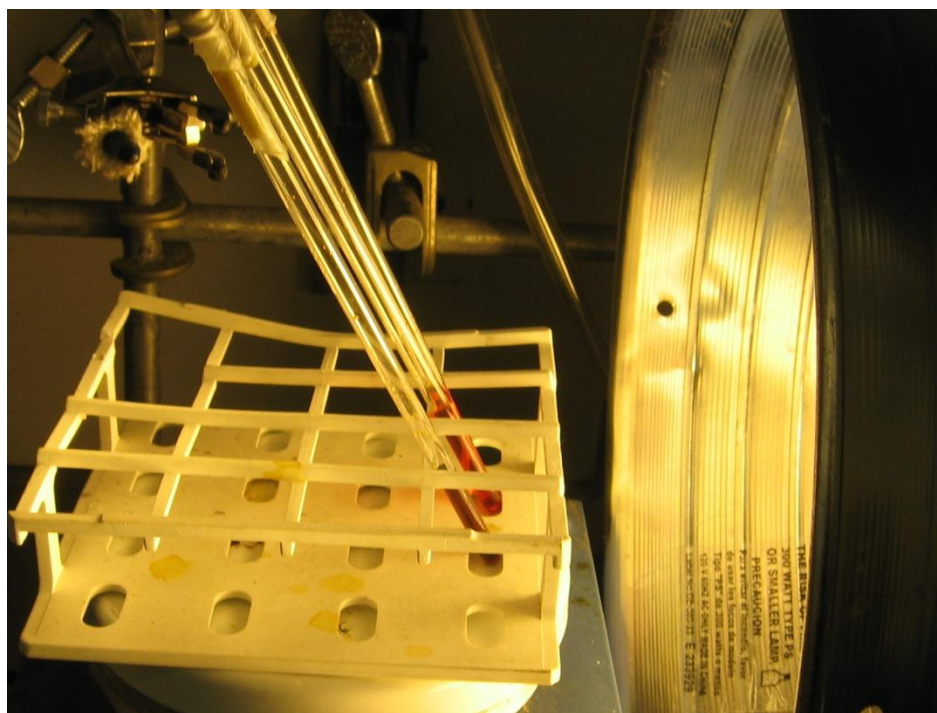
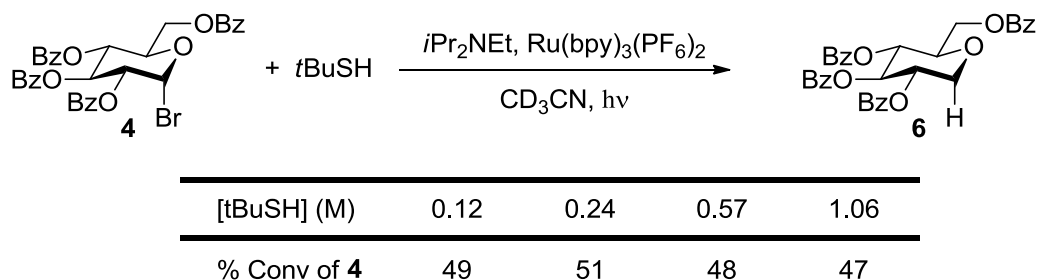


Figure 4.3: Experimental Setup for CFL Irradiation of NMR Tubes.

As the reaction times of *C*-glycoside formation are dependent on the alkene, we considered the possibility that radical conjugate addition is the rate limiting step rather than electron transfer to the substrate. To test if this was also the case with thiol trapping of the radical, the concentration of *t*BuSH was varied in a series of experiments, and the amount of consumed starting material after 3 hours of irradiation with a 14 W CFL was compared.¹⁰⁵ It was found that thiol concentration had no significant effect on the rate of the reaction, resulting in an average conversion of 49% (Scheme 4.3). This consistency indicates the radical trapping is fast, and therefore that the observed conversions reflect the rate of glucosyl radical generation. Since this may not be the case with alkene-trapping, the use of thiols is essential to probing the photoredox cycle.

¹⁰⁵ Andrews, R. S.; Becker, J. J.; Gagné, M. R., *Org. Lett.* **2011**, *13*, 2406-2409.



Scheme 4.3: Varying Concentration of Thiol on Consumption of **4**.

Rate Dependence on Reagent Concentration.

Based on the success of these initial control experiments, we then varied the concentration of glucosyl bromide **4**. It was found that the rate directly depended on the initial concentration of glucosyl bromide **4**, suggesting a rate-limiting single-electron transfer (SET) from photogenerated $\text{Ru}(\text{bpy})_3^+$ to **4** (Figure 4.4). Since the rate equation for electron transfer would presumably be dependent both on **[4]** and $[\text{Ru}(\text{bpy})_3^+]$, we then turned our attention to probing the factors that affect the steady state concentration of active catalyst.

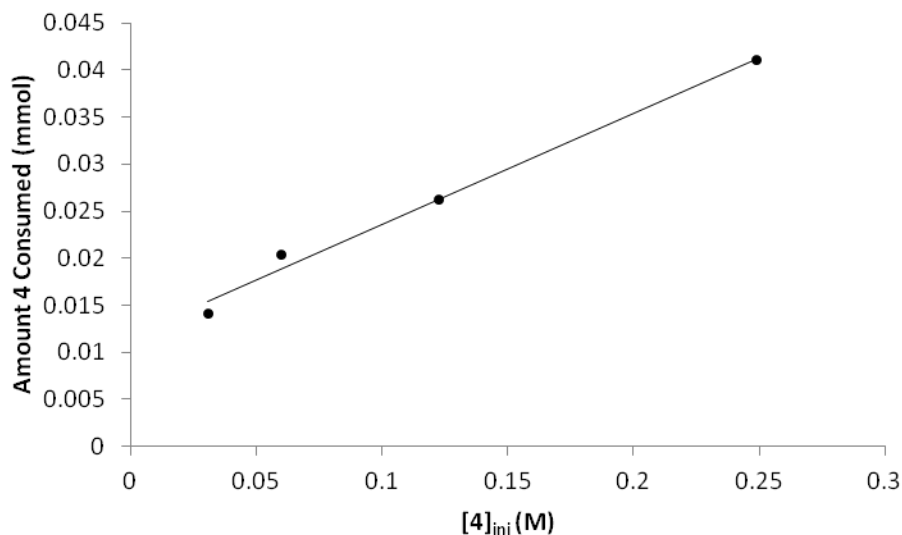


Figure 4.4: Amount of **1** consumed after 3 h of irradiation with a 14 W CFL light source versus initial concentration of **1**. Reaction conditions: 6.0 mM $\text{Ru}(\text{bpy})_3^{2+}$, 0.37 M Et_3N , 0.24 M $t\text{BuSH}$ in CD_3CN .

Varying the initial concentration of catalyst revealed two distinct regions. Under dilute conditions (<4 mM), the rate of the reaction was proportional to $[\text{Ru}(\text{bpy})_3^{2+}]$, whereas the rate plateaued at concentrations >4 mM (Figure 4.5). The observation of a plateau could arise from a photon-limited scenario where catalyst concentration exceeds photon flux.

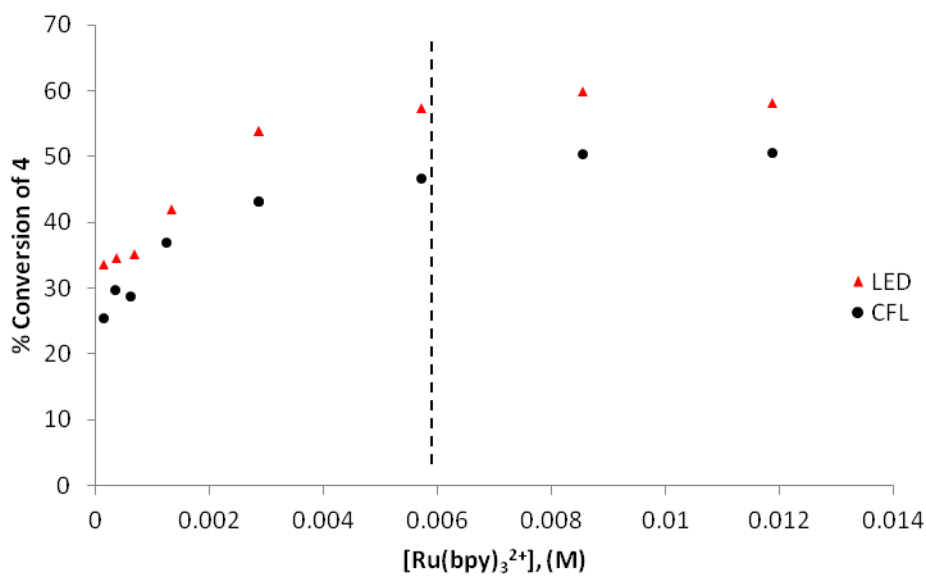


Figure 4.5: Conversion after 3 h of irradiation with increasing $[\text{Ru}(\text{bpy})_3^{2+}]$ for CFL and blue LED light sources. Reaction conditions: 0.37 M EtNiPr₂, 0.24 M *t*BuSH, 0.12 M **1** in CD₃CN.

In order to test this hypothesis, we constructed an experimental apparatus that utilizes 12" blue LED strips, which have been reported to generate a higher flux at the MLCT absorption wavelength (1W, $\lambda_{\text{max}} = 435$ nm). To ensure consistent flux for each NMR vessel, a Liebig's reflux condenser was wrapped with a single LED strip in a 5 cm vertical span. Four of these condensers were connected in serial, and cool water was passed through them to ensure a consistent reaction temperature, as the LED strips generate significant heat (~ 50 °C in the condenser without water-cooling). An NMR tube was passed through a septum and placed in each condenser as shown in Figure 4.6. Control experiments to test the consistency of the chambers resulted in a 60-61% conversion for each reaction, confirming that each chamber was receiving the same approximate flux.

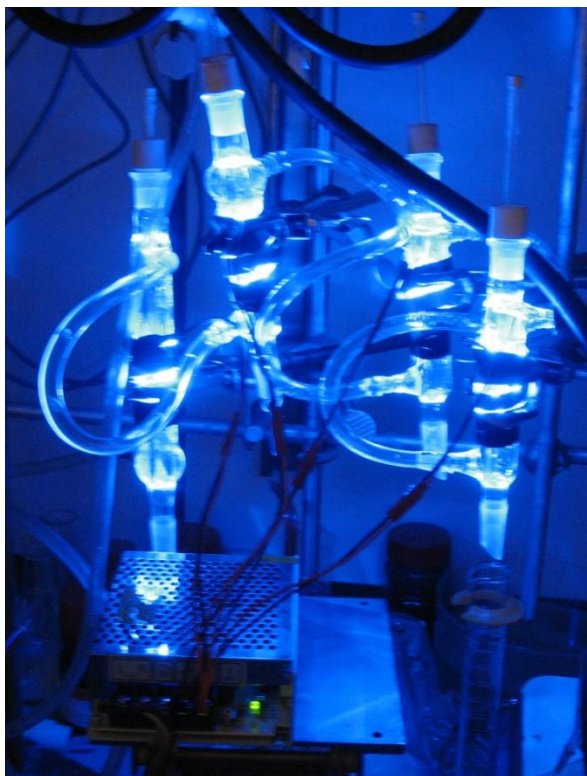


Figure 4.6: Experimental Setup for the Irradiation of NMR Tubes with Blue LEDs.

The amount of **4** consumed at all catalyst concentrations was determined to be flux dependent, as repeating the experiments in Figure 4.5 using the described blue LED apparatus resulted in higher conversions (Figure 4.5). This is consistent with the hypothesis that these reactions are photon-limited. A similar saturation in conversion was observed with increasing concentrations of amine (Figure 4.7).

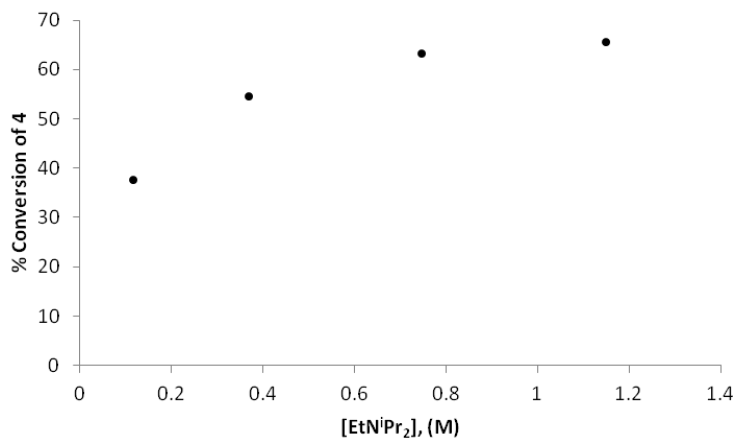


Figure 4.7: % Conversions after 3 h of irradiation as a function of initial EtNiPr₂ concentration. Reaction conditions: 5.9 mM Ru(bpy)₃²⁺, 0.24 M *t*BuSH, 0.12 M **1** in CD₃CN.

The rate of bimolecular quenching of Ru(bpy)₃²⁺ has been described in typical Marcus terms as proceeding through an encounter complex prior to electron transfer and formation of the successor complex.¹⁰⁴ The rate of electron transfer is dependent on several factors, including complex reorganization energy, ΔG° between the precursor and successor complex, and electronic coupling of the charged states. The efficiency of the overall reaction is related to k_{esc} vs k_{bt} and the rate of electron transfer has been shown to be sensitive to solvent effects (Scheme 4.1).^{104,106} Examples of the effect of solvent on the rate of electron transfer reactions have been reported. Based on these results and those reported by Stephenson,¹⁰⁷ solvent composition was a logical place to look for improved efficiencies in our system.

¹⁰⁶ a) Sun, H.; Yoshimura, A.; Hoffman, M. Z., *J. Phys. Chem.* **1994**, 98, 5058-5064. b) Clark, C. D.; Hoffman, M. Z., *J. Phys. Chem.* **1996**, 100, 7526-7532. c) Clark, C. D.; Hoffman, M. Z., *J. Phys. Chem.* **1996**, 100, 14688-14693. d) Fedurco, M.; Sartoretti, C. J.; Augustynski, J., *J. Phys. Chem. B* **2001**, 105, 2003-2009.

¹⁰⁷ Nguyen, J. D.; Tucker, J. W.; Konieczynska, M. D.; Stephenson, C. R. J., *J. Am. Chem. Soc.* **2011**, 133, 4160-4163.

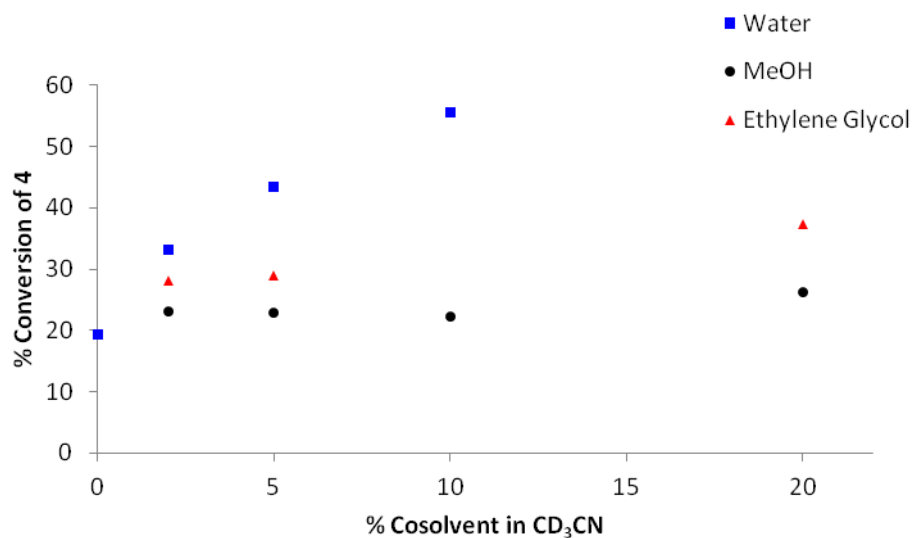


Figure 4.8: % conversion of **1** (20 min) after photolysis with blue LEDs versus cosolvent additive. Conditions: 5.9 mM Ru(bpy)₃²⁺, 0.37 M EtNiPr₂, 0.24 M *t*BuSH, and 0.12 M **1** in CD₃CN.

To determine the effect of solvation on the rate of glucosyl radical generation, we varied the amount of water, ethylene glycol, methanol and DMF in acetonitrile. As shown in Figure 4.8, water dramatically increased the efficiency of the reaction, reaching 55% conversion in only 20 minutes in 10% aqueous acetonitrile as compared to over 3 hours under anhydrous conditions. By comparison, DMF and ethanol (not shown) were ineffective at increasing the rate, and ethylene glycol was moderately effective. Higher concentrations of water (>10%) resulted in the formation of a biphasic mixture in the NMR tubes which showed minimal reactivity.

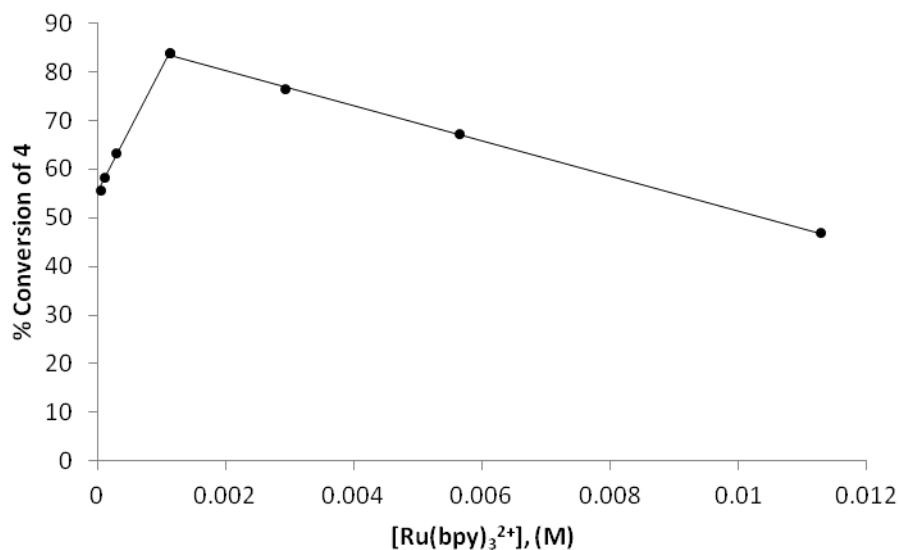


Figure 4.9: Conversion after 20 min of irradiation with blue LEDs with increasing $[\text{Ru}(\text{bpy})_3^{2+}]$. Reaction conditions: 0.33 M EtNiPr_2 , 0.22 M $t\text{BuSH}$, 0.11 M **1** in 10:1 $\text{CD}_3\text{CN}:\text{H}_2\text{O}$.

When the effect of the initial concentration of $\text{Ru}(\text{bpy})_3^{2+}$ on the rate of radical generation was re-evaluated in 10% aqueous acetonitrile, a surprising trend emerged. As seen before, low initial concentrations of photocatalyst led to a strong linear increase in rate with respect to $[\text{Ru}(\text{bpy})_3^{2+}]$ (Figure 4.9). However, instead of increased photocatalyst concentrations leading to a conversion plateau, a strong inverse linear relationship was observed. Additionally, the crossover point between high and low concentrations was changed from 4 mM to 1 mM.

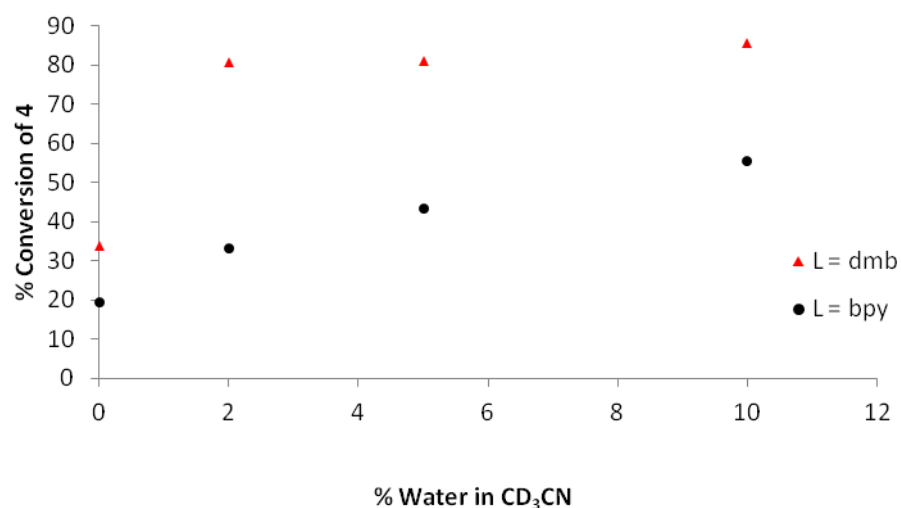


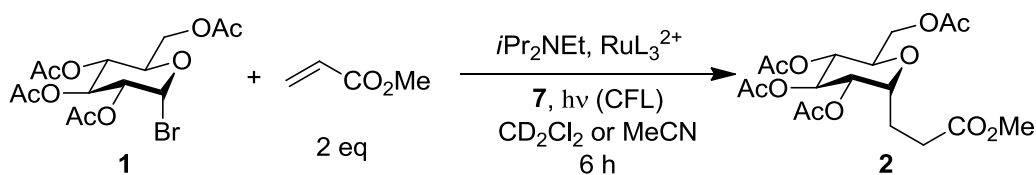
Figure 4.10: Conversion after 20 min of irradiation with blue LEDs for $\text{Ru}(\text{L})_3^{2+}$. Reaction conditions: 6.0 mM $\text{Ru}(\text{L})_3^{2+}$, 0.37 M EtNiPr_2 , 0.24 M $t\text{BuSH}$, 0.12 M **1** in $\text{CD}_3\text{CN}/\text{H}_2\text{O}$.

It has been reported that hydrophobic catalysts are more effective at solvating after electron transfer, decreasing the propensity of the catalyst to undergo back electron transfer and increasing the efficiency.¹⁰⁸ To test this, $\text{Ru}(\text{dmb})_3^{2+}$ ($\text{dmb} = 4,4'$ -dimethyl-2,2'-bipyridine) was used as the catalyst at varying concentrations of water in acetonitrile (Figure 4.10). At all concentrations of water, $\text{Ru}(\text{dmb})_3^{2+}$ resulted in higher conversions, (32% vs 20% under anhydrous conditions). However, adding only 2% water in acetonitrile resulted in a dramatic increase in conversion, achieving >80% conversion in only 20 minutes of irradiation. Further increasing the concentration of water failed to significantly improve the rate of radical generation (up to 10% water in CD_3CN).

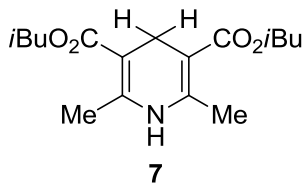
¹⁰⁸ a) Tazuke, S.; Kitamura, N.; Kawanishi, Y., *J. Photochem.* **1985**, 29, 123-138. b) Bock, C. R.; Connor, J. A.; Gutierrez, A. R.; Meyer, T. J.; Whitten, D. G.; Sullivan, B. P.; Nagle, J. K., *Chem. Phys. Lett.* **1979**, 61, 522-525. c) Monserrat, K.; Foreman, T. K.; Graetzel, M.; Whitten, D. G., *J. Am. Chem. Soc.* **1981**, 103, 6667-6672.

Application to C-Glycoside Synthesis.

Table 4.1: Yield and Conversion of C-Glycoside Synthesis with Optimized Conditions.



Entry	L	Solvent	% Conversion	%Yield (brsm)
1	bpy	MeCN	81	54 (67)
2	dmb	MeCN	100	75
3	bpy	CD_2Cl_2	39	38 (99)
4	dmb	CD_2Cl_2	90	84 (93)



We then applied our improved glycosyl radical generation conditions to the conjugate addition of these radicals into alkenes to determine if the required reaction time decreased. Initial attempts in anhydrous acetonitrile showed higher conversions with $\text{Ru}(\text{dmb})_3^{2+}$, achieving full conversion in 6 hours, whereas $\text{Ru}(\text{bpy})_3^{2+}$ resulted in only 81% conversion (Table 4.1, entry 1). While the predicted rate increase was observed, hydrolysis of the substrate dramatically lowered the yields, as was seen in MeCN in the optimization reported in Chapter 3. Switching the solvent back to methylene chloride resulted in higher yields based on remaining starting material (Table 4.1, entries 3 and 4). Importantly, $\text{Ru}(\text{dmb})_3^{2+}$ resulted in 90% conversion in 6 hours as compared to 39%

conversion for Ru(bpy)₃²⁺ in the same time span, which is consistent with the thiol glycosyl radical trapping experiments.

Conclusion.

The photoredox cycle has been shown to be dependent on several variables, including the hydrophobicity of the catalyst and the polarity of the solvent and cosolvent. The knowledge gained from these experiments led to an improved synthesis of C-glycosides, whereby the required reaction time was significantly reduced. These experiments demonstrate the applicability of these mechanistic studies to improving synthetic problems. Current work focuses on further investigations into the efficiencies of the photoredox cycle and applications to a wider variety of photoredox reactions, including large-scale syntheses.

Experimental Section.

General. All reagents were reagent grade quality and used as received from Aldrich or Acros unless otherwise indicated. All reactions were conducted under inert conditions (Ar or N₂) using flame dried or oven dried glassware cooled under inert atmosphere unless otherwise indicated. Anhydrous acetonitrile (MeCN or CD₃CN) and N,N-diisopropylethylamine (EtNⁱPr₂) were distilled from CaH₂ prior to use. α-D-glucopyranosyl bromide tetrabenzoate (**4**) was synthesized according to a literature procedure.¹⁰⁹ Ru(bpy)₃Cl₂ and Ru(dmb)₃Cl₂ were synthesized by reported procedures,⁹⁸ and Ru(bpy)₃(PF₆)₂ and Ru(dmb)₃(PF₆)₂ were synthesized in an analogous manner to reported anion metatheses.⁹⁹ All NMR spectra were recorded on Bruker Avance 600 MHz with Cryoqnp probe, a Bruker 500 MHz with bbo probe, or a 400 MHz with bbfo probe using Topshim at STP. All deuterated solvents were used as received from Cambridge Isotope Laboratories, Inc, unless otherwise noted. ¹H NMR and ¹³C NMR chemical shifts are reported in δ units, parts per million (ppm) relative to the chemical shift of residual solvent or an external standard. Reference peaks for

¹⁰⁹ Dowlut, M.; Hall, D. G.; Hindsgaul, O. *J. Org. Chem.* **2005**, 70, 9809.

chloroform-*d* in ^1H NMR and ^{13}C NMR spectra were set at 7.26 ppm and 77.0 ppm, respectively. The reference peak for acetonitrile- d_3 in ^1H NMR was set at 1.94 ppm. Reaction vessels were covered in foil to protect them from light during manipulations prior to irradiation.

Reaction apparatuses.

Compact fluorescent light bulb (14 W):

NMR tubes were placed approximately 8-10 cm away from a 14 W CFL with a focusing cone (see Figure 4.3).

Blue LEDs:

NMR tubes were placed inside a reflux condenser around which 12 inch blue LED light strips (from www.creativelightings.com) were wrapped in a 5 cm vertical span (see image below). Four of these reflux condensers were placed in serial, and water was used to keep the reactions at room temperature ($23\text{ }^\circ\text{C} \pm 1\text{ }^\circ\text{C}$), as the LED strips generated significant amounts of heat. The flow of the water was regulated to keep the temperature between the first and fourth reflux condensers within $1\text{ }^\circ\text{C}$ of each other.

Procedures.

Varying concentration of $^t\text{BuSH}$:

A 10 mL round bottom flask under Ar was charged with **4** (201 mg, 0.305 mmol), EtN^iPr_2 (160 μL , 0.915 mmol, 3 eq), $\text{Ru}(\text{bpy})_3(\text{PF}_6)_2$ (13 mg, 0.015 mmol), 1,3,5-trimethoxybenzene (41.6 mg as an internal standard), and 2.5 mL CD_3CN . 500 μL of this solution was transferred to oven dried NMR tubes containing 7 μL , 14 μL , 34 μL , and 68 μL of 2-methyl-2-propanethiol, each. The NMR tubes were degassed by three freeze-pump-thaw cycles, and the reactions were irradiated with a 14 W compact fluorescent light bulb for 3 hours. ^1H NMR monitoring ($d_1 = 5\text{ }\mu\text{sec}$) before and after the reaction was used to determine the % conversion.

[<i>t</i> BuSH] (mM)	0.12	0.24	0.57	1.06
% Conversion of 4	49	51	48	47

Average % conversion: $48.8 \pm 3.5\%$

Varying concentration of **4**:

A 10 mL round bottom flask under Ar was charged with 2-methyl-2-propanethiol (69 μ L, 0.61 mmol) *i*Pr₂NEt (160 μ L, 0.915 mmol, 3 eq), Ru(bpy)₃(PF₆)₂ (13 mg, 0.015 mmol), 1,3,5-trimethoxybenzene (42.1 mg as an internal standard), and 2.5 mL CD₃CN. 500 μ L of this solution was transferred to oven dried NMR tubes containing 10.1 mg, 19.7 mg, 40.4 mg, and 82.0 mg of **4**, each. The NMR tubes were degassed by three freeze-pump-thaw cycles, and the reactions were irradiated with a 14 W compact fluorescent light bulb for 3 hours. ¹H NMR monitoring (*d*₁ = 5 μ sec) before and after the reaction was used to determine the % conversion.

[4] (mM)	0.031	0.060	0.122	0.249
mmol of 4 consumed	0.014	0.020	0.026	0.041

Varying concentration of EtNⁱPr₂:

4 (809.7 mg, 1.228 mmol), 2-methyl-2-propanethiol (275 μ L, 2.44 mmol), Ru(bpy)₃(PF₆)₂ (51.0 mg, 0.059 mmol), and 1,3,5-trimethoxybenzene (~200 mg as an internal standard) was brought to a final volume of 5 mL in CD₃CN. Oven dry NMR tubes were charged with 250 μ L of this stock solution and 10 μ L, 32 μ L, 65 μ L, and 100 μ L of EtNⁱPr₂. The reactions were then diluted to a final volume of 0.5 mL with CD₃CN, and the solutions were degassed by three freeze-pump-thaw cycles. The

reactions were then irradiated with a 14 W compact fluorescent light for 3 hours. ^1H NMR monitoring ($d_1 = 5 \mu\text{sec}$) before and after the reaction was used to determine the % conversion.

[EtN ⁱ Pr ₂] (mM)	0.12	0.37	0.75	1.15
% conversion of 4 (CFL)	37.6	54.5	63.3	65.5

Varying amount of cosolvent:

4 (809.2 mg, 1.228 mmol), EtNⁱPr₂ (638 μL , 3.66 mmol), 2-methyl-2-propanethiol (275 μL , 2.44 mmol), Ru(bpy)₃(PF₆)₂ (51.0 mg, 0.059 mmol), and 1,3,5-trimethoxybenzene (~200 mg as an internal standard) was brought to a final volume of 5 mL in CD₃CN. Oven dry NMR tubes were charged with 250 μL of this stock solution and 10 μL , 25 μL , 50 μL , and 100 μL of cosolvent was added (see table below). The reactions were then diluted to a final volume of 0.5 mL with CD₃CN, and the solutions were degassed by three freeze-pump-thaw cycles. The reactions were then irradiated with blue LEDs for 3 hours. ^1H NMR monitoring ($d_1 = 5 \mu\text{sec}$) before and after the reaction was used to determine the % conversion.

Table 4.2: % Conversion of **4 for various cosolvent concentrations**

Cosolvent	2% cosolvent	5% cosolvent	10% cosolvent	20% cosolvent
MeOH	23.3	23.0	22.4	26.3
DMSO	23.9	23.5	<i>a</i>	<i>a</i>
Ethylene Glycol	28.3	29.1	ND	37.4
H ₂ O	33.2	43.5	55.7	<i>b</i>

ND: Not determined. *a*: At higher concentrations of DMSO, the reaction suffered from hydrolysis of the substrate, and conversion was not determined for these concentrations. *b*: **1** was insoluble in >10% aqueous acetonitrile.

Varying concentration of catalyst under anhydrous conditions (representative example):

4 (807.2 mg, 1.22 mmol), EtNⁱPr₂ (638 μ L, 3.66 mmol), 2-methyl-2-propanethiol (275 μ L, 2.44 mmol), and 1,3,5-trimethoxybenzene (~200 mg as an internal standard) was brought to a final volume of 5 mL in CD₃CN. Oven dry NMR tubes were charged with 250 μ L of this stock solution and varying amounts of a stock solution of Ru(bpy)₃(PF₆)₂ was added (see manuscript for final concentrations). The reactions were then diluted to a final volume of 0.5 mL with CD₃CN, and the solutions were degassed by three freeze-pump-thaw cycles. The reactions were then irradiated with a 14 W compact fluorescent light bulb or blue LEDs for 3 hours. ¹H NMR monitoring (d₁ = 5 μ sec) before and after the reaction was used to determine the % conversion.

Varying concentration of catalyst under aqueous conditions:

4 (801.6 mg, 1.215 mmol), EtNⁱPr₂ (638 μ L, 3.66 mmol), 2-methyl-2-propanethiol (275 μ L, 2.44 mmol), and 1,3,5-trimethoxybenzene (~200 mg as an internal standard) was brought to a final volume of 5 mL in CD₃CN. Oven dry NMR tubes were charged with 250 μ L of this stock solution, and varying amounts of a stock solution of Ru(bpy)₃(PF₆)₂ was added. The reactions were then diluted to a final volume of 0.5 mL with CD₃CN, and an additional 50 μ L of H₂O was added. The solutions were degassed by three freeze-pump-thaw cycles. The reactions were then irradiated with a 14 W compact fluorescent light bulb or blue LEDs for 3 hours. ¹H NMR monitoring (d₁ = 5 μ sec) before and after the reaction was used to determine the % conversion.

Blue LED apparatus control experiment:

To determine the consistency of the LED apparatus (see picture above), 4 trial experiments were conducted, one in each of the LED “chambers”. A 10 mL round bottom flask under Ar was charged with **4** (204 mg, 0.309 mmol), 2-methyl-2-propanethiol (69 μ L, 0.61 mmol), EtNⁱPr₂ (160 μ L, 0.915 mmol), Ru(bpy)₃(PF₆)₂ (12.8 mg, 0.015 mmol), 1,3,5-trimethoxybenzene (43.4 mg as an internal standard), and 2.5 mL CD₃CN. 500 μ L of this solution was transferred to oven dried NMR tubes, which were then degassed by three freeze-pump-thaw cycles, and the reactions were irradiated with

blue LEDs for 3 hours. ^1H NMR monitoring ($d_1 = 5\ \mu\text{sec}$) before and after the reaction was used to determine the % conversion.

Trial #	1	2	3	4
% Conversion of 4	59.8	60.8	61.3	60.8

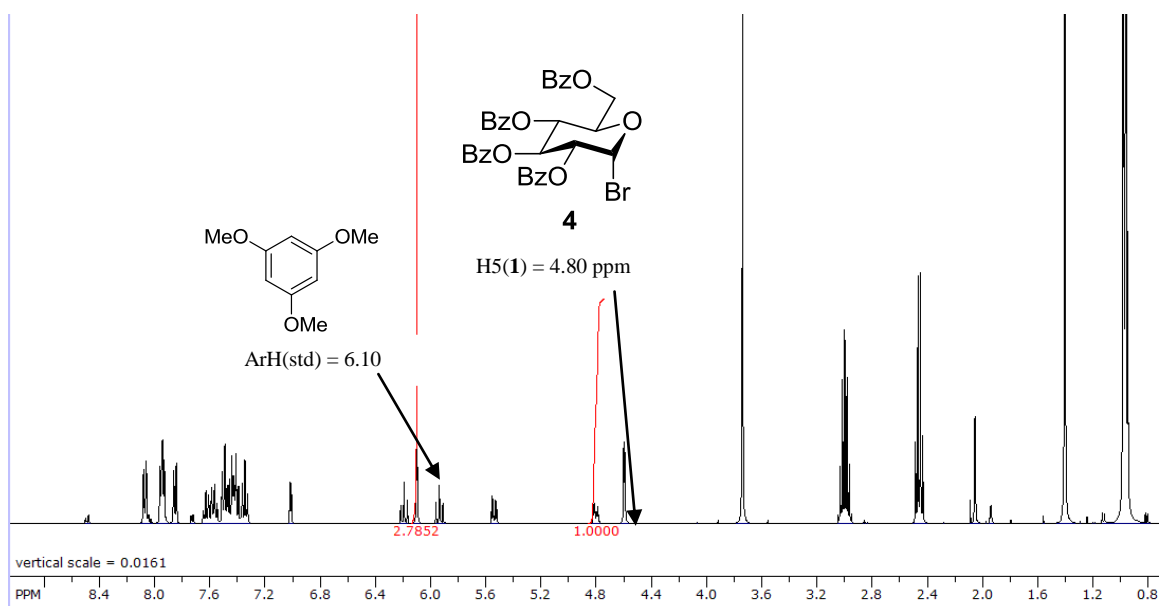
Average % conversion: $60.7 \pm 1.1\%$

Radical coupling with electron-deficient alkenes (representative procedure):

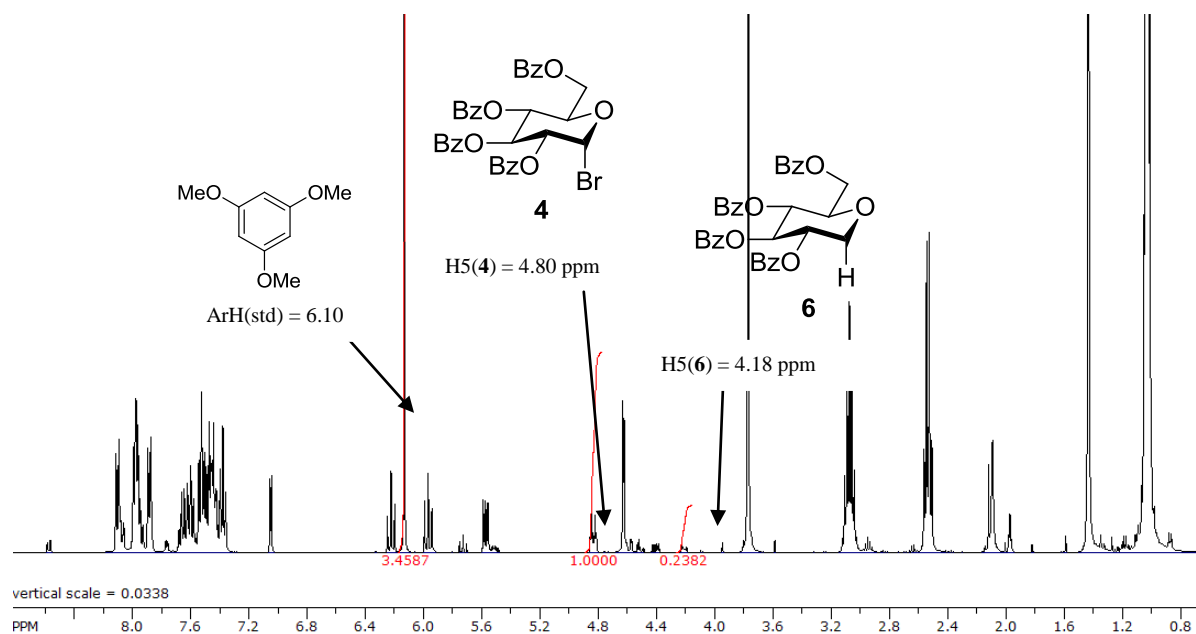
A dry 10 mL Schlenk tube under Ar was charged with **1** (50 mg, 0.12 mmol), $\text{RuL}_3(\text{PF}_6)_2$ (0.006 mmol), diethyl 1,4-dihydro-2,6-dimethyl-3,5-pyridinedicarboxylate (HEH, 34 mg, 0.134 mmol) and 1 mL MeCN (for anhydrous reactions) or 0.9 mL MeCN and 0.1 mL H_2O (for aqueous reactions). EtN^iPr_2 (64 μL , 0.37 mmol) was added, and the heterogeneous solution was degassed by three freeze-pump-thaw cycles. Methyl acrylate (22 μL , 0.24 mmol) was added, and the vessels were irradiated with blue LEDs. Anhydrous reactions were quenched by passing the reaction through a plug of silica in ether and concentrated *in vacuo*. Aqueous reactions were transferred to a separatory funnel with 10 mL EtOAc and 10 mL H_2O . The layers were separated, and the aqueous layer was extracted 3 x EtOAc. The combined organic layers were successively rinsed 1 x HCl (1M), 1 x sat. $\text{NaHCO}_3(\text{aq})$, 1 x brine, dried with MgSO_4 , filtered, and concentrated *in vacuo*. 1,3,5-trimethoxybenzene was added as a quantitative internal ^1H NMR standard for determination of yield and conversion ($d_1 = 5\ \mu\text{sec}$).

Sample ^1H NMR for quantitation of % conversion:

Initial spectrum (CD_3CN , 400 MHz):



Final spectrum (CD_3CN , 400 MHz):



% Conversion of **1** = 19.5; % Yield of **2** = 19.2% (98% brsm)

Chapter 5 - Large Scale Synthesis of C-Glycoconjugates

Synthesis of C-Glycoconjugates.

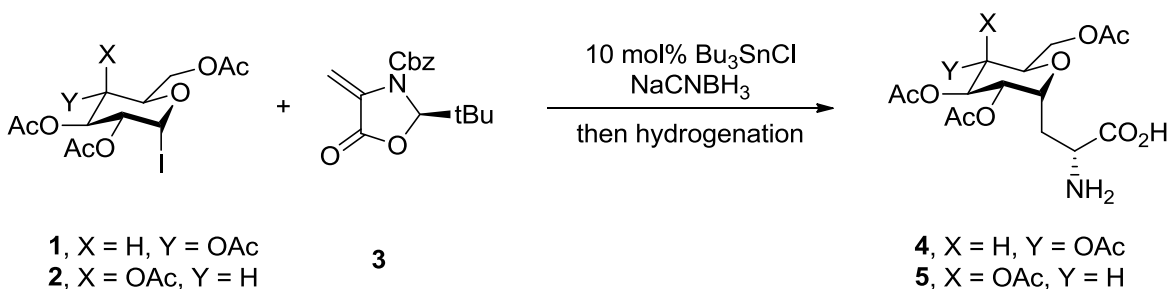
Having developed an effective method for the radical-mediated synthesis of C-glycosides, we hoped to apply our techniques to the preparation of C-analogs of glycoconjugates, which represent an essential class of biological glycosides with varied functions.⁶ Glycoproteins are involved in intercellular recognition events such as the immune response, and glycosphingolipids, which are glycosylated-lipids, are found on the cell membrane of organisms ranging in complexity from bacteria to humans. Moreover, glycoproteins represent the fastest growing class of therapeutics due to the favorable pharmacokinetic properties imparted by the glycan.^{8,9-10} As discussed in Chapter 1, a common feature of these glycoconjugates is the metabolic instability of the *O*-glycosidic linkage, often as a result of enzymatic cleavage.¹¹ This instability has inspired the development of C-linked glycoconjugates as stable biological isosteres in order to further improve the desired properties of the molecule, such as bioavailability.^{11,12,20} While extensive effort has been invested into developing methods of C-glycosylation, improved methods are still in demand.

Several syntheses of C-glycoamino acids have been reported,¹¹⁰ some of which will be presented here for comparison. While many unnatural C-glycosyl amino acids have been synthesized, this report will focus only on isosteres of the natural amino acids serine and alanine. Axon and Beckwith report a tin-mediated glycosyl radical addition into chiral alkene **3** to form the C-

¹¹⁰ Dondoni, A.; Marra, A., *Chem. Rev.* **2000**, *100*, 4395-4421.

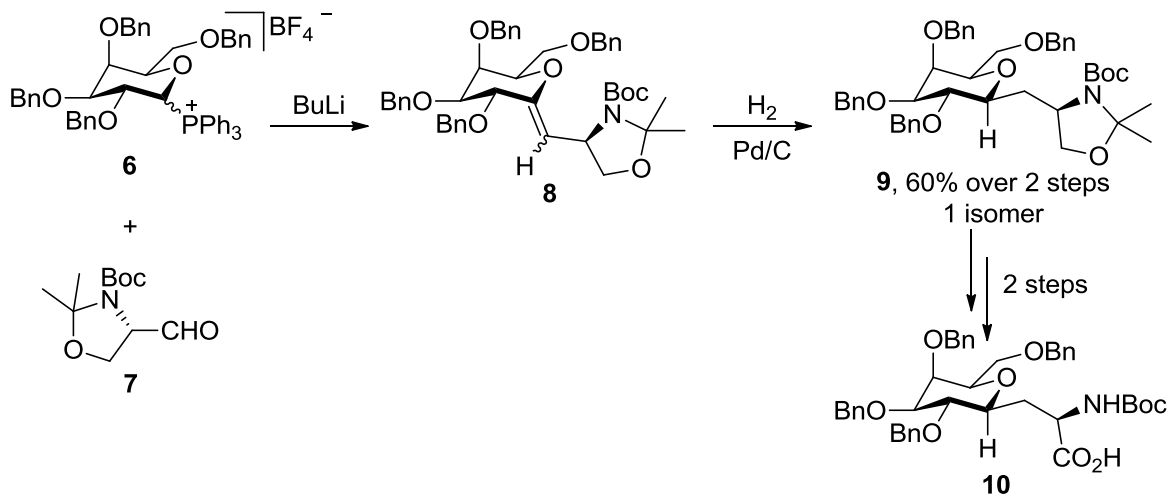
alanine (**4** or **5**) after hydrogenolysis in high yields and excellent diastereoselectivity (Scheme 5.1).¹¹¹

This reaction was general for both glucosyl and galactosyl iodides.



Scheme 5.1: Synthesis of C-Alanine via Radical Addition into a Chiral Alkene.

Lieberknecht and co-workers formed C1 exo-olefin **8** through a Wittig reaction with galactosyl triphenylphosphonium salt **6**, available from the benzyl-protected C1 methyl ether in one step (Scheme 5.2).¹¹² Garner aldehyde (**7**) is a common precursor for C-glycosyl amino acid syntheses and can be purchased, although it is often cheaper to synthesize the material from serine.

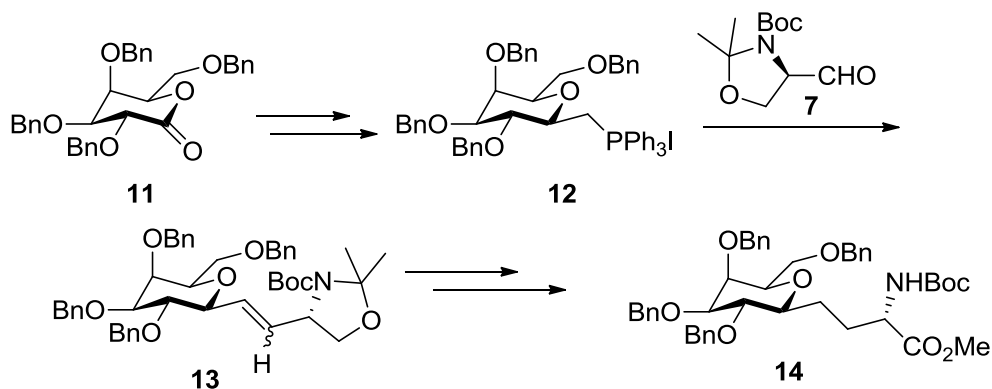


Scheme 5.2: Wittig-Approach to β -C-Alanine Glycoamino Acid.

¹¹¹ Axon, J. R.; Beckwith, A. L. J., *J. Chem. Soc., Chem. Commun.* **1995**, 549-550.

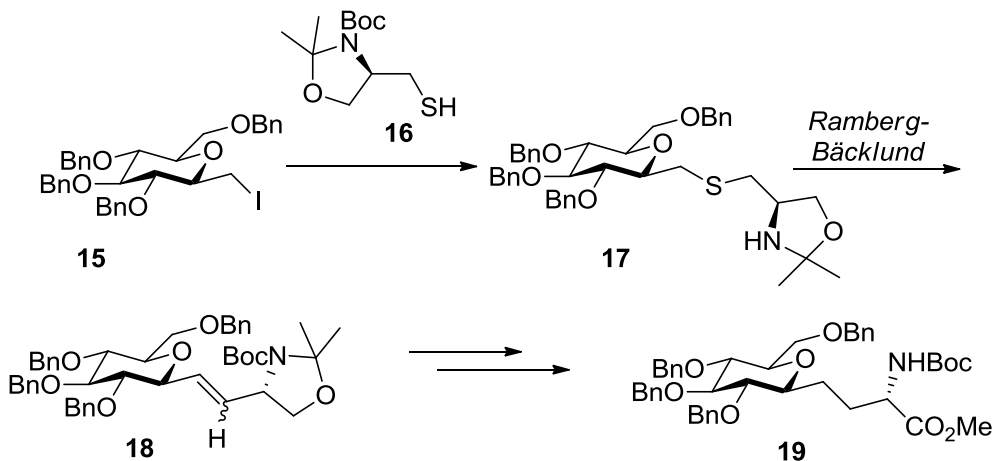
¹¹² Lieberknecht, A.; Griesser, H.; Krämer, B.; Bravo, R. D.; Colinas, P. A.; Grigera, R. I. J., *Tetrahedron* **1999**, 55, 6475-6482.

Hydrogenation of the olefin isomers provided intermediate **9**, which was deprotected and oxidized to generate the C-alanine product **10**. In a related approach, Dondoni and co-workers report the synthesis of galactosyl β -C-glycosyl serines through the methylene-linked glycosyl phosphonium salt **12** (Scheme 5.3).¹¹³



Scheme 5.3: Wittig-Approach to Glycosyl C-Serines.

A complimentary method to access a glucosyl derivative of key intermediate **13** (Scheme 5.3) in the synthesis of C-serines was reported by Taylor and co-workers (Scheme 5.4).¹¹⁴

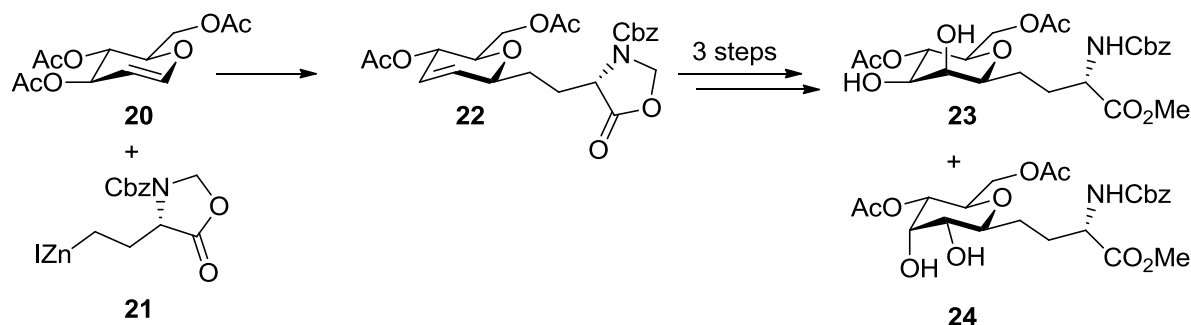


Scheme 5.4: Synthesis of β -C-Serine via Ramberg-Bäcklund Rearrangement.

¹¹³ Dondoni, A.; Marra, A.; Massi, A., *Tetrahedron* **1998**, 54, 2827-2832.

¹¹⁴ D. Campbell, A.; E. Paterson, D.; J. K. Taylor, R.; M. Raynham, T., *Chem. Commun.* **1999**, 1599-1600.

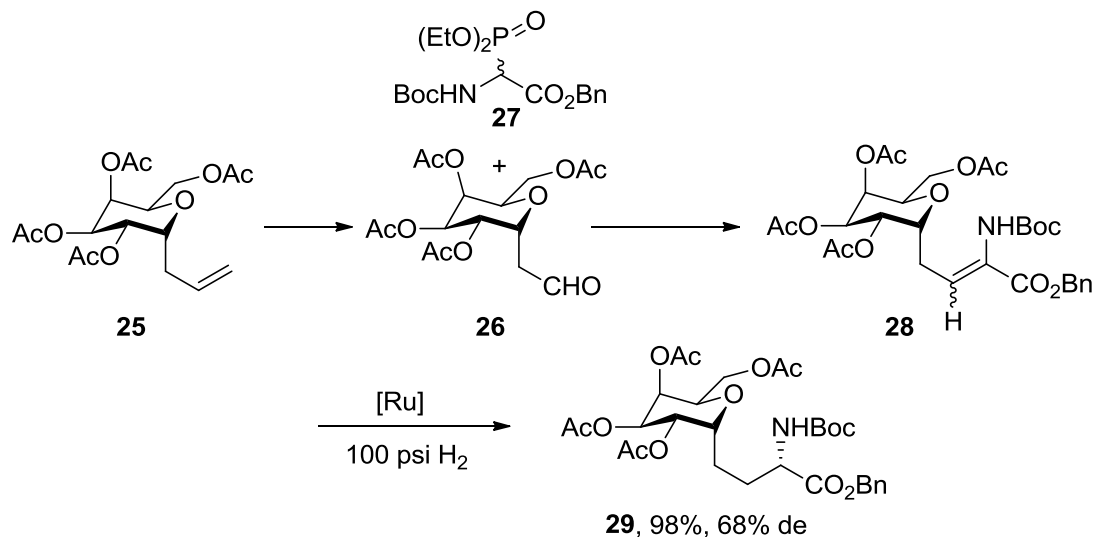
S_N2 substitution of glycosyl iodide **15** with thiol **16** results in thioether **17**. Oxidation followed by Ramberg-Bäcklund rearrangement leads to exo-alkene **18**, which is then reduced and elaborated into protected glycosyl *C*-serine **19**. This approach avoids the generation of stoichiometric amounts of triphenylphosphine oxide in the formation of the key carbon-carbon bond.



Scheme 5.5: Synthesis of *C*-Serines via Nucleophilic Addition of Chiral Zinc Reagent to Glycal.

Thorn and Gallagher have reported a catalyst-free synthesis of *C*-serines by the S_N2' addition of chiral zinc reagent **21** to triacetoxyl glucal **20** (Scheme 5.5).¹¹⁵ This leads to the trisubstituted *C*-glycoside **22**, which gives the final product after dihydroxylation. However, this was found to be non-selective and gave a 1:1 mixture of diastereomers (**23** and **24**).

¹¹⁵ Thorn, S. N.; Gallagher, T., *Synlett* **1996**, 856-858.



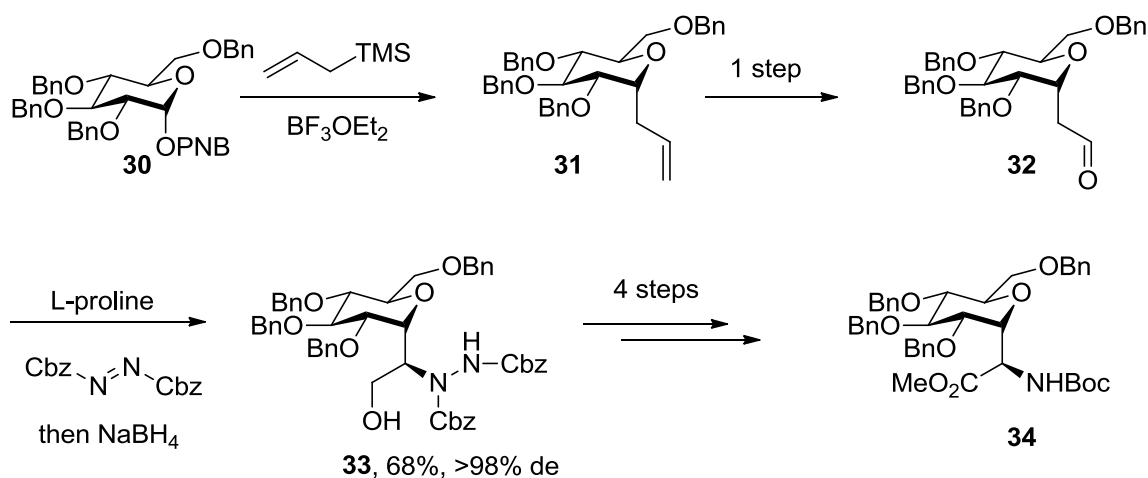
Scheme 5.6: Synthesis of α -C-Serine via Olefination and Asymmetric Hydrogenation.

Toone and co-workers report the synthesis of C-linked serines through Horner-Emmons olefination of galactosyl aldehyde **26**, synthesized from allyl-C-glycoside **25**, with phosphonate **27** (Scheme 5.6).¹¹⁶ Asymmetric catalytic hydrogenation with a chiral ruthenium catalyst under elevated pressures of H₂ resulted in the desired protected C-galactosy serine **29**, albeit in a modest diastereomeric excess.

Dondoni and co-workers have reported an asymmetric organocatalytic α -amination reaction for the synthesis of C-amino acids (Scheme 5.7).¹¹⁷ An example for the synthesis of α -C-glycines is shown in Scheme 5.7. Nucleophilic substitution of glycoside **30** results in α -allyl glycoside **31**, which can be oxidatively cleaved to generate aldehyde **32**. α -Amination of the aldehyde followed by *in situ* reduction leads to amino alcohol **33**, which can be converted into the protect amino acid in four synthetic steps. The reaction works equally well with the β -anomer of aldehyde **32**.

¹¹⁶ Debenham, S. D.; Debenham, J. S.; Burk, M. J.; Toone, E. J., *J. Am. Chem. Soc.* **1997**, *119*, 9897-9898.

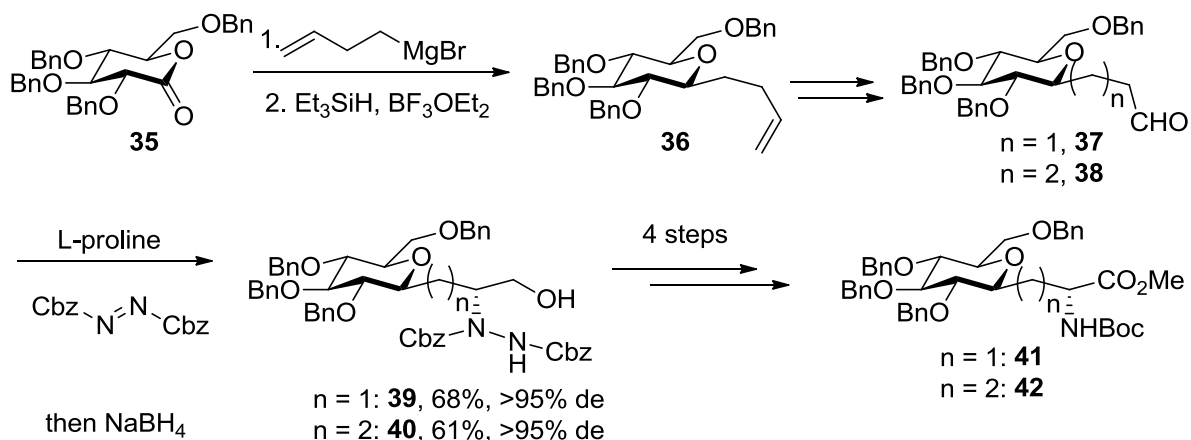
¹¹⁷ Nuzzi, A.; Massi, A.; Dondoni, A., *Org. Lett.* **2008**, *10*, 4485-4488.



Scheme 5.7: Organocatalytic α -Amination of Aldehydes for C-Alanine Synthesis.

The authors then apply the methodology to longer chain-length aldehydes for the synthesis of alanine and serine analogs. For C-alanine and C-serine analogs, these syntheses begin by reacting 4-butenylmagnesium bromide with glycosyl lactone **35**, which yields alkene **36** after subsequent reduction by Et_3SiH under Lewis acidic conditions (Scheme 5.8).¹¹⁸ Alkene **36** can be elaborated into two different aldehydes (**37**: $n = 1$, **38**: $n = 2$) to provide the C-amino acids after α -amination and subsequent derivatizations. Importantly, L-proline provides the *R*-configuration at the amino acid, whereas D-proline provides the *S*-configuration, demonstrating the catalyst-controlled stereoselectivity.

¹¹⁸ Cipolla, L.; Nicotra, F.; Vismara, E.; Guerrini, M., *Tetrahedron* **1997**, 53, 6163-6170.

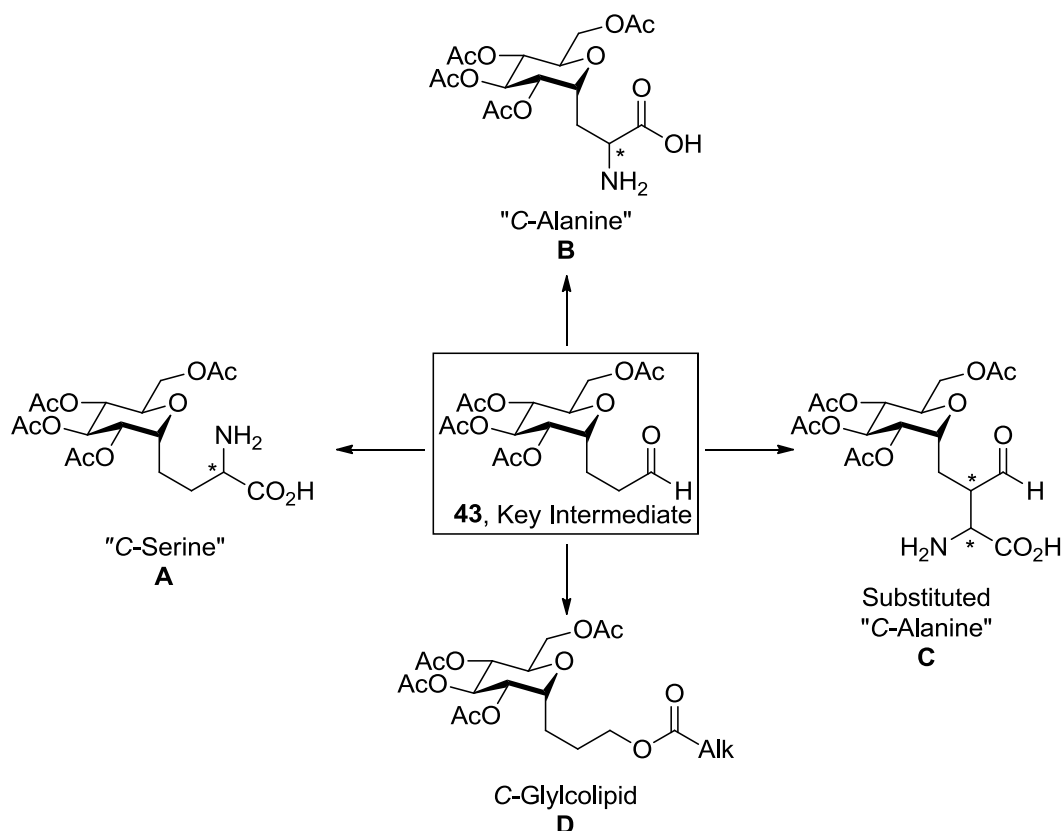


Scheme 5.8: Organocatalytic α -Amination of Aldehydes for C-Serine Synthesis.

Planned Synthesis of C-Glycoamino acids via Key Aldehyde Intermediate.

Each of the reported processes effectively generates the desired C-amino acid but also has significant drawbacks. These processes require multiple synthetic steps and often require the synthesis of complex aglycones for C-glycosylation. The use of expensive or toxic reagents, harsh conditions (strong acid or base), and the use of chiral starting materials all serve to limit these syntheses. Recent advances in organocatalytic modification of aldehydes could allow for the synthesis of a variety of amino acid derivatives from a single aldehyde intermediate, similar to that proposed by Dondoni.¹¹⁷ To this end, we envisioned aldehyde **43** could serve as a common intermediate for the divergent synthesis of C-glycoconjugates (Scheme 5.9). By utilizing established asymmetric organocatalytic derivatizations, aldehyde **43** could be elaborated into C-serines (Scheme 5.9, pathway **A**) and substituted C-alanines (Scheme 5.9, pathways **B** and **C**). Reduction and acylation could similarly allow for the synthesis of a simple C-glycolipid (Scheme 5.9, pathway **D**). The use of asymmetric catalysis to create the late-stage amino acid stereocenter theoretically allows for the synthesis of either epimer, which is a key feature of this approach. In our reported light-mediated glycosyl radical method of C-glycoside synthesis, we were able to synthesize aldehyde **43** in one step from commercially available acetobromo-d-glucose **44**, acrolein, and $i\text{Pr}_2\text{NEt}$ along

with readily prepared Hantzsch ester **45** and $\text{Ru}(\text{bpy})_3(\text{PF}_6)_2$. This provides an attractive entry point into the synthesis of these complex C-amino acids.

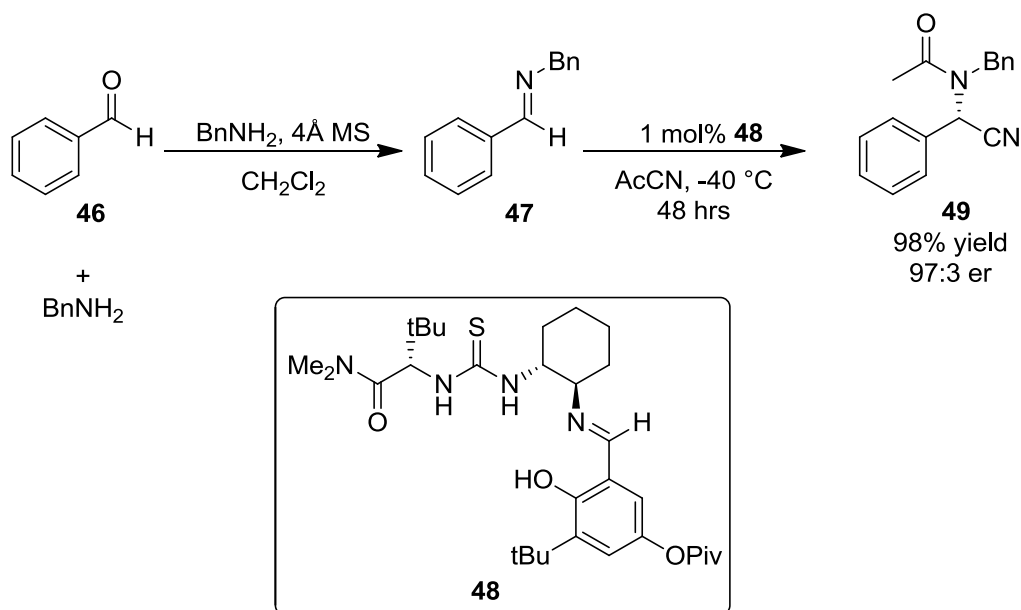


Scheme 5.9: Planned Synthesis of C-Glycoconjugates from Common Aldehyde Intermediate.

For the synthesis of C-glycosyl serines, we envisioned forming the key stereocenter and functional groups in one combined step in an asymmetric Strecker cyanation reaction. Pan and List have recently reported this reaction for the one-pot asymmetric cyanation of aryl and alkyl aldehydes Scheme 5.10).¹¹⁹ In these reactions, Jacobsen thiourea **48** is used as an organocatalyst to both promote the reaction and to control the stereoselectivity. This methodology is particularly attractive due to the *in situ* formation of the necessary imine and the use of AcCN instead of more volatile sources of cyanide, which pose a greater health hazard. As the elaboration of the aminocyanide to the

¹¹⁹ Pan, S. C.; List, B., *Org. Lett.* **2007**, 9, 1149-1151.

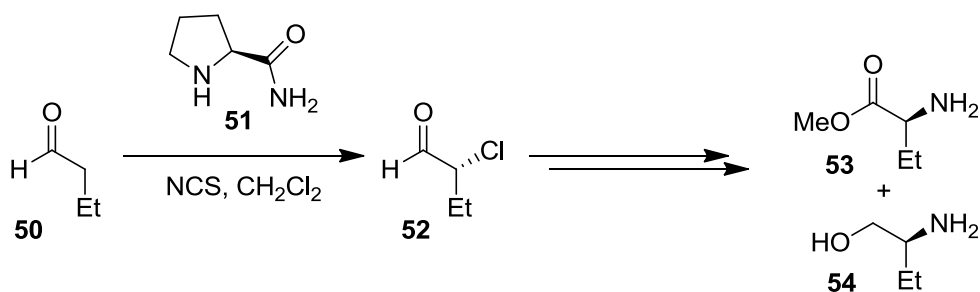
free amino acid has been reported for these reactions and catalyst **48** is commercially available, this methodology serves as an excellent source of inspiration for our synthesis of *C*-serines.



Scheme 5.10: One-Pot Organocatalytic Asymmetric Strecker Cyanation of Aldehydes.

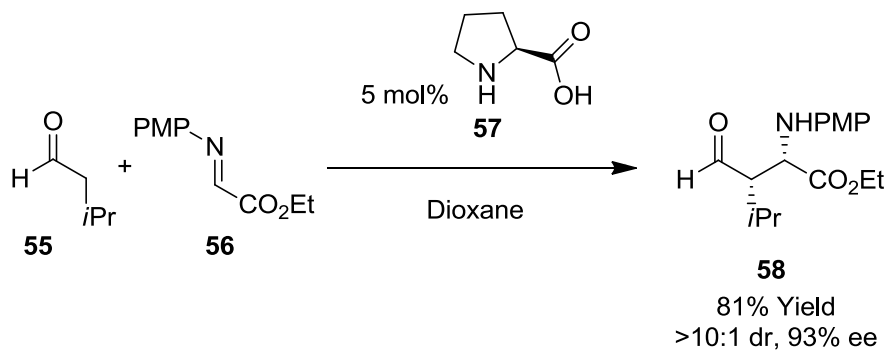
Jørgensen co-workers have reported a direct organocatalytic α -chlorination of alkyl aldehydes for the synthesis of amino acids (Scheme 5.11).¹²⁰ In their protocol, alkyl aldehyde is exposed to a slight excess of *N*-chlorosuccinimide (NCS) in the presence of L-prolinamide as the catalyst to achieve generally high yields and enantioselectivities. As α -chloro aldehydes are often unstable under acidic or basic conditions, subsequent oxidation or reduction yields the carboxylic acid or alcohol, respectively. The authors report the synthesis of amino acids and alcohols from these substrates after substitution with NaN_3 (**53** and **54**). Again, the readily available starting materials make this reaction particularly attractive for our planned synthesis of unsubstituted *C*-alanines.

¹²⁰ Halland, N.; Branton, A.; Bachmann, S.; Marigo, M.; Jørgensen, K. A., *J. Am. Chem. Soc.* **2004**, *126*, 4790-4791.



Scheme 5.11: L-Prolinamide Catalyzed α -Chlorination of Aldehydes for Amino Acid Synthesis.

Barbas and co-workers have reported the proline-catalyzed α -substitution of aldehyde with iminoglyoxalate **56** in order to form amino acid derivatives (**58**, Scheme 5.12).¹²¹ The reaction proceeds in high yields and enantioselectivities at room temperature in a variety of solvents. Iminoglyoxalate **56** is readily synthesized from ethyl glyoxalate and 4-methoxyaniline and is stable at room temperature for weeks. We therefore chose to model our initial attempts after this methodology, and we hoped this would provide access to more complicated C-glycosyl amino acid derivatives.



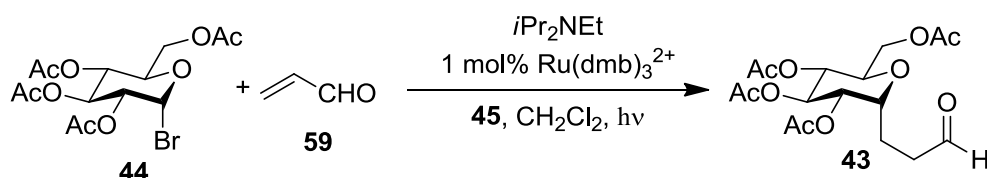
Scheme 5.12: α -Substitution of Aldehydes with Iminoglyoxalate **56 for Amino Acid Synthesis.**

For the synthesis of glycolipids, we planned a simple NaBH_4 reduction followed by acylation with lauroyl chloride. While this does not provide access to a C-analog of a naturally occurring glycolipid, it does serve as a model for unnatural glycolipids. Moreover, it serves as an example of the utility provided by aldehyde intermediate **43**.

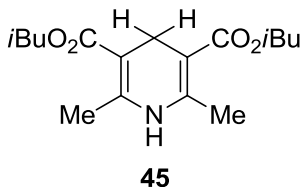
¹²¹ Córdova, A.; Watanabe, S.-i.; Tanaka, F.; Notz, W.; Barbas, C. F., *J. Am. Chem. Soc.* **2002**, *124*, 1866-1867.

Each of the planned glycoconjugate syntheses requires only commercially available or readily-synthesized starting materials and provides the desired protected glycoamino acid in three or fewer steps from aldehyde **43**. When combined with the one-step synthesis of the key intermediate, our planned syntheses are competitive with the most efficient syntheses of C-amino acids in terms of steps. Since these syntheses rely on readily available starting materials, the cost and time of the overall process is significantly reduced, which allows for potential adaptation to large-scale processes. However, large quantities of key intermediate **43** are required for the development of the planned protocols, and the largest reaction successfully conducted in our laboratory prior to this project was limited to a 1.2 mmol scale. This corresponds to approximately 466 mg of **44** assuming a quantitative yield, which is insufficient for the first step in a divergent series of multistep reactions. Thus, our initial goal was to synthesize substantial quantities of **43**.

Large Scale Synthesis of C-Glycosides.



	time (h)	mmol 44	% Conv	TOF (h ⁻¹)
25 mL flask	24	2.43	85	3.5
5 mm NMR tube	1	0.06	73	70



Scheme 5.13: Conversion and TOF Based on Vessel Size.

In order to increase the scale of the reaction, a 1 g “batch” reaction was attempted in a 50 mL round bottom flask (25 mm in diameter) using our light-mediated radical conjugate addition into

acrolein (Scheme 5.13).⁹¹ While 85% conversion was obtained, the reaction required 24 hours of irradiation on this scale for a net turnover frequency (TOF) of 3.5 h⁻¹. A comparable reaction on a 25 mg-scale reaction in a 5 mm diameter NMR tube afforded 73% conversion after only one hour of irradiation, a TOF of 70 h⁻¹ (Scheme 5.13). This is a general trend we have observed in our investigations; thinner reaction vessels generally result in faster reaction rates. For a potential explanation of this, we considered the absorption profile of these reaction mixtures at relevant concentrations. The molar extinction coefficients for RuL₃²⁺ complexes are high, in the range of 14000 M⁻¹cm⁻¹ for L = bpy to 170000 M⁻¹cm⁻¹ for L = dmb, and we considered the possibility the reactions were light-starved. This is consistent with our previous observations as described in Chapter 4. In this scenario, the light source fails to provide sufficient photons to irradiate the entire reaction volume. A simple analysis of the absorption profile at relevant concentrations of Ru(dmb)₃²⁺ at increasing vessel diameters using the Beer-Lambert law is shown in Figure 5.1.

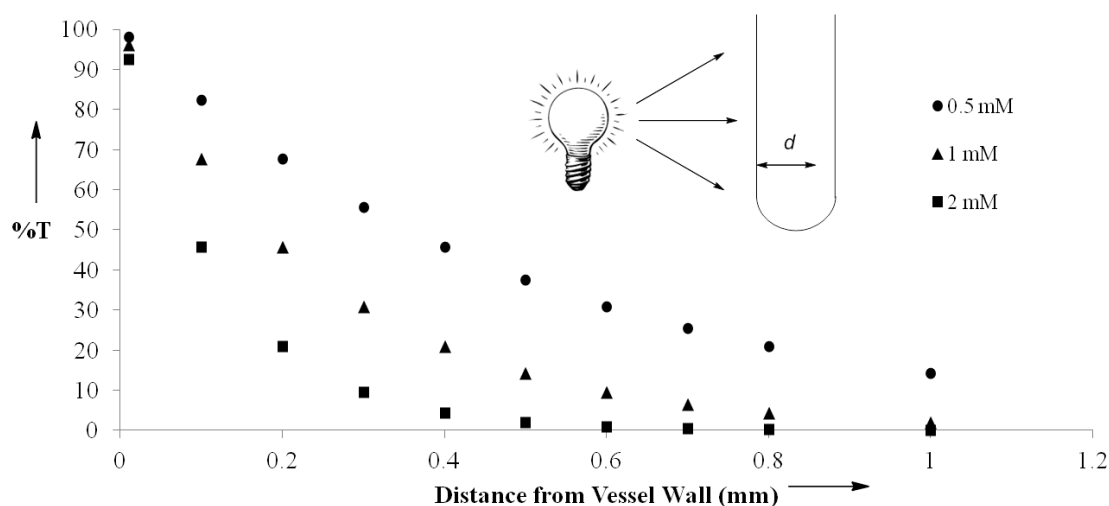


Figure 5.1: % Transmittance vs distance (d) from the Wall from the Beer-Lambert law. Circle = 0.5 mM Ru(dmb)₃²⁺, triangle = 1 mM Ru(dmb)₃²⁺, square = 2 mM Ru(dmb)₃²⁺.

From this analysis, it can be concluded the vast majority of the reaction volume receives negligible light. At 1 mM catalyst loading, 98% of the incident light is absorbed within 1 mm of the vessel wall. Since the absorption of photons is required to generate “active catalyst” (i.e. RuL₃⁺ as the

reductant), this 1 mm volume represents the “active volume” of the vessel. The remaining volume in the vessel only serves to dilute the concentration of the reagents, which in turn decreases the forward rate of the reaction. This is consistent with lower TOFs observed in larger diameter vessels. By extension, continually thinner vessels should provide increased rates of reaction by increasing the concentration of the reagents within the “active volume”. However, thinner reaction vessels would decrease the overall scale of the reaction and limit the amount of material produced in a given “batch” reaction. Our solution to obtaining sufficiently thin reaction vessel diameters without sacrificing reaction volume was a photo-flow reactor, which allows for the reaction mixture to be continuously flowed through tubing around a light source. In this manner, the rate of the reaction is rendered independent of the reaction scale, which is opposite of “batch” reactions.

The basic design principle for photoflow reactors was initially reported by Booker-Milburn in 2005 for large-scale UV-initiated cycloadditions.¹²² Since this time, several more examples of photo-flow reactor designs have been reported,¹²³ the most recent of which was reported by Lévesque and Seeberger.¹²⁴ In the report, the authors detail the large-scale synthesis of the anti-malarial drug artemisinin through a continuous-flow reactor that incorporated multiple synthetic steps, including a photo-mediated step, into a single reactor. With this reactor design, the authors estimated the reactor was capable of synthesizing 200 g of artemisinin per day and that 1500 of these relatively simple and

¹²² Hook, B. D. A.; Dohle, W.; Hirst, P. R.; Pickworth, M.; Berry, M. B.; Booker-Milburn, K. I., *J. Org. Chem.* **2005**, *70*, 7558-7564.

¹²³ a) Vaske, Y. S. M.; Mahoney, M. E.; Konopelski, J. P.; Rogow, D. L.; McDonald, W. J., *J. Am. Chem. Soc.* **2010**, *132*, 11379-11385. b) Laurino, P.; Kikkeri, R.; Azzouz, N.; Seeberger, P. H., *Nano Lett.* **2011**, *11*, 73-78. c) Lévesque, F.; Seeberger, P. H., *Org. Lett.* **2011**, *13*, 5008-5011. d) Gutierrez, A. C.; Jamison, T. F., *Org. Lett.* **2011**, *13*, 6414-6417. e) Bourne, R. A.; Han, X.; Poliakov, M.; George, M. W., *Angew. Chem., Int. Ed.* **2009**, *48*, 5322-5325.

¹²⁴ Lévesque, F.; Seeberger, P. H., *Angew. Chem., Int. Ed.* **2012**, *51*, 1706-1709.

inexpensive reactors could satisfy the annual global demand for this drug. This example clearly demonstrates the potential of photo-flow reactors not only in small-scale laboratory experiments but also in large-scale process chemistry for the synthesis of advanced therapeutics. We hoped to contribute to this thriving area of research through the development of reactors for highly-absorbing photosensitizers to compliment photoreactors designed for the poorly-absorbing sensitizers typically employed in these UV-light mediated processes.

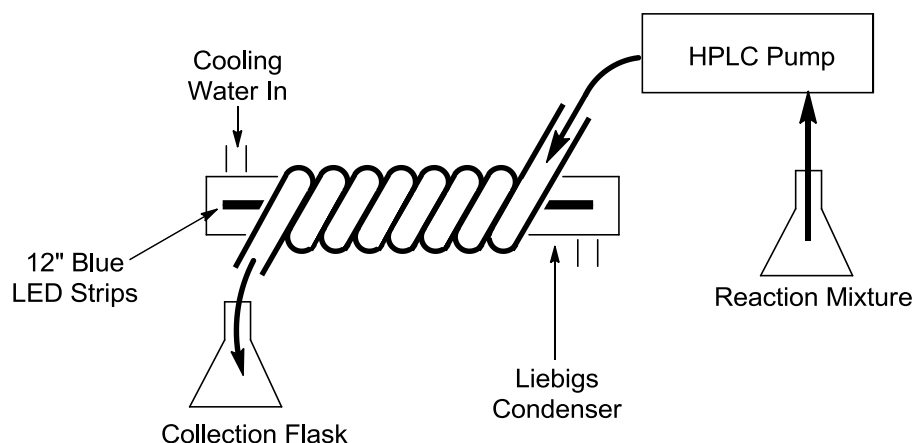


Figure 5.2: Diagram of the Designed Photo-flow Reactor.

Our reactor design utilizes fluorinated ethylene propylene (FEP) tubing coiled around the outside of a Liebig condenser with three 12" blue LED strips on the inside (Figure 5.2). FEP tubing is versatile, flexible, and chemically resistant and has excellent light transmission properties. In order to mitigate the thermal output of the LEDs, cooling water is passed through the water jacket of the condenser. A prep-HPLC pump precisely controls the flow rate of the reaction mixture through the tubing in order to control the reaction time. As opposed to the Booker-Milburn design, only a single layer of tubing can be used, as the extra layers would receive negligible light. The ends of the tubing were fitted with Swagelok connectors to allow for several "modules" to be connected in series to increase the residence time without decreasing flow rate, which would decrease the amount of product produced per hour.

Evaluation of Photo-Flow Reactor.

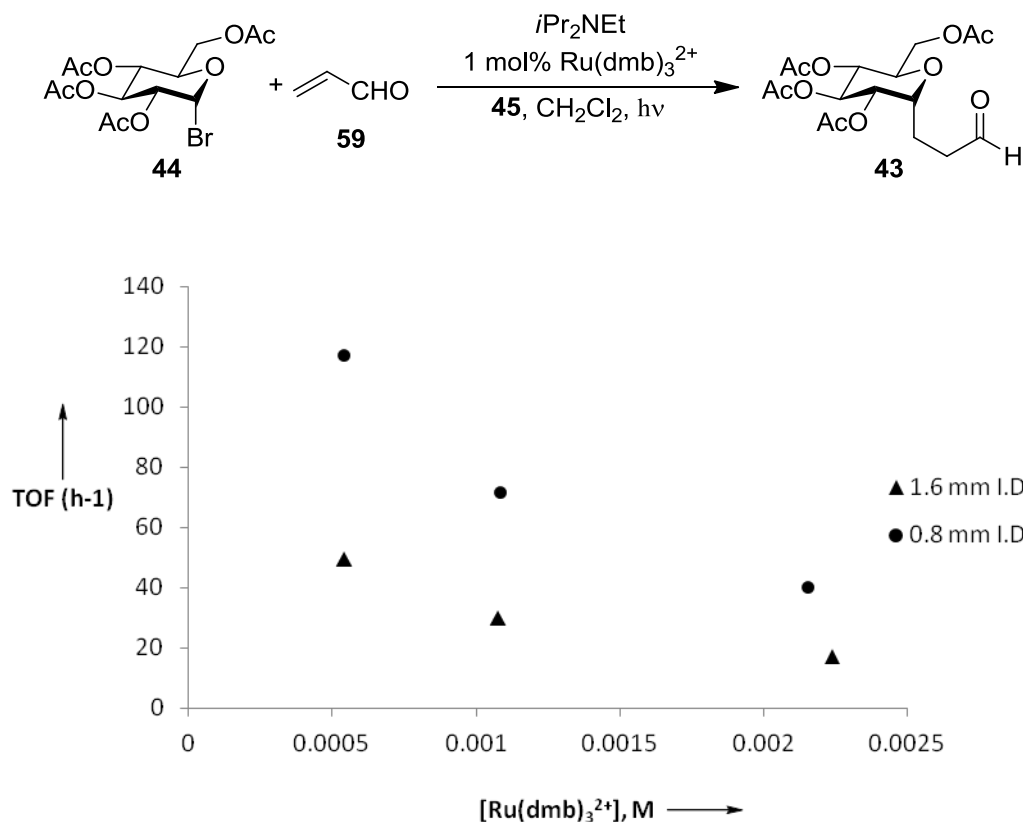


Figure 5.3: TOF vs $[\text{Ru(dmb)}_3^{2+}]$ at Two Tubing Diameters; circle = 1/32" ID FEP tubing, triangle = 1/16" FEP tubing.

The efficiency of this flow reactor design was evaluated at three concentrations of catalyst and two diameters of tubing. At 1.6 mm I.D. tubing and 1.1 mM $[\text{Ru(dmb)}_3^{2+}]$, a 30 h^{-1} net TOF was observed for one module at a flow rate of 0.1 mL/min (Figure 5.3). Increasing the photocatalyst concentration to 2.2 mM resulted in lower TOFs (17 h^{-1}), and decreasing the photocatalyst concentration to 0.5 mM increased the observed rate of reaction (TOF = 50 h^{-1}). As predicted by the analysis in Figure 5.1, we found thinner reaction tubing significantly increased the rate of the reaction. At 1.1 mM $[\text{Ru(dmb)}_3^{2+}]$ in 0.8 mm I.D. tubing, a TOF of 72 h^{-1} was observed, a two-fold increase in rate. A similar inverse relationship between catalyst concentration and conversion was observed for the thinner tubing, and 0.5 mM of catalyst resulted in the highest observed TOFs for this

reaction (120 h^{-1}). From these results, it is clear the photoflow reactor resulted in significantly higher TOFs than observed in “batch” reactions, with thinner tubing diameters resulting in higher TOFs. These observations support the analysis presented in Figure 5.1 and our hypothesis that higher rates of reaction can be obtained in thinner reaction vessels.

Table 5.1: 24-hour Continuous Flow Reaction for Ac- and Piv-Protected Sugars.

$\text{P} = \text{Ac}, \mathbf{44}$
 $\text{P} = \text{Piv}, \mathbf{60}$

$\text{P} = \text{Ac}, \mathbf{43}$
 $\text{P} = \text{Piv}, \mathbf{61}$

Entry	Substrate	Eq of 59	# of Modules	Product	% Conv ^a	% Yield ^a
1	OAc	2	2	43	>97	70 (65 ^b)
2	OAc	4	2	43	>97	85 (77 ^b)
3	OPiv	4	2	61	75	ND ^c
4	OPiv	4	3	61	>97	85 (46 ^b)

^aDetermined by ^1H NMR ^bIsolated yield.

For our final reactor design, we chose 1.6 mm I.D. FEP tubing and 1 mM Ru(dmb)_3^{2+} concentrations, as these conditions led to the highest yields based on remaining starting material. On an 18.2 mmol scale with two modules connected in series, we were able to obtain full conversion and a 70% yield (4.5 g) of **43** after 24 hours of continuous flowing (Table 5.1, entry 1). The yields were unexpectedly low for this reaction, but higher yields (85%) were observed by increasing the concentration of the alkene to provide 5.5 g of **43** (Table 5.1, entry 2). This is significantly higher than the previous theoretical best of 0.8 g of **43** in the 24 hour “batch” reaction (*vide supra*).

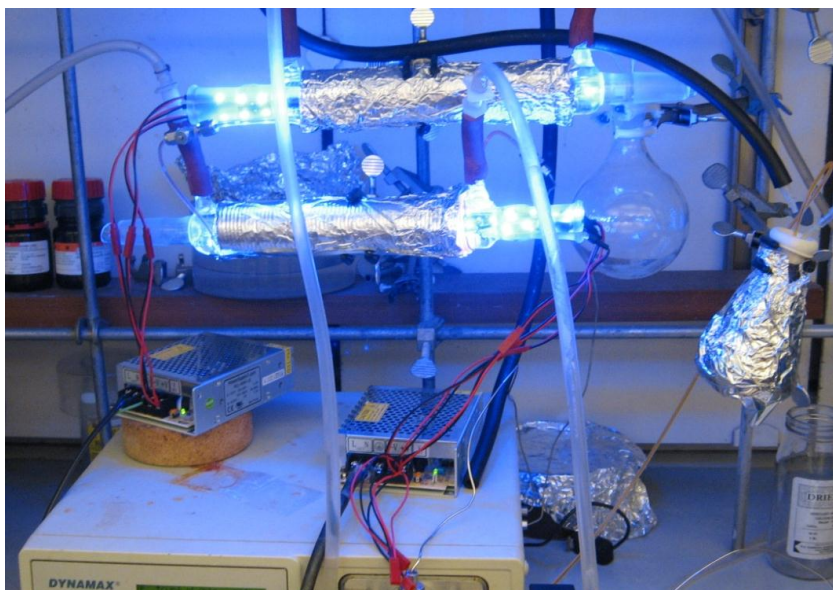


Figure 5.4: Experimental Setup for the Synthesis of Acetate-Protected C-Glycosides.

Pivaloate protected substrate **60** was slower to react, reaching only 75% conversion with two modules of the flow reactor (Table 5.1, entry 3). Simply attaching a third module to the reactor allowed for full conversion of the substrate, which demonstrates the flexibility of the reactor design (Figure 5.5).

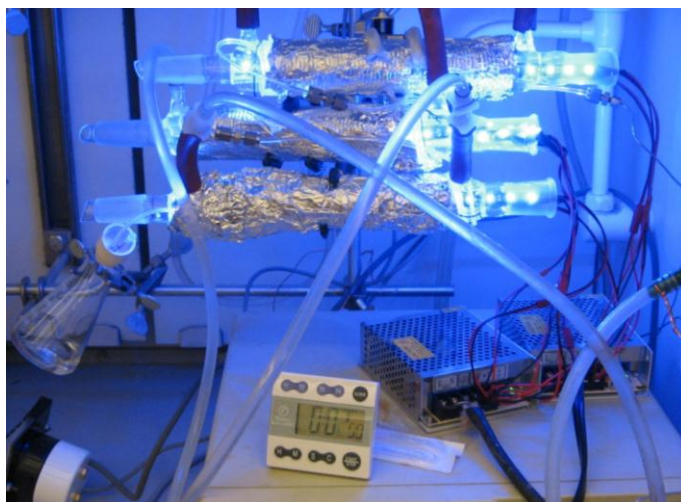
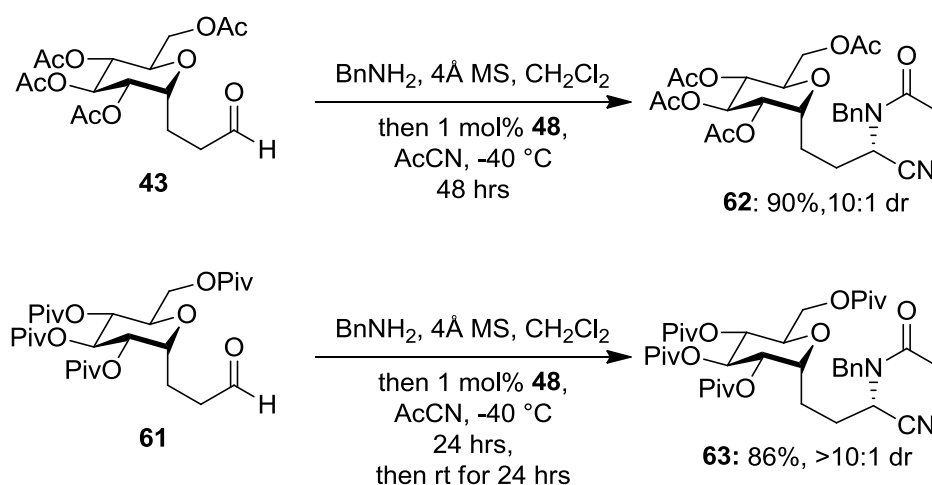


Figure 5.5: Experimental Setup for the Synthesis of Pivaloate-Protected C-Glycosides.

Synthesis of C-Glycoconjugates.

With substantial quantities of **43** in hand, we turned our attention to synthesis of C-linked serines. One-pot asymmetric Strecker cyanation of **43** with Jacobsen thiourea **48** at low temperatures provided the aminonitrile **62** in good yields and diastereoselectivities (Scheme 5.14). Pivaloate-protected **61** reacted more sluggishly in these reactions and required warmer temperatures to reach full conversion but afforded higher diastereoselectivities, providing only one diastereomer (**63**). The stereoselectivity of cyanation in these reactions was assigned by analogy to the original report.¹¹⁹

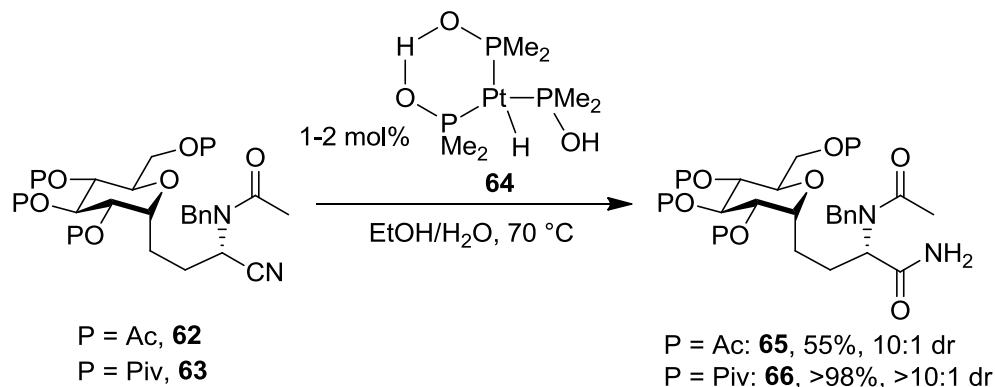


Scheme 5.14: One-Pot Organocatalytic Synthesis of Glycosyl Amino Nitriles.

Attempts to hydrolyze nitrile **62** or **63** through conventional methods (e.g. 65% w/w H₂SO₄) were unsuccessful and provided either deprotection or no reaction. Alcoholysis attempts with HCl in MeOH were similarly unsuccessful. As an alternative path, hydration with Parkin's catalyst afforded the primary amide with no observable epimerization for both acetate- and pivaloate-protected substrates (Scheme 5.15).¹²⁵ Acetate substrates provided lower yields, and no attempts were made to improve this through optimization of the conditions.

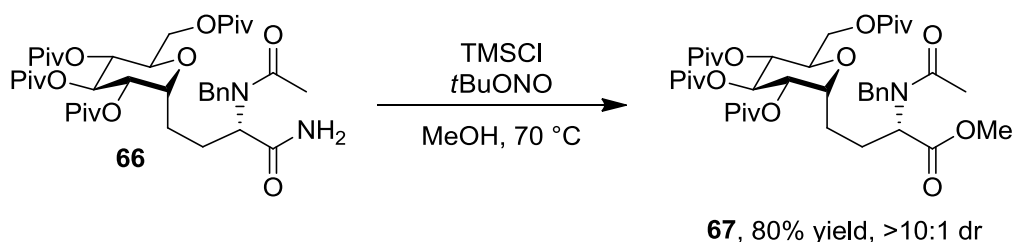
¹²⁵ a) Ghaffar, T.; Parkins, A. W., *Tetrahedron Lett.* **1995**, 36, 8657-8660. b) Ghaffar, T.; Parkins, A. W., *J.*

Mol. Catal. A: Chem. **2000**, 160, 249-261.



Scheme 5.15: Platinum-Catalyzed Hydration of Nitrile to Amide.

Alcoholysis of the primary amide in the presence of *t*BuONO and TMSCl in MeOH provided the carboxylic ester in one step in excellent yields (Scheme 5.16).¹²⁶ The structure of **67** was confirmed by single crystal X-ray diffraction.¹²⁷



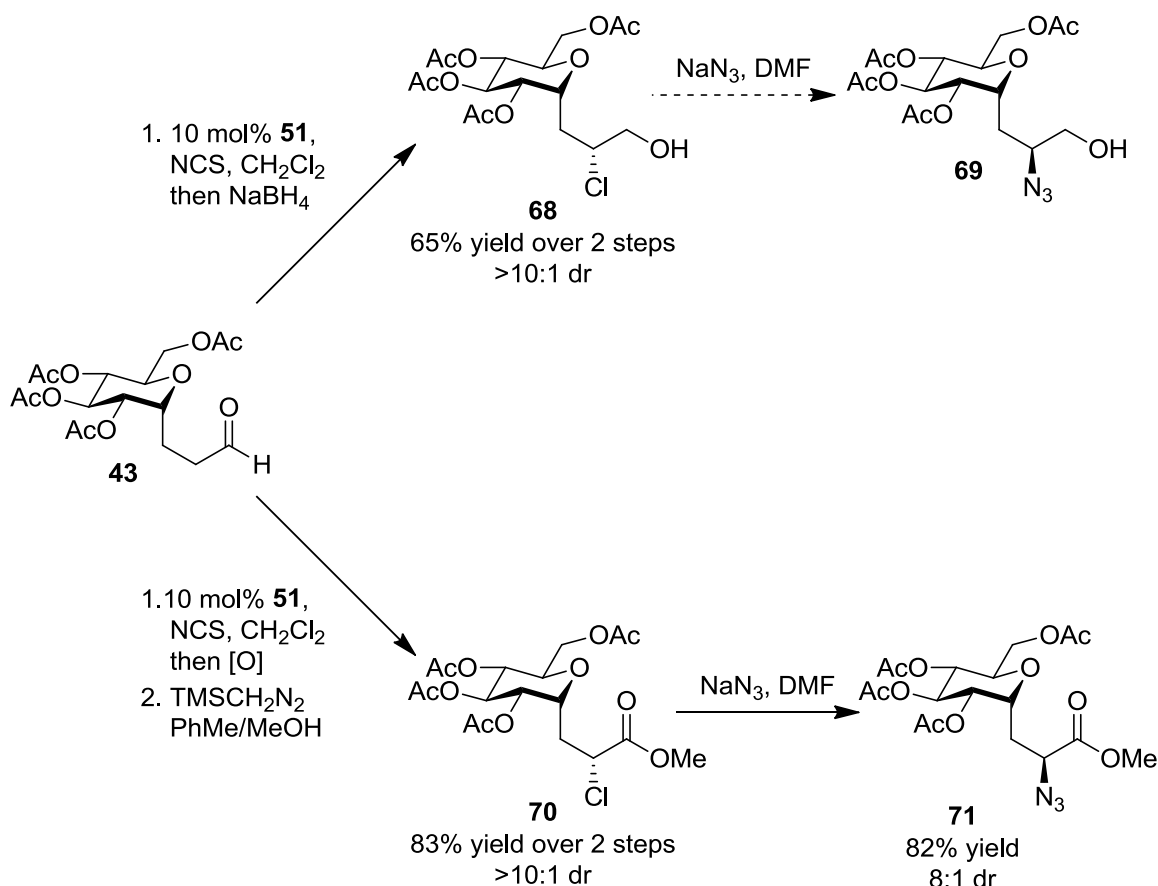
Scheme 5.16: Alcoholysis of Primary Amide to Methyl Ester.

These conditions were problematic for acetate-protected **65**, presumably due to the generation of strong acid (i.e. HCl) under the reaction conditions. Regardless, >100 mg of the pivaloate-protected C-serine was synthesized in a total of four steps in 31% overall yield from readily available materials. The process is high yielding, efficient, and amenable to larger scale reactions due to the low catalyst loadings used throughout the process.

¹²⁶ Lee, J. G.; Seo, Y. S., *Bull. Korean Chem. Soc.* **1995**, *16*, 377-379.

¹²⁷ Registry number: CCDC 869982. These data can be obtained free of charge from

<http://www.ccdc.cam.ac.uk/cgi-bin/catreq.cgi>.



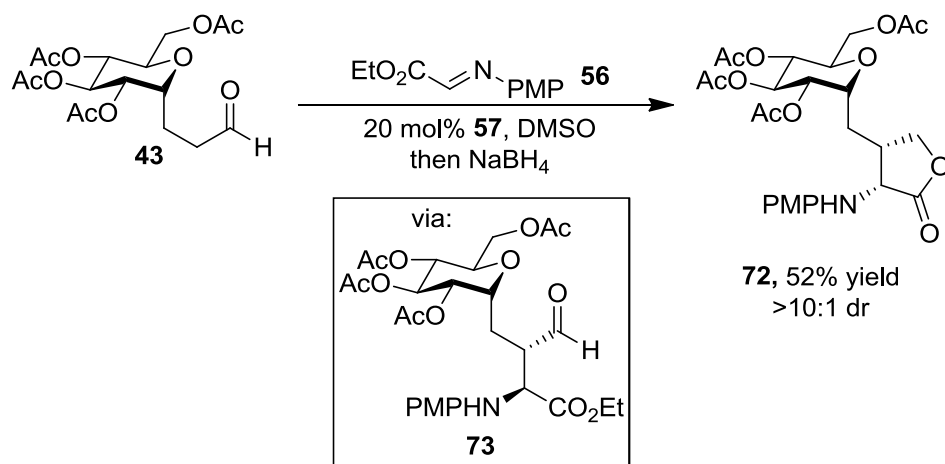
Scheme 5.17: α -Chlorination of Aldehydes and Subsequent Derivatization to Azido Ester.

For the synthesis of C-glycosyl alanine derivatives, diastereoselective α -chlorination under L-prolinamide catalysis in the presence of NCS provided chloroaldehyd, which was reduced or oxidized in order to provide the chloroalcohol (**68**) or chloroester (**70**) respectively (Scheme 5.17).¹²⁰ While sodium azide displacement of chloroalcohol **68** failed to produce any detectable product, chloroester cleanly provided corresponding azidoester **71** at room temperature, although some loss of diastereoselectivity was observed. Thus, the protected glucosyl alanine derivative **71** was synthesized in three steps in 52% overall yield from commercially available material. The stereochemistry of α -chlorination was determined by single crystal X-ray diffraction of chloroalcohol **68**.¹²⁸

¹²⁸ Registry number: CCDC 869983. These data can be obtained free of charge from

<http://www.ccdc.cam.ac.uk/cgi-bin/catreq.cgi>.

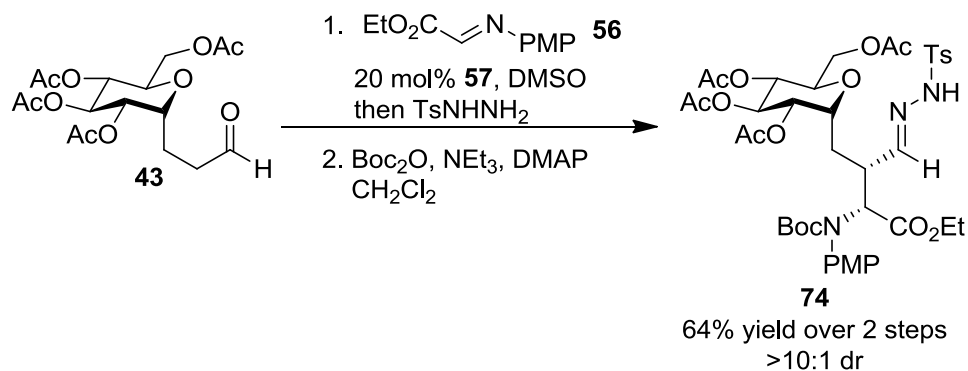
Proline-catalyzed enamine addition into iminoglyoxalate **56** proceeded smoothly to provide α -substituted aldehyde **73** in high diastereoselectivity (Scheme 5.18).¹²¹ However, this product was found to be particularly sensitive and readily decomposed at room temperature in a few hours. Attempts to stabilize the molecule by reducing the aldehyde to the alcohol *in situ* resulted in formation of lactone **72** in modest yields, but this method failed to reliably produce the desired product on larger scales (>50 mg).



Scheme 5.18: α -Addition of Aldehyde into Iminoglyoxalate, Reduction, and Lactonization.

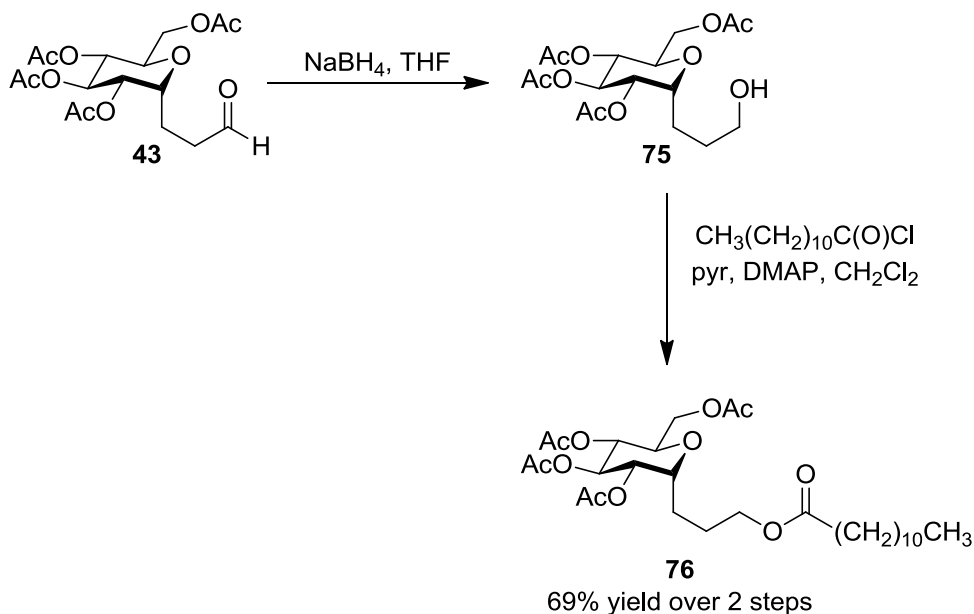
Instead, it was found that *in situ* protection of the aldehyde as the tosyl hydrazone followed by Boc protection of the amine provided a reasonably stable product (**74**, Scheme 5.19).¹²⁹

¹²⁹ No decomposition of **74** was observed after storing the pure solid at -20 °C for weeks.



Scheme 5.19: α -Addition of Aldehyde into Iminoglyoxalate and Protection.

Simple reduction of aldehyde **43** with NaBH_4 cleanly provided alcohol **75**, which was then acylated with lauroyl chloride in order to provide model glycolipid **76** (Scheme 5.20). While not a naturally occurring lipid, this compound represents the potential of aldehyde **43** to be derivatized into new classes of biologically relevant compounds.



Scheme 5.20: Synthesis of Model C-glycolipid.

Through the development of a continuous-flow photoreactor, we were able to overcome the inherent limitations of a photon-starved reaction in order to increase the rate of reaction without sacrificing the scale of the reaction. Highly-absorbing RuL_3^{2+} catalysts can create strong

concentration gradients near the surface of the vessel, which serves to limit the rate of the reaction. We were able to confirm and overcome the light-starved nature of the reaction through tubing size/TOF relationships. Thinner reaction vessels corresponded to higher TOFs, and this concept was applied to a large-scale continuous flow reaction to produce >5 g of a key intermediate in 24 hours. This intermediate was then elaborated into a series biologically-relevant C-glycoconjugates in short order, demonstrating the ability of this approach to improve on existing approaches to important C-glycosides.

Conclusion and Future Work.

We have designed a simple yet efficient flow reactor system as a solution to light-starved large scale photo-redox reactions. Highly-absorbing RuL_3^{2+} absorb the majority of the incident light near the surface of the reaction vessel, creating a concentration gradient that localizes the photo-activated catalyst near the surface. It was found that formal TOFs could be increased as compared to traditional “batch” reactions through the use of thin (~1 mm) diameter FEP tubing in a continuous flow reactor, which consequently renders the reaction time independent of scale. This photo-flow reactor was applied to the synthesis of a key C-glycoside intermediate, which in turn was converted into a series of C-linked glycoconjugates.

While our flow reactor design provided higher TOFs for the light-mediated RuL_3^{2+} catalyzed synthesis of C-glycosides, there is still room for improvement, especially in terms of reaction efficiencies. Assuming a quantum efficiency of unity ($\phi = 1$) for the conversion of a photon to a molecule of C-glycoside product, a 4.86 mmol reaction (e.g. 2.0 g of **44**) would require 7 minutes of irradiation from three 1 W blue LED strips ($\lambda = 452$ nm). At 0.5 mol% of Ru(dmb)_3^{2+} , the reaction reached approximately 60% conversion in 45 minutes in 0.8 mm I.D. tubing in the photo-flow

reactor. We estimate the flow reactor is 100 times less efficient than the theoretical maximum output, and we hope to increase these efficiencies in future systems and reactor designs.

As the light-mediated $\text{Ru}(\text{bpy})_3^{2+}$ catalyzed method of radical generation involves several elementary steps, there are many potential sources of inefficiency in this reaction. For example, the rate of electron transfer from a trialkylamine to $^3\text{Ru}(\text{bpy})_3^{2+}$ is thermodynamically disfavored, resulting in a slow electron transfer reaction with a highly favored competing back-electron transfer (Scheme 4.1). As a result, electron transfer from trialkylamines has a low quantum yield ($\phi = 0.007$ for NEt_3), whereas reductive quenching by aryl amines has been shown to be significantly faster and more efficient.¹³⁰ By taking advantage of more favorable reductive quenchers, it might be possible to significantly improve the efficiency of the reaction. Applying similar methods to those described in Chapter 4 allows for the simple investigation of the reaction parameters, such as the effect of the reductive quencher, solvent, and organic substrate, to determine how to further improve efficiency. When combined with our photo-flow reactor design, the reaction rates obtained should be increased further to provide highly-efficient reactions that require minimal irradiation time, allowing for higher flow rates. In turn, more material can be made in a shorter time span and with less-intense sources of light, such as sunlight. Thus increasing the efficiency of the reaction even further allows for many potentially attractive enhancements of this reaction.

Experimental Section.

All reagents were reagent grade quality and used as received from Aldrich or Acros unless otherwise indicated. All reactions were conducted under inert conditions (Ar or N_2) unless otherwise indicated. Anhydrous THF was purchased from Acros and stored over molecular sieves. Anhydrous CH_2Cl_2 was passed through a column of alumina. N,N -diisopropylethylamine ($i\text{Pr}_2\text{NEt}$) were distilled from CaH_2 prior to use. α -D-glucopyranosyl bromide tetraacetate (**44**) was synthesized according to a literature

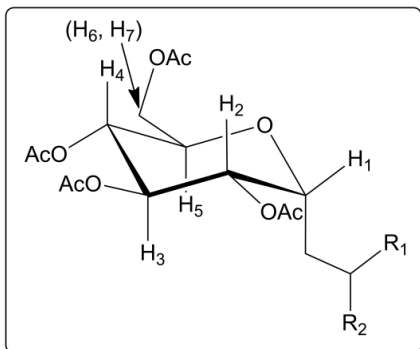
¹³⁰ Rivarola, C. R.; Bertolotti, S. G.; Previtali, C. M., *Photochem. Photobiol.* **2006**, 82, 213-218.

procedure, and α -D-glucopyranosyl bromide tetrapivaloate (**60**) was synthesized in an analogous manner.¹³¹ Ru(bpy)₃Cl₂ and Ru(dmb)₃Cl₂ were synthesized by reported procedures,⁹⁸ and Ru(bpy)₃(PF₆)₂ and Ru(dmb)₃(PF₆)₂ were synthesized in an analogous manner to reported anion metatheses.⁹⁹ Iminoglyoxalate **56** was synthesized according to literature procedure and stored in a desiccator.¹³² Platinum complex **64** was synthesized according to literature procedure.¹²⁵ Column chromatography was performed using Silicycle silica gel 60 as the solid support. All NMR spectra were recorded on Bruker Avance 600 MHz, 500 MHz, or 400 MHz spectrometer at STP and with CDCl₃ as the NMR solvent unless otherwise indicated. All deuterated solvents were used as received from Cambridge Isotope Laboratories, Inc. ¹H NMR and ¹³C NMR chemical shifts are reported in δ units, parts per million (ppm) relative to the chemical shift of residual solvent. Reference peaks for chloroform in ¹H NMR and ¹³C NMR spectra were set at 7.26 ppm and 77.0 ppm, respectively. High-resolution mass spectra (HRMS) were obtained using a Micromass Q-ToF Ultima or Agilent Accurate LC-TOF Mass Spectrometer (ESI+, 175 eV). Melting point was recorded on Uni-melt (Thomas Hoover) capillary melting point apparatus. Specific rotations were obtained using a Jasco DIP-1000 or Jasco P-1010 polarimeter with CH₂Cl₂ as the solvent.

Proton labeling. For the purpose of spectral assignment, the proton labeling outlined in the following box was used throughout the text.

¹³¹ Floyd, N.; Vijayakrishnan, B.; Koeppe, J. R.; Davis, B. G., *Angew. Chem., Int. Ed.* **2009**, 48, 7798-7802.

¹³² De Lamo Marin, S.; Catala, C.; Kumar, S. R.; Valleix, A.; Wagner, A.; Mioskowski, C. *Eur. J. Org. Chem.* **2010**, 3985-3989.



Absorption Profile Calculation:

$$\text{Abs} = \epsilon \times l \times c$$

$$\%T = 10^{-(\epsilon \times l \times c)}$$

$\%T$ = % transmittance

ϵ = molar absorptivity coefficient, $17000 \text{ M}^{-1}\text{cm}^{-1}$ for Ru(dmb)_3^{2+}

l = path length, distance from vessel wall (d), 0 – 0.1 cm

c = concentration of catalyst, 0.5, 1.0, or 2.0 M

Table 5.2: Calculation of % Transmittance Based on Path Length and $[\text{Ru(dmb)}_3^{2+}]$

Distance from Vessel Wall (cm)	% T (1 mM)	% T (2 mM)	% T (0.5 mM)
0.001	96.16	92.47	98.06
0.01	67.61	45.71	82.22
0.02	45.71	20.89	67.61
0.03	30.90	9.55	55.59
0.04	20.89	4.36	45.71
0.05	14.12	2.00	37.58
0.06	9.55	0.91	30.90
0.07	6.46	0.42	25.41
0.08	4.36	0.19	20.89

0.1	2.00	0.04	14.12
0.16	0.19	0.0004	4.36

General flow reactor details: 12 inch, 1W blue LED strips were purchased from www.creativelightings.com and connected to a 40W power supply purchased from the same supplier. FEP tubing was purchased from www.newageindustries.com.

Flow reactor design A:

Into a Liebig's condenser was placed 3 12" strips of 1W blue LEDs. These strips were connected to a 40W power supply. 8.23 m of 1.59 mm I.D. FEP Teflon tubing was wrapped around the condenser in a single layer and secured at either end with copper wire (Figure 5.6). The tubing inlet was fitted with a Swagelok adapter and connected to a Dynamax SD-300 HPLC pump, and the outlet was placed in an appropriate collection vessel. The calculated residence volume is 15.9 mL.

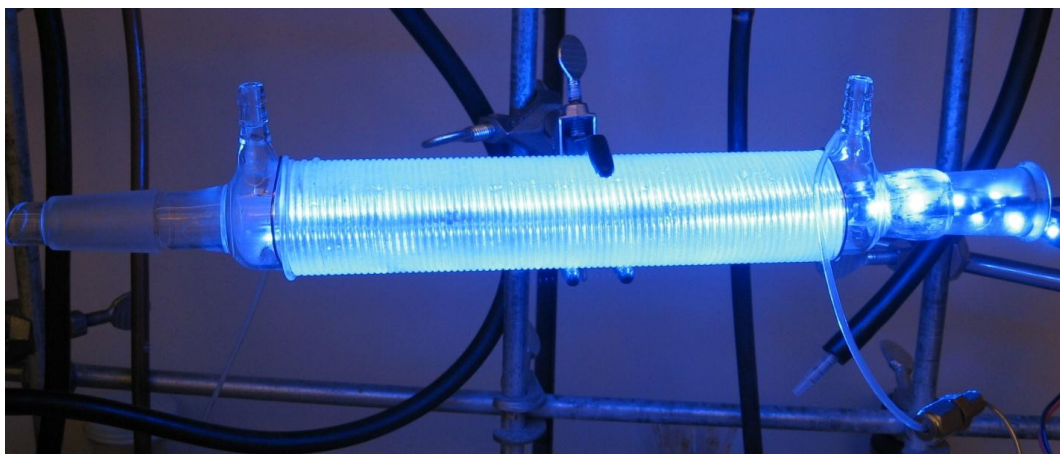


Figure 5.6: Flow Reactor Design A.

Flow reactor design B:

Into a Liebig's condenser was placed 3 12" strips of 1W blue LEDs. These strips were connected to a 40W power supply. 11.00 m of 0.79 mm I.D. FEP Teflon tubing was wrapped around the condenser in a single layer and secured at either end with copper wire. The tubing inlet was fitted with a Swagelok adapter and connected to a Dynamax SD-300 HPLC pump, and the outlet was placed in an appropriate collection vessel. The calculated residence volume is 5.7 mL.

Flow Reactor Procedures

General Procedure. An Erlenmeyer flask is charged with glucosyl bromide (1 eq), Hantzsch ester (2.1 eq), $\text{Ru(dmb)}_3(\text{PF}_6)_2$, and either 1,3,5-trimethoxybenzene or 1,4-dimethoxybenzene as an internal standard. The flask is sealed with a rubber septum and flushed with N_2 for 15 min. CH_2Cl_2 (0.12 M of substrate) and $i\text{Pr}_2\text{NEt}$ (3 eq) are added, and the solution is sparged with N_2 for 10 min. Freshly distilled acrolein (**3**, 2 or 4 eq) was added, resulting in a homogeneous orange solution. An inlet line with a filter was passed through the septum cap and into the reaction mixture, and the inlet line and pump head were primed with the reaction solution. The LEDs were turned on, and the flow rate was set to 0.1 mL/min. Cooling water was passed through the jacket on the condenser to ensure consistent reaction temperature. The reactor was allowed to run until all the reaction mixture was removed from the reaction flask, at which point the inlet line was placed into a beaker of CH_2Cl_2 . The reactor was allowed to continue to flow until all reaction mixture had been collected. The crude mixture was analyzed by ^1H NMR ($d_1 = 5.0 \mu\text{sec}$) for conversion and yield. For isolation of the product, silica was added (~5 g of silica per 1 g of substrate), and the heterogeneous mixture was concentrated *in vacuo*. The mixture was dry-loaded onto a silica gel column, and flash column chromatography afforded the product as a white or off-white solid.

Analysis of Flow Reactor Design and Catalyst Concentration.

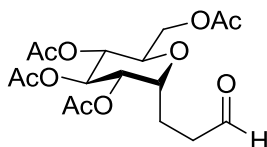
The analysis was performed using the general procedure listed above using 2.0 g **2** (4.86 mmol), 0.65 mL acrolein (9.72 mmol), 2.54 mL $i\text{Pr}_2\text{NEt}$ (14.6 mmol), 43.8 mg $\text{Ru(dmb)}_3(\text{PF}_6)_2$ (0.46 mmol), 3.16

g *i*Bu-HEH (10.2 mmol) and 688.8 mg p-dimethoxybenzene in 40 mL CH₂Cl₂. After the reaction time listed in Table 5.3, 1 mL samples were collected at 10 minute intervals, concentrated *in vacuo*, and analyzed by ¹H NMR for conversion and yield. The averages for the samples are reported (Table 5.3).

Table 5.3: Conversion, Yield, and TOF of Flow Reactor Based on Design.

Reactor Design	[Ru(dmb) ₃ ²⁺] (mM)	Time (h)	% Conv	%Yield (brsm)	TOF (h ⁻¹)
A	1.1	2	57	53 (93)	30
A	2.2	1.8	63	52 (83)	17
A	0.5	2.1	50	43 (86)	50
B	1.1	0.75	52	41 (80)	72
B	2.1	0.75	58	51 (89)	40
B	0.5	0.75	42	35 (82)	120

24-hour Continuous Flow Experiments.



3-(2,3,4,6-tetra-O-acetyl-α-D-glucopyranosyl)propionaldehyde (43).

“Batch” Reaction:

A flame dry 50 mL Schlenk flask (25 mm in diameter) under Ar was charged with glucosyl bromide **44** (1 g, 2.43 mmol), Ru(dmb)₃(PF₆)₂ (23 mg, 0.024 mmol, 1 mol%), *i*Bu-HEH (**45**) (1.58 g, 5.1 mmol, 2.1 eq) and p-dimethoxybenzene (489.3 mg) as an internal standard. The flask was evacuated and backfilled with Ar. Dry CH₂Cl₂ (20 mL) and *i*Pr₂NEt (1.27 mL, 7.29 mmol, 2 eq) were added, and the homogenous solution was sparged with N₂ for 10 min. Acrolein (**59**) was added (0.324 mL,

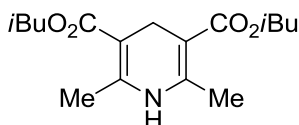
4.86 mmol, 2 eq). A 100 mL beaker was wrapped with one 12" blue LED strip, and the reaction flask was placed in the center of this beaker. The reaction was stirred vigorously for 24 hours, after which an aliquot was taken for analysis. ^1H NMR showed an 85% conversion to product, corresponding to a formal TOF of 3.5 h^{-1} .

NMR Reaction:

A 1 dram septum vial under Ar was charged with glucosyl bromide **44** (150 mg, 0.36 mmol), $i\text{Pr}_2\text{NEt}$ (0.190 mL, 1.09 mmol, 3 eq), acrolein (**59**) (50 μL , 0.73 mmol, 2 eq), 1,3,5-trimethoxybenzene (60 mg) as an internal standard, and 1.5 mL CD_2Cl_2 . A second 1 dram septum vial under Ar was charged with $\text{Ru(dmb)}_3(\text{PF}_6)_2$ (5.7 mg) in 1 mL CD_2Cl_2 (6.04 μM). An NMR tube under Ar was charged with 0.25 mL of the glucosyl bromide stock solution, 0.125 mL of $\text{Ru(dmb)}_3(\text{PF}_6)_2$ stock solution (1 mol %), and 40 mg $i\text{Bu-HEH}$ (**45**) (0.129 mmol, 2.1 eq). The solution was degassed with three freeze-pump-thaw cycles. The vessel was irradiated with a 27 W CFL at ~5 cm from the bulb for 60 min. The mixture was analyzed by ^1H NMR to give a 73% conversion, corresponding to a formal TOF of 70 h^{-1} .

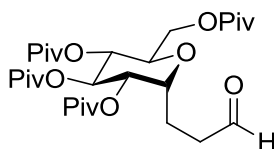
24- hour flow reactor:

According to the general procedure listed above, 7.5 g glucosyl bromide **44** (18.2 mmol), 4.86 mL acrolein (**59**) (72.8 mmol), 9.5 mL $i\text{Pr}_2\text{NEt}$ (54.6 mmol), 172 mg $\text{Ru(dmb)}_3(\text{PF}_6)_2$ (0.182 mmol), 11.8 g $i\text{Bu-HEH}$ (**45**) (38.2 mmol), 2.5 g p -dimethoxybenzene and 150 mL CH_2Cl_2 were combined. Reactor design A was modified by connected two modules in series via Swagelok connectors (Figure 5.6). The flow reactor was operated according to the general procedure for 24 hours, resulting in >97% conversion and 5.46 g of **43** (14.1 mmol, 77% yield) after silica gel flash column chromatography in EtOAc/hexanes. The ^1H NMR spectrum matched previously reported spectra.^{67b}



Diisobutyl 2,6-dimethyl-1,4-dihydropyridine-3,5-dicarboxylate (*i*Bu-HEH, **45**)

This compound was synthesized according to modified literature procedure.¹³³ A 1L round bottom flask was charged with isobutyl acetoacetate (100 mL, 0.628 mol, 2 eq), NH₄OAc (36.5 g, 0.474 mol, 1.5 eq), and paraformaldehyde (9.5 g, 0.316 mol, 1 eq). The heterogeneous mixture was heated to 70 °C with vigorous stirring until the mixture precipitated as a solid. The solid was heated for an additional 15 minutes, cooled to room temperature, and recrystallized from hot isopropyl alcohol. The solid was washed with isopropyl alcohol and pentanes and dried *in vacuo* to afford 64.9 g of *i*Bu-HEH as a yellow powder (0.209 mol, 66% yield). The ¹H NMR spectrum matched previously reported spectra.¹³⁴



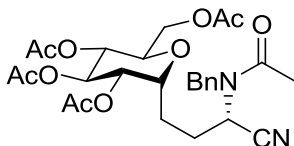
3-(2,3,4,6-tetra-*O*-pivaloyl- α -D-glucopyranosyl)propionaldehyde (**61**).

According to the general procedure listed above, 10.5 g glucosyl bromide **60** (18.2 mmol), 4.86 mL acrolein (**59**) (72.8 mmol), 9.5 mL *i*Pr₂NEt (54.6 mmol), 172 mg Ru(dmb)₃(PF₆)₂ (0.182 mmol), 11.8 g *i*Bu-HEH (**45**) (38.2 mmol), 2.42 g *p*-dimethoxybenzene and 150 mL CH₂Cl₂ were combined and passed through three connected modules of reactor design A (Figure 5.6), resulting in >97% conversion and an 85% yield by ¹H NMR. Flash column chromatography in Et₂O/hexanes followed by recrystallization from hexamethyldisiloxane to yield 4.62 g of **61** (8.30 mmol, 46% yield). [α]_D²⁰ = +63.6 (c = 1.4). ¹H NMR (600 MHz, CDCl₃): δ 9.82 (s, 1H, CHO), 5.42 (t, ³*J*(H,H) = 9.6, 1H, *H*3), 5.10 (dd, ³*J*(H,H) = 6.2 and 10 Hz, 1H, *H*2), 5.04 (t, ³*J*(H,H) = 9.8 Hz, 1H, *H*4), 4.16 (ddd, ³*J*(H,H) = 3.1, 6.2, and 12.5 Hz, 1H, *H*1), 4.09 (dd, ³*J*(H,H) = 1.8 and 12.3 Hz, 1H, *H*6/7), 4.02 (dd, ³*J*(H,H) =

¹³³ Zolfigol, M. A.; Safaiee, M., *Synlett* **2004**, 0827-0828.

¹³⁴ Yang, J. W.; List, B., *Org. Lett.* **2006**, 8, 5653-5655.

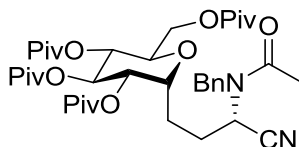
5.7 and 12.3 Hz, 1H, *H*6/7), 3.78 (ddd, $^3J(\text{H,H}) = 1.6, 5.6$ and 10 Hz 1H, *H*5), 2.62-2.56 (m, 2H, CH_2CHO) 2.14-2.10 (m, 1H, $-\text{CH}_2-$), 1.87-1.83 (m, 1H, $-\text{CH}_2-$), 1.22 (s, 9H), 1.18 (s, 9H), 1.16 (s, 9H), 1.12 (s, 9H). ^{13}C NMR (150 MHz, CDCl_3): δ 200.6, 178.0, 177.09, 177.07, 176.6, 72.2, 70.4, 69.8, 68.9, 68.3, 62.4, 39.2, 38.84, 38.77, 38.74, 38.71, 27.16, 27.15, 27.11, 27.0, 17.7. HRMS (ESI): m/z $[\text{M}+\text{Na}]^+$ found 579.3129, calcd 579.3140 for $\text{C}_{29}\text{H}_{48}\text{O}_{10}$. m.p. = 110-112°C.



(1*S*)-*N*-benzylacetamido-3-(2,3,4,6-tetra-*O*-acetyl- α -D-glucopyranosyl)-propanenitrile (62**).**

This compound was prepared according to modified literature procedure.¹¹⁹ A 1 dram spetum vial was charged with **43** (100 mg, 0.25 mmol) and 80 mg 4Å molecular sieves. The vial was evacuated and backfilled with Ar, then CH_2Cl_2 (1 mL) and BnNH_2 (33 μL , 0.3 mmol, 1.2 eq) were added. The heterogeneous solution was allowed to stir at room temperature for 2 hours, then **48** (1.4 mg, 0.0025 mmol, 1 mol%) was added. The resulting yellow solution was placed in a -40°C bath and stirred for 10 min, then AcCN (30 μL , 0.375 mmol, 1.5 eq) was added. After stirring for 48 hours at -40°C , the reaction was allowed to warm to room temperature, filtered through a plug of silica in EtOAc, and concentrated *in vacuo*. The crude mixture was analyzed by ^1H NMR to give a 10:1 dr. Silica gel flash column chromatography in 55/45 EtOAc/hexanes provided 123 mg of **62** (90% yield) as a white powder. $[\alpha]_D^{20} = +34.8$ ($c = 3.6$). ^1H NMR (500 MHz, CDCl_3): δ 7.38 (t, $^3J(\text{H,H}) = 7.2$ Hz, 2H), 7.33 (m, 1H), 7.23 (d, $^3J(\text{H,H}) = 7.4$ Hz, 2H) 5.47 (t, $^3J(\text{H,H}) = 6.4$ Hz, 1H, CHCN), 5.22 (t, $^3J(\text{H,H}) = 9.0$ Hz, 1H, *H*3), 5.01 (dd, $^3J(\text{H,H}) = 6.0$ and 8.9 Hz, 1H, *H*2), 4.94 (t, $^3J(\text{H,H}) = 9.0$ Hz, 1H, *H*4), 4.77 (d, $^3J(\text{H,H}) = 17.4$ Hz, 1H, PhCH_2N), 4.60 (d, $^3J(\text{H,H}) = 17.4$ Hz, 1H, PhCH_2N), 4.18 (dd, $^3J(\text{H,H}) = 4.8$ and 12.1 Hz, 1H, *H*6/7), 3.98-3.94 (m, 2H, *H*6/7), 3.70 (m, 1H, *H*5), 2.14 (s, 3H, NAc), 2.05 (s, 3H), 2.03 (s, 3H), 2.02 (s, 3H), 2.01 (s, 3H). 1.90-1.86 (m, 2H), 1.66 (m, 1H), 1.56-1.51 (m, 1H). ^{13}C NMR (100 MHz, CDCl_3): δ 171.1, 170.5, 169.8, 169.52, 169.45, 135.8, 129.2, 128.2,

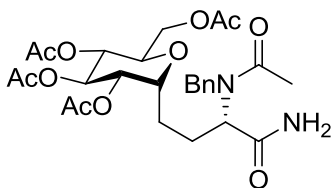
126.2, 117.3, 71.6, 70.0, 69.8, 68.4, 62.0, 50.4, 46.3, 27.8, 21.97, 21.86, 20.66, 20.60. HRMS (ESI): m/z $[M+Na]^+$ found 569.2104, calcd 569.2106 for $C_{27}H_{34}N_2O_{10}$. m.p. = 61-65°C.



(1S)-N-benzylacetamido-3-(2,3,4,6-tetra-O-pivaloyl-α-D-glucopyranosyl)-propanenitrile (63).

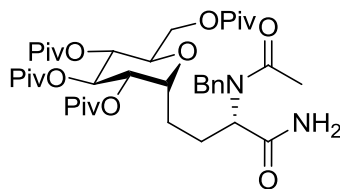
This compound was prepared according to modified literature procedure.¹¹⁹ A 20mL septum vial was charged with **61** (800 mg, 1.44 mmol), 4 Å MS (400 mg) and placed under Ar. CH_2Cl_2 (5 mL) was added, and then freshly distilled $BnNH_2$ (165 μ L, 1.5 mmol, 1.05 eq) was added. The heterogeneous mixture was allowed to stir for 2 hours at room temperature, and then **48** was added (7 mg, 0.012 mmol, 0.8 mol %). The mixture was cooled to -40 °C for 10 min, and AcCN (150 μ L, 2.11 mmol, 2.5 eq) was added. Allowed to stir 24 hours, then the solution was allowed to warm to rt and stir for an additional 24 hours. The reaction mixture was quenched by passing through a plug of silica in EtOAc in a well-ventilated hood. The crude mixture was concentrated *in vacuo* and analyzed by 1H NMR to give a dr >20:1. Silica gel flash column chromatography in EtOAc/Hex provided **63** (0.887g, 86% yield) as a white solid. Further purification was possible through recrystallization from hexamethyldisiloxane/TBME. $[\alpha]_D^{25} = 46.17$ ($c = 1.00$). 1H NMR (400 MHz, $CDCl_3$): δ 7.40 (t, $^3J(H,H) = 7$ Hz, 2H), 7.34 (m, 1H), 7.22 (d, $^3J(H,H) = 7.3$ Hz, 2H) 5.50 (t, $^3J(H,H) = 7.1$ Hz, 1H, $CHCN$), 5.33 (t, $^3J(H,H) = 9.6$ Hz, 1H, $H3$), 5.04-5.00 (m, 2H, $H2 + H4$), 4.75 (d, $^3J(H,H) = 17.6$ Hz, 1H, $PhCH_2N$), 4.58 (d, $^3J(H,H) = 17.2$ Hz, 1H, $PhCH_2N$), 4.04 (m, 1H, $H1$), 4.00 (s, 2H, $H6/7$), 3.66 (dt, $^3J(H,H) = 7.1$ 3.2 Hz, 3.2 Hz, and 9.6 Hz, 1H, $H5$), 2.11 (s, 3H, NAc), 1.94-1.89 (m, 2H), 1.71-1.60 (m, 1H, $-CH_2CHCN$), 1.54-1.41 (m, 1), 1.20 (s, 9H), 1.17 (s, 9H), 1.16 (s, 9H), 1.12 (s, 9H). ^{13}C NMR (100 MHz, $CDCl_3$): δ 178.0, 177.0, 176.97, 176.5, 171.1, 135.8, 129.2, 128.3, 126.2, 117.3, 71.8, 70.5, 69.8, 69.0, 68.1, 62.3, 50.4, 45.9, 38.8, 38.75, 38.69, 27.6, 27.15, 27.12, 27.0, 21.9,

21.5. HRMS (ESI): m/z $[M+H]^+$ found 715.4160, calcd 715.4164 for $C_{39}H_{58}N_2O_{10}$. m.p. = 123-125°C.



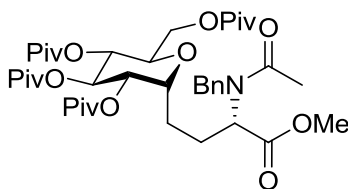
(2S)-N-benzylacetamido-4-(2,3,4,6-tetra-O-acetyl-α-D-glucopyranosyl)-butylamide (65).

This compound was synthesized according to modified literature procedure.¹²⁵ A 20 mL vial was charged with **62** (143 mg, 0.265 mmol), **64** (1.1 mg, 0.0026 mmol, 1 mol%), absolute EtOH (3.2 mL), and H₂O (0.8 mL). The reaction mixture was heated to 70 °C. After 1 hour, an additional 1.1 mg of **64** (0.0026 mmol, 1 mol%) was added. After 7 hours, the reaction was cooled to room temperature, passed through a plug of silica in EtOAc, and concentrated *in vacuo*. The crude reaction mixture was analyzed by ¹H NMR to give a 10:1 dr. Silica gel flash column chromatography in MeOH/CH₂Cl₂ gave 82 mg of **65** (55% yield) as a white powder. $[\alpha]_D^{20} = +5.9$ (c = 2.3). ¹H NMR (400 MHz, CDCl₃): δ 7.34 (t, ³J(H,H) = 7.0 Hz, 2H), 7.27 (m, 1H), 7.17 (d, ³J(H,H) = 7.4 Hz, 2H) 6.52 (s, 1H, NH), 5.33 (s, 1H, NH), 5.23 (t, ³J(H,H) = 9.4 Hz, 1H, H3), 5.01 (dd, ³J(H,H) = 6.0 and 9.6 Hz, 1H, H2), 4.96 (t, ³J(H,H) = 9.4 Hz, 1H, H4), 4.58 (at, ³J(H,H) = 18.3 Hz, 2H, PhCH₂N), 4.20 (dd, ³J(H,H) = 4.7 and 12.3 Hz, 1H, H6/7), 4.04 (dd, ³J(H,H) = 2.1 and 12.3 Hz, 1H, H6/7), 4.00 (ddd, ³J(H,H) = 3.0, 5.9, and 12.0 Hz, 1H, H1), 3.84-3.82 (m, 1H, H5), 2.21-2.13 (m, 1H) 2.10 (s, 3H, NAc), 2.05-1.95 (15H, Ac), 1.75-1.71 (m, 1H), 1.42-1.34 (m, 2H). ¹³C NMR (100 MHz, CDCl₃): δ 173.1, 171.9, 170.7, 170.1, 169.6, 136.9, 129.0, 127.6, 125.9, 77.2, 72.4, 70.5, 70.4, 68.6, 68.3, 61.2, 56.5, 49.1, 23.7, 22.37, 22.31, 20.7, 20.68, 20.62. HRMS (ESI): m/z $[M+Na]^+$ found 587.2198, calcd 587.2211 for $C_{27}H_{36}N_2O_{11}$. m.p. = 75-80 °C.



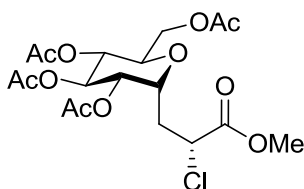
(2S)-N-benzylacetamido-4-(2,3,4,6,-tetra-O-pivaloyl-α-D-glucopyranosyl)-butylamide (66).

This compound was synthesized according to modified literature procedure.¹²⁵ A 1 dram vial was charged with **63** (100 mg, 0.14 mmol), **64** (1.2 mg, 0.0028 mmol, 2 mol%), absolute EtOH (1.6 mL), and H₂O (0.4 mL). The reaction mixture was heated to 70 °C. After 7 hours, the reaction was cooled to room temperature, passed through a plug of silica in EtOAc, and concentrated *in vacuo* to give 103 mg **66** (>98% yield, dr >10:1) as a white powder. Analytically pure material was obtained by silica gel flash column chromatography in 75/25 EtOAc/hexanes. $[\alpha]_D^{20} = +4.4$ (c = 1.6). ¹H NMR (400 MHz, CDCl₃): δ 7.36 (t, ³J(H,H) = 7.0 Hz, 2H), 7.28 (m, 1H), 7.17 (d, ³J(H,H) = 7.3 Hz, 2H) 6.54 (s, 1H, NH), 5.32 (s, 1H, NH), 5.32 (t, ³J(H,H) = 9.7 Hz, 1H, H₃), 5.08-5.00 (m, ²H, H₂ + H₄), 4.94 (dd, ³J(H,H) = 4.8 and 10.1 Hz, 1H), 4.56 (s, 2H, PhCH₂N) 4.10-4.04 (m, ³H), 3.79 (dq, ³J(H,H) = 2.4 and 10.2 Hz, 1H), 2.23-2.12 (m, 1H), 2.08 (s, 3H, NAc), 1.83-1.73 (m, 1H), 1.48-1.43 (m, 1H), 1.39-1.30 (m, 1H), 1.19 (s, 9H), 1.15 (s, 9H), 1.13 (s, 9H), 1.11 (s, 9H). ¹³C NMR (150 MHz, CDCl₃): δ 178.1, 177.1, 177.0, 176.4, 173.0, 171.9, 136.8, 128.9, 127.6, 126.0, 72.4, 70.7, 70.1, 68.4, 68.0, 62.2, 56.7, 49.3, 38.8, 38.68, 38.66, 27.15, 27.11, 27.08, 27.0, 23.6, 22.3, 21.8. HRMS (ESI): *m/z* [M+H]⁺ found 733.4283, calcd 733.4275 for C₃₉H₆₀N₂O₁₁. m.p. = 84-86 °C.



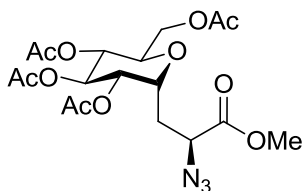
(2S)-methyl-N-benzylacetamido-4-(2,3,4,6,-tetra-O-pivaloyl-α-D-glucopyranosyl)-butanoate (67).

This compound was synthesized according to modified literature procedure.¹²⁶ A 1 dram vial was charged with **66** (200 mg, 0.272 mmol). The vial was evacuated and backfilled with Ar, and dry MeOH (4 mL) was added. *t*-Butyl nitrite (54 μ L, 0.41 mmol, 1.5 eq) then freshly distilled TMSCl (70 μ L, 0.546 mmol, 2 eq) were added. The homogeneous reaction mixture was heated to 60 °C. After 4 h, the reaction mixture was cooled to rt and transferred to a separatory funnel with 20 mL H₂O. The aqueous layer was extracted 3 x 20 mL Et₂O, and the combined organic layers were dried with MgSO₄, filtered, and concentrated *in vacuo*. Silica gel flash column chromatography in 30/70 to 40/60 EtOAc/hexanes gave 164 mg of **12** (80% yield) as a white powder. The product exists as a 3.5:1 mixture of rotamers in CDCl₃ and 3.5:1 in tol-d₈ at room temperature. Heating a mixture of 10 mg of **12** in 0.5 mL of dry tol-d₈ resulted in coalescence of the rotamers at 350 K which returned to a 3.5:1 mixture upon cooling to room temperature. Analysis of the ¹H spectrum in tol-d₈ at 380 K indicates a >10:1 dr. $[\alpha]_D^{20} = +33.2$ (c = 1.1). ¹H NMR (400 MHz, CDCl₃): Major rotamer: δ 7.39 (t, ³*J*(H,H) = 7.0 Hz, 2H), 7.31 (m, 1H), 7.24 (d, ³*J*(H,H) = 7.2 Hz, 2H), 5.31 (t, ³*J*(H,H) = 9.5 Hz, 1H, *H*3), 5.04-4.98 (m, 2H, *H*2 + *H*4), 4.60 (t, ³*J*(H,H) = 7.1 Hz, 1H), 4.54 (s, 2H, PhCH₂N), 4.10-4.00 (m, 3H), 3.70 (ddd, ³*J*(H,H) = 1.8, 4.8, and 9.9 Hz, 1H, *H*5), 3.60 (s, 3H, -OMe), 2.21-2.10 (m, 1H) 2.11 (s, 3H, NAc), 1.80-1.69 (m, 1H), 1.66-1.60 (m, 1H), 1.40-1.30 (m, 2H), 1.20 (s, 9H), 1.15 (s, 18H), 1.11 (s, 9H). Diagnostic peaks from minor rotamer: δ 4.42 (d, ³*J*(H,H) = 15.2 Hz, 1H), 4.31 (t, ³*J*(H,H) = 7.3 Hz, 1H). 3.45 (s, 3H, -OMe), 2.24 (s, 3H, NAc). ¹³C NMR (100 MHz, CDCl₃): δ 178.1, 177.1, 176.9, 176.5, 171.4, 171.1, 136.5, 128.9, 128.4, 127.9, 126.8, 72.6, 70.7, 70.1, 68.6, 68.3, 62.4, 57.5, 52.1, 51.4, 38.8, 38.72, 38.69, 27.18, 27.11, 27.0, 25.2, 22.1, 22.0. HRMS (ESI): *m/z* [M+Na]⁺ found 770.4091, calcd 770.4086 for C₄₀H₆₁NO₁₂. m.p. = 50-55°C.



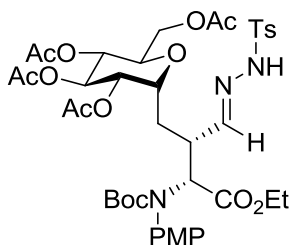
(2R)-methyl-2-chloro-3-(2,3,4,6-tetra-O-acetyl- α -D-glucopyranosyl)propanoate (70).

This compound was synthesized according to modified literature procedure.¹²⁰ A 1 dram vial was charged with **43** (100 mg, 0.25 mmol) and L-prolinamide (**51**) (3 mg, 0.026 mmol, 10 mol%), evacuated, and backfilled with Ar. Dry CH₂Cl₂ (1 mL) and *N*-chlorosuccinimide (43 mg, 0.332 mmol, 1.3 eq) were added. The reaction was allowed to stir for 24 hours at room temperature. The solution was transferred to a 20 mL vial with 3 mL ^{*t*}BuOH, then 3 mL 1M KH₂PO_{4(aq)} and 3 mL 1M KMnO_{4(aq)} were added. The purple solution was allowed to stir 1 min and then cooled to 0 °C. The reaction was acidified to pH 3 with 1M HCl_(aq) and transferred to a separatory funnel. The aqueous layer was extracted 3 x EtOAc, and the combined organic layers were rinsed 3 x H₂O, 1 x NaHCO_{3(aq)}, 1 x brine, dried with Na₂SO₄, filtered, and concentrated *in vacuo*. The crude reaction mixture was transferred to a 20 mL vial, evacuated, and placed under Ar. Dry PhMe (2 mL) and dry MeOH (5 mL) were added. TMSCH₂N₂ (2 M in hexanes) was added dropwise until a yellow color persisted, and the mixture was allowed to stir 5 min. The reaction was quenched with 1 drop AcOH, transferred to a separatory funnel, and diluted with H₂O and EtOAc. The layers were separated, and the aqueous layer was extracted 3 x EtOAc. The combined organic layers were rinsed 1 x brine, dried with MgSO₄, filtered, and conc *in vacuo*. The crude reaction mixture was analyzed by ¹H NMR to give a 10:1 dr. Silica gel flash column chromatography in EtOAc/hexanes afforded 97 mg of **70** (83% yield over 2 steps) as a white powder. [α]_D²⁵ = +29.5 (c = 1.0). ¹H NMR (400 MHz, CDCl₃): δ 5.24 (t, ³*J*(H,H) = 8.6 Hz, 2H, *H*3), 5.11 (dd, ³*J*(H,H) = 5.4 and 8.8 Hz, 1H, *H*2), 4.99 (t, ³*J*(H,H) = 8.8 Hz, 1H, *H*4), 4.43 (ddd, ³*J*(H,H) = 2.5, 5.4 and 12 Hz, 1H), 4.41 (dd, ³*J*(H,H) = 3.2 and 5.6 Hz, 1H), 4.24 (dd, ³*J*(H,H) = 5.4 and 12 Hz, 1H), 4.10 (dd, ³*J*(H,H) = 3 and 12.2 Hz, 1H), 3.87 (ddd, ³*J*(H,H) = 3, 5.3 and 8.5 Hz, 1H), 3.82 (s, 3H, -OMe), 2.55 (ddd, ³*J*(H,H) = 4, 11.7, and 15.5 Hz, 1H, -CH₂-), 2.10 (s, 3H, OAc), 2.08 (s, 3H, OAc), 2.04 (s, 6H, OAc), 1.97-2.06 (m, 1H, -CH₂-). ¹³C NMR (100 MHz, CDCl₃): δ 170.6, 169.9, 169.8, 169.4, 69.9, 69.8, 68.9, 68.2, 61.8, 53.3, 53.1, 31.4, 20.7. HRMS (ESI): *m/z* [M+Na]⁺ found 475.0970, calcd 475.0978 for C₁₈H₂₅ClO₁₁. m.p. = 74-77 °C.



(2S)-methyl-2-azido-3-(2,3,4,6-tetra-O-acetyl- α -D-glucopyranosyl)propanoate (71).

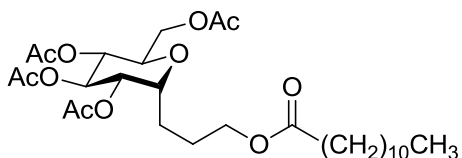
A 20 mL vial was charged with **70** (48 mg, 0.106 mmol), 100 mg NaN₃ (14.5 eq) in 4 mL DMF. The heterogeneous solution was allowed to stir at room temperature for 6 hours. The reaction mixture was transferred to a separatory funnel with 20 mL Et₂O and 20 mL H₂O. The layers were separated, and the aqueous layer was extracted 2x Et₂O (20 mL). The combined organic layers were washed 3x H₂O, 1x brine, dried with MgSO₄, filtered, and concentrated *in vacuo*. Crude ¹H NMR showed a dr of 8:1 based on ratio of –OMe peaks. Silica gel flash column chromatography in Et₂O/Hexanes provided **14** (40 mg, 82% yield) as a clear oil. $[\alpha]_D^{20} = 59.7$ (c = 0.7). ¹H NMR (400 MHz, CDCl₃): major diastereomer: δ 5.23 (t, ³J(H,H) = 8.8 Hz, 1H, H3), 5.07 (dd, ³J(H,H) = 5.5 and 9.1 Hz, 1H, H2), 5.00 (t, ³J(H,H) = 8.7 Hz, 1H, H4), 4.35 (ddd, ³J(H,H) = 3.0, 5.4 and 11.0 Hz, 1H, H?), 4.25 (dd, ³J(H,H) = 5.0 and 12.3 Hz, 1H, H?), 4.11 (dd, ³J(H,H) = 5.5 and 6.5 Hz, 1H, H?), 4.04 (dd, ³J(H,H) = 2.7 and 12.2 Hz, 1H, H?), 3.90 (ddd, ³J(H,H) = 2.8, 4.8 and 8.3 Hz, 1H, H?) 3.82 (s, 3H, -OMe) 2.24 (ddd, ³J(H,H) = 5.4, 11.2 and 15.2 Hz, 1H, -CH₂-) 2.10 (s, 3H, Ac), 2.06-2.02 (m, 1H, -CH₂-), 2.08 (s, 3H, Ac), 2.04 (s, 6H, Ac). ¹³C NMR (100 MHz, CDCl₃): δ 170.7, 170.0, 169.9, 269.4, 69.9, 69.8, 69.52, 69.49, 68.2, 61.8, 59.1, 27.8, 20.71, 20.66, 20.63. HRMS (ESI): *m/z* [M+Na]⁺ found 482.1379, calcd 482.1381 for C₁₈H₂₅N₃O₁₁.



Ethyl 2-(N-Boc-N-(4-methoxyphenyl)amino)-3-tosylhydrazono-(4-[2,3,4,6,-tetra-*O*-acetyl- α -D-glucopyranosyl])butanoate (74).

This compound was synthesized according to modified literature procedure.¹²¹ A 1 dram vial was charged with **43** (100 mg, 0.25 mmol) and **56** (57 mg, 0.275 mmol, 1.1 eq). Dry DMSO (2 mL) and L-proline (**57**) (6 mg, 0.052 mmol, 20 mol%) were added, and the reaction was allowed to stir for 1 hour at room temperature. TsNHNH₂ (100 mg, 0.537 mmol, 2 eq) was added in one portion, and the reaction was allowed to stir for an additional hour. The reaction was transferred to a separatory funnel and diluted with 20 mL Et₂O and 20 mL half-saturated NH₄Cl_(aq). The layers were separated, and the aqueous layer was extracted 3 x Et₂O. The combined organic layers were rinsed 1 x NaHCO_{3(aq)}, 1 x brine, dried with MgSO₄, filtered, and concentrated *in vacuo* in a <25 °C bath. Higher bath temperatures results in decomposition of the product. The crude mixture was transferred to a 20 mL vial, evacuated, and placed under Ar. Dry CH₂Cl₂ (3 mL), NEt₃ (140 μ L, 1.0 mmol, 4 eq), DMAP (5 mg, 0.041 mmol, 15 mol%) and Boc₂O (170 mg, 0.78 mmol, 3 eq) were added. The reaction was allowed to stir 30 min then quenched with H₂O. The mixture was transferred to a separatory funnel and diluted with CH₂Cl₂ and H₂O. The layers were separated, and the aqueous layer was extracted 3 x CH₂Cl₂. The combined organic layer was rinsed 1 x 1M HCl_(aq), 1 x sat. NaHCO_{3(aq)}, 1 x brine, dried with MgSO₄, filtered, and concentrated *in vacuo*. The crude mixture was analyzed by ¹H NMR to give a >10:1 dr. Immediate silica gel flash column chromatography in Et₂O/hexanes afforded 114 mg of **16** (68% yield) as a white solid. The material was stable for >1 week when stored at -20 °C as a solution or a solid, and a solution in CDCl₃ is stable for ~1-2 days at room temperature. $[\alpha]_D^{25} = 31.0$ (c = 0.7). ¹H NMR (400 MHz, CDCl₃): δ 7.98 (d, 1H, HC=N), 7.85 (d, ³J(H,H) = , 2H), 7.31 (d, ³J(H,H) = 2H), 6.75 (d, ³J(H,H) = , 2H), 6.68 (d, ³J(H,H) = , 2H), 5.28 (t, ³J(H,H) = 9.6, 1H, H3), 5.12 (dd, ³J(H,H) = 6.2 and 10 Hz, 1H, H2), 5.00 (t, ³J(H,H) = 9.8 Hz, 1H, H4), 4.49 (d, ³J(H,H) = 3.1, 6.2, and 12.5 Hz, 1H,), 4.42 (br s, 1H, NH), 4.34 (s, 1H, H6/7), 4.20 (dd, ³J(H,H) = , 1H, H6/7), 4.19-4.14 (m, 3H, OCH₂CH₃ + H5), 4.05 (dd, ³J(H,H) = , 1H,) 3.92 (ddd,

$^3J(\text{H,H}) = , 1\text{H, H5})$ 3.72 (s, 3H, -OMe), 3.22 (pent, $^3J(\text{H,H}) = , 1\text{H})$, 2.43 (s, 3H, Me), 2.23 (ddd, $^3J(\text{H,H}) = , 1\text{H})$ 2.03 (s, 3H), 2.01 (s, 3H), 2.00 (s, 6H), 1.35 (s, 9H, Boc) 1.20 (t, $^3J(\text{H,H}) = , 3\text{H})$ ^{13}C NMR (150 MHz, CDCl_3): δ 173.6, 171.4, 170.6, 169.9, 169.45, 169.40, 153.0, 149.8, 144.8, 140.0, 135.3, 129.4, 128.3, 115.6, 114.7, 85.4, 70.2, 69.9, 69.7, 69.4, 68.2, 61.9, 61.5, 58.4, 55.6, 41.7, 34.6, 31.5, 27.7, 23.6, 22.6, 21.6, 20.61, 20.6, 20.57, 14.1. HRMS (ESI): m/z $[\text{M}+\text{Na}]^+$ found 886.3016, calcd 886.3039 for $\text{C}_{40}\text{H}_{53}\text{N}_3\text{O}_{16}\text{S}$. m.p. = 60 °C (dec).



3-(2,3,4,6,-tetra-*O*-acetyl- α -D-glucopyranosyl)propyl dodecanoate (76).

A 1 dram vial was charged with **1** (200 mg, 0.515 mmol), evacuated, and backfilled with Ar. Dry THF (2 mL) and NaBH_4 (78 mg, 2.06 mmol, 4 eq) were added, and the heterogeneous solution was stirred at room temperature. After 30 min, the reaction was cooled to 0 °C and quenched with H_2O . The mixture was diluted with 10 mL EtOAc and 10 mL H_2O , and the layers were separated. The aqueous layer was extracted 3 x 10 mL EtOAc, and the combined organic layers were rinsed 1 x brine, dried with MgSO_4 , filtered, and concentrated *in vacuo*. The crude reaction mixture was transferred to a 20 mL vial, backfilled, and placed under Ar. CH_2Cl_2 (3 mL), NEt_3 (144 μL , 0.82 mmol, 1.6 eq), DMAP (6 mg, 0.049 mmol, 0.1 eq), and lauroyl chloride (126 μL , 0.545 mmol, 1.05 eq) were added. The homogenous solution was allowed to stir at room temperature for 24 hours. The reaction was quenched with 10 mL H_2O and diluted with 10 mL CH_2Cl_2 . The layers were separated, and the aqueous layer was extracted 3 x 10 mL CH_2Cl_2 . The combined organic layers were rinsed 1 x 1M $\text{HCl}_{(\text{aq})}$, 1 x $\text{NaHCO}_{3(\text{aq})}$, 1 x brine, dried with MgSO_4 , filtered, and concentrated *in vacuo*. Silica gel flash column chromatography in 20/80 to 30/70 EtOAc/hexanes gave 204 mg of the **17** (69% yield) as a clear oil. $[\alpha]_{\text{D}}^{20} = +34.2$ ($c = 3.2$). ^1H NMR (400 MHz, CDCl_3): δ 5.30 (t, $^3J(\text{H,H}) = 9.2$,

1H, *H3*), 5.08 (dd, $^3J(\text{H,H}) = 5.7$ and 9.4 Hz, 1H, *H2*), 4.97 (t, $^3J(\text{H,H}) = 9.2$ Hz, 1H, *H4*), 4.23 (dd, $^3J(\text{H,H}) = 5.4$ and 12.2 Hz, 1H, *H6/7*), 4.17 (ddd, $^3J(\text{H,H}) = 3.4$, 5.6 and 11.2 Hz, 1H, *H1*), 4.05-4.12 (m, 3H, *H6/7* + $\text{CH}_2\text{-O}_2\text{C}$), 3.80 (ddd, 1H, $^3J(\text{H,H}) = 2.6$, 5.4 , and 9.1 Hz, *H5*), 2.29 (t, $^3J(\text{H,H}) = 7.5$ Hz, 2H), 2.08 (s, 3H, OAc), 2.05 (s, 3H, OAc), 2.04 (s, 3H, OAc), 2.03 (s, 3H, OAc), 1.75-1.84 (m, 2H), 1.51-1.68 (m, 4H), 1.19-1.34 (m, 16H), 0.87 (t, , $^3J(\text{H,H}) = 6.6$ Hz, 3H). ^{13}C NMR (100 MHz, CDCl_3): δ 173.8, 170.6, 170.1, 169.6, 169.5, 72.3, 70.28, 70.26, 68.7, 63.5, 62.2, 34.3, 31.9, 29.6, 29.4, 29.3, 29.2, 29.16, 25.0, 24.4, 22.6, 22.0, 20.68, 20.63 14.1. HRMS (ESI): m/z $[\text{M}+\text{Na}]^+$ found 595.3083, calcd 595.3089 for $\text{C}_{29}\text{H}_{48}\text{O}_{11}$.

Bibliography

- Abrecht, S.; Scheffold, R. *Chimia* **1985**, *39*, 211.
- Adlington, R. M.; Baldwin, J. E.; Basak, A.; Kozyrod, R. P. *J. Chem. Soc., Chem. Comm.* **1983**, *17*, 944-945.
- Anderson, T. J.; Jones, G. D.; Vicic, D. A., *J. Am. Chem. Soc.* **2004**, *126*, 8100-8101.
- Andrews, R. S.; Becker, J. J.; Gagné, M. R., *Angew. Chem., Int. Ed.* **2010**, *49*, 7274-7276.
- Andrews, R. S.; Becker, J. J.; Gagné, M. R., *Org. Lett.* **2011**, *13*, 2406-2409.
- Araki, Y.; Kobayashi, N.; Watanabe, K.; Ishido, Y., *J. Carbohydr. Chem.* **1985**, *4*, 565-585.
- Axon, J. R.; Beckwith, A. L. J., *J. Chem. Soc., Chem. Commun.* **1995**, 549-550.
- Ballardini, R.; Varani, G.; Indelli, M. T.; Scandola, F.; Balzani, V., *J. Am. Chem. Soc.* **1978**, *100*, 7219-7223.
- Beau, J.-M.; Gallagher, T.; Driguez, H.; Thiem, J., Nucleophilic C-glycosyl donors for C-glycoside synthesis. In *Glycoscience Synthesis of Substrate Analogs and Mimetics*, Springer Berlin / Heidelberg: 1997; Vol. 187, pp 1-54.
- Beau, J.-M.; Sinaÿ, P., *Tetrahedron Lett.* **1985**, *26*, 6185-6188.
- Beau, J.-M.; Sinaÿ, P., *Tetrahedron Lett.* **1985**, *26*, 6189-6192.
- Bellosta, V.; Czernecki, S., *J. Chem. Soc., Chem. Commun.* **1989**, 199-200.
- Bihovsky, R.; Selick, C.; Giusti, I., *J. Org. Chem.* **1988**, *53*, 4026-4031.
- Bisht, H. S.; Chatterjee, A. K., *J. Macromol. Sci. Pol. R.* **2001**, *41*, 139-173.
- Blom, P.; Ruttens, B.; Van Hoof, S.; Hubrecht, I.; Van der Eycken, J.; Sas, B.; Van hemel, J.; Vandenkerckhove, J. *J. Org. Chem.* **2005**, *70*, 10109-10112.
- Bock, C. R.; Connor, J. A.; Gutierrez, A. R.; Meyer, T. J.; Whitten, D. G.; Sullivan, B. P.; Nagle, J. K., *Chem. Phys. Lett.* **1979**, *61*, 522-525.
- Bourne, R. A.; Han, X.; Poliakoff, M.; George, M. W., *Angew. Chem., Int. Ed.* **2009**, *48*, 5322-5325.
- Broomhead, J. A.; Young, C. G. *Inorg. Synth.* 1990, *28*, 338.
- Burstall, F. H., *J. Chem. Soc.* **1936**, 173-175.
- Carey, F. A.; Sundberg, R. J. In *Advanced Organic Chemistry, Part A*, 4th ed.; Kluwer Academic / Plenum Publishers: New York, 2000; pp 151-156.

- Carey, F. A.; Sundberg, R. J. In *Advanced Organic Chemistry, Part A*, 4th ed.; Kluwer Academic / Plenum Publishers: New York, 2000; pp 220-222.
- Cheng, J.-P.; Lu, Y.; Zhu, X.-Q.; Sun, Y.; Bi, F.; He, J., *J. Org. Chem.* **2000**, *65*, 3853-3857.
- Cipolla, L.; Nicotra, F.; Vismara, E.; Guerrini, M., *Tetrahedron* **1997**, *53*, 6163-6170.
- Ciszewski, J. T.; Mikhaylov, D. Y.; Holin, K. V.; Kadirov, M. K.; Budnikova, Y. H.; Sinyashin, O.; Vicic, D. A., *Inorg. Chem.* **50**, 8630-8635.
- Clark, C. D.; Hoffman, M. Z., *J. Phys. Chem.* **1996**, *100*, 14688-14693.
- Clark, C. D.; Hoffman, M. Z., *J. Phys. Chem.* **1996**, *100*, 7526-7532.
- Collins, P.; Ferrier, R., *Monosaccharides. Their Chemistry and Their Roles in Natural Products*. West Sussex, England, 1995.
- Córdova, A.; Watanabe, S.-i.; Tanaka, F.; Notz, W.; Barbas, C. F., *J. Am. Chem. Soc.* **2002**, *124*, 1866-1867.
- Czernecki, S.; Dechavanne, V., *Can. J. Chem.* **1983**, *61*, 533-540.
- Czernecki, S.; Ville, G., *J. Org. Chem.* **1989**, *54*, 610-612.
- D. Campbell, A.; E. Paterson, D.; J. K. Taylor, R.; M. Raynham, T., *Chem. Commun.* **1999**, 1599-1600.
- Danishefsky, S.; Allen, J. R., *Angew. Chem., Int. Ed.* **2000**, *39*, 836-863.
- De Lamo Marin, S.; Catala, C.; Kumar, S. R.; Valleix, A.; Wagner, A.; Mioskowski, C. *Eur. J. Org. Chem.* **2010**, 3985-3989.
- Debenham, S. D.; Debenham, J. S.; Burk, M. J.; Toone, E. J., *J. Am. Chem. Soc.* **1997**, *119*, 9897-9898.
- DeLaive, P. J.; Sullivan, B. P.; Meyer, T. J.; Whitten, D. G., *J. Am. Chem. Soc.* **1979**, *101*, 4007-4008.
- Dondoni, A.; Marra, A., *Chem. Rev.* **2000**, *100*, 4395-4421.
- Dondoni, A.; Marra, A.; Massi, A., *Tetrahedron* **1998**, *54*, 2827-2832.
- Doores, K. J.; Gamblin, D. P.; Davis, B. G., *Chem. Eur. J.* **2006**, *12*, 656-665.
- Dowlut, M.; Hall, D. G.; Hindsgaul, O. *J. Org. Chem.* **2005**, *70*, 9809.
- Du, J.; Yoon, T. P., *J. Am. Chem. Soc.* **2009**, *131*, 14604-14605.
- Dupuis, J.; Giese, B.; Rüegge, D.; Fishcer, H.; Korth, H. G.; Sustmann, R., *Angew. Chem., Int. Ed. Engl.* **1984**, *23*, 896-898.

Dwek, R. A., *Chem. Rev.* **1996**, *96*, 683-720.

Evans D. A. *Aldrichim. Acta* **1982**, *15*, 23-32.

Evans, D. A.; Chapman, K. T.; Bisaha, J., *J. Am. Chem. Soc.* **1988**, *110*, 1238-1256.

Fedurco, M.; Sartoretti, C. J.; Augustynski, J., *J. Phys. Chem. B* **2001**, *105*, 2003-2009.

Fischer, C.; Fu, G. C., *J. Am. Chem. Soc.* **2005**, *127*, 4594-4595.

Floyd, N.; Vijayakrishnan, B.; Koeppe, J. R.; Davis, B. G., *Angew. Chem., Int. Ed.* **2009**, *48*, 7798-7802.

Forbes, M. D. E. *Photochem. Photobiol.* **1997**, *65*, 73.

Friesen, R. W.; Loo, R. W., *J. Org. Chem.* **1991**, *56*, 4821-4823.

Friesen, R. W.; Sturino, C. F., *J. Org. Chem.* **1990**, *55*, 2572-2574.

Furst, L.; Matsuura, B. S.; Narayanam, J. M. R.; Tucker, J. W.; Stephenson, C. R. J., *Org. Lett.* **2010**, *12*, 3104-3107.

Ghaffar, T.; Parkins, A. W., *J. Mol. Catal. A: Chem.* **2000**, *160*, 249-261.

Ghaffar, T.; Parkins, A. W., *Tetrahedron Lett.* **1995**, *36*, 8657-8660.

Ghosez, A.; Göbel, T.; Giese, B. *Chem. Ber.* **1988**, *121*, 1807-1811.

Giese, B., *Angew. Chem., Int. Ed.* **1983**, *22*, 753-764.

Giese, B., *Angew. Chem., Int. Ed.* **1989**, *28*, 969-980.

Giese, B.; Dupuis, J., *Angew. Chem., Int. Ed. Engl.* **1983**, *22*, 622-623.

Giese, B.; Dupuis, J.; Nix, M. *Org. Synth.* **1987**, *65*, 236-239.

Giese, B.; González-Gómez, J. A.; Witzel, T., *Angew. Chem., Int. Ed.* **1984**, *23*, 69-70. c) Giese, B.; Witzel, T., *Angew. Chem., Int. Ed.* **1986**, *25*, 450-451.

Gnas, Y.; Glorius, F., *Synthesis* **2006**, *2006*, 1899-1930.

Gong, H.; Andrews, R. S.; Zuccarello, J. L.; Lee, S. J.; Gagné, M. R., *Org. Lett.* **2009**, *11*, 879-882.

Gong, H.; Gagné, M. R., *J. Am. Chem. Soc.* **2008**, *130*, 12177-12183.

Gong, H.; Sinisi, R.; Gagné, M. R., *J. Am. Chem. Soc.* **2007**, *129*, 1908-1909.

- Gonzalez-Aseguinolaza, G.; de Oliveira, C.; Tomaska, M.; Hong, S.; Bruna-Romero, O.; Nakayama, T.; Taniguchi, M.; Bendelac, A.; Van Kaer, L.; Koezuka, Y.; Tsuji, M., *Proc. Natl. Acad. Sci. U.S.A.* **2000**, *97*, 8461-8466.
- González-Bobes, F.; Fu, G. C., *J. Am. Chem. Soc.* **2006**, *128*, 5360-5361.
- Goodwin, T. E.; Crowder, C. M.; White, R. B.; Swanson, J. S.; Evans, F. E.; Meyer, W. L., *J. Org. Chem.* **1983**, *48*, 376-380.
- Gotanda, K.; Matsugi, M.; Suemura, M.; Ohira, C.; Sano, A.; Oka, M.; Kita, Y. *Tetrahedron* **1999**, *55*, 10315-1324.
- Gutierrez, A. C.; Jamison, T. F., *Org. Lett.* **2011**, *13*, 6414-6417.
- Halland, N.; Braunton, A.; Bachmann, S.; Marigo, M.; Jørgensen, K. A., *J. Am. Chem. Soc.* **2004**, *126*, 4790-4791.
- Hanessian, S.; Pernet, A. G., *Can. J. Chem.* **1974**, *52*, 1266-1279.
- Hansch, C.; Leo, A.; Taft, R. W., *Chem. Rev.* **1991**, *91*, 165-195.
- Hartwig, J. F., *Organotransition Metal Chemistry: From Bonding to Catalysis*. University Science Books: Sausalito. 2010; pp. 877-965.
- Hayakawa, Y.; Rovero, S.; Forni, G.; Smyth, M. J., *Proc. Natl. Acad. Sci. U.S.A.* **2003**, *100*, 9464-9469.
- Hedstrand, D. M.; Kruizinga, W. H.; Kellogg, R. M., *Tetrahedron Lett.* **1978**, *19*, 1255-1258.
- Herscovici, J.; Delatre, S.; Antonakis, K., *Tetrahedron Lett.* **1991**, *32*, 1183-1186
- Hirao, T.; Shiori, J.; Okahata, N., *Bull. Chem. Soc. Jpn.* **2004**, *77*, 1763-1764.
- Hong, S.; Wilson, M. T.; Serizawa, I.; Wu, L.; Singh, N.; Naidenko, O. V.; Miura, T.; Haba, T.; Scherer, D. C.; Wei, J.; Kronenberg, M.; Koezuka, Y.; Van Kaer, L., *Nat. Med.* **2001**, *7*, 1052-1056.
- Hook, B. D. A.; Dohle, W.; Hirst, P. R.; Pickworth, M.; Berry, M. B.; Booker-Milburn, K. I., *J. Org. Chem.* **2005**, *70*, 7558-7564.
- Hosomi, A.; Sakata, Y.; Sakurai, H., *Carbohydr. Res.* **1987**, *171*, 223-232.
- Hultin, P. G., *Curr. Top. Med. Chem.* **2005**, *5*, 1299-1331. d) Compain, P.; Martin, O. R., *Bioorg. Med. Chem.* **2001**, *9*, 3077-3092.
- Hutchinson, D. K.; Fuchs, P. L., *J. Am. Chem. Soc.* **1987**, *109*, 4930-4939.
- Ischay, M. A.; Anzovino, M. E.; Du, J.; Yoon, T. P., *J. Am. Chem. Soc.* **2008**, *130*, 12886-12887.

- Ischay, M. A.; Lu, Z.; Yoon, T. P., *J. Am. Chem. Soc.* **2010**, *132*, 8572-8574.
- Ishitani, O.; Yanagida, S.; Takamuku, S.; Pac, C., *J. Org. Chem.* **1987**, *52*, 2790-2796.
- Jones, G. D.; Martin, J. L.; McFarland, C.; Allen, O. R.; Hall, R. E.; Haley, A. D.; Brandon, R. J.; Kononova, T.; Desrochers, P. J.; Pulay, P.; Vicic, D. A., *J. Am. Chem. Soc.* **2006**, *128*, 13175-13183.
- Jones, G. D.; McFarland, C.; Anderson, T. J.; Vicic, D. A., *Chem. Commun.* **2005**, 4211-4213.
- Juaristi, E.; Cuevas, G., *Tetrahedron* **1992**, *48* (24), 5019-5087.
- Julliard, M.; Chanon, M., *Chem. Rev.* **1983**, *83*, 425-506.
- Juris, A.; Balzani, V.; Barigelletti, F.; Campagna, S.; Belser, P.; von Zelewsky, A., *Coord. Chem. Rev.* **1988**, *84*, 85-277.
- Kakimi, K.; Guidotti, L. G.; Koezuka, Y.; Chisari, F. V., *J. Exp. Med.* **2000**, *192*, 921-930.
- Kamigaito, M.; Ando, T.; Sawamoto, M., *Chem. Rev.* **2001**, *101*, 3689-3746.
- Kavarnos, G. J.; Turro, N. J., *Chem. Rev.* **1986**, *86*, 401-449.
- Kikuchi, A.; Nieda, M.; Schmidt, C.; Koezuka, Y.; Ishihara, S.; Ishikawa, Y.; Tadokoro, K.; Durrant, S.; Boyd, A.; Juji, T.; Nicol, A., *Br. J. Cancer* **2001**, *85*, 741-746.
- Kitamura, N.; Kim, H. B.; Okano, S.; Tazuke, S., *J. Phys. Chem.* **1989**, *93*, 5750-5756.
- Korth, H. G.; Sustmann, R.; Gröninger, K. S.; Witzel, T.; Giese, B., *J. Chem. Soc., Perkin Trans. 2* **1986**, 1461-1464.
- Kraus, G. A.; Molina, M. T., *J. Org. Chem.* **1988**, *53*, 752-753.
- Kuburan, B.; Lindhardt, R. J., *Curr. Org. Chem.* **2000**, *4*, 653-677.
- Laurino, P.; Kikkeri, R.; Azzouz, N.; Seeberger, P. H., *Nano Lett.* **2011**, *11*, 73-78.
- Lebedeva, N. V.; Forbes, M. D. E. Acrylic Polymer Radicals: Structural Characterization and Dynamics in Carbon-Centered Radicals and Radical Cations. In *Wiley Series on Reactive Intermediates in Chemistry and Biology*; Forbes, M.D.E., Ed; Wiley: New York, 2010, Vol. 3; p 323-355.
- Lee, J. G.; Seo, Y. S., *Bull. Korean Chem. Soc.* **1995**, *16*, 377-379.
- Lee, K. Y.; Lee, C. G.; Na, J. E.; Kim, J. N., *Tetrahedron Lett.* **2005**, *46*, 69-74.
- Lemieux, R. U.; Hendricks, K. B.; Stick, R. V.; James, K., *J. Am. Chem. Soc.* **1975**, *97*, 4056-4062.
- Lévesque, F.; Seeberger, P. H., *Angew. Chem., Int. Ed.* **2012**, *51*, 1706-1709.

- Lévesque, F.; Seeberger, P. H., *Org. Lett.* **2011**, *13*, 5008-5011.
- Levy, D. E.; Tang, C., *The Chemistry of C-Glycosides*. Pergamon: Tarrytown, 1995.
- Lieberknecht, A.; Griesser, H.; Krämer, B.; Bravo, R. D.; Colinas, P. A.; Grigera, R. I. J., *Tetrahedron* **1999**, *55*, 6475-6482.
- Lin, C. H.; Lin, H. C.; Yang, W. B., *Curr. Top. Med. Chem.* **2005**, *5*, 1431-1457.
- Lin, X.; Phillips, D. L., *J. Org. Chem.* **2008**, *73*, 3680-3688.
- Liu, P. S., *J. Org. Chem.* **1987**, *52*, 4717-4721.
- Liu, Y.; Gallagher, T., *Org. Lett.* **2004**, *6*, 2445-2448.
- Maidan, R.; Goren, Z.; Becker, J. Y.; Willner, I., *J. Am. Chem. Soc.* **1984**, *106*, 6217-6222.
- Maity, S. K.; Dutta, S. K.; Banerjee, A. K.; Achari, B.; Singh, M. *Tetrahedron* **1994**, *50*, 6965-6974.
- Marcaurelle, L. A.; Bertozzi, C. R., *Chem. Eur. J.* **1999**, *5*, 1384-1390.
- Mashraqui, S. H.; Kellogg, R. M., *Tetrahedron Lett.* **1985**, *26*, 1453-1456.
- Masui, H.; Murray, R. W. *Inorg. Chem.* **1997**, *36*, 5118.
- Mathews, C. K.; van Holde, K. E.; Ahern, K. G., *Biochemisry*. 3rd Ed.; Addison Wesley Longman, Publishers, San Francisco, 2000; pp. 278-312.
- Mathews, C. K.; van Holde, K. E.; Ahern, K. G., *Biochemisry*. 3rd Ed.; Addison Wesley Longman, Publishers, San Francisco, 2000; pp. 594-624.
- Matyjaszewski, K.; Xia, J., *Chem. Rev.* **2001**, *101*, 2921-2990.
- Monserrat, K.; Foreman, T. K.; Graetzel, M.; Whitten, D. G., *J. Am. Chem. Soc.* **1981**, *103*, 6667-6672.
- Motoyama, Y.; Kurihara, O.; Murata, K.; Aoki, K.; Nishiyama, H. *Organometallics* **2000**, *19*, 1025-1034.
- Nagib, D. A.; Scott, M. E.; MacMillan, D. W. C., *J. Am. Chem. Soc.* **2009**, *131*, 10875-10877.
- Nagy, J. O.; Wang, P.; Gilbert, J. H.; Schaefer, M. E.; Hill, T. G.; Callstrom, M. R.; Bednarski, M. D., *J. Med. Chem.* **1992**, *35*, 4501-4502.
- Nakagawa, R.; Motoki, K.; Ueno, H.; Iijima, R.; Nakamura, H.; Kobayashi, E.; Shimosaka, A.; Koezuka, Y., *Cancer Res.* **1998**, *58*, 1202-1207.
- Narayanam, J. M. R.; Stephenson, C. R. J., *Chem. Soc. Rev.* **2011**, *40*, 102-113.

- Narayanam, J. M. R.; Tucker, J. W.; Stephenson, C. R. J., *J. Am. Chem. Soc.* **2009**, *131*, 8756-8757.
- Nguyen, J. D.; Tucker, J. W.; Konieczynska, M. D.; Stephenson, C. R. J., *J. Am. Chem. Soc.* **2011**, *133*, 4160-4163.
- Nicewicz, D. A.; MacMillan, D. W. C., *Science* **2008**, *322*, 77-80.
- Nicotra, F.; Driguez, H.; Thiem, J., Synthesis of C-glycosides of biological interest In *Glycoscience Synthesis of Substrate Analogs and Mimetics*, Springer Berlin / Heidelberg: 1997; Vol. 187, pp 55-83.
- Nishiyama, H.; Kondo, M.; Nakamura, T.; Itoh, K. *Organometallics* **1991**, *10*, 500-508.
- Nuzzi, A.; Massi, A.; Dondoni, A., *Org. Lett.* **2008**, *10*, 4485-4488.
- Okada, K.; Okamoto, K.; Morita, N.; Okubo, K.; Oda, M., *J. Am. Chem. Soc.* **1991**, *113*, 9401-9402.
- Osborn, H. M. I.; Evans, P. G.; Gemmell, N.; Osborne, S. D., *J. Pharm. Pharmacol.* **2004**, *56*, 691-702.
- Pac, C.; Ihama, M.; Yasuda, M.; Miyauchi, Y.; Sakurai, H., *J. Am. Chem. Soc.* **1981**, *103*, 6495-6497.
- Pan, S. C.; List, B., *Org. Lett.* **2007**, *9*, 1149-1151.
- Parsons, A. T.; Campbell, M. J.; Johnson, J. S. *Org. Lett.* **2008**, *10*, 2541.
- Patten, T. E.; Matyjaszewski, K., *Acc. Chem. Res.* **1999**, *32*, 895-903.
- Peng, C., Wang, Y., Wang, J.; *J. Am. Chem. Soc.* **2008**, *130*, 1566-1567.
- Perreault, C.; Goudreau, S. R.; Zimmer, L. E.; Charette, A. B. *Org. Lett.* **2008**, *10*, 689-692, and references therein.
- Phapale, V. B.; Buñuel, E.; García-Iglesias, M.; Cárdenas, D. J., *Angew. Chem., Int. Ed.* **2007**, *46*, 8790-8795.
- Postema, M. H. D., *C-Glycoside Synthesis*. CRC Press, Inc.: Boca Raton, 1995.
- Powell, D. A.; Maki, T.; Fu, G. C., *J. Am. Chem. Soc.* **2005**, *127*, 510-511.
- Praly, J.-P.; Ardakani, A. S.; Bruyère, I.; Marie-Luce, C.; Bing Qin, B., *Carbohydr. Res.* **2002**, *337*, 1623-1632.
- Ramnauth, J.; Poulin, O.; Bratovanov, S. S.; Rakhit, S.; Maddaford, S. P., *Org. Lett.* **2001**, *3*, 2571-2573.
- Ravindranathan Karcha, K. P.; Jennings, H. J. *J. Carbohydr. Chem.* **1990**, *9*, 777-781.
- Readman, S. K.; Marsden, S. P.; Hodgson, A., *Synlett* **2000**, 1628-1630.

- Rivarola, C. R.; Bertolotti, S. G.; Previtali, C. M., *Photochem. Photobiol.* **2006**, 82, 213-218.
- Rondinini, S. B.; Mussini, P. R.; Crippa, F.; Sello, G., *Electrochem. Commun.* **2000**, 2, 491-496.
- SanMartin, R.; Tavassoli, B.; Walsh, K. E.; Walter, D. S.; Gallagher, T., *Org. Lett.* **2000**, 2, 4051-4054.
- Schmidt, R. R.; Dietrich, H., *Angew. Chem., Int. Ed. Engl.* **1991**, 30, 1328-1329.
- Sears, P.; Wong, C.-H., *Angew. Chem., Int. Ed.* **1999**, 38, 2300-2324.
- Shulman, M. L.; Shiyan, S. D.; Khorlin, A. Y., *Carbohydr. Res.* **1974**, 33, 229-235.
- Sibi, M. P.; Sausker, J. B. *J. Am. Chem. Soc.* **2002**, 124, 984-991.
- Spencer, R. P.; Schwartz, J., *J. Org. Chem.* **1997**, 62, 4204-4205.
- Spencer, R. P.; Schwartz, J., *Tetrahedron* **2000**, 54, 2103-2112.
- Struwe, W. B.; Cosgrave, E. F. J.; Byrne, J. C.; Saldova, R.; Rudd, P. M.; Owens, R.; Nettleship, J., Glycoproteomics in Health and Disease. In *Functional and Structural Proteomics of Glycoproteins*, Springer Netherlands: 2011; pp 1-38.
- Sun, H.; Yoshimura, A.; Hoffman, M. Z., *J. Phys. Chem.* **1994**, 98, 5058-5064.
- Takahashi, O.; Yamasaki, K.; Kohno, Y.; Ohtaki, R.; Ueda, K.; Suezawa, H.; Umezawa, Y.; Nishio, M., *Carbohydr. Res.* **2007**, 342, 1202-1209.
- Takeo, K.; Nakagen, M.; Teramoto, Y.; Nitta, Y. *Carbohydr. Res.* **1990**, 201, 261-275.
- Tazuke, S.; Kitamura, N.; Kawanishi, Y., *J. Photochem.* **1985**, 29, 123-138.
- Teplý, F., *Collect. Czech. Chem. Commun.* **2011**, 76, 859-917.
- Thorn, S. N.; Gallagher, T., *Synlett* **1996**, 856-858.
- Toshima, K.; Tatsuta, K., *Chem. Rev.* **1993**, 93, 1503-1531.
- Tucker, J. W.; Narayanam, J. M. R.; Krabbe, S. W.; Stephenson, C. R. J., *Org. Lett.* **2009**, 12, 368-371.
- Tucker, J. W.; Stephenson, C. R. J. *J. Org. Chem.* **2012**, 77, ASAP. DOI: 10.1021/jo202538x.
- Uegaki, H.; Kotani, Y.; Kamigaito, M.; Sawamoto, M., *Macromolecules* **1997**, 30, 2249-2253.
- Varki, A., *Essentials of glycobiology*. Cold Spring Harbor Laboratory Press: Cold Spring Harbor, N.Y., 2009.

Varki, A., *Glycobiology* **1993**, *3*, 97-130.

Vaske, Y. S. M.; Mahoney, M. E.; Konopelski, J. P.; Rogow, D. L.; McDonald, W. J., *J. Am. Chem. Soc.* **2010**, *132*, 11379-11385.

Vaupel, A.; Knochel, P., *J. Org. Chem.* **1996**, *61*, 5743-5753.

Xiong, D.-C.; Zhang, L.-H.; Ye, X.-S., *Org. Lett.* **2009**, *11*, 1709-1712.

Yang, G.; Franck, R. W.; Bittman, R.; Samadder, P.; Arthur, G., *Org. Lett.* **2001**, *3*, 197-200.

Yang, G.; Schmieg, J.; Tsuji, M.; Franck, R. W., *Angew. Chem., Int. Ed.* **2004**, *43*, 3818-3822.

Yang, J. W.; List, B., *Org. Lett.* **2006**, *8*, 5653-5655.

Yoon, T. P.; Ischay, M. A.; Du, J., *Nat Chem* **2010**, *2*, 527-532.

Yougai, S.; Miwa, T., *J. Chem. Soc., Chem. Commun.* **1983**, 68-69.

Zen, J.-M.; Liou, S.-L.; Kumar, A. S.; Hsia, M.-S., *Angew. Chem., Int. Ed.* **2003**, *42*, 577-579.

Zhou, J. S.; Fu, G. C., *J. Am. Chem. Soc.* **2004**, *126*, 1340.

Zhou, J.; Fu, G. C., *J. Am. Chem. Soc.* **2003**, *125*, 12527-12530.

Zhou, J.; Fu, G. C., *J. Am. Chem. Soc.* **2003**, *125*, 14726-14727.

Zolfigol, M. A.; Safaiee, M., *Synlett* **2004**, 0827-0828.

Zou, W., *Curr. Top. Med. Chem.* **2005**, *5*, 1363-1391.